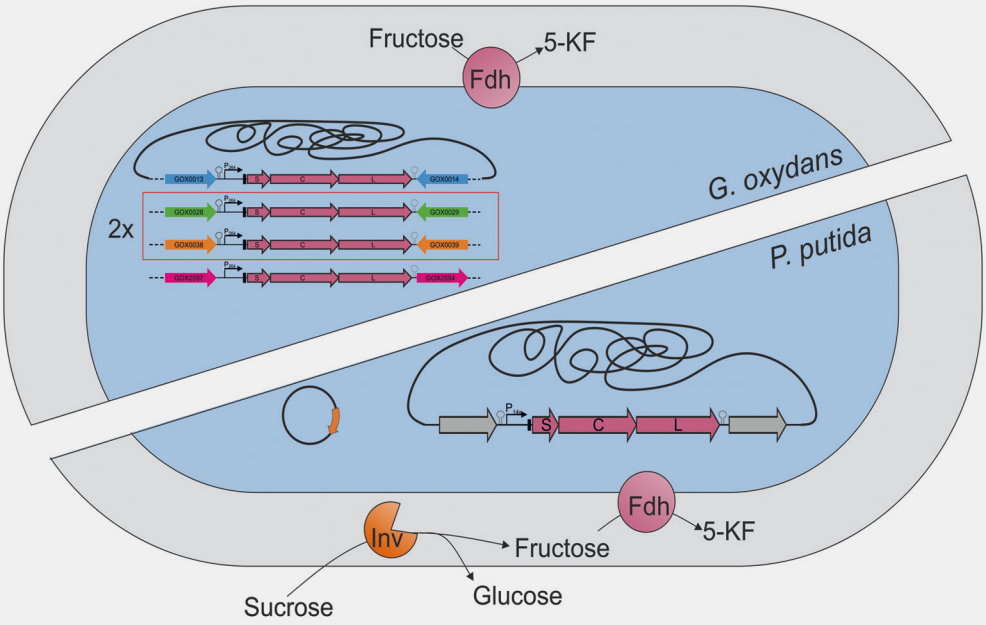

Strain development of *Gluconobacter oxydans* and *Pseudomonas putida* for production of the sweetener 5-ketofructose

Karen Wohlers

Schlüsseltechnologien / Key Technologies
Band / Volume 252
ISBN 978-3-95806-612-0

Mitglied der Helmholtz-Gemeinschaft

JÜLICH
Forschungszentrum

Schriften des Forschungszentrums Jülich
Reihe Schlüsseltechnologien / Key Technologies Band / Volume 252

Forschungszentrum Jülich GmbH
Institut für Bio-und Geowissenschaften
Biotechnologie (IBG-1)

Strain development of *Gluconobacter oxydans* and *Pseudomonas putida* for production of the sweetener 5-ketofructose

Karen Wohlers

Schriften des Forschungszentrums Jülich
Reihe Schlüsseltechnologien / Key Technologies Band / Volume 252

ISSN 1866-1807 ISBN 978-3-95806-612-0

Bibliografische Information der Deutschen Nationalbibliothek.
Die Deutsche Nationalbibliothek verzeichnet diese Publikation in der
Deutschen Nationalbibliografie; detaillierte Bibliografische Daten
sind im Internet über http://dnb.d-nb.de abrufbar.

Herausgeber und Vertrieb:	Forschungszentrum Jülich GmbH Zentralbibliothek, Verlag 52425 Jülich Tel.: +49 2461 61-5368 Fax: +49 2461 61-6103 zb-publikation@fz-juelich.de www.fz-juelich.de/zb
Umschlaggestaltung:	Grafische Medien, Forschungszentrum Jülich GmbH
Druck:	Grafische Medien, Forschungszentrum Jülich GmbH
Copyright:	Forschungszentrum Jülich 2022

Schriften des Forschungszentrums Jülich
Reihe Schlüsseltechnologien / Key Technologies, Band / Volume 252

D 61 (Diss. Düsseldorf, Univ., 2021)

ISSN 1866-1807
ISBN 978-3-95806-612-0

Vollständig frei verfügbar über das Publikationsportal des Forschungszentrums Jülich (JuSER)
unter www.fz-juelich.de/zb/openaccess.

The results described in this dissertation have been published in peer-reviewed journals in the following articles:

Battling, S*., Wohlers, K.*, Igwe, C., Kranz, A., Pesch, M., Wirtz, A., Baumgart, M., Büchs, J., Bott, M. (2020). Novel plasmid-free *Gluconobacter oxydans* strains for production of the natural sweetener 5-ketofructose. Microbial Cell Factories, 19(1), 54 (https://dx.doi.org/10.1186/s12934-020-01310-7)
*Shared first author

Wohlers, K., Wirtz, A., Reiter, A., Oldiges, M., Baumgart, M., Bott, M. (2021). Metabolic engineering of *Pseudomonas putida* for production of the natural sweetener 5-ketofructose from fructose or sucrose by periplasmic oxidation with a heterologous fructose dehydrogenase. Microbial Biotechnology (https://doi.org/10.1111/1751-7915.13913)

Content

Summary

Consumption of added sugar is a health threat since it can cause obesity and type 2 diabetes. Consequently, there is an increasing demand for sugar substitutes. Available sweeteners, however, have different drawbacks resulting in a need for alternative sugar substitutes. The natural metabolite 5-ketofructose (5-KF) is a promising sweetener candidate. It is not metabolized by the human body and probably not metabolized by the human gut microbiome while having a comparable sweet taste as fructose. 5-KF can be produced from fructose via oxidation by the membrane-bound fructose dehydrogenase (Fdh) of *Gluconbacter japonicus*, encoded by the *fdhSCL* genes. Recent studies showed the production of the sweetener with heterologous strains of the industrially relevant acetic acid bacterium *Gluconobacter oxydans*. As *G. oxydans* possesses no Fdh, plasmid-based *fdhSCL* expression was applied in previous studies. For production of a food additive, however, antibiotic-free production is desirable.

Aiming at plasmid- and antibiotic-free 5-KF production, in this study the *fdhSCL* genes were integrated into the chromosome of engineered *G. oxydans* IK003.1. Four different genomic integration sites were selected, including three intergenic regions and one gene replacement, to compare the effects of the genomic environment. The four integration strains were successfully constructed, and all allowed functional expression of the *fdhSCL* genes with minor differences in 5-KF production. However, the efficiency and velocity of 5-KF production was lower compared to plasmid-based *fdhSCL* expression. To improve the plasmid-free production of the sweetener, the two best integration sites were combined in a double integration strain, *G. oxydans* IK003.1::*fdhSCL*^{2} containing two chromosomal *fdhSCL* copies. This strain showed accelerated 5-KF production, approaching that of the strain with plasmid-based *fdhSCL* expression.

Methods for genetic engineering and expression systems for *G. oxydans* are still limited. *G. oxydans* needs complex medium components for good growth and has a low biomass yield. Hence, in the second part of this study, the well-established organism *Pseudomonas putida* was selected as alternative 5-KF production host. Tn*7*-based chromosomal integration of the *fdhSCL* genes enabled *P. putida* to produce 5-KF from fructose in mineral salts medium. In a batch fermentation with 150 g/L fructose, a product concentration of 129 ± 5 g/L 5-KF was reached. Overall, shake flask experiments, bioreactor cultivations and whole-cell biotransformations demonstrated a competitive ability of *P. putida*::*fdhSCL* to produce 5-KF when compared to a *G. oxydans fdhSCL* integration strain. The substrate spectrum of *P. putida*::*fdhSCL* was expanded by plasmid-based expression of *inv1417*, encoding a periplasmic invertase of *G. japonicus*. Inv1417 enabled 5-KF production from sucrose as cheaper substrate at rates comparable to production from fructose.

All in all, a set of potent *G. oxydans* and *P. putida* 5-KF producers was generated in this study, providing a good starting point for further process development and industrial implementation of microbial 5-KF production.

Zusammenfassung

Der zunehmende Zuckerkonsum stellt eine große gesundheitliche Bedrohung dar, weil übermäßiger Konsum zu Übergewicht und Typ 2 Diabetes führen kann. Folglich gibt es eine zunehmende Nachfrage nach Zuckerersatzstoffen. Aufgrund verschiedener Nachteile der bereits erhältlichen Süßstoffe gibt es einen Bedarf an alternativen Zuckerersatzstoffen. Der natürliche Metabolit 5-Ketofructose (5-KF) ist ein vielversprechender Süßstoff-Kandidat. 5-KF hat einen ähnlich süßen Geschmack wie Fructose und wird nicht vom menschlichen Körper und vermutlich auch nicht vom Darm-Mikrobiom verstoffwechselt. 5-KF wird durch Oxidation von Fructose mit der membrangebundenen Fructose-Dehydrogenase (Fdh) aus *Gluconobacter japonicus*, kodiert durch die *fdhSCL*-Gene, gebildet. Frühere Studien haben sich auf die 5-KF-Produktion mit heterologen Stämmen des industriell relevanten Essigsäurebakteriums *Gluconobacter oxydans* konzentriert. Da *G. oxydans* selbst keine Fdh besitzt, wurden die *fdhSCL*-Gene bisher plasmid-basiert exprimiert. Für die Produktion eines Süßstoffs wäre jedoch eine antibiotika-freie Herstellung wünschenswert.

Um eine plasmid- und antibiotika-freie 5-KF-Produktion zu ermöglichen, wurden die *fdhSCL*-Gene in das Chromosom des optimierten *G. oxydans*-Stammes IK003.1 integriert. Um den Einfluss der genomischen Umgebung zu testen, wurden vier verschiedene genomische Integrationsorte ausgewählt, drei intergene Regionen und ein Genaustausch. Alle vier Integrationsstämme wurden erfolgreich konstruiert und zeigten nur leichte Unterschiede in der 5-KF Produktion. Allerdings waren die Effizienz und Geschwindigkeit der 5-KF-Bildung geringer als bei den Stämmen mit plasmid-basierter *fdhSCL*-Expression. Um die plasmid-freie Produktion des Süßstoffs zu steigern, wurde die beiden besten Integrationsorte in einer Doppelintegrante, *G. oxydans* IK003.1::*fdhSCL*^{2} mit zwei chromosomalen *fdhSCL*-Kopien kombiniert. Dieser Stamm zeigte eine beschleunigte 5-KF-Produktion, die nahe an die Rate von Stämmen mit plasmid-basierter *fdhSCL*-Expression heranreichte.

Die Methoden zur genetischen Modifikation sowie die verfügbaren Expressionssystemen für *G. oxydans* sind noch recht begrenzt. *G. oxydans* benötigt komplexe Mediums-Bestandteile für gutes Wachstum und erreicht nur eine geringe Biomasse-Ausbeute. Daher wurde das methodisch gut etablierte Bakterium *Pseudomonas putida* als alternativer Wirt für die 5-KF Produktion ausgewählt. Eine Tn*7*-basierte chromosomale Integration der *fdhSCL*-Gene befähigte *P. putida* zur 5-KF Produktion aus Fructose in Minimalmedium. In einer Batch-Fermentation mit 150 g/L Fructose wurden Produktkonzentrationen von 129 ± 5 g/L 5-KF erreicht. Insgesamt wurde

gezeigt, dass *P. putida*::*fdhSCL* im Vergleich mit einem *G. oxydans fdhSCL*-Integrationsstamm vergleichbare Aktivitäten bezüglich der 5-KF-Produktion zeigt und somit ein geeigneter Wirtsorganismus ist. Um statt Fructose das günstigere Substrat Saccharose für die 5-KF-Produktion einsetzen zu können, wurde das Gen *inv1417*, codierend für eine periplasmatische Invertase aus *G. japonicus*, in *P. putida*::*fdhSCL* plasmid-kodiert exprimiert. Der resultierende Stamm zeigte ausgehend von Saccharose eine 5-KF-Produktionsrate, die vergleichbar war mit der Rate aus Fructose.

Zusammenfassend wurden in dieser Arbeit verschiedene *G. oxydans* und *P. putida* 5-KF-Produzentenstämme generiert und charakterisiert, die eine gute Grundlage für die weitere Bioprozess-Entwicklung sowie eine industrielle Umsetzung darstellen.

Abbreviations

5-KF	5-Ketofructose
ADI	Amount of daily intake
ATP	Adenosine triphosphate
BMI	Body Mass Index
DCPIP	2,6-dichlorophenolindophenol
EDP	Entner-Doudoroff pathway
EFSA	European Food Safety Authority
EMP	Embden-Meyerhoff pathway
FAD	Flavin adenine dinucleotide
FDA	Food and Drug Administration
Fdh	Fructose dehydrogenase
GA3P	Glyceraldehyde-3-phosphate (GA3P)
GAPDH	Glyceraldehyde-3-phosphate dehydrogenase
Gcd	Glucose dehydrogenase (membrane-bound, *P. putida*)
GdhM	Glucose dehydrogenase (membrane-bound, *G. oxydans*)
HPLC	High performance liquid chromatography
mSldAB	Membrane-bound polyol/sorbitol dehydrogenase (*G. oxydans*)
MSM	Mineral salts medium
NAD^+/NADH	Nicotinamide adenine dinucleotide, oxidized/reduced
$NADP^+$/NADPH	Nicotinamide adenine dinucleotide phosphate, oxidized/reduced
NMR	Nuclear magnetic resonance
OD_{600}	Optical density, measured at 600 nm
OMP	Outer membrane protein
PEP	Phosphoenolpyruvate
PPP	Pentose phosphate pathway
PQQ	Pyrroloquinoline quinone
PTS	Phosphotransferase system
RDCI	Recommended daily calorie intake
Reb	Rebaudioside
SPE	Solid phase extraction
TCA	Tricarboxylic acid
WHO	World Health Organization
Δ	Deletion

1 Introduction

1.1 Sugar consumption and sweeteners

1.1.1 Health problems caused by sugar consumption

According to the world health organization (WHO), obesity has almost tripled between 1975 and 2016 and in 2016 39 % of adults worldwide were overweight (body mass index (BMI) ≥ 25) and 13 % were obese (BMI ≥ 30) (WHO, 2020). In Germany even 54 % of adults were overweight and 18 % obese in 2014/15 (Schienkiewitz, et al., 2017, Stricker, et al., 2021). Despite regional variation in overweight augmentation, obesity is an increasing health threat around the world. In 2000, the WHO recognized obesity as a global epidemic (WHO Consultation on Obesity and World Health Organization, 2000). One discussed cause for weight gain, overweight and obesity is the excessive consumption of free sugars (WHO, 2020, Stricker, et al., 2021). However, it is difficult to precisely link consumption of added sugars to obesity since bodyweight can be influenced by many factors. Sugar as component of the diet is just one of the factors (Mitchell, et al., 2011, van Buul, et al., 2014, Rippe and Angelopoulos, 2016).

In addition to the possible linkage to obesity, the consumption of added sugars, mostly as sucrose or high fructose corn sirup (HFCS), often in forms of processed food or sugar-sweetened beverages, is discussed as cause or risk factor for several health problems, in particular the metabolic syndrome, type-2 diabetes, cardio-vascular diseases, and dental caries (Malik, et al., 2010, de Koning, et al., 2011, Moynihan and Kelly, 2014, Yang, et al., 2014, DiNicolantonio, et al., 2015, Moynihan, 2016, Rippe and Angelopoulos, 2016).

These problems could be solved, or risk factors could be reduced by an altered, sugar-reduced diet. The WHO and the German Society for Nutrition (Deutsche Gesellschaft für Ernährung) for instance recommend an intake of free sugars of < 10 % of the recommended daily calorie intake (RDCI). Based on the RDCI of 2000 kcal for an adult, this corresponds to 50 g sugar or 17 sugar cubes or 500 mL orange juice (Stricker, et al., 2021). Reducing the sugar consumption without sacrificing the desired sweet taste can be achieved with sugar substitutes or sweeteners.

1.1.2 Sweeteners on the market

The sweetener market already offers a broad variety of sweeteners with different traits for various applications. However, most available sugar substitutes have disadvantages or are controversially discussed. The available sweeteners can be divided in nutritive, and non-nutritive or intensive sweeteners, by having a caloric content similar to sugar or having no or a low caloric content. Non-nutritive sweeteners can be subdivided in artificial and natural sweeteners (Carocho, et al., 2017, Ruiz-Ojeda, et al., 2019). An overview is shown in Figure 3.

Nutritive sweeteners are sugar alcohols or polyols that are used as sugar substitutes because they do not interfere with insulin levels and have no cariogenic properties and are used

for example in sugar-free chewing gum (Deshpande and Jadad, 2008, Carocho, et al., 2017). The group of sugar alcohols comprises erythritol, isomaltose, lactitol, mannitol, sorbitol, and xylitol. Polyols are sweeteners with a reduced caloric content compared to sucrose and a comparable or slightly lower sweetness. However, polyols are most applied where the low glycemic and non-cariogenic properties are needed. They are natural compounds that occur for example in fruits (Livesey, 2003, Grembecka, 2015, Moriconi, et al., 2020). While some polyols, primarily the smaller molecules, for examples erythritol, are mostly absorbed by diffusion in the small intestine, high percentages of others, for example lactitol, are predominantly fermented by the gut microbiome in the distal small intestine or in the large intestine. The fermentation can lead to gastrointestinal problems like flatulence, abdominal discomfort, or laxative effects and can alter the composition of the microbiome (Lenhart and Chey, 2017, Ruiz-Ojeda, et al., 2019). Due to the laxative effect, the daily intake of polyols is limited in order to avoid gastrointestinal discomfort (Ghosh and Sudha, 2012).

Non-nutritive artificial sweeteners are synthesized by chemical or biotechnological processes. The group of artificial sweeteners includes acesulfame-K, aspartame, cyclamate, saccharine and sucralose (Chattopadhyay, et al., 2014). An overview of the respective structures is shown in Figure 1.

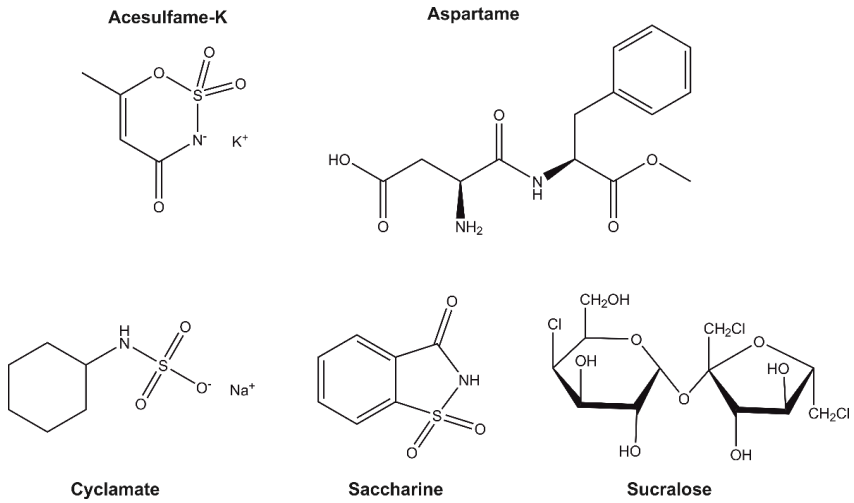

Figure 1 Chemical structures of different artificial sweeteners

Since the sweet taste of a compound cannot be predicted, artificial sweeteners were accidental discoveries (Mazur, et al., 1969). In comparison to sucrose, they are 200-600-fold sweeter and only small amounts are therefore necessary for generating a sweet taste. Consequently their caloric content can be neglected (Moriconi, et al., 2020).

Although the sweeteners on the market are all approved by the Food and Drug Administration (FDA) in the USA or the European Food Safety Authority (EFSA) with different

acceptable amounts of daily intake (ADI), their influence on the human body, its microbiome and potential health threats are evaluated controversially (Mattes and Popkin, 2009, Tandel, 2011, Sharma, et al., 2016, Moriconi, et al., 2020). Aspartame for example was shown to have carcinogenic effects in rats even in amounts below ADI (Soffritti, et al., 2006). Sucralose was described to change the gut microbiome and influence the cholesterol bile acid metabolism in mice (Uebanso, et al., 2017). Though intended to reduce health risk factors by using sweeteners instead of sugar, some studies relate the consumption of artificial sweeteners with the risk to develop metabolic syndrome or type 2 diabetes (Fagherazzi, et al., 2013, Pepino, 2015). Similarly controversial is the effect of artificial sweeteners in weight control. Some studies show a positive effect (Miller and Perez, 2014), while others show adverse effects linking consumption of artificial sweeteners with weight gain (Chia, et al., 2016, Azeez, et al., 2019).

The group of **non-nutritive natural sweeteners** contains different natural compounds with a high sweetness. The use of sweeteners of this group is increasing due to customer demands for natural food additives. The most prominent sweetener of this group is stevia or steviol glycosides. Steviol glycosides are extracted from the leaves of *Stevia rebaudiana* Bertoni. The extracted steviol glycosides (E957) contain different compounds, stevioside (5-10%), rebaudioside (Reb) A (2-5%), Reb C (1%), dulcoside A (0.5%), Reb D, E and F (0.2%), of which Reb A is the sweetest. Selected steviol glycosides are shown in Figure 2.

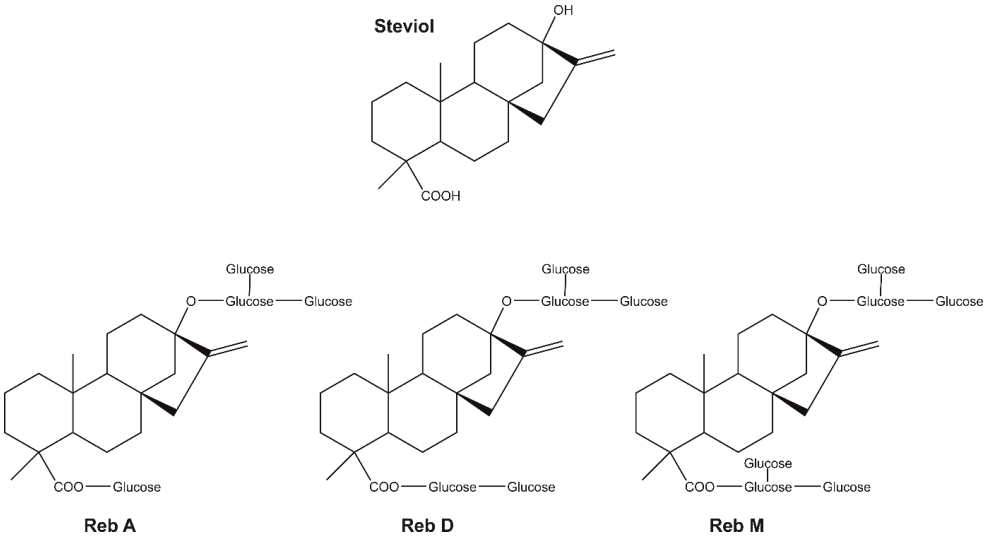

Figure 2 Structure of steviol and selected steviol glycosides. Adapted from Olsson, et al. (2016).

The mixture is 250-300-fold sweeter than sucrose, but unfortunately some of the components have a bitter taste, limiting the use as sweetener (Carocho, et al., 2017, Momtazi-Borojeni, et al., 2017). Hence, microbial production processes of certain steviol glycosides without bitter taste like Reb D or Reb M have been developed. The steviol glycosides differ in their number of glucose

molecules, Reb D and Reb M have with five and six glucose molecules the most (Olsson, et al., 2016, Zhao, et al., 2018).

Thaumatin is another example for a natural non-nutritive sweetener. It is a mixture of similar 207 amino acid proteins, with a sweetness 2000-3000-fold higher than sucrose (Carocho, et al., 2017). It is extracted from the plant *Thaumatococcus danielli* Bennett, which is naturally found in the rain forests in Nigeria, Ghana, Cameroon, and the Ivory Coast and hence production is limited (Frey, 2012). Different approaches of heterologous production with various microbial hosts have been reported in literature. However, many of these studies resulted in an inactive form without the desired sweet tase. Eventually, production of sweet thaumatin II could be achieved for example with refolding of inclusion bodies synthesized with *Escherichia coli* (Daniell, et al., 2000, Masuda, 2017, Joseph, et al., 2019). Also, different studies on the recombinant thaumatin production in different plants have been described in literature. While there is no industrial process yet, the recent publication of a techno-economic analysis suggests that large-scale production of the sweetener might come (Firsov, et al., 2018, Kelada, et al., 2021). Sensory drawbacks of thaumatin are the slow development of the sweet taste and a characteristic licorice-like aftertaste (Carocho, et al., 2017, Firsov, et al., 2018). Additionally, thaumatin-like proteins were found to be allergens and allergic reactions were reported for chewing gum factory workers processing a thaumatin-containing powder (Breiteneder, 2004, Tschannen, et al., 2017).

Nutritive	**Polyols** • Erythritol • Isomaltose • Lactitol • Mannitol • Sorbitol • Xylitol	Comparably sweet as sucrose	+ Non-cariogenic + Suited for diabetics - Uptake limited - Laxative
Non-nutritive	**Artificial** • Acesulfame-K • Aspartame • Cyclamate • Saccharine • Sucralose	200-600 x sweeter than sucrose	+ Sweet taste without calories - Under suspicion to cause health problems
	Natural • Steviol glycosides • Thaumatin	250-3000 x sweeter than sucrose	+ Natural sweet taste without calories - Licorice-like aftertaste
	Natural, new • 5-Keto-D-fructose	Comparably sweet as sucrose	+ Natural sweet taste without calories + Fructose like taste / no aftertaste + Not metabolized by the gut microbiome

Figure 3 Schematic overview of available sweeteners together with the new potential sweetener 5-KF. Sweeteners can be grouped into nutritive and non-nutritive sweeteners. Non-nutritive sweeteners can be further divided in artificial sweeteners and natural sweeteners. Some examples, their sweetness as well as advantages (+) and disadvantages (-) for each group are listed.

The overview of different sweeteners in Figure 3 shows the variety of available nutritive and non-nutritive sweeteners, but also points out the drawbacks and limitations of the different

compounds. Especially the controverse discussion or suspicion of health threats from the artificial sweeteners explains the demand for new, preferably natural sweeteners.

1.2 5-Ketofructose as new natural sweetener

1.2.1 Characteristics of the potential sweetener 5-KF

5-Keto-D-fructose (5-KF) is an interesting new sweetener that is not yet produced commercially. 5-KF is a natural compound that can be found in botrytized grapes, in wine as well as in honey and vinegar (Barbe, et al., 2001, Blasi, et al., 2008, Siemen, et al., 2018). It is almost comparable sweet as fructose. A sensory test showed no differentiation in sweetness intensity or quality of a 60 mM fructose and a 70 mM 5-KF solution (Herweg, et al., 2018). It is considered as a non-nutritive sweetener since it is not metabolized by the human body (Wyrobnik, et al., 2009) and likely also not metabolized by the gut microbiome, as recently demonstrated by a study with 15 representative intestinal species (Schiessl, et al., 2021). Hence, 5-KF possesses promising traits as a new sweetener.

1.2.2 5-KF synthesis

5-KF was first described in 1934, when the diketone was synthesized chemically and called 5-fructonose (Micheel and Horn, 1934). Microbial synthesis of 5-KF was first reported in 1952 via a 2-fold oxidation of D-mannitol by *Acetobacter suboxydans* and in 1960 from D-fructose by different *Acetobacter* strains together with the sweet taste of the compound (Isbell and Karabinos, 1952, Terada, et al., 1960).

Later a membrane-bound fructose dehydrogenase was found to be responsible for this reaction (Ameyama, et al., 1981b) (1.2.5). Additionally, 5-KF was described as intermediate in kojic acid fermentation from sorbose by *Acetobacter* species (Terada, et al., 1961) and as intermediate formed from D-sorbitol in formation of the γ-pyrones kojic acid, 3-oxykojic acid and 5-oxymaltol by *A. suboxydans* (Sato, et al., 1967). The first patent for fermentative 5-KF production was filed in 1963 (Kinoshita and Terada, 1963).

While 5-KF synthesis first seemed limited to acetic acid bacteria, also two strains of *Pseudomonas convexa* were reported to convert L-sorbose to 5-KF (Longley and Perlman, 1972). Additionally, 5-KF production from L-sorbose via an L-sorbose oxidase was described for the Basidiomycete *Trametes sanguinea* (Yamada, et al., 1966b) and by the flavin adenine dinucleotide-(FAD)-dependent pyranose oxidase of the Basidiomycete *Peniophora gigantea* (Danneel, et al., 1993). Immobilized *P. gigantea* pyranose oxidase was described in a lab-scale conversion of L-sorbose to 5-KF (Huwig et al. 1994), and an engineered *P. gigantea* pyranose oxidase was shown to convert L-sorbose to 5-KF more efficiently (Schneider, et al., 2012). Enzymatic synthesis of 5-KF was achieved from fructose-6-phosphate in a transaldolase reaction with hydroxy pyruvic

aldehyde (Grazi, et al., 1962). An overview of the different microbial and enzymatic formation and degradation possibilities is shown in Figure 4.

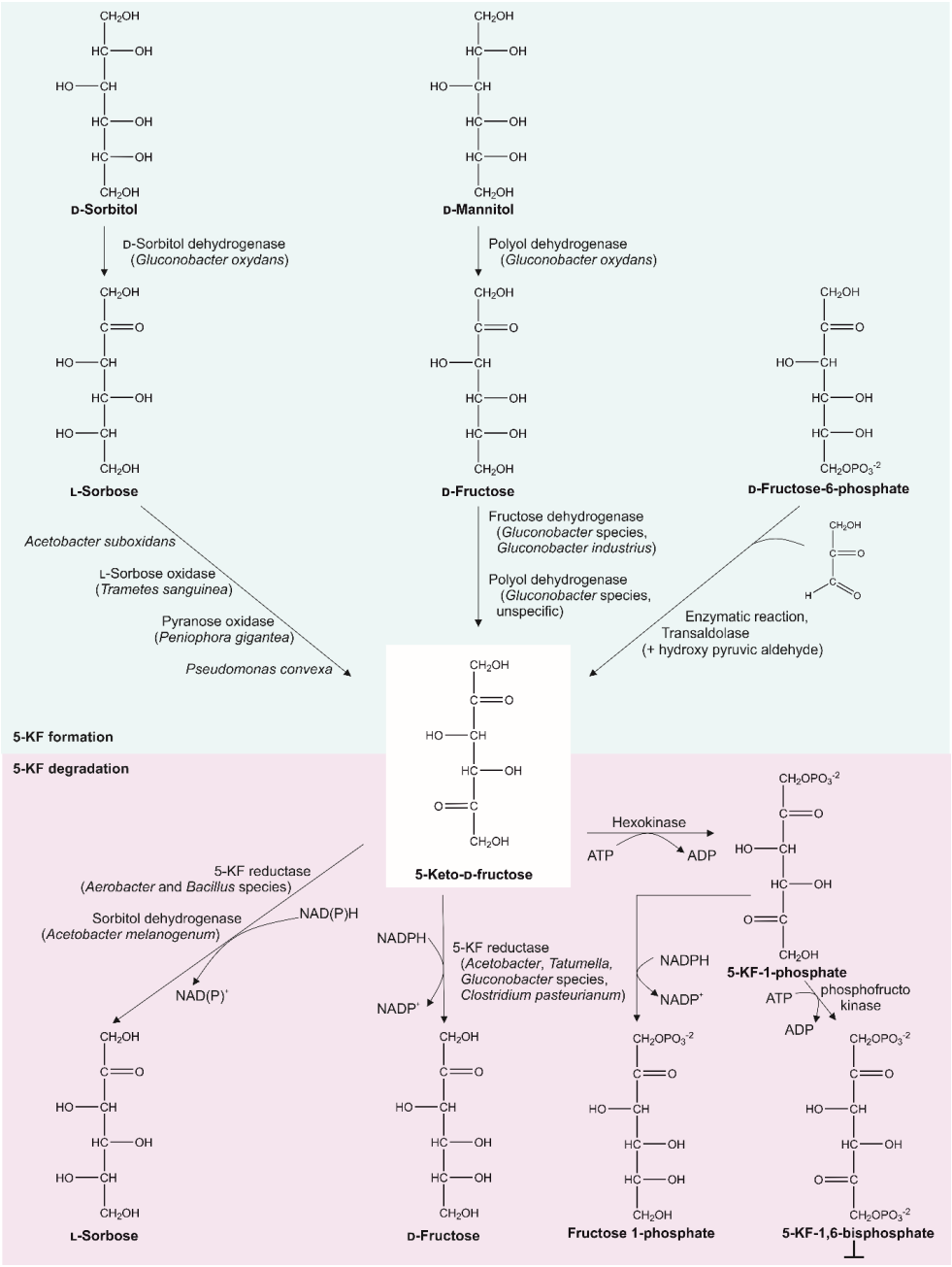

Figure 4 Overview on microbial and enzymatic formation and degradation of 5-KF. Depicted are 5-KF formation from different substrates (upper panel) and different products starting from 5-KF (lower panel). Responsible microorganisms and enzymes reported in literature are indicated.

1.2.3 5-KF degradation

After discovery of microbial 5-KF production an enzyme for 5-KF degradation, a 5-KF reductase from *Acetobacter albidus* IFO 3250 was described to catalyze the nicotinamide adenine dinucleotide phosphate (NADPH)-dependent reaction of 5-KF to fructose (Aida and Yamada, 1964). Further 5-KF reductases were later identified in *Erwinia citreus*, *Gluconobacter cerinus*, *Acetobacter melanogenum*, *Gluconobacter industrius*, *Tatumella morbirosei*, *G. oxydans* 621H, *G. japonicus* LMG 26773, *G. japonicus* LMG 1281, and *Clostridium pasteurianum*. The reductases enable the strains to use 5-KF as carbon and energy source (Avigad, et al., 1966, Sasajima and Isono, 1968, Englard and Avigad, 1975a, Ameyama, et al., 1981a, Schrimsher, et al., 1988, Schiessl, et al., 2021). Only recently, the 5-KF reductase of *Gluconobacter* sp. CHM43 was characterized and classified as shikimate reductase family member (Nguyen, et al., 2021b). Another type of NADPH-dependent 5-KF reductases, yielding L-sorbose instead of fructose, initially found in baker's yeast, was detected in *Bacillus subtilis* var. *aterneum*, *Aerobacter cloacae*, *Bacillus subtilis* 168-2, *Proteus vulgaris*, *Aerobacter aerogenes*, *Bacillus megaterium*, *Bacillus brevis* 9999, and a *Corynebacterium* sp. mutant (Englard, et al., 1970, Englard and Avigad, 1975b, Yagi, et al., 1989). An nicotinamide adenine dinucleotide (NADH)-dependent activity reducing 5-KF to sorbose was described for a sorbitol dehydrogenase of *A. melanogenum* (Sasajima and Isono, 1968).

Direct phosphorylation of 5-KF at C_1 was described for a yeast hexokinase, yielding a mono-phosphate ester. The following reduction with a *G. cerinus* NADPH-dependent 5-KF reductase resulted in fructose-1-phosphate (Avigad and Englard, 1968). 5-KF-1-phosphate could also be further phosphorylated by yeast phosphofructokinase to yield 5-KF-1,6-bisphosphate, which competitively inhibited fructose-1,6-bisphosphate aldolase and fructose l,6-diphosphatase for fructose-1,6-bisphosphate (Avigad and Englard, 1974).

For *G. cerinus* IFO 3267, containing an endogenous fructose dehydrogenase, coexistence of fructose oxidation and 5-KF reduction was shown by isotope labeling. Continuous fructose oxidation and 5-KF reutilization were postulated to play a role in $NADP^+$ regeneration. This hypothesis was supported with a mutant without fructose oxidation activity that showed poor growth on fructose as sole carbon source and better growth upon 5-KF addition (Mowshowitz, et al., 1974a, Mowshowitz, et al., 1974b).

1.2.4 Chemical structures of 5-KF

Regarding the structure of 5-KF, first a hemiacetal form for both carbonyl groups (Figure 5A) was proposed according to spectrometric analysis (Avigad and Englard, 1965). Subsequently the 5-keto-D-fructose structure (D-threo-2,5-hexudiolose) with the second carbonyl group at C_5 was confirmed with tritiated fructose and stereospecificity of the 5-KF reductase. Also the internal hemiacetal form was confirmed by a molecular model and the earlier suggested 6-aldo-D-fructose form, reported by Weidenhagen and Bernsee (1960) was refuted (Englard, et al., 1965).

X-ray analysis and ^{13}C nuclear magnetic resonance (NMR) spectroscopy of the crystalline form revealed a dimer of a furanose and a pyranose form, linked by C-O-C bonds (Figure 5B) (Hansen, et al., 1976, Brewer, et al., 1982). NMR analysis of 5-KF in dimethyl-d_6 sulfoxide showed a spirane dimer of one furanose and one pyranose ring, like the crystalline structure, while 5-KF in D_2O showed in more than 95% a β-pyranose form with a hydrated 5-ketogroup, forming a *gem*-diol (Figure 5C), while only about 2% of 5-KF were found in the β-furanose form (Figure 5D) (Blanchard, et al., 1982). The β-5-keto-D-fructopyranose *gem*-diol hydrate form was also confirmed by a more recent NMR analysis (Herweg, et al., 2018, Siemen, et al., 2018).

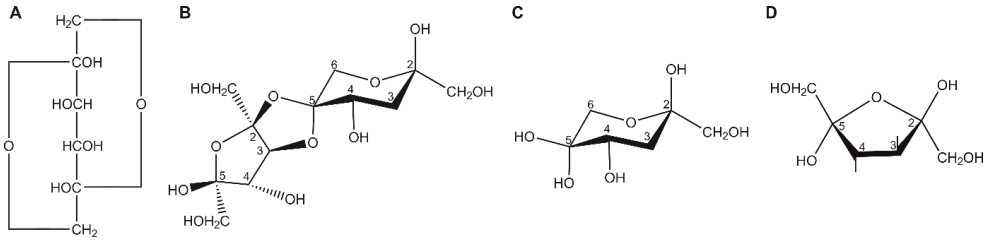

Figure 5 Structures of 5-KF. Depicted are the first proposed hemiacetal form (A), the dimeric form of a furanose and a pyranose form, linked by C-O-C bonds (B), the monomeric pyranose C_5 *gem*-diol hydrate found in aquatic solution (C) and the monomeric 2β,5α-furanose form (D). Structures adapted from Brewer, et al. (1982), Blanchard, et al. (1982) and (Avigad and Englard, 1965)

1.2.5 Membrane-bound fructose dehydrogenase and its application in 5-KF production

5-KF can be produced by fructose oxidation via the membrane-bound fructose dehydrogenase (Fdh, EC 1.1.99.11). D-Fructose dehydrogenase activity was first described in 1966 for the particulate fraction (membrane fraction) of *G. cerinus* var. *ammoniacus* ASAI IFO 3267. The oxidation was described to be NAD- and NADP- independent and 2,6-dichlorophenolindophenol (DCPIP) was found as most effective artificial electron acceptor (Yamada, et al., 1966a).

In 1981 Fdh was first purified from the membrane fraction of *G. industrius* IFO 3260. This strain was chosen because it showed the highest Fdh activity among various tested *Gluconobacter* spp. The characterization showed three components, a dehydrogenase subunit, a cytochrome *c* subunit and a third subunit with unknown function. An acidic pH optimum of 4.0-4.5, a temperature optimum of 25 °C, a strong substrate specificity for fructose, and the unsuitability of NADH, NADPH and oxygen as electron acceptors, were reported (Ameyama, et al., 1981b). In 2013 the Fdh of *G. japonicus* NBRC 3260 (formerly *G. industrius* IFO 3260), was purified and further characterized (Kawai, et al., 2013). The genes encoding the Fdh subunits were identified and sequenced based on the N-terminal amino acid sequence of the large subunit FdhL. The *fdhSCL* genes were found in a polycistronic operon, encoding a small (18 kDa), a cytochrome *c* (51 kDa), and a large subunit (68 kDa). This confirmed the three subunits reported from the first

purification. The operon starts with a TTG start codon for *fdhS*. Exchange of the TTG to an ATG start codon significantly increased Fdh activity in the heterologous host *G. oxydans* (Kawai, et al., 2013). FdhC has three CXXCH motifs for heme binding and in FdhL the FAD binding motif GXGXXG was found. Covalent binding of three heme *c* moieties and one FAD was shown experimentally (Kawai, et al., 2013). The small subunit FdhS was predicted to have a Tat signal peptide and for the cytochrome *c* subunit FdhC a Sec signal peptide was predicted. No signal peptide was found for the large subunit FdhL. Since FdhL contains covalently bound FAD, a co-secretion with the small subunit via the Tat-pathway was proposed. Expression of only *fdhSL* showed that the cytochrome *c* subunit is the membrane-anchor of the enzyme, links the Fdh complex to the respiratory chain and is responsible for ubiquinone reduction (Kawai, et al., 2013). A schematic overview of FdhSCL is shown in Figure 6.

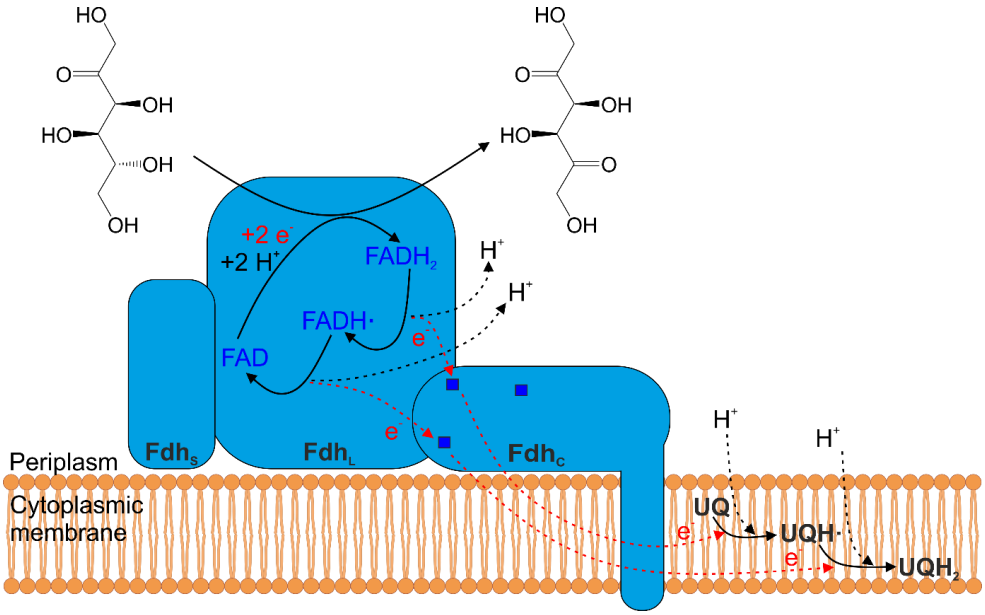

Figure 6 Schematic overview of the membrane-bound fructose-dehydrogenase. Fructose is oxidized in the periplasm to 5-KF via the heterotrimeric membrane-bound fructose dehydrogenase complex (Fdh), consisting of a small (FhdS), a cytochrome *c* subunit (FhdC) with three hemes *c* (blue boxes) and a large subunit with a covalently bound FAD as prosthetic group. The electrons and protons are transferred to FAD, resulting in reduced $FADH_2$. The electrons are each transferred to a heme *c*, while the protons are released to the periplasm. An FADH· semiquinone is formed as intermediate. The electrons from the hemes *c* are transferred to ubiquinone (UQ) together with protons from the periplasm, forming a semiquinone radical (UQH·). The formed ubiquinol (UQH2) is regenerated in the respiratory chain, using oxygen as electron acceptor, yielding one water molecule per fructose molecule oxidized.

Fdh has a high specificity towards D-fructose and can be used to quantify D-fructose amounts down to 0.01 µmol (Ameyama, et al., 1981b). For example, a diagnostic colorimetric assay applying Fdh for the exact determination of serum D-fructose has been described (Hui, et

al., 2009). With Fdh in direct electron transfer (DET) electrodes, D-fructose can directly transfer electrons to the electrode. These electrodes can function as electrochemical biosensors for absolute fructose quantification without calibration via the coulometric method, since all measured fructose is converted into electric charge in the coulometric biosensor (Kamitaka, et al., 2006, Tsujimura, et al., 2009). The direct electron transfer from Fdh to the electrodes without mediator is facilitated by heme *c* in FdhC (Kawai, et al., 2014). Another possible application of Fdh was demonstrated as part of an enzyme cascade in a biofuel cell. Fdh together with an invertase and a glucose oxidase in a ferrocene-modified polymer layer on a carbon electrode, paired with an air breathing platinum cathode can be used to generate an electric current from sucrose. Biofuel cells like these are researched as potential power source for small electronic devices (Hickey, et al., 2013). Furthermore, Fdh was used as a model membrane-bound enzyme immobilized in liquid crystalline cubic mesophases, where it remains active for several days, allowing good stability for different applications of immobilized Fdh. For example the aforementioned biosensor or biofuel cell are applications where the immobilization method could increase the lifetime (Sun, et al., 2016). This work, however, focuses on the use of Fdh in 5-KF production.

Previous studies expressed *fdhSCL* of *G. japonicus* IFO 3260 heterologously in *Gluconobacter oxydans*, a classic host for periplasmic oxidation instead of using the natural host *G. japonicus* (Herweg, et al., 2018, Siemen, et al., 2018). The genome sequence of *G. japonicus* IFO 3260 is not yet available and *G. japonicus* has not yet been extensively studied, while *G. oxydans* is a reasonably characterized host, already applied in industry since many decades (see 1.3). Heterologous *fdhSCL* expression in *G. oxydans* was shown to be beneficial compared to homologous expression in the natural host (Kawai, et al., 2013). Heterologous plasmid-based *fdhSCL* expression in *G. oxydans* 621H resulted in high 5-KF/fructose yields and product titers of almost 500 g/L were achieved in a fed-batch process (Herweg, et al., 2018, Siemen, et al., 2018). More recently, 5-KF production has also been described with a natural host. D-Mannitol was oxidized to D-fructose and then further oxidized to 5-KF by *Gluconobacter frateurii* CHM 43 (Adachi, et al., 2020).

1.3 *Gluconobacter oxydans*

The genus *Gluconobacter* was first described in 1935, comprising some previous *Acetobacter* strains (Asai, 1935, Gupta, et al., 2001), and *Gluconobacter oxydans* is the type species (Sievers and Swings, 2015). *G. oxydans* is a Gram-negative acetic acid bacterium belonging to the alphaproteobacteria. The ellipsoidal to rod-shaped cells are obligately aerobic and use oxygen as terminal electron acceptor (Gupta, et al., 2001, Sievers and Swings, 2015). *G. oxydans* is naturally found in sugary niches like fruits and flowers. It can live in acidic and highly osmotic sugar-rich habitats (Gupta, et al., 2001, Sievers and Swings, 2015, Zahid, et al., 2015).

G. oxydans has a special carbon metabolism that is characterized by its membrane-bound dehydrogenases with their catalytic center located in the periplasm (see 1.3.1). The various dehydrogenases are also the reason for *G. oxydans*' application in industrial biotechnology (Gupta, et al., 2001, Deppenmeier, et al., 2002). It's oxidation abilities are used for example in the production of dihydroxyacetone from glycerol via the membrane-bound glycerol/polyol dehydrogenase (mSldAB) (Hekmat, et al., 2003, Gätgens, et al., 2007), and for oxidation of D-sorbitol to L-sorbose via mSldAB in vitamin C production (Reichstein and Grüssner, 1934, Bremus, et al., 2006), and for oxidation of 1-amino-1-deoxy-D-sorbitol to 6-amino-6-deoxy-L-sorbose, likewise catalyzed by mSldAB as step in production of miglitol, an antidiabetic drug (Schedel, 2000, Ke, et al., 2019).

The 2.7 Mbp genome of *G. oxydans* 621H, an often used and well characterized strain, that was also used as strain background in this work, was sequenced in 2005 and resequenced in 2017 (Prust, et al., 2005, Kranz, et al., 2017). The genome sequence facilitated strain optimization via directed genetic modifications and allowed deeper insights into the strain's metabolism and physiology (Deppenmeier and Ehrenreich, 2009).

Genetic engineering of *G. oxydans* is possible since plasmid systems for homologous recombination, based on either *upp*- or *codBA*-counter selection, are available (Kostner, et al., 2013, Peters, et al., 2013a). Plasmid-based expression is possible with the broad host range vector pBBR1 (Kovach, et al., 1995). Different native promotors, either of selected membrane-bound dehydrogenases (Mientus, et al., 2017) or of ribosomal proteins (Kallnik, et al., 2010) with different strength are described for expression (Fricke, et al., 2021a). While those native promotors were mostly constitutive or repressed by glucose, only recently the first inducible promotor systems have been described for heterologous expression in *G. oxydans* (Fricke, et al., 2020, Fricke, et al., 2021b). So far, knowledge on regulation in *G. oxydans* is very limited, but is further being investigated (Hanke, et al., 2012, Li, et al., 2016, Schweikert, et al., 2021).

1.3.1 Membrane bound dehydrogenases in *G. oxydans*

G. oxydans possesses various membrane-bound dehydrogenases with periplasmic activity that are bound to the cytoplasmic membrane and linked to the respiratory chain. The dehydrogenases allow regio- and stereoselective incomplete oxidation of various sugars, alcohols, and polyols. This direct oxidation or non-phosphorylative pathway is sometimes called oxidative fermentation and needs no substrate uptake into the cytosol. Substrates and oxidation products only need to pass the outer membrane via porins to enter the periplasmic space (Deppenmeier, et al., 2002, Adachi, et al., 2003). There are two types of membrane-bound dehydrogenases, quinoproteins and flavoproteins, that have either pyrroloquinoline quinone (PQQ) or covalently bound FAD as prosthetic groups. These prosthetic groups transfer the electrons to ubiquinone. Ubiquinol is reoxidized by ubiquinol oxidases, which transfer the electrons to molecular oxygen forming

water. Hence, the membrane-bound dehydrogenases are linked to the respiratory chain, making oxygen essential for periplasmic oxidation (Matsushita, et al., 1994).

The genome sequence and experiments with a series of multideletion strains revealed that *G. oxydans* 621H has nine different membrane-bound dehydrogenases with a periplasmic active center (Prust, et al., 2005, Peters, et al., 2013b). With regard to the number of accepted substrates, the alcohol dehydrogenase mADH and the polyol dehydrogenase mSldAB are the most important dehydrogenases (Peters, et al., 2013b, Mientus, et al., 2017). The quinoprotein mSldAB as major polyol dehydrogenase in *G. oxydans* 621H oxidizes for example glycerol, D-sorbitol and D-mannitol (Matsushita, et al., 2003, Peters, et al., 2013b). For an mSldAB homolog, the membrane-bound glycerol dehydrogenase of *Gluconobacter thailandicus*, the oxidation of fructose to 5-KF has been described as additional reaction (Ano, et al., 2017).

1.3.2 The respiratory chain of *G. oxydans*

The primary, membrane-bound dehydrogenases oxidize different substrates and transfer the electrons via ubiquinone to the respiratory chain, where the terminal oxidases transfer the electrons to the terminal electron acceptor oxygen to generate energy for growth (Matsushita, et al., 1994). Besides a non-proton-translocating NADH:ubiquinone oxidoreductase (*ndh*, GOX1675), the respiratory chain of *G. oxydans* 621H contains two quinol oxidases, a cytochrome *bd* oxidase (*cydAB* genes, GOX0278-0279) and a cytochrome bo_3 oxidase (*cyoBACD*, GOX1911-1914) (Prust, et al., 2005, Richhardt, et al., 2013b). The cyanide insensitive *bd* oxidase has a lower oxygen affinity but a higher V_{max}, compared to the bo_3 oxidase (Miura, et al., 2013). In deletion strains and overexpression experiments of both oxidases, the bo_3 oxidase was found to play a key role in the respiratory chain of *G. oxydans* (Richhardt, et al., 2013b). In addition to the terminal oxidases, genes for a cytochrome bc_1 complex (*qcrABC*, GOX0565-0567) and a soluble cytochrome c_{522} (*cycA*, GOX0258) were found in the genome, however, no cytochrome *c* oxidase is present, which could transfer the electrons from the bc_1 complex to oxygen (Prust, et al., 2005, Richhardt, et al., 2013b). Nevertheless, the bc_1 complex was found to play a physiological role, at least at low pH (Hanke, et al., 2012). Besides oxygen availability, in *G. oxydans* the pH can influence the regulation of the respiratory chain. It was found that the *bd* oxidase genes are about twofold upregulated at an acidic pH of 4.0 compared to a pH of 6.0, leading to an increased cyanide insensitivity of the respiratory chain at acidic pH (Matsushita, et al., 1989, Hanke, et al., 2012). An overview of the respiratory chain in *G. oxydans* is shown in Figure 7.

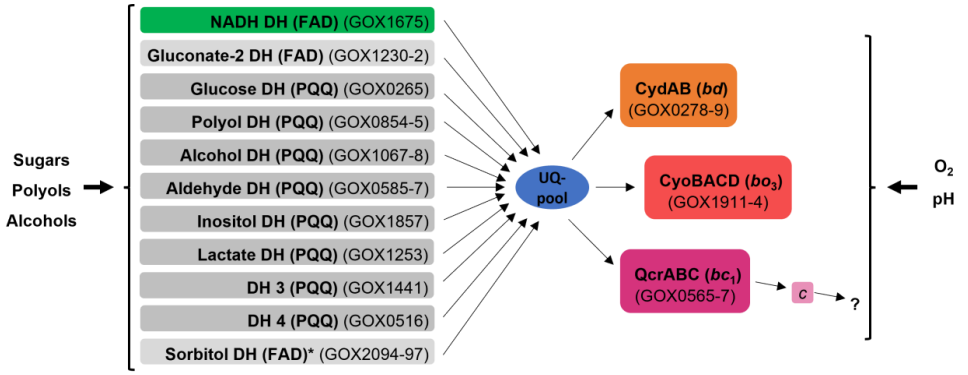

Figure 7 Scheme of the respiratory chain of *G. oxydans* 621H. Electrons are transferred to ubiquinone (UQ) by the membrane-bound dehydrogenases (DH) that are either FAD- or PQQ-dependent and by the NADH dehydrogenase. Ubiquinol is subsequently regenerated by the terminal *bd* and bo_3 quinol oxidases. Whether the cytochrome bc_1 complex is also involved is unclear, as no cytochrome *c* oxidase is present. DH 3 and DH 4 are uncharacterized PQQ-dependent dehydrogenases of a yet unknown substrate spectrum (Peters, et al., 2013b). * The sorbitol dehydrogenase is inactive due to a stop codon mutation in *G. oxydans* 621H. The dehydrogenases oxidize available sugars, polyols, or alcohols. Expression of the oxidase genes is influenced by the oxygen availability and the pH. (Locus tags for the *G. oxydans* 621H genome are indicated.)

1.3.3 Carbon metabolism in *G. oxydans*

G. oxydans has a special carbon metabolism, as it lacks the Embden-Meyerhoff pathway (EMP) due to the absence of phosphofructokinase and has an incomplete tricarboxylic acid (TCA) cycle since it lacks succinyl-CoA synthetase, and succinate dehydrogenase (Greenfield and Claus, 1972, Prust, et al., 2005, Deppenmeier and Ehrenreich, 2009). Instead, it uses the pentose phosphate pathway (PPP) and the Entner–Doudoroff pathway (EDP). In a study with deletion strains of key enzymes of either pathways, the PPP was shown to be the most important pathway for cytoplasmic glucose utilization (Richhardt, et al., 2013a). However, only a minor portion of the available sugar and sugar alcohol substrates is processed through the cytoplasmic carbon metabolism, as the majority is incompletely oxidized in the periplasm and subsequently released to the medium as end products, characterizing the special metabolism of *G. oxydans*. In a ^{13}C flux analysis it was revealed that in the first growth phase of glucose-grown *G. oxydans* only 10 % of the glucose enters the cytoplasm, of which a majority is directly oxidized by a cytosolic glucose dehydrogenase to gluconate and only a small portion is phosphorylated. Also, some of the gluconate formed in the periplasm by the membrane-bound glucose dehydrogenase is transported into the cytoplasm, where a small part is phosphorylated. Overall, only a minor portion of the initial glucose enters the cytoplasm and even less is processed via the PPP, which was shown to be the most frequented pathway (Hanke, et al., 2013). While the versatile oxidation activities are key to the industrial applications of *G. oxydans*, incomplete oxidation is a disadvantage with respect to biomass yield, which is only in the range of 0.1 g/g glucose and thus much lower than the one of bacteria like *E. coli* (0.5 g/g) (Ng, 1969, Krajewski, et al., 2010, Kiefler, et al., 2017).

1.3.4 *G. oxydans* IK003.1

The engineered strain *G. oxydans* IK003.1 was used in this work. It is based on the 621 H wild type and was optimized towards an improved biomass yield when grown on glucose (Kiefler, et al., 2017). In the *G. oxydans* wild type the majority of available glucose is oxidized by the membrane-bound glucose dehydrogenase GdhM to gluconate, which can be further oxidized to 2-ketogluconate (Hanke, et al., 2013). This causes an inefficient biomass formation, which is represented by the low biomass yield of 0.1 g cell dry weight/g glucose. To optimize the biomass yield, direct glucose oxidation was one of the targets for strain engineering by Kiefler, et al. (2017). In total, the soluble glucose dehydrogenase gene *gdhS*, the pyruvate decarboxylase gene *pdc* and the membrane-bound glucose dehydrogenase gene *gdhM* were replaced by the *Acetobacter pasteurianus* succinate dehydrogenase genes *sdhCDAB* and flavinylation factor gene *sdhE*, the NADH dehydrogenase gene *ndh* from *G. oxydans* DSM3504 and the *Gluconacetobacter diazotrophicus* succinyl-CoA-synthetase genes *sucCD*, respectively. By this approach, direct glucose oxidation was prevented to increase the biomass yield by avoiding glucose loss. The incomplete TCA cycle was complemented with the aim to allow a complete oxidation of glucose in the cytoplasm for a more efficient biomass formation. However, this was not achieved by the expression of the missing TCA cycle genes, since pyruvate was accumulated by the strain instead of acetate, indicating a bottleneck in pyruvate oxidation to acetyl-CoA. Nevertheless, the metabolic engineering approaches enabled an increase of the biomass yield of strain IK003.1 by 60 % compared to the reference strain *G. oxydans* 621H Δ*upp* (Kiefler, et al., 2017).

1.4 *Pseudomonas putida*

Pseudomonas putida is a ubiquitous Gram-negative soil and plant root-associated bacterium of the group of gammaproteobacteria (Palleroni, 2015). It can adapt to physicochemical and nutritional niches and shows outstanding tolerance towards organic solvents (Nelson, et al., 2002, Blank, et al., 2008, Nikel, et al., 2014). The most studied strain is *P. putida* KT2440, which was derived from *P. putida* mt-2 (formerly *Pseudomonas arvilla*), a *m*-toluate degrading soil isolate. Strain KT2440 lacks the pWW0 plasmid, responsible for degradation of aromatic substrates (Murray, et al., 1972, Bagdasarian, et al., 1981, Nikel and de Lorenzo, 2018). Revelation of the 6.18 Mbp genome sequence of strain KT2440 in 2002 and its revised version in 2016 allowed systemic insights into its metabolism and demonstrated the non-pathogenic character of the strain, as it lacked key virulence factors of the pathogenic close relative *Pseudomonas aeruginosa* (Nelson, et al., 2002, Belda, et al., 2016). *P. putida* KT2440 is classified as host-vector system safety level 1 (HV-1) by the FDA, meaning it is safe to work with (Kampers, et al., 2019).

Due to its versatile metabolism and tolerance towards xenobiotics *P. putida* is an interesting and well-studied organism. Consequently, a big toolbox including different modification techniques and expression systems is available (Loeschcke and Thies, 2015,

Martínez-García and de Lorenzo, 2017, Nikel and de Lorenzo, 2018). Besides a system for homologous recombination (Martínez-García and de Lorenzo, 2011), a system for site-directed Tn*7*-based transposon-integration (Zobel, et al., 2015) for chromosomal integration in *P. putida* is available. Additionally, gene repression via CRISPR interference is possible (Tan, et al., 2018). Plasmid-based expression is possible with various vector backbones and a multitude of inducible promoter systems (Martínez-García and de Lorenzo, 2017). Of special interest for 5-KF production with *P. putida* from alternative substrates is the fact that different examples of enzyme surface display for either the wild type, engineered or surfome-streamlined *P. putida* are reported in literature (Lee, et al., 2005, Martínez-García, et al., 2020, Tozakidis, et al., 2020). The reduction of the surfome, surface exposed proteins which are for example involved in attachment and biofilm formation, was reported to improve the suitability of *P. putida* for heterologous protein anchoring to the outer membrane (Martínez-García, et al., 2020)

P. putida has not only a potent endogenous metabolism but is also an interesting *chassis* for heterologous pathways. Among others, the production of rhamnolipids, the terpenoid zeaxanthin, prodigiosin, aromatic products like phenol and *p*-coumaric acid with *P. putida* was shown (Wierckx, et al., 2005, Loeschcke, et al., 2013, Loeschcke and Thies, 2015, Calero, et al., 2016, Nikel and de Lorenzo, 2018, Tiso, et al., 2020). Moreover, the solvent tolerance of *P. putida* and its ability to withstand industrial-scale stress conditions make it an excellent industrial host (Ankenbauer, et al., 2020). Currently, rhamnolipids and different Polyhydroxyalkanoates (PHAs) are already industrially produced with *P. putida* and the production of furandicarboxylic acid (FDCA), a building block for the recyclable polymer polyethylene furanoate (PEF) is planned to start in 2023 (Poltronieri and Kumar, 2017, Tiso, et al., 2020, Weimer, et al., 2020, Avantium, 2021). In addition to the broad product spectrum, the utilization of lignin- and plastic-derived compounds by engineered *P. putida* strains is of interest for sustainable biotechnological processes (Kohlstedt, et al., 2018, Li, et al., 2020, Ackermann, et al., 2021, Elmore, et al., 2021, Tiso, et al., 2021).

For this work, however, the recently shown xylonate production with *P. putida* via periplasmic oxidation by its native membrane-bound glucose dehydrogenase (Dvořák, et al., 2020) is the most relevant application of the versatile host since it demonstrates the ability of *P. putida* for product formation via periplasmic oxidation.

1.4.1 Membrane bound dehydrogenases in *P. putida*

Like *G. oxydans*, *P. putida* possesses a membrane-bound PQQ-dependent glucose dehydrogenase (Gcd), which plays an important role in glucose metabolization (del Castillo, et al., 2007, Nikel, et al., 2015). The gluconate formed by glucose oxidation plays an important role in the natural habitat of *P. putida*, the soil, where excreted gluconate can solubilize phosphate from poorly soluble calcium mineral phosphates like hydroxyapatite or tricalcium phosphate, promoting plant

growth (Castagno, et al., 2011, An and Moe, 2016). In glucose metabolization it also plays an important physiological role for the cells themselves, since a major portion of the hexose is first oxidized, subsequently taken up as gluconate and phosphorylated to phosphogluconate (Nikel, et al., 2015, Kohlstedt and Wittmann, 2019).

Gluconate can also be oxidized via a second membrane-bound dehydrogenase, which *G. oxydans* and *P. putida* have in common, gluconate dehydrogenase (Gad). The enzyme consists of three subunits, encoded by PP_3382-3384, a cytochrome *c* subunit, which is predicted to be membrane associated and have a Sec signal peptide, a large FAD-containing subunit without signal peptide, and a small subunit with a Tat signal peptide. It oxidizes gluconate to 2-ketogluconate (Kumar, et al., 2013, Winsor, et al., 2016). Regarding its subunits and prosthetic groups, Gad resembles *G. japonicus* Fdh.

1.4.2 The respiratory chain of *P. putida*

The branched respiratory chain of *P. putida* contains a proton-pumping complex type I NADH dehydrogenase, two non-proton-pumping type II NADH dehydrogenases, two ubiquinol oxidases (cytochrome bo_3 and a cyanide-insensitive *bd*-type oxidase CIO), a cytochrome bc_1 complex, and three cytochrome *c* oxidases (cytochrome aa_3 and two cytochrome cbb_3 oxidases, cbb_3-1 and cbb_3-2) (Nelson, et al., 2002, Morales, et al., 2006, Ebert, et al., 2011). An overview of the respiratory chain of *P. putida* is shown in Figure 8.

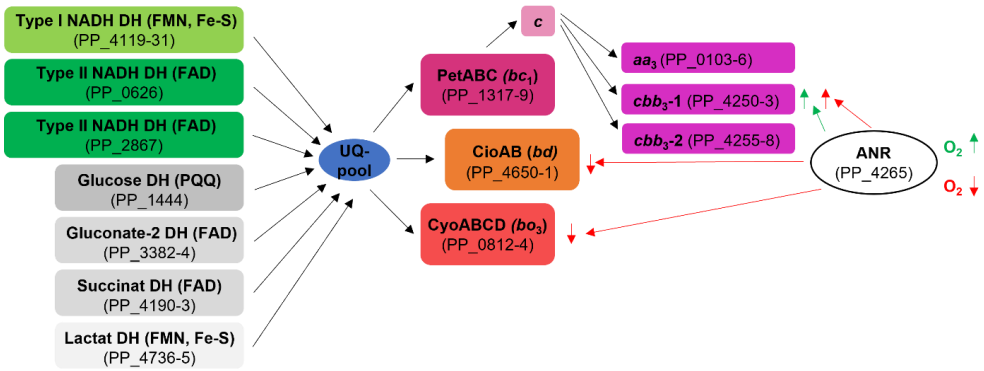

Figure 8 Scheme of the respiratory chain of *P. putida*. Electrons are transferred to ubiquinone (UQ) by the membrane-bound glucose dehydrogenase (DH), gluconate DH, succinate DH, lactate DH and by the NADH dehydrogenases. Ubiquinol is subsequently regenerated by the terminal cytochrome *bd* and cytochrome bo_3 quinol oxidases or the cytochrome bc_1 complex, which further transfers the electron via cytochrome *c* to the terminal cytochrome aa_3 or cytochrome cbb_3 oxidases. Expression of the oxidases is regulated by the global ANR regulator depending on the oxygen availability. During exponential phase or at high oxygen tension (green arrows), ANR upregulates expression of the cbb_3-1 oxidase and in early stationary phase or during oxygen limitation (red arrows) ANR downregulates expression of the *bd* and bo_3 oxidases and upregulates expression of the cbb_3-1 oxidase (Ugidos, et al., 2008). Locus tags for the *P. putida* KT2440 genome (Belda, et al., 2016) are indicated.

Expression of the bo_3, *bd* and ccb_3-1 terminal oxidases in *P. putida* was shown to be coordinated by the oxygen-responsive global regulator ANR (Ugidos, et al., 2008). ANR is one of three FNR-family proteins in *P. putida*, each with a different O_2 sensitivity, modulating O_2-responsive gene expression (Ibrahim, et al., 2015).

1.4.3 Carbon metabolism in *P. putida*

The carbon metabolism of *P. putida* was predominantly analyzed for the commonly used hexose glucose. Glucose enters the periplasm via the sugar-specific porin OprB (Saravolac, et al., 1991, del Castillo, et al., 2007, Coines, et al., 2019). From the periplasm glucose can either be directly taken up into the cytoplasm via the ABC transporter GtsABCD, where it is subsequently phosphorylated to glucose 6-phosphate by the glucokinase Glk or be processed via periplasmic oxidation. A major portion of glucose is oxidized to gluconate by the membrane-bound glucose dehydrogenase Gcd. Gluconate is either taken up into the cytoplasm via the gluconate transporter Gnt and then phosphorylated by the gluconokinase GnuK or it is further oxidized in the periplasm to 2-ketogluconate by the membrane-bound gluconate dehydrogenase Gad. 2-Ketogluconate is then taken up by the 2-ketogluconate transporter KguT and subsequently phosphorylated by the 2-ketogluconate kinase KguK (del Castillo, et al., 2007). The phosphorylated metabolites then enter the central carbon metabolism. Flux studies showed that direct glucose uptake only plays a minor role, while the initial oxidation to gluconate and subsequent gluconate uptake is the major route (Nikel, et al., 2015, Kohlstedt and Wittmann, 2019). *P. putida* KT2440 encodes the needed enzymes for the EDP, the PPP and an incomplete EMP, lacking the 6-phosphofructo-1-kinase (Pfk) (Nelson, et al., 2002, Belda, et al., 2016). A combined cyclic, so called EDEMP cycle, using enzymes of all three routes was shown to be used by *P. putida* for glucose metabolization (Nikel, et al., 2015). Sugar processing via this route leads to high regeneration rates for NADPH, which can be interconverted to NADH by the soluble and the membrane-bound, proton-translocating pyridine nucleotide transhydrogenases (SthA and PntAB) (Nikel, et al., 2016, Kohlstedt and Wittmann, 2019). Additionally, the periplasmic glucose oxidation leads to an ATP surplus, compared to direct glucose uptake via GtsABCD. Only one ATP per glucose is needed for the phosphorylation of gluconate or 2-ketogluconate, while for the direct glucose uptake one ATP is needed for the transport and one for the phosphorylation. Together the high NAD(P)H and ATP regeneration likely support the organisms robustness (Ebert, et al., 2011, Nikel, et al., 2015, Kohlstedt and Wittmann, 2019).

For this work however, fructose is the more important carbon source. Fructose is taken up as fructose-1-phosphate via the only sugar phosphotransferase system (PTS) in *P. putida*. PTS^{Fru} consists of FruA, a fusion protein of EIIB-EIIC, and FruB, a fusion protein of EIIA-HPr-EI, encoded by the *fruBKA* operon, together with the 1-phosphofructokinase FruK (Velázquez, et al., 2007, Pflüger and de Lorenzo, 2008). *fruB* deletion strains cannot grow on fructose, indicating

that fructose can only be taken up via PTS^{Fru} (Velázquez, et al., 2007, Chavarría, et al., 2013). Fructose-1-phosphate is phosphorylated by FruK to fructose-1,6-bisphosphate, enabling further processing directly via the EMP, or after cleavage of one phosphate group by 1,6-bisphosphatase as fructose-6-phosphate via the EDP, and PPP (Sawyer, et al., 1977, Lessie and Phibbs, 1984, Velázquez, et al., 2007, Chavarría, et al., 2012). Regarding the uptake of the sole PTS sugar fructose via PTS^{Fru} in *P. putida* additionally some regulatory effects are important. The *fruBKA* operon is repressed by FruR, a catabolite repressor/activator (Cra) protein and fructose-1-phospate is needed as FruR effector to allow *fruBKA* expression (Chavarría, et al., 2014, Chavarría, et al., 2016). Cra additionally represses the expression of one glyceraldehyde-3-phosphate (GA3P) dehydrogenase (GAPDH) gene (PP_3443) and thus regulates the central carbon metabolism at the GA3P branching point. Upon fructose availability and effector binding, additional GAPHDH is available, ensuring efficient phosphoenolpyruvate (PEP) for PEP-dependent fructose uptake via PTS^{Fru} (Chavarría, et al., 2016). In addition to PTS^{Fru}, *P. putida* possesses a second PTS, PTS^{Ntr}. It was first believed to sense the balance between N and C in the cell, but was later shown to control various metabolic functions, and thus is a key regulatory device. Both PTSs were shown to be interconnected via exchange of phosphoryl-groups (Cases, et al., 2001, Pflüger and de Lorenzo, 2008, Chavarría, et al., 2012, Wolf, et al., 2015).

1.4.4 Heterologous sucrose metabolism in *P. putida*

In addition to glucose and fructose, for this work sucrose as cheap alternative carbon source is of importance. *P. putida* is naturally not able to metabolize the disaccharide, however, two engineering approaches with heterologous genes toward sucrose consumption in *P. putida* were reported so far. The *cscA* and *cscB* genes of *E. coli* W, encoding an invertase and a sucrose permease were expressed from plasmids or in Tn*5* transposon integration strains (Löwe, et al., 2017). While the reference strain without *cscAB* showed no growth with sucrose as sole carbon source, the strain with plasmid-based or transposon-integrated *cscAB* expression was able to grow with sucrose as sole carbon source. However, growth of the expression strain with sucrose was slower than growth of the reference strain with a combination of glucose and fructose. The expression of *cscA* alone was also shown to allow growth with sucrose as sole carbon source at a comparable growth rate and biomass yield, as with *cscAB*. CscA is a cytoplasmic enzyme, and sucrose should not be taken up into the cell without CscB since no sucrose specific porins or transporters are known in *P. putida*. The sucrose cleavage of the invertase CscA alone was explained with nonspecific leakage of the enzyme out of the cell, since a small portion of invertase activity was detected in the supernatant (Löwe, et al., 2017).

Improved growth on sucrose was shown when using the newly identified sucrose metabolism gene cluster of the close relative *Pseudomonas protegens* Pf-5. The *cscRABY* gene cluster (PFL_3236-3239), encodes a repressor, a sucrose hydrolase, a permease and a porin

(Löwe, et al., 2020). Plasmid-based expression of *cscRABY* allowed growth with sucrose as sole carbon source. The expression of *cscRAB*, without *cscY*, encoding a porin, was not sufficient to enable growth in M9 medium with sucrose as sole carbon source, suggesting a crucial role or the porin in sucrose consumption. However, *cscRAB* expressing cells from M9 precultures, compared to cells from LB precultures, were able to grow with sucrose as sole carbon source, despite lacking the CscY porin. This different behavior is explained with the difference of a glycolytic regime when grown in M9 medium with glucose as sole carbon source, compared to a gluconeogenetic regime in LB-grown cells, as these different lifestyles require a different composition of the outer membrane. The difference in precultures was shown to influence the permeability for sucrose, likely by altering the outer membrane composition. Overall, this study demonstrated the importance of porins for sucrose uptake when using an intracellular sucrose cleavage in *P. putida* (Löwe, et al., 2020).

1.5 Aims of this thesis

Plasmid-based 5-KF production with a heterologous *G. oxydans* strain expressing *fdhSCL* was already described in literature. For production of 5-KF as a food additive, antibiotic-free production would be desirable. Consequently, the first part of this thesis aimed at plasmid-free 5-KF production via chromosomally encoded Fdh. For *G. oxydans,* however, not many genomic integration sites were known since recent studies mainly focused on metabolic engineering with gene replacements. Therefore, criteria for the selection of integration sites should be defined, sites should be chosen based on the results of an RNAseq analysis (Kranz, et al., 2018), and the *G. japonicus fdhSCL* genes should then be integrated at the selected sites in the chromosome via homologous recombination. The resulting recombinant strains should then be tested for 5-KF production from fructose and the different integration sites compared with respect to their influence on *fdhSCL* expression and 5-KF production. The second aim was the use of alternative substrates like sucrose or starch for 5-KF production by employing surface-displayed heterologous enzymes (invertase, amylase, glucose isomerase) that convert these substrates to fructose. As model enzyme for establishing surface display in *G. oxydans*, amylase was selected.

Although *G. oxydans* is a well-established host for oxidative biotransformations, it has several disadvantages for industrial production, such as the low biomass yield, the need for complex media components, and the restricted molecular toolbox available. Hence, in the second part of this thesis, the possibility for 5-KF production with an alternative host lacking these disadvantages should be tested. For various reasons, the well-established workhorse *P. putida* was chosen as an attractive new host for 5-KF production. Suitable *fdhSCL* expression strains should be constructed and their efficiency for 5-KF production from fructose should be compared with the corresponding *G. oxydans* strains. Furthermore, the substrate spectrum for 5-KF synthesis should be extended to sucrose by expression of a heterologous invertase.

2 Results

The overarching aim of this thesis was the construction and characterization of strains of *Gluconobacter oxydans* and *Pseudomonas putida* for the efficient production of the natural sweetener 5-ketofructose (5-KF) from fructose and alternative substrates. The results were published in two original articles in peer-reviewed journals.

In the publication "Novel plasmid-free *Gluconobacter oxydans* strains for production of the natural sweetener 5-ketofructose" (Microbial Cell Factories (2020) 19:54) the generation and characterization of chromosomal *fdhSCL* integration strains based of *G. oxydans* IK003.1 was described. Four chromosomal integration sites for heterologous expression were selected. In three cases the *fdhSCL* genes were inserted into intergenic regions, whereas in one case the *fdhSCL* genes replaced a known defective gene in the chromosome. Integration of *G. japonicus fdhSCL* genes enabled plasmid-free 5-KF production with only slightly varying levels for the four different strains. As the 5-KF production rates were much lower than that of a strain with plasmid-borne *fdhSCL* genes, the double integration strain IK003.1::*fdhSCL*^{2} was constructed, which showed an approximately two-fold increased 5-KF production rate when compared to the single integration strains. RT-qPCR showed that different 5-KF production rates were related to different *fdh* expression levels in the respective strains. In cooperation with M.Sc. Svenja Battling at the Institute of Biochemical Engineering headed by Prof. Jochen Büchs at RWTH Aachen University, bioprocess optimization was performed for a selected *fdhSCL* integration strain. Overall, this study demonstrated the possibility for plasmid- and antibiotic-free 5-KF production with *G. oxydans*.

5-KF production from fructose and sucrose with *P. putida* as alternative host is described in the publication "Metabolic engineering of *Pseudomonas putida* for production of the natural sweetener 5-ketofructose from fructose or sucrose by periplasmic oxidation with a heterologous fructose dehydrogenase" (Microbial Biotechnology, doi: 10.1111/1751-7915.13913). Tn*7*-based genomic integration of the *G. japonicus fdhSCL* genes enabled *P. putida* to oxidize fructose to 5-KF. In a fed-batch fermentation high titers and yields of 5-KF were reached, comparable to the corresponding *G. oxydans* strain. Plasmid-based expression of the *G. japonicus inv1417* gene encoding an invertase enabled sucrose metabolization. With sucrose as substrate, production times almost comparable to fructose as substrate were reached and in a pulsed fed-batch fermentation high 5-KF concentrations comparable to the fructose fermentation were reached. In summary, this study established *P. putida* as an efficient alternative host for 5-KF production.

2.1 Novel plasmid-free *Gluconobacter oxydans* strains for production of the natural sweetener 5-ketofructose

Battling, S*., Wohlers, K.*, Igwe, C., Kranz, A., Pesch, M., Wirtz, A., Baumgart, M., Büchs, J., Bott, M. (2020). Microbial Cell Factories 19(1), 54
*Shared first author

Author contributions:

- SB designed and performed the characterization and optimization experiments in shake flasks with online monitoring (RAMOS), scale up and fermentation experiments, analyzed the data and drafted the manuscript. Figures 3, 4 and 5 resulted from these experiments.
- KW designed and constructed the four integration strains, performed the shake flask cultivations and the RT-qPCR experiment, analyzed the data, and drafted the manuscript. Figures 1, 2, 6 and 7 resulted from these experiments.
- CI performed the scale up experiments.
- AK selected the integration sites.
- MP performed some of the shake flask cultivations with online monitoring.
- AW set up HPLC method A.
- MBo, JB and MBa supervised the study, assisted in data interpretation, and participated in drafting the manuscript.
- Overall contribution KW: 40%

Battling *et al. Microb Cell Fact* (2020) 19:54
https://doi.org/10.1186/s12934-020-01310-7

Microbial Cell Factories

RESEARCH Open Access

Novel plasmid-free *Gluconobacter oxydans* strains for production of the natural sweetener 5-ketofructose

Svenja Battling[1†], Karen Wohlers[2†], Chika Igwe[1], Angela Kranz[2], Matthias Pesch[1], Astrid Wirtz[2], Meike Baumgart[2], Jochen Büchs[1*] and Michael Bott[2*]

Abstract

Background: 5-Ketofructose (5-KF) has recently been identified as a promising non-nutritive natural sweetener. *Gluconobacter oxydans* strains have been developed that allow efficient production of 5-KF from fructose by plasmid-based expression of the fructose dehydrogenase genes *fdhSCL* of *Gluconobacter japonicus*. As plasmid-free strains are preferred for industrial production of food additives, we aimed at the construction of efficient 5-KF production strains with the *fdhSCL* genes chromosomally integrated.

Results: For plasmid-free 5-KF production, we selected four sites in the genome of *G. oxydans* IK003.1 and inserted the *fdhSCL* genes under control of the strong P264 promoter into each of these sites. All four recombinant strains expressed *fdhSCL* and oxidized fructose to 5-KF, but site-specific differences were observed suggesting that the genomic vicinity influenced gene expression. For further improvement, a second copy of the *fdhSCL* genes under control of P264 was inserted into the second-best insertion site to obtain strain IK003.1::*fdhSCL*^{2}. The 5-KF production rate and the 5-KF yield obtained with this double-integration strain were considerably higher than for the single integration strains and approached the values of IK003.1 with plasmid-based *fdhSCL* expression.

Conclusion: We identified four sites in the genome of *G. oxydans* suitable for expression of heterologous genes and constructed a strain with two genomic copies of the *fdhSCL* genes enabling efficient plasmid-free 5-KF production. This strain will serve as basis for further metabolic engineering strategies aiming at the use of alternative carbon sources for 5-KF production and for bioprocess optimization.

Keywords: *Gluconobacter oxydans*, Sweetener, Chromosomal integration, 5-ketofructose, Fructose dehydrogenase

Background

The strictly aerobic acetic acid bacterium *Gluconobacter oxydans* contains at least eight membrane-bound dehydrogenases catalyzing the rapid chemo-, regio-, and stereoselective oxidation of sugars, alcohols, and polyols in the periplasm to organic acids, aldehydes, and ketones [1]. The resulting electrons are transferred via ubiquinone to the terminal cytochrome bo_3 oxidase [2] or a cyanide-insensitive *bd*-type oxidase [3], both of which reduce oxygen to water. Due to the distinctive properties of the membrane-bound dehydrogenases, *G. oxydans* has become an important workhorse for oxidative biotransformations in biotechnology [4–8]. The first industrial application of *G. oxydans* was in vitamin C production via the Reichstein-Grüssner process [9], where the sorbitol dehydrogenase catalyzes the oxidation of D-sorbitol to L-sorbose [10]. Other products whose synthesis

*Correspondence: jochen.buechs@avt.rwth-aachen.de; m.bott@fz-juelich.de
†Svenja Battling and Karen Wohlers contributed equally to this manuscript
[1] AVT-Biochemical Engineering, RWTH Aachen University, Forckenbeckstraße 51, 52074 Aachen, Germany
[2] IBG-1: Biotechnology, Institute of Bio- and Geosciences, Forschungszentrum Jülich, 52425 Jülich, Germany

involves *G. oxydans* include dihydroxyacetone [11] or the anti-diabetic drug miglitol [12, 13].

Due to the vigorous incomplete periplasmic substrate oxidation of *G. oxydans,* only a small fraction of the carbon source is taken up into the cytoplasm and enters the central carbon metabolism, which is characterized by an incomplete glycolysis and an incomplete tricarboxylic acid (TCA) cycle [14]. Glucose is metabolized predominantly via the oxidative pentose phosphate pathway and to some extent via the Entner–Doudoroff pathway [15]. Pyruvate is partly converted to acetate as final product by pyruvate decarboxylase and acetaldehyde dehydrogenase [16]. As a consequence of the small fraction of substrate metabolized within the cell, the biomass yield of *G. oxydans* is quite low (about 0.1 g cell dry weight/g glucose). As this causes increased costs for biomass synthesis, metabolic engineering was used to create *G. oxydans* strains with improved biomass yield on glucose by reducing or avoiding its oxidation to gluconate [16, 17]. One of the resulting strains, IK003.1, which is derived from the parent strain 621H, lacks both the membrane-bound and the soluble glucose dehydrogenase as well as pyruvate decarboxylase. It has a 60% increased biomass yield on glucose and accumulates pyruvate instead of acetate [17].

Excess sugar consumption is associated with obesity and various diseases such as cardiovascular diseases or type II diabetes [18–20]. Thus, the food industry aims at the replacement of nutritive sugars such as sucrose or high-fructose corn syrup by non-nutritive sugar substitutes such as sucralose [21]. Various artificial and natural sweeteners are already available on the market, but most of them have drawbacks. Polyols such as D-sorbitol or D-xylitol show laxative effects [18], whereas compounds such as acesulfame K or steviol glycosides have a bitter off-taste [22]. 5-Keto-D-fructose (5-KF) is considered as a potential non-nutritive natural sweetener [23], which has been found e.g. in white wine [24, 25]. It shows a sweet taste quality identical to that of fructose and has a similar intrinsic sweet threshold concentration of 16.4 mmol/L [26]. Therefore, the development of processes for the production of 5-KF has recently gained attention.

G. oxydans is able to oxidize fructose to 5-KF when cultivated with fructose [25] or with mannitol, which is initially oxidized to fructose [27]. However, the enzyme responsible for 5-KF formation in *G. oxydans* is not known yet. In contrast, fructose dehydrogenase (FDH), a membrane-bound enzyme catalyzing the periplasmic oxidation of fructose to 5-KF with ubiquinone as electron acceptor, has been isolated and characterized from *Gluconobacter japonicus* NBRC3260 (formerly *Gluconobacter industrius* IFO3260) [28, 29]. It is a heterotrimeric enzyme composed of a small subunit with a putative Tat signal peptide (FdhS), a Sec-secreted cytochrome *c* subunit with three CXXCH motifs for covalent heme attachment and a C-terminal transmembrane helix anchoring the entire complex to the membrane (FdhC), and a large subunit with a covalently bound flavin adenine dinucleotide (FAD) cofactor (FdhL). It lacks a signal peptide and is presumably exported via the Tat system in complex with FdhS. The corresponding genes are organized in the polycistronic *fdhSCL* transcription unit [29]. Plasmid-based expression of the *G. japonicus fdhSCL* genes under the control of an *adhAB* promoter in a Δ*adhA* mutant of *G. oxydans* NBRC12528 lead to 20-fold higher FDH activity compared to *G. japonicus* wild-type cells, confirming the successful synthesis of FDH in this heterologous host [29].

The application of FDH for the targeted production of 5-KF was reported only recently [30]. A strain of *G. oxydans* 621H expressing the *fdhSCL* genes of *G. japonicus* under the control of the strong constitutive promoter P264 on the broad host range plasmid pBBR1p264-*fdhSCL*-ST showed good growth on fructose and formed 5-KF with a yield of 89 mol% 5-KF per fructose. Moreover, when combined with a second *G. oxydans* strain secreting the sucrase SacC of *Zymomonas mobilis*, this bacterial community was able to convert either purified sucrose or sucrose present in sugar beet extract to glucose and fructose and oxidize the latter to 5-KF with molar yields of > 90% and > 80%, respectively [30]. Most recently, 5-KF production from sucrose was reported for a *G. oxydans* strain with a chromosomal *fdhSCL* integration and plasmid-based expression of an invertase, resulting in conversion of 84 ± 2 mol% of the fructose units of sucrose into 5-KF [31]. *G. oxydans* carrying the expression plasmid pBBR1p264-*fdhSCL*-ST was also used for bioprocess development. When cultivated in a 2 L bioreactor with constant fructose feeding, 5-KF up to 489 g/L, yields up to 0.98 g 5-KF/g fructose and space-time yields up to 8.2 g/L/h were reached, demonstrating the efficiency of this 5-KF production process [26].

Considering an industrial implementation, 5-KF production with plasmid-free strains would be desirable. Therefore, the current study aimed at the development and characterization of *G. oxydans* strains with genomically integrated *fdhSCL* genes. Initially, four strains of *G. oxydans* IK003.1, each harboring a single copy of the *fdhSCL* genes at different genomic loci, were constructed and analyzed regarding 5-KF production. Based on these results, a strain carrying two genomic *fdhSCL* copies under control of the P264 promoter was constructed, which showed even better growth on fructose than the single-copy strains and formed 5-KF with yields of up to 0.82 g/g.

Results and discussion

Selection of genomic integration sites for the *fdhSCL* genes and design of integration constructs

In this study, we wanted to generate plasmid-free *G. oxydans* strains for the production of 5-KF by genomic integration of the FDH genes *fdhSCL* from *G. japonicus*. Because the genomic vicinity can influence the expression of integrated genes, we selected four different integration sites in the genome of *G. oxydans* IK003.1. For one of the insertions, the genes GOX2096-GOX2095 (GOX_RS11750) for a sorbitol dehydrogenase large subunit were replaced by the *fdhSCL* genes. GOX2096-GOX2095 represent an authentic frameshift in *G. oxydans* 621H leading to an inactive enzyme [14, 32]. Therefore, the replacement does not lead to a metabolic deficiency. In the case of the other three integration sites, the *fdhSCL* genes were inserted into intergenic regions (IGRs) without deleting any part of the genome. The IGRs were chosen based on the following criteria: (i) the genomic positions should be close to the origin of replication to profit from a positive gene dosage effect; (ii) the positions should be located between the 3′-ends of two convergent genes to avoid an interference with the regulation of neighboring genes; (iii) the expression levels of the adjacent genes should vary for the three sites to test the influence of the genomic vicinity on *fdhSCL* expression; (iv) the chromosomal gene upstream of the *fdhSCL* genes should possess a terminator to enable comparison of the three loci without readthrough from an upstream promoter. Applying those criteria and using RNAseq data [33] for the evaluation of the expression levels of the neighbouring genes, the following positions were selected: igr1 between GOX0013 and GOX0014, igr2 between GOX0028 and GOX0029, and igr3 between GOX0038 and GOX0039. The exact integration sites were positioned directly downstream of the terminator of the upstream gene, as predicted with the online tool ARNold [34].

The *fdhSCL* integration fragments were composed of 500 bp upstream DNA of the respective insertion site followed by the strong constitutive P264 promotor, the consensus ribosome binding site (RBS) AGGAG [33], the *fdhSCL* genes with an ATG start codon instead of TTG for *fdhS*, which was shown to be beneficial for 5-KF production [29], the bidirectional 100 bp terminator region downstream of GOX0028, which led to efficient termination according to RNA seq data [33], and 500 bp downstream DNA of the respective insertion site. The integration fragments were inserted into the suicide vector pAJ63a [35] and transferred into *G. oxydans* IK003.1 by conjugation, followed by a two-step homologous recombination protocol as outlined in the Methods section. The resulting integration strains were checked via colony-PCR and named IK003.1-igr1::*fdhSCL*, IK003.1-igr2::*fdhSCL*, IK003.1-igr3::*fdhSCL*, and IK003.1 Δ*sdh*::*fdhSCL* (Fig. 1).

Shake flask cultivations with different *G. oxydans* IK003.1::*fdhSCL* strains with 18 g/L and 80 g/L fructose

Shake flask cultivations with offline sampling, using the four integration strains as well as IK003.1 as reference, were performed to assess whether the integration strains produce more 5-KF than the parental strain. Cultivations were performed with 18 g/L fructose (=100 mM). Growth, fructose consumption, and 5-KF formation are

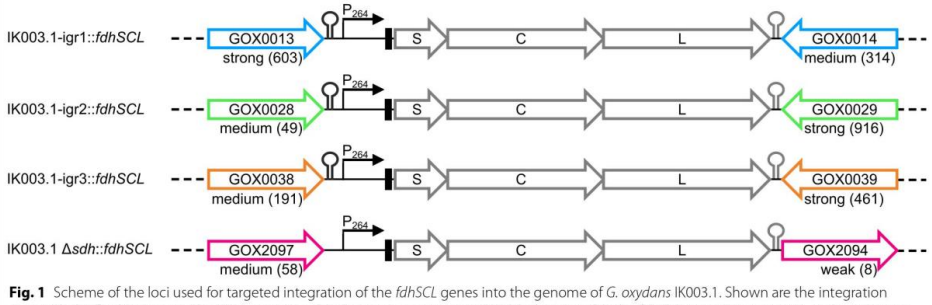

Fig. 1 Scheme of the loci used for targeted integration of the *fdhSCL* genes into the genome of *G. oxydans* IK003.1. Shown are the integration sites with the flanking genes, the P264 promoter (black arrow), a consensus RBS (black rectangle), the *fdhSCL* genes (gray arrows), and terminators (black hairpin = native, gray hairpin = inserted). The transcription strength of the flanking genes (strong, medium, weak) and the normalized read count (given by Fragments Per Kilobase of transcript per Million mapped reads (FPKM) values in brackets) are also indicated. FPKM values were determined via RNAseq with *G. oxydans* 621H grown on mannitol (exponential growth phase) [33]. To differentiate the transcription levels, the FPKM values (range of 0–446,627) were grouped in the lowest 25% (0–38, weak), the median 50% (38–318, medium) and the highest 25% (318–446,627, strong)

shown in Fig. 2. After 29 h of cultivation, when no further growth was observed, IK003.1-igr3::*fdhSCL*, IK003.1-igr2::*fdhSCL*, and IK003.1 Δ*sdh*::*fdhSCL* had completely consumed the fructose, resulting in higher 5-KF concentrations than observed for IK003.1-igr1::*fdhSCL* with 2.5 g/L residual fructose. The integration strains showed 15–22% higher growth rates (0.31 h^{-1} –0.33 h^{-1}) than the reference strain IK003.1 (0.27 h^{-1}) and reached higher final cell densities. Due to the lack of the *fdhSCL* genes, IK003.1 cannot generate energy by periplasmic fructose oxidation, which explains slower growth and lower biomass formation. Nevertheless, the reference strain produced small amounts of 5-KF, reaching a yield of 0.04 g/g. Low 5-KF production has also previously been described for *G. oxydans* grown on mannitol [27]. Here fructose oxidation to 5-KF was presumably catalyzed by the membrane-bound polyol dehydrogenase mSldAB, since a side activity for fructose oxidation has been described for a *Gluconobacter thailandicus* mSldAB homolog [36]. All integration strains formed 5-KF, but the kinetics differed (Fig. 2b). Strain IK003.1-igr3::*fdhSCL* showed the fastest 5-KF production, strains IK003.1-igr2::*fdhSCL* and IK003.1 Δ*sdh*::*fdhSCL* were somewhat slower, and IK003.1-igr1::*fdhSCL* was much slower than the other strains. The 5-KF yields after 29 h were comparable for the three fastest strains (0.76 g/g for IK003.1-igr3::*fdhSCL* and IK003.1-igr2::*fdhSCL*, 0.74 g/g for IK003.1 Δ*sdh*::*fdhSCL*), but lower for IK003.1-igr1::*fdhSCL* (0.61 g/g). This experiment already showed an influence of the integration site on 5-KF production with the ranking IK003.1-igr3::*fdhSCL* > IK003.1-igr2::*fdhSCL* > IK003.1 Δ*sdh*::*fdhSCL* > IK003.1-igr1::*fdhSCL*. This ranking was later confirmed in additional experiments.

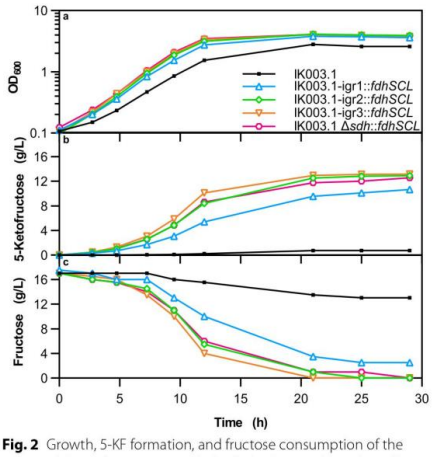

Fig. 2 Growth, 5-KF formation, and fructose consumption of the indicated *G. oxydans* strains in shake flasks. Depicted is **a** the cell density as OD_{600}, **b** the 5-KF concentration, and **c** the fructose concentration determined by HPLC (method A). The strains were cultivated in 100 mL complex medium with 18 g/L fructose in 500 mL baffled shake flasks at 30 °C, 130 rpm, a shaking diameter of 50 mm, and 85% humidity. Shown are mean values of biological duplicates

To further investigate the four different integration sites, cultivations with online monitoring of respiratory activity in shake flasks were performed using the Respiration Activity MOnitoring System (RAMOS). Measuring the oxygen transfer rate (OTR) and the carbon dioxide transfer rate (CTR) provides extremely useful information about the metabolic activities and the physiological state of the microorganisms [37, 38]. 5-KF production from fructose is an oxidation reaction catalyzed by FDH and the electrons are transferred in the respiratory chain to oxygen as the final electron acceptor [26, 39]. Hence, 5-KF formation contributes to the OTR kinetics in addition to other catabolic activities of the *G. oxydans* strains. Cultivations with online monitoring of the respiratory activity were performed to obtain additional information on the growth behavior of the four integration strains using IK003.1 and the plasmid-containing strain IK003.1 pBBR1p264-*fdhSCL*-ST as reference (Additional file 1: Fig. S1). Increasing the fructose concentration from 18 g/L to 80 g/L led to a decrease of the 5-KF yield for all four integration strains, reaching values between 0.36 g/g and 0.58 g/g (Additional file 1: Table S1). Residual fructose concentrations of 25 g/L to 45 g/L were detected for the integration strains (Additional file 1: Table S1). IK003.1 pBBR1p264-*fdhSCL*-ST reached a much higher yield of 0.88 g/g.

The kinetics of OTR, CTR, and the respiratory quotient (RQ = CTR/OTR) observed for the six strains (Additional file 1: Fig. S1a–c) are likely caused by differences in the fructose oxidation rate, as a consequence of varying *fdhSCL* expression levels, which will be discussed below. The plasmid-containing strain IK003.1 pBBR1p264-*fdhSCL*-ST presumably has the highest FDH activity and showed the highest OTR. The maximal total oxygen consumption (TOC) of 220 mmol/L was reached already after 19 h (Additional file 1: Fig. S1d). Due to the rapid oxidation of fructose to 5-KF, less fructose is available for uptake and intracellular oxidation, resulting in the lowest total carbon dioxide evolution (TCE) of 50 mmol/L for IK003.1 pBBR1p264-*fdhSCL*-ST (Additional file 1: Fig. S1e). The reference strain IK003.1 had only a very low activity for fructose conversion to 5-KF and a very low maximal TOC of 80 mmol/L. The CTR was also quite low for IK003.1, because the strain may be energy-limited in the absence of FDH-based respiration, resulting

in a maximal TCE of only 75 mmol/L. The 5-KF production of the four integration strains was slower than in the plasmid-based strain, resulting in a lower OTR. A maximal TOC of 250 mmol/L was reached for the integration strains at the end of the cultivation, except for IK003.1-igr1::*fdhSCL*. At the same time, more fructose was taken up and catabolized within the cell, resulting in higher CTR. The maximal TCE is two to four times higher for all integration strains in comparison with the plasmid-containing strain (Additional file 1: Fig. S1e). The kinetics of the RQ reflects these differences (Additional file 1: Fig. S1c).

Another parameter that probably influences the kinetics of OTR and CTR is the pH value. Strain IK003.1 forms pyruvate (pK_a 2.49) instead of acetate (pK_a 4.78), leading to a stronger acidification of the medium. In the experiment shown in Additional file 1: Fig. S1, pyruvate formation is dependent on the rate of intracellular fructose catabolism and thus should be reflected by the CTR value. Consequently, the integration strains should show a stronger acidification than the plasmid-containing strain and IK003.1, which was confirmed by the pH values measured after 29 h of cultivation (Additional file 1: Table S1). The pH influences the FDH activity and thus fructose consumption. The pH optimum for FDH is around 4 and activity decreases slightly at higher pH values, but strongly at lower pH, with no activity observed at pH 3 [29]. It is therefore likely that the OTR and CTR kinetics observed for the integration strains with a slow decrease after the maximum (Additional file 1: Fig. S1) and the incomplete fructose consumption (Additional file 1: Table S1) is caused by inhibition of FDH and other enzymes, such as those of the pentose phosphate pathway [40], due to acidification.

Influence of buffering on growth and 5-KF production during cultivation of IK003.1-igr1::*fdhSCL* with 80 g/L fructose in a RAMOS device

The decreasing pH during the cultivation had presumably a negative influence on growth and product formation during the cultivation. Therefore, it was investigated whether pH control has a positive effect on growth and product formation. $CaCO_3$ is sometimes used in shake flask cultivations for buffering, but it has several disadvantages including turbidity of the medium [41]. Therefore, 2-(*N*-morpholino)ethansulfonic acid (MES) buffer with a pK_a value of 6.1 was used [42]. Strain IK003.1-igr1::*fdhSCL* was chosen to compare cultivations without buffer and with 50 mM, 100 mM, and 150 mM MES buffer.

The addition of MES buffer had a strongly positive effect on 5-KF formation (Fig. 3). As expected, the pH value at the end of the cultivation increased from 3.3 for unbuffered cultivation to 4–4.7 for the cultivations with MES buffer (Fig. 3a). Fructose was completely consumed in the buffered cultures, resulting in a significantly increased 5-KF formation of up to 71 g/L and an increase of the yield from 0.56 g/g for the unbuffered culture to 0.86 g/g for the culture with 50 mM MES (Fig. 3a). At 100 mM and 150 mM MES, the 5-KF concentration and the yield were lower than at 50 mM MES, but the final OD_{600} was higher (4.1 for 0 mM MES, 4.9 for 50 mM MES, 5.4 for 100 mM MES, 5.9 for 150 mM MES). Higher pH values thus favor biomass formation and decrease 5-KF production.

The OTR kinetics of cultivations with the different MES concentrations showed clear differences (Fig. 3b). The maximal OTR of all MES-buffered cultures was about 50 mmol/L/h and thus 2.5-fold higher than for the unbuffered culture. At 100 mM and 150 mM MES, the OTR slowed down compared to 50 mM MES. This is most likely due to the higher osmolality of the medium, which increased from 0.56 Osmol/kg for unbuffered medium to 0.78 Osmol/kg for medium with 150 mM MES. The negative influence of osmolality on growth of *G. oxydans* has already been described [41, 43].

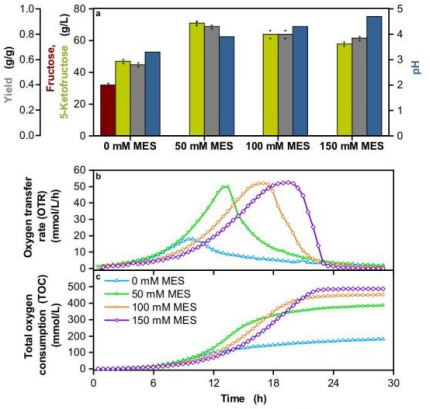

Fig. 3 Cultivation of *G. oxydans* IK003.1-igr1::*fdhSCL* in a RAMOS device with 80 g/L fructose and different MES buffer concentrations. Depicted is **a** the residual fructose concentration (red), the 5-KF concentration (green), the yield g/g (grey), and the pH (blue), **b** the oxygen transfer rate (OTR) and **c** the total oxygen consumption (TOC). Cultivations were performed at 30 °C, 350 rpm, $V_L = 10$ mL in 250 mL flasks, $pH_{start} = 6$ and a shaking diameter of 50 mm in complex medium with 80 g/L fructose and MES buffer at concentrations of 0 mM, 50 mM, 100 mM and 150 mM. Shown are mean values of duplicates and the concentrations determined for fructose and 5-KF in the two experiments as well as the resulting yields are shown as stars

The kinetics of TOC is shown in Fig. 3c. As expected from the OTR kinetics, the TOC values of the MES-containing cultures were much higher than that of the unbuffered culture. Increasing MES concentrations correlated with increased TOC values, which can be explained by the fact that higher MES concentration led to higher biomass formation and thus a higher fraction of fructose was metabolized intracellularly, leading to more reducing equivalents per fructose than its simple oxidation to 5-KF.

Despite the increased lag phase, the positive effect of MES buffer regarding pH, TOC, OD_{600}, and yield predominates. Therefore, subsequent shake flasks experiments were conducted with 150 mM MES buffer, which led to the highest TOC and the highest pH at the end of the cultivation. This was important for further experiments with fructose concentrations up to 210 g/L performed in shake flasks (Additional file 1: Fig. S5, Tab. S2).

Comparison of different *G. oxydans* strains during cultivation in a RAMOS device with 80 g/L fructose and 150 mM MES buffer

Based on the positive effect of MES buffering on 5-KF production by IK003.1-igr1::*fdhSCL*, these conditions were used to compare the four different integration strains among each other, with the parent strain IK003.1, and with the plasmid-containing strain IK003.1 pBBR1p264-*fdhSCL*-ST (Fig. 4).

As expected from the previous experiments, all strains except for IK003.1 consumed fructose completely and the final pH values varied between 4.3 and 4.6. 5-KF formation by the four integration strains was very similar (57–59 g/L), corresponding to yields of 0.71–0.75 g/g (Fig. 4a). Compared to the unbuffered cultures (Additional file 1: Table S1) this was an increase of 1.2- to 2-fold. The plasmid-containing strain formed 65 g/L 5-KF corresponding to a yield of 0.84 g/g.

The final OD_{600} of the integration strains ranged between 6.9 and 8.3 (Fig. 4a). In view of the comparable 5-KF formation of the four strains, these differences were unexpected and apparently are a consequence of the different genomic integration sites. The plasmid-containing strain had a much lower final OD_{600} of only 3.3 compared to the integration strains. As discussed above, this is caused by the higher copy number resulting in more *fdhSCL* transcript, resulting in faster fructose oxidation and a lower amount of fructose entering the cell. Additionally, a longer period of fructose oxidation by FDH also provides a longer period of energy supply for biomass formation from components of the yeast extract. Once fructose has been exhausted, growth is no longer sustained.

The statements made above are supported by the OTR and CTR kinetics (Fig. 4b, c). The plasmid-based strain

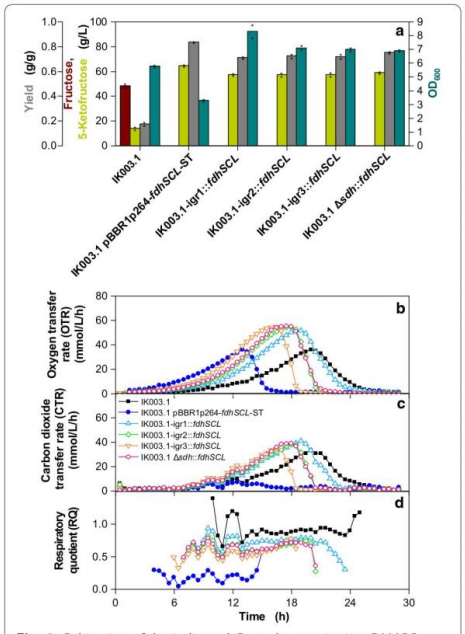

Fig. 4 Cultivation of the indicated *G. oxydans* strains in a RAMOS device with 80 g/L fructose and 150 mM MES. Depicted is **a** the residual fructose concentration and the 5-KF concentration (determined by HPLC method B), the yield g/g, and the optical density (OD_{600}) after 29 h, **b** the oxygen transfer rate (OTR), **c** the carbon dioxide transfer rate (CTR), and **d** the respiratory quotient (RQ, shown for OTR values above 5 mmol/L/h). The strains were cultivated in complex medium with 80 g/L fructose and 150 mM MES at 30 °C, 350 rpm, $V_L = 10$ mL in 250 mL flasks, $pH_{start} = 6$ and a shaking diameter of 50 mm. Shown are mean values of duplicates and the values determined for optical density, the concentrations of fructose and 5-KF, and the resulting yields in the two experiments are shown as stars

reached its OTR maximum of 36 mmol/L/h already after 13 h, whereas the integration strains reached their maximum of ~ 55 mmol/L/h after 17 h –19 h (Fig. 4b). CTR was very low for the plasmid-based strain and much higher for the integration strains. This is in line with a higher intracellular fructose catabolism and a presumably higher consumption of yeast extract components (Fig. 4c). For strain IK003.1, both OTR and CTR were retarded compared to the integration strains. These kinetics are due to slow intracellular oxidation of fructose. In line with these data, the RQ value for IK003.1 was the highest of all strains (about 0.9), whereas the RQ of the plasmid-based strain was very low with a value of

about 0.2. The integration strains showed RQ values in the range of 0.6–0.8 (Fig. 4d).

This experiment revealed that when using buffered conditions, the *fdhSCL* integration strains approached the 5-KF titer and the yield of the strain with plasmid-based *fdhSCL* expression. With respect to the four genomic integration sites, the differences in 5-KF titer and yield were rather small, but IK003.1-igr3::*fdhSCL* showed the fastest growth followed by IK003.1 Δ*sdh*::*fdhSCL* and IK003.1-igr2::*fdhSCL*.

Scale up and fermentation in 2 L fermenter with IK003.1-igr3::*fdhSCL*

An important step for the industrial implementation of 5-KF production with a plasmid-free strain is the design and establishment of a suitable fermentation process. As a first step, a scale up from shake flasks to a 2 L fermenter was performed with strain IK003.1-igr3::*fdhSCL*, which was the best performing integration strain so far. To allow a direct comparison between shake flask (RAMOS system) and fermenter, the same medium, initial pH, and temperature were used for both cultivation devices. The shake flask was filled with inoculated medium by sterile transfer of a sample of the fermenter culture to ensure optimal comparability. In shake flask cultivations with 80 g/L fructose, no oxygen limitation was detected in the RAMOS devices. Hence, for a successful scale-up, oxygen limitation in the fermenter had to be avoided. For that reason, the dissolved oxygen tension (DOT) was kept above 30% by adjusting the agitation speed, whereas the aeration rate in the fermenter was kept constant at 1 vessel volume per minute (vvm). To verify the successful scale-up, online data (OTR, CTR, RQ) and offline data (OD_{600}, pH, fructose and 5-KF concentration) were measured and compared. The results are shown in Additional file 1: Fig. S2. No significant differences in both, online and offline data, were found. Additional fermentations were performed as first optimization steps and confirmed the consistency of online and offline data (Additional file 1: Fig. S3 and Fig. S4). Hence, the scale up to a 2 L fermenter was successful and the process could be further optimized.

Higher product concentrations are desirable for an industrial application. To achieve higher 5-KF titers, the fructose concentration in batch fermentations was increased. To identify the optimal initial fructose concentration for the cultivation of IK003.1-igr3::*fdhSCL*, an experiment in shake flasks was performed using the RAMOS device and fructose concentrations between 80 g/L and 210 g/L. IK003.1-igr3::*fdhSCL* completely consumed fructose up to 210 g/L and the highest yield of 0.86 g/g was reached for the cultivation with 160 g/L fructose (Additional file 1: Fig. S5 and Table S2).

In a previous study, a 5-KF production process in a 2 L fermenter with the plasmid-based strain *G. oxydans* 621H pBBR1p264-*fdhSCL*-ST was described. This strain carried the same plasmid as IK003.1 pBBR1p264-*fdhSCL*-ST. *G. oxydans* 621H is not optimized for biomass formation from glucose and produces acetate rather than pyruvate. A batch fermentation with 150 g/L fructose was performed, reaching a 5-KF yield of 0.87 g/g [26]. To compare our genomic integration strain IK003.1-igr3::*fdhSCL* with this strain, a 2 L batch fermentation was performed under similar conditions (Fig. 5). An initial fructose concentration of 150 g/L was used to allow a direct comparison. Due to pH control by KOH addition, MES buffer was not included in the medium. The pH was set to 5, promoting both growth of *G. oxydans* and FDH activity. The DOT was maintained above 30% and antifoam was added twice during the cultivation. The OTR reached a maximum of 53 mmol/L/h after approx. 20 h and decreased sharply after 27 h, indicating the complete consumption of fructose (Fig. 5a). The OD_{600} increased

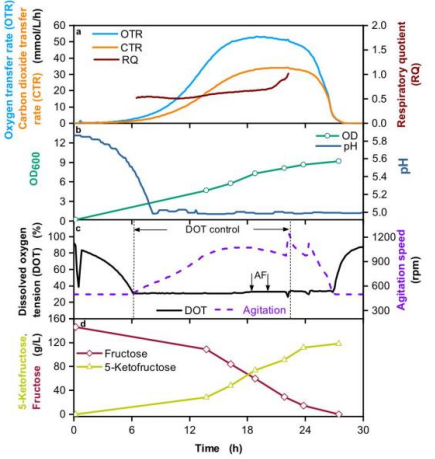

Fig. 5 Cultivation of *G. oxydans* IK003.1-igr3::*fdhSCL* in a 2 L fermenter with pH control. Depicted is **a** the oxygen and carbon dioxide transfer rates (OTR and CTR), the respiratory quotient (RQ, shown for OTR values above 5 mmol/L/h), **b** optical density (OD_{600}) and pH, **c** dissolved oxygen tension (DOT) and agitation speed, antifoam (AF) agent addition, and period of DOT control (indicated by arrows), **d** fructose and 5-KF concentrations. The cultivation was performed in complex medium with 150 g/L fructose with 1 L filling volume, DOT ≥ 30% controlled by agitation speed (500–1200 rpm), aeration rate (Q) = L/min, T = 30 °C, $pH_{control} \geq 5$

over time and reached a final value of 9.2 (Fig. 5b), which is 1.7-fold higher compared with *G. oxydans* 621H pBBR1p264-*fdhSCL*-ST [26]. This difference is presumably caused by a somewhat higher fraction of fructose metabolized within the IK003.1 pBBR1p264-*fdhSCL*-ST cells and possibly also by the genetic alterations introduced into strain IK003.1 [17]. Most importantly, the 5-KF yield IK003.1-igr3::*fdhSCL* was 0.84 g/g and thus only slightly smaller than the 5-KF yield of 0.87 g/g determined for the plasmid-based strain [26].

Shake flask cultivation of double integration strain IK003.1::*fdhSCL*^{2}

The results described above were obtained with integration strains containing a single genomic *fdhSCL* copy and a resulting lower expression rate compared to plasmid-based *fdhSCL* expression (see below). To further improve the potential for plasmid-free 5-KF production, the double integration strain IK003.1::*fdhSCL*^{2} was constructed using the two most potent integration sites igr3 and igr2 for *fdhSCL* integration. The performance of this strain was compared to the parent single integration strains IK003.1-igr2::*fdhSCL* and IK003.1-igr3::*fdhSCL* and to the plasmid-based strain IK003.1 pBBR1p264-*fdhSCL*-ST in a shake flask experiment. Growth curves, fructose consumption, and 5-KF formation are shown in Fig. 6.

The growth rate of strain IK003.1::*fdhSCL*^{2} (0.32 h^{-1}) was close to that of the plasmid-based strain (0.33 h^{-1}) and slightly higher than that of the single integration strains (0.28–0.29 h^{-1}). The final OD_{600} after 30 h of the double integration strain (3.5) was lower than that of IK003.1-igr2::*fdhSCL* (4.1) and IK003.1-igr3::*fdhSCL* (4.1) and higher than that of the plasmid-based strain (2.3). Most importantly, the double integration strain IK003.1::*fdhSCL*^{2} was clearly faster than the single integration strains with respect to fructose consumption and 5-KF formation, but still slower than the plasmid-based strain. In a further experiment, the IK003.1::*fdhSCL*^{2} strain was compared with the parent single integration strains in a RAMOS cultivation device with 80 g/L fructose and 150 mM MES buffer (initial pH 6.0). As shown in Additional file 1: Fig. S6, the OTR kinetics confirmed faster fructose consumption by the double integration strain, reaching maximal OTR values at about 12 h, whereas the single integration strains reached the maximum after about 17 h. Under these conditions, IK003.1::*fdhSCL*^{2} reached a final 5-KF yield of 0.82 g/g, close to that of IK003.1 pBBR1p264-*fdhSCL* (0.84 g/g) obtained in the experiment shown in Fig. 4.

The properties of IK003.1::*fdhSCL*^{2} showed that doubling of the copy number of the *fdhSCL* genes and thus presumably a higher rate of *fdhSCL* transcription is sufficient to significantly increase the rate of fructose consumption and 5-KF formation. In the plasmid-based strain, the copy number of the *fdhSCL* genes is presumably above 20, as the copy number of the parent vector was determined to be 23 ± 6 in *G. oxydans* Δ*hsdR* [44]. In this case, the increase in *fdhSCL* copy number did not lead to tenfold higher rates of fructose consumption and 5-KF production, showing that there were other factors that limit fructose oxidation.

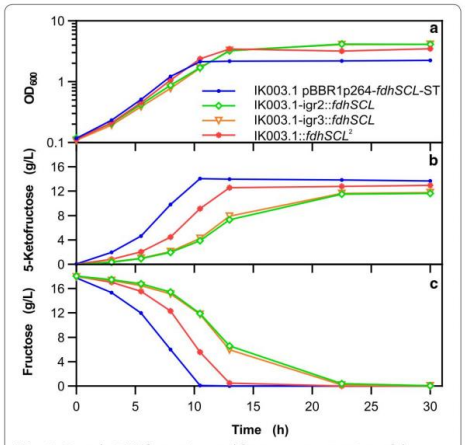

Fig. 6 Growth, 5-KF formation, and fructose consumption of the indicated *G. oxydans* strains. Depicted are **a** the growth as OD_{600}, **b** the 5-KF and **c** the fructose concentration (determined by HPLC method A). The strains were cultivated in 100 mL complex medium with 18 g/L fructose in 500 mL baffled shake flasks at 30 °C, 130 rpm, a shaking diameter of 50 mm and 85% humidity. Shown are mean values of biological duplicates

Analysis of *fdhSCL* expression by RT-qPCR

To validate that different *fdhSCL* transcription levels are responsible for the phenotypic differences of single integration strains, reverse transcription quantitative PCR (RT-qPCR) was performed with the single integration strains, the double integration strain, and the plasmid-based strain using RNA from cells in the exponential growth phase. The *gap* gene (GOX0508), encoding glyceraldehyde 3–phosphate dehydrogenase, was tested as reference. It has been used as reference gene for RT-qPCR in *G. oxydans* before [45, 46]. However, with this reference gene we failed to detect the difference between single integration strains and the double integration strain, suggesting that *gap* expression is not constant under the experimental conditions employed and thus not a suitable reference gene (data not shown). We therefore used the gene for a ribosomal protein as reference,

namely GOX0264 encoding the ribosomal protein L35. The results obtained for the *fdhSCL*/GOX0264 mRNA ratios are shown in Fig. 7, normalized to the mRNA ratio of the plasmid-based strain (5.03), which was set as 1.

The *fdh* mRNA ratio of the four single integration strains varied between 3.5% and 6.6% of the value measured for the plasmid-based strain, which fits with a copy number of about 20 for pBBR1p264 in *G. oxydans* [44]. In the double integration strain, the *fdh* mRNA ratio was about twice as high (14% of the level of the plasmid-based strain), roughly corresponding to the sum of the values measured for IK003.1-igr2::*fdhSCL* and IK003.1-igr3::*fdhSCL* (12%). These results confirm the different expression levels expected from the *fdhSCL* copy numbers of the different strains. The *fdhSCL* transcription levels observed for the different integration strains correlated with the 5-KF production levels in the order IK003.1::$fdhSCL^2$ > IK003.1-igr3::*fdhSCL* > IK003.1-igr2::*fdhSCL* > IK003.1 Δ*sdh*::*fdhSCL* > IK003.1-igr1::*fdhSCL*.

Despite the usage of the same promoter and terminator structures, *fdhSCL* expression in the four different integration sites varied, indicating that the genomic vicinity of the target gene had an influence on the expression. It has been reported that RNA polymerase activity increases with proximity to the origin of replication [47] and that transcription speed is influenced by the codon composition [48]. However, both factors are not applicable to the differences observed here for the four single integration strains, since all four sites are close to the origin and contain the same DNA sequence. Genome architecture and DNA supercoiling are known to influence bacterial gene expression with DNA gyrase playing an important role by introducing negative supercoils or relaxing positive supercoils introduced by RNA polymerase [47, 49, 50]. In *Escherichia coli,* an increase in gyrase cleavage sites was found downstream of highly transcribed operons [51]. Furthermore, nucleoid-associated proteins influence DNA folding and gene expression [52, 53]. Such mechanisms, which have not been studied at all in *G. oxydans*, are likely to contribute to the variation in *fdhSCL* expression at the four different integration sites.

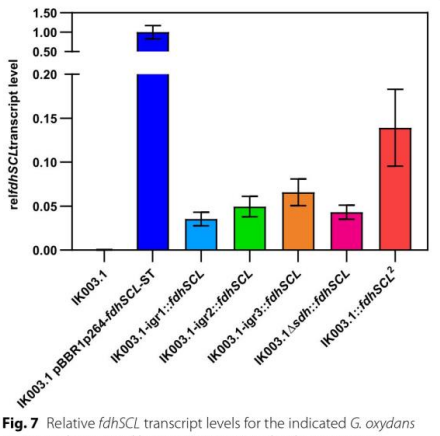

Fig. 7 Relative *fdhSCL* transcript levels for the indicated *G. oxydans* strains as determined by RT-qPCR. Depicted is the transcript ratio *fdhSCL*/GOX0264 normalized to the transcript ratio of the plasmid-based strain IK003.1 pBBR1p264-*fdhSCL*-ST, which was set as 1.0. Shown are the mean values of at least three biological replicates and technical duplicates, with standard deviation as error bars

Conclusions

In this study, four different integration sites for heterologous genes were identified in the genome of *G. oxydans*, all enabling successful expression. The integration into the intergenic region of convergent genes flanked by terminators is thus a favorable option for future engineering studies requiring genomic expression of foreign genes. The position-dependent effects on gene expression observed in our experiments suggests that a comparison of different integration sites might be worthwhile. Chromosomal *fdhSCL* expression should enable stable expression and in fact we never observed loss of the ability for 5-KF production during growth for up to 30 generations and handling of the strains over several months. Furthermore, chromosomal expression avoids the necessity to use antibiotics required for plasmid-based *fdhSCL* expression. Plasmid loss can be an issue in the case of plasmid-based expression, however, no evidence for this has been observed in the case pBBR1p264-*fdhSCL*-ST. Another advantage of genomic *fdhSCL* expression is that it facilitates further metabolic engineering of the strains, for example toward utilization of alternative substrates. As doubling the genomic copy number of the *fdhSCL* genes correlated with twofold increased 5-KF synthesis rates, additional *fdhSCL* integrations could further increase 5-KF production. Also, the use of a promoter stronger than P264 could further enhance *fdhSCL* expression. Besides genetic optimization, process optimization is an obvious method to improve 5-KF production. In summary, our study provided the efficient *G. oxydans* strain IK003.1::$fdhSCL^2$ for plasmid-free 5-KF production that will serve as basis for future strain and process development.

Methods

Strains, plasmids and oligonucleotides

All strains and plasmids used in this study are listed in Table 1. Oligonucleotides were obtained from Eurofins

Table 1 Strains and plasmids used in this study

Strain or plasmid	Relevant characteristics	Source or references
E. coli		
DH5α	F– *endA1* Φ80d*lacZ*ΔM15 Δ(*lacZYA-argF*)U169 *recA1 relA1 hsdR17*(rK–mK+) *deoR supE44 thi-1 gyrA96 phoA* λ–, strain used for cloning	[57]
S17-1	*ΔrecA, endA1, hsdR17, supE44, thi-1, tra+*, strain used for conjugation of *G. oxydans*	[62]
G. oxydans		
IK003.1	*G. oxydans* 621H Δ*upp* Δ*gdhS*::*sdhCDABE* Δ*pdc*::*ndh* Δ*gdhM*::*sucCD*	[17]
IK003.1-igr1::*fdhSCL*	IK003.1 with the *fdhSCL* genes of *G. japonicus* under the control of the P264 promoter integrated between GOX0013 and GOX0014 (GOX_RS01200 and GOX_RS01205)	This work
IK003.1-igr2::*fdhSCL*	IK003.1 with the *fdhSCL* genes of of *G. japonicus* under the control of the P264 promoter integrated between GOX0028 and GOX0029 (GOX_RS01280 and GOX_RS01285)	This work
IK003.1-igr3::*fdhSCL*	IK003.1 with the *fdhSCL* genes of *G. japonicus* under the control of the P264 promoter integrated between GOX0038 and GOX0039 (GOX_RS01330 and GOX_RS01335)	This work
IK003.1 Δ*sdh*::*fdhSCL*	IK003.1 with the *fdhSCL* genes of *G. japonicus* under control of the P264 promoter replacing the genes GOX2095-6 (GOX_RS11750) encoding an inactive sorbitol dehydrogenase (authentic genomic frameshift)	This work
IK003.1::*fdhSCL*^{2}	IK003.1-igr2::*fdhSCL* with an additional copy of the *fdhSCL* genes of *G. japonicus* under the control of the P264 promoter integrated between GOX0038 and GOX0039	This work
Plasmids		
pBBR1p264-*fdhSCL*-ST	pBBR1MCS-2 derivative containing the promoter region of GOX0264 upstream of the *fdhSCL* genes of *G. japonicus* NBRC3260 with a C-terminal Strep-tag II-encoding sequence fused to the 3′-end of *fdhL*	[30]
pAJ63a	Km^R, FU^S, derivative of pk18mobGII, integration vector for Δ*upp* based counter-selection	[35]
pAJ63a-igr1::*fdhSCL*	Km^R, FU^S, derivative of pAJ63a for integration of the *fdhSCL* genes under the control of the P264 promoter between GOX0013 and GOX0014 (GOX_RS01200 and GOX_RS01205)	This work
pAJ63a-igr2::*fdhSCL*	Km^R, FU^S, derivative of pAJ63a for integration of the *fdhSCL* genes under the control of the P264 promoter between GOX0028 and GOX0029 (GOX_RS01280 and GOX_RS01285)	This work
pAJ63a-igr3::*fdhSCL*	Km^R, FU^S, derivative of pAJ63a for integration of the *fdhSCL* genes under the control of the P264 promoter between GOX0038 and GOX0039 (GOX_RS01330 and GOX_RS01335)	This work
pAJ63a Δ*sdh*::*fdhSCL*	Km^R, FU^S, derivative of pAJ63a for integration of the *fdhSCL* genes under the control of the P264 promoter with simultaneous deletion of GOX2095-6 (GOX_RS11750)	This work

Genomics (Ebersberg, Germany) and are shown in Additional file 1: Table S3.

Media composition

G. oxydans strains were cultivated in complex medium containing 5 g/L yeast extract (Karl Roth GmbH, Karlsruhe, Germany or BD Biosciences, Heidelberg, Germany), 2.5 g/L $MgSO_4 \times 7\ H_2O$, 1 g/L $(NH_4)_2SO_4$, 1 g/L KH_2PO_4. The initial pH was adjusted to 6 with KOH [54]. The media were supplemented with 50 µg/mL cefoxitin and 10 µM thymidine, and for plasmid-carrying strains 50 µg/mL kanamycin was added. For the precultures, 40 g/L mannitol was added as carbon source and main cultures were conducted with different fructose concentrations as indicated in the respective experiments. *E. coli* strains were cultivated in lysogeny broth-based media [55] at 37 °C and 130 rpm, and 50 µg/mL kanamycin was added for plasmid-carrying strains.

Generation of *fdhSCL* integration strains

To generate the *fdhSCL* integration strains, derivatives of pAJ63a [35] containing the *fdhSCL* genes of *G. japonicus* with promoter and terminator and flanked by about 500 bp DNA regions up- and downstream of the selected integration site were constructed. The required DNA fragments were amplified from suitable templates with the Phusion High Fidelity PCR Master Mix (New England Biolabs, Frankfurt am Main, Germany). The *fdhSCL* fragment with an ATG start codon for *fdhS* instead of the native TTG start codon was amplified from pBBR1p264-*fdhSCL*-ST [30] with the oligonucleotides RBS-ATG-fdhSCL-fwd, containing a consensus RBS, and fdhSCL-rev [33]. For all integration constructs, a 508 bp fragment covering the strong promoter of GOX0264 was amplified from pBBR1p264 [44] using the oligonucleotides P264-fwd and P264-rev-RBS-overlap with an overlap to the RBS and *fdhS*. A 100 bp bidirectional terminator region downstream of GOX0028 containing an overlap to *fdhL* was amplified with the oligonucleotides Term-GOX0028-fwd-fdhL-overlap and Term-GOX0028-rev

from genomic DNA of strain IK003.1, which was isolated with the DNeasy Blood and Tissue Kit (Qiagen, Hilden, Germany). Two individual flanking regions of about 500 bp up- and downstream the respective integration sites were amplified from *G. oxydans* IK003.1 genomic DNA using specific oligonucleotide pairs with overlaps to the pAJ63a backbone, digested with PstI and KpnI, the promotor region and the terminator region to assemble all fragments via Gibson assembly [56]. The resulting fusion constructs were used to transform *E. coli* DH5α by the RbCl method [57]. Plasmids of positive clones were isolated using the QIAprep Spin Miniprep Kit (Qiagen, Hilden, Germany) and verified by sequencing (Eurofins Genomics, Ebersberg, Germany). Then the plasmids were transferred into the donor strain *E. coli* S17-1 for integration into *G. oxydans* IK003.1 via conjugation as described previously [17]. Positive clones, containing genomically integrated *fdhSCL* genes but not the vector backbone, were selected with 60 µg/mL 5-fluorouracile [35]. Positive clones were checked via colony PCR using a forward primer that binds upstream the upstream flanking region and a reverse primer, binding downstream of the downstream flanking region. Since the generation of the *fdhSCL* double integration strain turned out to be more challenging than the single integration strains, an adapted protocol was applied. IK003.1-igr2::*fdhSCL* was conjugated with *E. coli* S17−1 pAJ63a-igr3::*fdhSCL* according to the above mentioned protocol, while recombination media for the second recombination step and the agar plates for selecting the positive clones contained fructose instead of mannitol, as a strain with two chromosomal *fdhSCL* copies was assumed to show improved growth on fructose in comparison to a strain with a single *fdhSCL* copy. The double integration strain was obtained after several attempts.

Cultivation in regular shake flasks

For biological replicates, individual 10 mL-precultures in 100 mL unbaffled shake flasks with complex medium containing 40 g/L mannitol were inoculated from agar plates and incubated for about 24 h at 30 °C and 250 rpm. Cells from these precultures were harvested for 15 min at 20 °C and 5.000*g*, washed once in the main culture medium and used to inoculate 100 mL main cultures in 500 mL baffled shake flasks to an OD_{600} (optical density at 600 nm) of 0.15 in complex medium with 18 g/L (100 mM) fructose. Main cultures were incubated at 30 °C and 130 rpm with a shaking diameter of 50 mm and 85% humidity (Shaker ISF1-X, Kuhner, Birsfelden, Switzerland).

Cultivation in a respiration activity monitoring system (RAMOS)

Online monitoring of the respiratory activity in shake flask cultivations was performed using the Respiration Activity MOnitoring System (RAMOS) developed at the chair of biochemical engineering (RWTH Aachen University) [37, 38]. Commercial versions of the RAMOS device can be acquired from Kühner AG (Birsfeld, Switzerland) or HiTec Zang GmbH (Herzogenrath, Germany). Eight 250 mL shake flasks (unbaffled) were cultivated in parallel with an initial filling volume of 10 mL, 350 rpm shaking frequency and 50 mm shaking diameter (Climo-Shaker ISF1-X, Kuhner, Birsfelden, Switzerland). The aeration rate was set to 10 mL/min (1 vvm). Each flask is equipped with a partial pressure sensor for oxygen and a differential pressure sensor to determine oxygen and carbon dioxide transfer rates (OTR and CTR). The respiratory quotient (RQ) is the quotient of CTR and OTR. [37, 38]. For strain maintenance, glycerol stocks were used. Cells cultivated in complex medium with mannitol were harvested during the exponential growth phase, centrifuged and re-suspended in fresh preculture medium with 200 g/L glycerol. The glycerol stocks were stored at − 80 °C.

Precultures were inoculated with 100 µL glycerol stock suspension (OD_{600} = 2.4) and cultivated at 30 °C for 11 h to 19 h. Main cultures were inoculated from pre-cultures starting with an OD_{600} of 0.1. Preculture cells were centrifuged for 3 min at 16,214*g* and room temperature, and resuspended in main culture medium. Samples for offline analysis were taken from Erlenmeyer flasks operated at the same conditions in parallel to the online measurement. If necessary, 2-(*N*-morpholino) ethansulfonic acid (MES) buffer (pH 6, adjusted with 3 M KOH) was added in different concentrations to main cultures.

Cultivation in 2 L bioreactors

Fermentation experiments were performed in a 2 L Sartorius BIOSTAT® Bplus stirred tank reactor (Sartorius, Goettingen, Germany). The temperature was set to 30 °C and aeration was set to 1 L/min with a filling volume of 1 L (1 vvm). The fermenter was equipped with a six blade rusthton turbine and 4 baffles. During cultivation, the dissolved oxygen tension (DOT) was measured using a VisiFerm™ DO 225 pO_2 sensor (Hamilton, Hoechst, Germany). The DOT was controlled at ≥ 30% by automatically adjusting the stirring rate between 500 rpm and 1500 rpm. The pH value was measured using a pH sensor (EasyFerm Plus K8 200, Hamilton, Hoechst, Germany). If necessary, pH was controlled with a 3 M KOH solution. Oxygen and carbon dioxide in the exhaust gas were measured using a DASGIP GA4 exhaust gas analyser

(DASGIP, Eppendorf, Jülich, Germany). 0.5 mL antifoam agent Plurafac LF 1300 (BASF, Ludwigshafen, Germany) was added at the beginning of each experiment and when needed to prevent foaming. During fermentation, samples were taken from the bioreactor for offline analysis. Volume change by KOH titration and sampling were considered for mass balancing.

The performance of scale-up from shake flasks to the fermenter was investigated by cultivating simultaneously in both cultivation systems. For this purpose, media composition, pH, temperature and oxygen supply (aeration rate) were kept constant for both cultivation systems. The shake flasks were filled with medium from a fermenter. Cultivation broth was sterilely transferred from the fermenter into shake flasks to ensure that media composition, pH and optical density were identical [58–60].

Offline analyses

The optical density of cultures at 600 nm (OD_{600}) was measured either with a Genesys 20 photometer (Thermo Scientific, Darmstadt, Germany) or with an Ultraspec 2100 UV–Visible Spectrophotometer (biochrom, Holliston MA, USA). The photometers have a linear range between 0.1 and 0.3 and samples were diluted with 0.9% (w/v) NaCl if necessary. The pH values were determined with a HI221 Basic pH (Hanna Instruments Deutschland GmbH, Vöhringen, Germany), which was calibrated using two standard buffer solutions at pH 4 and 7. The osmolality was determined using the cryoscopic Osmometer OSMOMAT® 030 (Genotec, Berlin, Germany).

Fructose consumption and 5-KF production were analyzed by HPLC of culture supernatants. 1 mL culture was centrifuged at 17,000*g* for 10 min and the supernatant was frozen at -20 °C until further analysis. Thawed samples were heated for 60 min at 60 °C (to avoid double peaks, probably caused by the existence of 5-ketofructose in an equilibrium of the keto and the germinal diol form [26]), filtered (0.2 µm syringe filter, Whatman™, GE Healthcare, Freiburg, Germany) and diluted with deionized water. Sugars were quantified using the same 5-KF standard with two different methods: HPLC method A: A 10 µL sample was measured in an Agilent LC-1100 system (Agilent, Santa Clara, CA, USA) equipped with a Carbo-Ca Guard Catridge (Phenomenex, Aschaffenburg, Germany) using a Rezex RCM-Monosaccharide 300, 7.8 mm column (Phenomenex, Aschaffenburg, Germany) for separation at 60 °C with water as eluent at a flow rate of 0.6 mL/min. 5-KF and fructose were detected with a refraction index detector (35 °C) [27]. 5-KF and fructose were calibrated in a range of 0.1 to 8 g/L, with retention times of 12.7 and 14.6 min, respectively. HPLC method B: An HPLC system of Shimadzu (Duisburg, Germany) was equipped with a precolumn Organic Acid Resin (40 × 8 mm, CS-Chromatographie Service, Langerwehe, Germany), the separating column Organic Acid Resin (250 × 8 mm, CS-Chromatographie Service, Langerwehe, Germany), and refraction index detector RID-20A (Shimadzu, Duisburg, Germany). The flow rate was set to 0.8 mL/min and an injection volume of 20 µL sample was used for analysis. 5 mM H_2SO_4 was used as mobile phase. Eluted components were detected and quantified using standard curves prepared with fructose and 5-KF solutions of known concentrations (0.032 g/L to 10 g/L). Evaporation during cultivations in the RAMOS device was determined gravimetrically and was taken into account for determination of fructose and 5-KF concentrations. Yields were calculated by dividing the produced 5-KF by the total fructose concentration and are indicated in g/g.

Analysis of gene expression by RT-qPCR

Strains were cultivated in shake flasks as described above and harvested in the exponential growth phase (after 7.25 h). 35 mL culture were mixed with 15 g ice, centrifuged for 5 min at 5.000*g* and 4 °C and the resulting cell pellet was shock-frozen in liquid nitrogen and stored at − 80 °C. RNA was isolated using QIAzol Lysis Reagent (Qiagen, Hilden, Germany) including the following steps: cell disruption in a Precellys 24 homogenizer (Bertin, Frankfurt am Main, Germany), chloroform extraction, isopropanol precipitation, an on-column DNA digest on RNeasy mini spin columns, with RNase-free DNase (Qiagen, Hilden, Germany). Purified RNA was subjected to a second DNA digest using the Ambion™ DNAfree™ DNA Removal Kit (Thermo Scientific, Waltham, MA USA). RNA was checked for integrity after the first or second DNase digest to exclude strong RNA degradation using a High Sensitivity RNA ScreenTape in the TapeStation 2200 (Agilent, Santa Clara, CA USA). Final RNA concentrations were determined using the Colibri microvolume spectrometer (Titerek-Berthold, Pforzheim, Germany).

cDNA was generated with SuperScript™ III Reverse Transcriptase (Thermo Scientific, Braunschweig, Germany) with the following protocol. 10 ng RNA, 150 ng random primers (Invitrogen, Thermo Scientific, Braunschweig, Germany) and 1 µL of 10 mM dNTP mix (Invitrogen, Thermo Scientific, Braunschweig, Germany) in a total volume of 14 µL were incubated for 5 min at 65 °C and cooled for 1 min at 4 °C. Subsequently, 4 µL 5× first strand buffer, 1 µL 0.1 mM DTT, and 1 µL SuperScript III reverse transcriptase were added and incubated for 5 min at 25 °C, 60 min at 50 °C and finally for 5 min at 70 °C for inactivation of reverse transcriptase. For all samples, additionally a no amplification control was generated with water instead of reverse transcriptase to exclude

genomic DNA contaminations in RT-qPCR. RT-qPCR was performed with a qTower instrument (Analytik Jena, Jena, Germany) using KAPA SYBR FAST qPCR Master Mix (Roche Diagnostics, Mannheim, Germany). 2 µL of cDNA or no template control were used for RT-qPCR. For each sample, at least three biological replicates with two technical replicates were measured.

To set up RT-qPCR, primers were designed using the online tool Primer3plus [61] and default qPCR settings with a target PCR product of 100–120 bp and an annealing temperature of 60 °C. Three different primer pairs for *fdhSCL*, two binding in *fdhS* and one in *fdhC*, one primer pair for GOX0264, and three primer pairs for *gap* (GOX0508) were designed and tested for PCR specificity. To optimize RT-qPCR conditions, all primer pairs were compared in a gradient from 57.1 to 63.9 °C regarding PCR specificity via agarose gel electrophoresis and melting curve analysis. The optimal temperature was determined to be 57.1 °C. Subsequently, the PCR efficiency was determined by running a RT-qPCR with an 8-step 1:10 dilution series of cDNA. Ct values were determined using qPCRsoft 3.1 (Analytik Jena). The optimal primer pairs were selected to quantitatively amplify cDNA fragments of *fdhC* (q-fdhC-fwd + q-fdhC-rev, PCR efficiency of 103.2%), of GOX0264 (q-GOX0264-fwd + q-GOX0264-rev, 103%), and of GOX0508 (q-gap-fwd2 + q-gap-rev2, 91.8%) Relative transcript levels were calculated from Ct values, considering the primer efficiencies, and normalized to the transcript levels of the plasmid strain.

Supplementary information

Supplementary information accompanies this paper at https://doi.org/10.1186/s12934-020-01310-7.

Additional file 1: Table S1. Offline data for cultivation of the indicated *G. oxydans* strains with 80 g/L fructose in a RAMOS device shown in Fig. S1**. Table S2.** Offline date for the cultivation of *G. oxydans* IK003.1-igr3::*fdhSCL* in a RAMOS device with different fructose concentrations shown in Fig. S5. **Table S3.** Oligonucleotides used in this study. **Figure S1.** Cultivation of the indicated *G. oxydans* strains with 80 g/L fructose in a RAMOS device with online monitoring. Depicted are (**a**) the oxygen transfer rate (OTR) (**b**) the carbon dioxide transfer rate (CTR) (**c**) the respiratory quotient (RQ shown for OTR values above 5 mmol/L/h), (**d**) the total oxygen consumption (TOC) and (**e**) the total carbon dioxide evolution (TCE). The strains were cultivated in complex medium with 80 g/L fructose at 30 °C, 350 rpm, V_L = 10 mL in 250 mL flasks, pH_{start} = 6 and a shaking diameter of 50 mm. Shown are mean values of duplicates. **Figure S2.** Scale-up of batch fermentation of *G. oxydans* IK003.1-igr3::*fdhSCL* from shake flasks (RAMOS device) to a 2 L fermenter with 80 g/L fructose and 150 mM MES. Depicted are (**a**) oxygen transfer rate (OTR) and carbon dioxide transfer rate (CTR), (**b**) growth as OD_{600} and pH, (**c**) dissolved oxygen tension (DOT), agitation speed during fermentation, addition of antifoam agent (AF), and period of DOT control (indicated by arrows) and (**d**) fructose and 5-ketofructose concentration as determined by HPLC (method B). Cultivations were performed in complex medium with 80 g/L fructose prepared in the fermenter. The shake flask experiment was started with a sterile sample from the fermenter at 30 °C, 350 rpm, V_L = 10 mL in 250 mL flasks, pH_{start} = 6 and a shaking diameter of 50 mm using the RAMOS system. Fermentation was performed with 1 L filling volume in a L fermenter, DOT was kept ≥ 30% by variation of the agitation speed (500–1250 rpm), aeration rate (Q) = 1 L/min, 30 °C. **Figure S3.** Cultivation of *G. oxydans* IK003.1-igr3::*fdhSCL* in a 2 L fermenter with 100 mM MES and 80 g/L fructose. Depicted is (**a**) the oxygen and carbon dioxide transfer rates (OTR and CTR), (**b**) optical density (OD_{600}) and pH, (**c**) dissolved oxygen tension (DOT) and agitation speed, and (**d**) fructose and 5-ketofructose concentrations. The cultivation was performed with 1 L filling volume, DOT ≥ 30% controlled by agitation speed (500–1500 rpm), aeration rate (Q) = 1 L/min, T = 30 °C. **Figure S4.** Cultivation of *G. oxydans* IK003.1-igr3::*fdhSCL* in a 2 L fermenter with 80 g/L fructose and pH control. Depicted is (**a**) the oxygen and carbon dioxide transfer rates (OTR and CTR), (**b**) optical density (OD_{600}) and pH, (**c**) dissolved oxygen tension (DOT) and agitation speed, and (**d**) fructose and 5-ketofructose concentrations. The cultivation was performed with 1 L filling volume, DOT ≥ 30% controlled by agitation speed (500–1500 rpm), aeration rate (Q) = 1 L/min, T = 30 °C. **Figure S5.** Cultivation of *G. oxydans* IK003.1-igr3::*fdhSCL* in a RAMOS device with different fructose concentrations and 150 mM MES (initial pH of 6). Depicted is the oxygen transfer rate during growth with the indicated concentrations of fructose in complex medium at 30 °C, 350 rpm, V_L = 10 mL in 250 mL flasks, pH_{start} = 6 and a shaking diameter of 50 mm. Shown are mean values of duplicates. **Figure S6.** Cultivation of the indicated *G. oxydans* strains in a RAMOS device with 80 g/L fructose and 150 mM MES (initial pH of 6). Depicted is (**a**) the 5-ketofructose concentration (HPLC method B), the yield g/g, the OD_{600} and the final pH after 29 h and (**b**) the oxygen transfer rate (OTR). Cultivations were performed in complex medium with 80 g/L fructose and 150 mM MES buffer at 30 °C, 350 rpm, V_L = 10 mL in 250 mL flasks, pH_{start} = 6 and a shaking diameter of 50 mm. Shown are mean values of duplicates.

Abbreviations

5-KF: 5-Keto-D-fructose; CTR: Carbon dioxide transfer rate; DOT: Dissolved oxygen tension; DNA: Deoxyribonucleic acid; FAD: Flavin adenine dinucleotide; FDH: Fructose dehydrogenase; FPKM: Fragments Per Kilobase of transcript per Million mapped reads; HPLC: High-performance liquid chromatography; IGRs: Intergenic regions; MES: 2-(N-Morpholino)ethansulfonic acid; OD_{600}: Optical density at 600 nm; ori: Origin of replication; OTR: Oxygen transfer rate; RAMOS: Respiration activity MOnitoring System; RBS: Ribosome binding site; RT-qPCR: Reverse transcription quantitative polymerase chain reaction; RQ: Respiratory quotient; TCA: Tricarboxylic acid cycle; TCE: Total carbon dioxide evolution; TOC: Total oxygen consumption; vvm: Vessel volume per minute.

Authors' contributions

SB designed and performed characterization and optimization experiments in shake flasks with online monitoring (RAMOS), scale up and fermentation experiments, analyzed the data and drafted the manuscript. KW constructed the integration strains, designed and performed the shake flask cultivations and the RT-qPCR, analyzed the data and drafted the manuscript. CI performed the scale up experiments. AK selected the integration sites. MP performed some of the shake flask cultivations with online monitoring. AW set up HPLC method A. MBo, JB and MBa supervised the study, assisted in data interpretation and participated in drafting the manuscript. All authors read and approved the final manuscript.

Funding

This work was financially supported by the Bundesministerium für Bildung und Forschung (BMBF) within Project No. 031B0370 by grants given to Michael Bott (031B0370B) and Jochen Büchs (031B0370C).

Availability of data and materials

The datasets supporting the conclusions of this article are included within the article and the additional file (Additional file1: Tables S1, S2, and S3, Figures S1, S2, S3, S4, S5, and S6).

Ethics approval and consent to participate

Not applicable.

Consent for publication

Not applicable.

Competing interests
The authors declare that they have no competing interest.

Received: 9 December 2019 Accepted: 17 February 2020
Published online: 04 March 2020

References

1. Matsushita K, Toyama H, Adachi O. Respiratory chains and bioenergetics of acetic acid bacteria. In: Rose AH, editor. Advances in Microbiol Physiology, vol. 36. Tempest DW: Academic Press; 1994. p. 247–301.
2. Richhardt J, Luchterhand B, Bringer S, Büchs J, Bott M. Evidence for a key role of cytochrome bo_3 oxidase in respiratory energy metabolism of *Gluconobacter oxydans*. J Bacteriol. 2013;195:4210–20.
3. Miura H, Mogi T, Ano Y, Migita CT, Matsutani M, Yakushi T, Kita K, Matsushita K. Cyanide-insensitive quinol oxidase (CIO) from *Gluconobacter oxydans* is a unique terminal oxidase subfamily of cytochrome *bd*. J Biochem. 2013;153:535–45.
4. De Muynck C, Pereira CS, Naessens M, Parmentier S, Soetaert W, Vandamme EJ. The genus *Gluconobacter oxydans*: comprehensive overview of biochemistry and biotechnological applications. Crit Rev Biotechnol. 2007;27:147–71.
5. Deppenmeier U, Hoffmeister M, Prust C. Biochemistry and biotechnological applications of *Gluconobacter* strains. Appl Microbiol Biotechnol. 2002;60:233–42.
6. Gupta A, Singh VK, Qazi GN, Kumar A. *Gluconobacter oxydans*: its biotechnological applications. J Mol Microbiol Biotechnol. 2001;3:445–56.
7. Hölscher T, Schleyer U, Merfort M, Bringer-Meyer S, Görisch H, Sahm H. Glucose oxidation and PQQ-dependent dehydrogenases in *Gluconobacter oxydans*. J Mol Microbiol Biotechnol. 2009;16:6–13.
8. Saichana N, Matsushita K, Adachi O, Frebort I, Frebortova J. Acetic acid bacteria: a group of bacteria with versatile biotechnological applications. Biotechnol Adv. 2015;33:1260–71.
9. Reichstein T, Grüssner A. Eine ergiebige Synthese der L-Ascorbinsäure (C-vitamin). Helv Chim Acta. 1934;17:311–28.
10. Pappenberger G, Hohmann HP. Industrial production of L-ascorbic acid (vitamin C) and D-isoascorbic acid. Adv Biochem Eng Biotechnol. 2014;143:143–88.
11. Gätgens C, Degner U, Bringer-Meyer S, Herrmann U. Biotransformation of glycerol to dihydroxyacetone by recombinant *Gluconobacter oxydans* DSM 2343. Appl Microbiol Biotechnol. 2007;76:553–9.
12. Ke X, Pan-Hong Y, Hu ZC, Chen L, Sun XQ, Zheng YG. Synergistic improvement of PQQ-dependent D-sorbitol dehydrogenase activity from *Gluconobacter oxydans* for the biosynthesis of miglitol precursor 6-(N-hydroxyethyl)-amino-6-deoxy-alpha-L-sorbofuranose. J Biotechnol. 2019;300:55–62.
13. Schedel M. Weiße biotechnologie bei Bayer healthcare product supply: mehr als 30 Jahre Erfahrung. Chem Ing Tec. 2006;78:485–9.
14. Prust C, Hoffmeister M, Liesegang H, Wiezer A, Fricke WF, Ehrenreich A, Gottschalk G, Deppenmeier U. Complete genome sequence of the acetic acid bacterium *Gluconobacter oxydans*. Nat Biotechnol. 2005;23:195.
15. Hanke T, Nöh K, Noack S, Polen T, Bringer S, Sahm H, Wiechert W, Bott M. Combined fluxomics and transcriptomics analysis of glucose catabolism via a partially cyclic pentose phosphate pathway in *Gluconobacter oxydans* 621H. Appl Environ Microbiol. 2013;79:2336–48.
16. Krajewski V, Simic P, Mouncey NJ, Bringer S, Sahm H, Bott M. Metabolic engineering of *Gluconobacter oxydans* for improved growth rate and growth yield on glucose by elimination of gluconate formation. Appl Environ Microbiol. 2010;76:4369–76.
17. Kiefler I, Bringer S, Bott M. Metabolic engineering of *Gluconobacter oxydans* 621H for increased biomass yield. Appl Microbiol Biotechnol. 2017;101:5453–67.
18. Carocho M, Morales P, Ferreira I. Sweeteners as food additives in the XXI century: a review of what is known, and what is to come. Food Chem Toxicol. 2017;107:302–17.
19. Hu FB, Malik VS. Sugar-sweetened beverages and risk of obesity and type 2 diabetes: epidemiologic evidence. Physiol Behav. 2010;100:47–54.
20. Yang Q, Zhang Z, Gregg EW, Flanders WD, Merritt R, Hu FB. Added sugar intake and cardiovascular diseases mortality among US adults. JAMA Intern Med. 2014;174:516–24.
21. Mattes RD, Popkin BM. Nonnutritive sweetener consumption in humans: effects on appetite and food intake and their putative mechanisms. Am J Clin Nutr. 2009;89:1–14.
22. Hellfritsch C, Brockhoff A, Stähler F, Meyerhof W, Hofmann T. Human psychometric and taste receptor responses to steviol glycosides. J Agric Food Chem. 2012;60:6782–93.
23. Wyrobnik DH, Wyrobnik IH, Silcoff ER: Agent for reducing the useable calorie content of food and for therapeutic reduction of weight, in particular for use in the case of adiposity (obesity). Patent Application No. US 2009/0060956A1; 2009.
24. Blasi M, Barbe JC, Dubourdieu D, Deleuze H. New method for reducing the binding power of sweet white wines. J Agric Food Chem. 2008;56:8470–4.
25. Barbe J-C, De Revel G, Joyeux A, Bertrand A, Lonvaud-Funel A. Role of botrytized grape micro-organisms in SO_2 binding phenomena. J Appl Microbiol. 2001;90:34–42.
26. Herweg E, Schöpping M, Rohr K, Siemen A, Frank O, Hofmann T, Deppenmeier U, Büchs J. Production of the potential sweetener 5-ketofructose from fructose in fed-batch cultivation with *Gluconobacter oxydans*. Bioresour Technol. 2018;259:164–72.
27. Richhardt J, Bringer S, Bott M. Mutational analysis of the pentose phosphate and Entner–Doudoroff pathways in *Gluconobacter oxydans* reveals improved growth of a *Δedd Δeda* mutant on mannitol. Appl Environ Microbiol. 2012;78:6975–86.
28. Ameyama M, Shinagawa E, Matsushita K, Adachi O. D-Fructose dehydrogenase of *Gluconobacter industrius* - purification, characterization, and application to enzymatic micro-determination of D-Fructose. J Bacteriol. 1981;145:814–23.
29. Kawai S, Goda-Tsutsumi M, Yakushi T, Kano K, Matsushita K. Heterologous overexpression and characterization of a flavoprotein-cytochrome *c* complex fructose dehydrogenase of *Gluconobacter japonicus* NBRC3260. Appl Environ Microbiol. 2013;79:1654–60.
30. Siemen A, Kosciow K, Schweiger P, Deppenmeier U. Production of 5-ketofructose from fructose or sucrose using genetically modified *Gluconobacter oxydans* strains. Appl Microbiol Biotechnol. 2018;102:1699–710.
31. Hoffmann JJ, Hovels M, Kosciow K, Deppenmeier U. Synthesis of the alternative sweetener 5-ketofructose from sucrose by fructose dehydrogenase and invertase producing *Gluconobacter* strains. J Biotechnol. 2020;307:164–74.
32. Kranz A, Vogel A, Degner U, Kiefler I, Bott M, Usadel B, Polen T. High precision genome sequencing of engineered *Gluconobacter oxydans* 621H by combining long nanopore and short accurate Illumina reads. J Biotechnol. 2017;258:197–205.
33. Kranz A, Busche T, Vogel A, Usadel B, Kalinowski J, Bott M, Polen T. RNAseq analysis of α-proteobacterium *Gluconobacter oxydans* 621H. BMC Genomics. 2018;19:24.
34. Naville M, Ghuillot-Gaudeffroy A, Marchais A, Gautheret D. ARNold: a web tool for the prediction of Rho-independent transcription terminators. RNA Biol. 2011;8:11–3.
35. Peters B, Junker A, Brauer K, Mühlthaler B, Kostner D, Mientus M, Liebl W, Ehrenreich A. Deletion of pyruvate decarboxylase by a new method for efficient markerless gene deletions in *Gluconobacter oxydans*. Appl Microbiol Biotechnol. 2013;97:2521–30.
36. Ano Y, Hours RA, Akakabe Y, Kataoka N, Yakushi T, Matsushita K, Adachi O. Membrane-bound glycerol dehydrogenase catalyzes oxidation of D-pentonates to 4-keto-D-pentonates, D-fructose to 5-keto-D-fructose, and D-psicose to 5-keto-D-psicose. Biosci Biotechnol Biochem. 2017;81:411–8.
37. Anderlei T, Büchs J. Device for sterile online measurement of the oxygen transfer rate in shaking flasks. Biochem Eng J. 2001;7:157–62.
38. Anderlei T, Zang W, Papaspyrou M, Büchs J. Online respiration activity measurement (OTR, CTR, RQ) in shake flasks. Biochem Eng J. 2004;17:187–94.
39. Deppenmeier U, Ehrenreich A. Physiology of acetic acid bacteria in light of the genome sequence of *Gluconobacter oxydans*. J Mol Microbiol Biotechnol. 2009;16:69–80.
40. Olijve W, Kok JJ. Analysis of growth of *Gluconobacter oxydans* in glucose containing media. Arch Microbiol. 1979;121:283–90.
41. Luchterhand B, Fischöder T, Grimm AR, Wewetzer S, Wunderlich M, Schlepütz T, Büchs J: Quantifying the sensitivity of *G. oxydans* ATCC 621H and DSM 3504 to osmotic stress triggered by soluble buffers. *J Ind Microbiol Biotechnol* 2015, 42:585-600.

42. Kandegedara A, Rorabacher DB. Noncomplexing tertiary amines as "better" buffers covering the range of pH 3–11. Temperature dependence of their acid dissociation constants. Anal Chem. 1999;71:3140–4.
43. Kiefler I. Strain development of *Gluconobacter oxydans*: Complementation of non-functional metabolic pathways and increase of carbon flux. Dissertation, University of Düsseldorf, Germany. 2016.
44. Kallnik V, Meyer M, Deppenmeier U, Schweiger P. Construction of expression vectors for protein production in *Gluconobacter oxydans*. J Biotechnol. 2010;150:460–5.
45. Schweiger P, Volland S, Deppenmeier U. Overproduction and characterization of two distinct aldehyde-oxidizing enzymes from *Gluconobacter oxydans* 621H. J Mol Microbiol Biotechnol. 2007;13:147–55.
46. Meyer M, Schweiger P, Deppenmeier U. Effects of membrane-bound glucose dehydrogenase overproduction on the respiratory chain of *Gluconobacter oxydans*. Appl Microbiol Biotechnol. 2013;97:3457–66.
47. Lal A, Dhar A, Trostel A, Kouzine F, Seshasayee AS, Adhya S. Genome scale patterns of supercoiling in a bacterial chromosome. Nat Commun. 2016;7:11055.
48. Großmann P, Lück A, Kaleta C. Model-based genome-wide determination of RNA chain elongation rates in *Escherichia coli*. Sci Rep. 2017;7:17213.
49. Dorman CJ, Dorman MJ. DNA supercoiling is a fundamental regulatory principle in the control of bacterial gene expression. Biophys Rev. 2016;8:89–100.
50. El Houdaigui B, Forquet R, Hindré T, Schneider D, Nasser W, Reverchon S, Meyer S. Bacterial genome architecture shapes global transcriptional regulation by DNA supercoiling. Nucleic Acids Res. 2019;47:5648–57.
51. Sutormin D, Rubanova N, Logacheva M, Ghilarov D, Severinov K. Single-nucleotide-resolution mapping of DNA gyrase cleavage sites across the *Escherichia coli* genome. Nucleic Acids Res. 2019;47:1373–88.
52. Landick R, Wade JT, Grainger DC. H-NS and RNA polymerase: a love–hate relationship? Curr Opin Microbiol. 2015;24:53–9.
53. Browning DF, Grainger DC, Busby SJW. Effects of nucleoid-associated proteins on bacterial chromosome structure and gene expression. Curr Opin Microbiol. 2010;13:773–80.
54. Richhardt J, Bringer S, Bott M. Role of the pentose phosphate pathway and the Entner-Doudoroff pathway in glucose metabolism of *Gluconobacter oxydans* 621H. Appl Microbiol Biotechnol. 2013;97:4315–23.
55. Bertani G. Studies on lysogenesis.I. The mode of phage liberation by lysogenic *Escherichia coli*. J Bacteriol. 1951;62:293–300.
56. Gibson DG. Enzymatic assembly of overlapping DNA fragments. Methods Enzymol. 2011;498:349–61.
57. Hanahan D. Studies on transformation of *Escherichia coli* with plasmids. J Mol Biol. 1983;166:557–80.
58. Seletzky JM, Noack U, Hahn S, Knoll A, Amoabediny G, Büchs J. An experimental comparison of respiration measuring techniques in fermenters and shake flasks: exhaust gas analyzer vs. RAMOS device vs. respirometer. J Ind Microbiol Biotechnol. 2007;34:123–30.
59. Seletzky JM, Noak U, Fricke J, Welk E, Eberhard W, Knocke C, Büchs J. Scale-up from shake flasks to fermenters in batch and continuous mode with *Corynebacterium glutamicum* on lactic acid based on oxygen transfer and pH. Biotechnol Bioeng. 2007;98:800–11.
60. Silberbach M, Maier B, Zimmermann M, Büchs J. Glucose oxidation by *Gluconobacter oxydans*: characterization in shaking-flasks, scale-up and optimization of the pH profile. Appl Microbiol Biotechnol. 2003;62:92–8.
61. Untergasser A, Nijveen H, Rao X, Bisseling T, Geurts R, Leunissen JA. Primer3Plus, an enhanced web interface to Primer3. Nucleic Acids Res. 2007;35:W71–4.
62. Simon R, Priefer U, Pühler A. A broad host range mobilization system for in vivo genetic engineering: transposon mutagenesis in Gram negative bacteria. Bio/Technology. 1983;1:784–91.

Publisher's Note

Additional file 1

Novel plasmid-free *Gluconobacter oxydans* strains for production of the natural sweetener 5-ketofructose

Svenja Battling[1†], Karen Wohlers[2†], Chika Igwe[1], Angela Kranz[2], Matthias Pesch[1], Astrid Wirtz[2], Meike Baumgart[2], Jochen Büchs[1]* and Michael Bott[2]*

1 AVT-Biochemical Engineering, RWTH Aachen University, Forckenbeckstraße 51, 52074 Aachen, Germany
2 IBG-1: Biotechnologie, Institut für Bio- und Geowissenschaften, Forschungszentrum Jülich GmbH, 52425 Jülich, Germany

*Correspondence: jochen.buechs@avt.rwth-aachen.de; m.bott@fz-juelich.de
†Svenja Battling and Karen Wohlers contributed equally to this manuscript

Table S1. Offline data for cultivation of the indicated *G. oxydans* strains with 80 g/L fructose in a RAMOS device

Table S2. Offline date for the cultivation of *G. oxydans* IK003.1-igr3::*fdhSCL* in a RAMOS device with different fructose concentrations

Table S3. Oligonucleotides used in this study.

Figure S1. Cultivation of the indicated *G. oxydans* strains with 80 g/L fructose in a RAMOS device with online monitoring.

Figure S2. Scale-up of batch fermentation of *G. oxydans* IK003.1-igr3::*fdhSCL* from shake flasks (RAMOS device) to a 2 L fermenter with 80 g/L fructose and 150 mM MES.

Figure S3. Cultivation of *G. oxydans* IK003.1-igr3::*fdhSCL* in a 2 L fermenter with 100 mM MES and 80 g/L fructose.

Figure S4. Cultivation of *G. oxydans* IK003.1-igr3::*fdhSCL* in a 2 L fermenter with 80 g/L fructose and pH control.

Figure S5. Cultivation of *G. oxydans* IK003.1-igr3::*fdhSCL* in a RAMOS device with different fructose concentrations and 150 mM MES (initial pH of 6)

Figure S6. Cultivation of the indicated *G. oxydans* strains in a RAMOS device with 80 g/L fructose and 150 mM MES (initial pH of 6).

Table S1. Offline data for cultivation of the indicated *G. oxydans* strains with 80 g/L fructose in a RAMOS device shown in Fig. S1.[1]

G. oxydans strain	Residual Fructose (g/L)	5-Ketofructose (g/L)	Yield (g/g)	OD_{600}	pH
IK003.1	69	3	0.04	3.6	3.8
IK003.1 pBBRp264-*fdhSCL*-ST	0	70	0.88	3.2	3.6
IK003.1-igr1::*fdhSCL*	45	29	0.36	3.2	3.4
IK003.1-igr2::*fdhSCL*	31	42	0.51	3.5	3.3
IK003.1-igr3::*fdhSCL*	25	47	0.58	3.8	3.3
IK003.1 Δ*sdh*::*fdhSCL*	32	38	0.47	3.6	3.3

[1] The data were measured after 29 h of cultivation. Fructose and 5-KF were determined by HPLC (method B). The yield represents $g_{5\text{-KF}}/g_{fructose,total}$. The strains were cultivated in complex medium with 80 g/L fructose at 30 °C, 350 rpm and a shaking diameter of 50 mm.

Table S2. Offline date for the cultivation of *G. oxydans* IK003.1-igr3::*fdhSCL* in a RAMOS device with different fructose concentrations shown in Fig. S5.[1]

Fructose (g/L)	Osmolality (Osmol/kg)	5-Ketofructose (g/L)	Yield (g/g)	OD_{600}	pH
80	0.8	60	0.77	5.30	5.0
100	0.9	75	0.77	5.30	4.9
120	1.1	96	0.80	5.00	4.8
160	1.4	141	0.86	4.60	4.7
180	1.6	150	0.84	4.00	4.7
210	1.8	164	0.78	3.50	4.9

[1]The values for 5-KF, yield, OD_{600} and pH were measured after 25 h (80 g/L -120 g/L fructose) and after 72 h (160 g/L – 210 g/L fructose).

Table S3. Oligonucleotides used in this study

Oligonucleotide	Sequence (5'→ 3') and properties[a]
Oligonucleotides for Cloning	
P264-fwd	CGTTGCGCCTGAATGAGAGGAAAG
P264-rev-RBS-overlap	**CCATCTGCAGTCCTCCTTTC**TTCGGTCTCCCTCGCCGTAAAC
RBS-ATG-fdhSCL-fwd	**GAAAGGAGGACTGCAGA**TGGAAAAAATAGCTGATTCCGGCCCTG
fdhSCL-rev	TTACCCCTGTTTCAGGTCATTGAG
Term-GOX0028-fwd-fdhL-overlap	**ATGACCTGAAACAGGGGTAA**GCGCGTTCCCGAGCGGTTC
Term-GOX0028-rev	AGACTGAAGTCTCGGTTCAGACAGATAAAAAAAG
FlA-igr1-fwd-pAJ-overlap	**TACGAATTCGAGCTCGGTAC**AACCTGACCAGCTCAACACTGGG
FlA-igr1-rev-fdhSCL-overlap	**CCTCTCATTCAGGCGCAACG**CCTCGTGAACTGAAAGACCG
FlB-igr1-fwd-Term-overlap	**CTGAACCGAGACTTCAGTCT**ATATCTCGCTCCTGCCCTGTG
FlB-igr1-rev-pAJ63a-overlap	**GCCAAGCTTGCATGCCTGCA**TTACGCTTATGCGTTCGCGCC
FlA-igr2-fwd-pAJ-overlap	**TACGAATTCGAGCTCGGTAC**TCTCACTTCAGCGCCGCCATC
FlA-igr2-rev-fdhSCL-overlap	**CCTCTCATTCAGGCGCAACG**AGACAGATAAAAAAAGCCGGTCCCGC
FlB-igr2-fwd-Term-overlap	**CTGAACCGAGACTTCAGTCT**GAACCGAGACTTCAGTCTGC
FlB-igr2-rev-pAJ63a-overlap	**GCCAAGCTTGCATGCCTGCA**CACGTCATCATGAAAGTGCATC
FlB-igr3-fwd-Term-overlap	**TACGAATTCGAGCTCGGTAC**CATCTGGCCGCCCATCCC
FlB-igr3-rev-pAJ63a-overlap	**CCTCTCATTCAGGCGCAACG**GCACTAATCCGAAAAGAGCGGTTG
FlB-igr3-fwd-Term-overlap	**CTGAACCGAGACTTCAGTCT**TCGATCAGACCTGTGTGTTC
FlB-igr3-rev-pAJ63a-overlap	**GCCAAGCTTGCATGCCTGCA**TTACGACATGGAACCGGGC
FlB-sdh-fwd-Term-overlap	**TACGAATTCGAGCTCGGTAC**CAGAGCCTGCAACCGGCG
FlB-sdh-rev-pAJ63a-overlap	**CCTCTCATTCAGGCGCAACG**TTTGATCTGAAGACATAGGAGATGCTG
FlB-sdh-fwd-Term-overlap	**CTGAACCGAGACTTCAGTCT**TGGTCTTTCCTTATTGGTGGAACGG
FlB-sdh-rev-pAJ63a-overlap	**GCCAAGCTTGCATGCCTGCA**TCGCCGGTTTCCTGCTTCTC
Oligonucleotides for sequencing and colony-PCR	
pAJ63a-seq-fwd	TGCTTCCGGCTCGTATGTTG
pAJ63a-seq-rev	GGATGTGCTGCAAGGCGATTAAG
fdh-seq-fwd2	GTGGTTATGCCATTTCTTCCCC
fdh-seq-fwd3	AACCGATGGTGCTGCACTC
fdh-seq-fwd4	CCCGCATACCAACTACTTCC
fdh-seq-rev	CCGGCATGACATCGACGG
Integr-igr1-seq-fwd	TGGCAATATTCTCGGCTTCAC
Integr-igr1-seq-rev	CGTGATCGAAACGCCTCTGC
Integr-igr2-seq-fwd	TCACCGCCACAGGCTTTG
Integr-igr2-seq-rev	GCTGGGTTCAGCCATAGC
Integr-igr3-seq-fwd	CAGCGAGGCCTATGCCAAAC
Integr-igr3-seq-rev	GATGATGCGGGCCTGGAC
Integr-sdh-seq-rev	GCTGATGCGGATGTCACGTC
Integr-sdh-seq-fwd	CGGGGTGTGTGGCATGTC
Oligonucleotides for RT-qPCR	
q-fdhS-fwd1	AGCCTAACAGTCGCAGCAAT
q-fdhS-rev1	AAGCGGAAAGCTGCATAAAA
q-fdhS-fwd2	CCCACGCTCATCCAGATTAT
q-fdhS-rev2	GGGACGGCTGATACATGAGT
q-fdhC-fwd	TACCCACAATGACGACTGGA
q-fdhC-rev	ACTGATTGGGCGCTAGAAGA
q-GOX0264-fwd	AGACCAAGTCGTCGGTCAAG
q-GOX0264-rev	GTTGGTGCGCTTCATCTTCT
q-gap-fwd1	TCCGACTTCAACCATGACAA
q-gap-rev1	TTGTCGTACCACGAGCAGAC
q-gap-rev1b	GTTGTCGTACCACGAGCAGA
q-gap-fwd2	ATGATCAGGCTGTTGCCTTC
q-gap-rev2	TTGTCGCCATCAACGATCTG

[a] overlaps for Gibson Assembly in bold

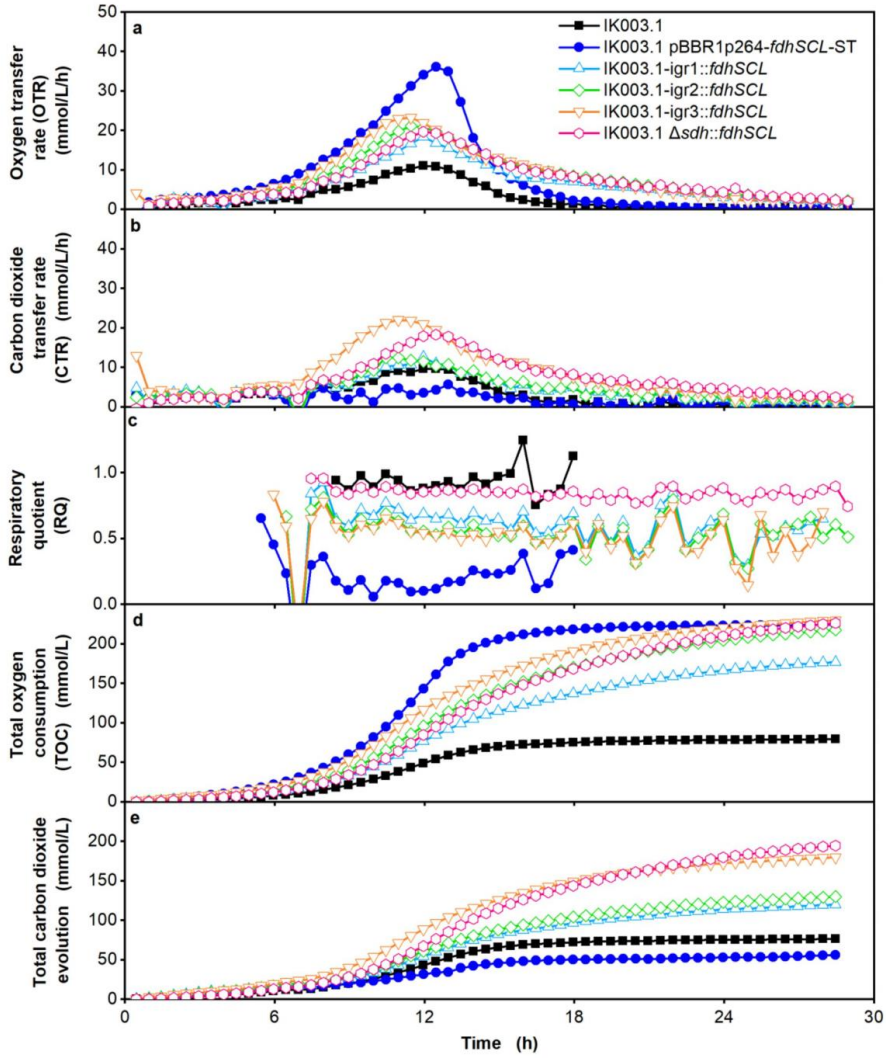

Figure S1. Cultivation of the indicated *G. oxydans* strains with 80 g/L fructose in a RAMOS device with online monitoring. Depicted are (**a**) the oxygen transfer rate (OTR), (**b**) the carbon dioxide transfer rate (CTR), (**c**) the respiratory quotient (RQ shown for OTR values above 5 mmol/L/h), (**d**) the total oxygen consumption (TOC) and (e) the total carbon dioxide evolution (TCE). The strains were cultivated in complex medium with 80 g/L fructose at 30 °C, 350 rpm, V_L = 10 mL in 250 mL flasks, pH_{start} = 6 and a shaking diameter of 50 mm. Shown are mean values of duplicates.

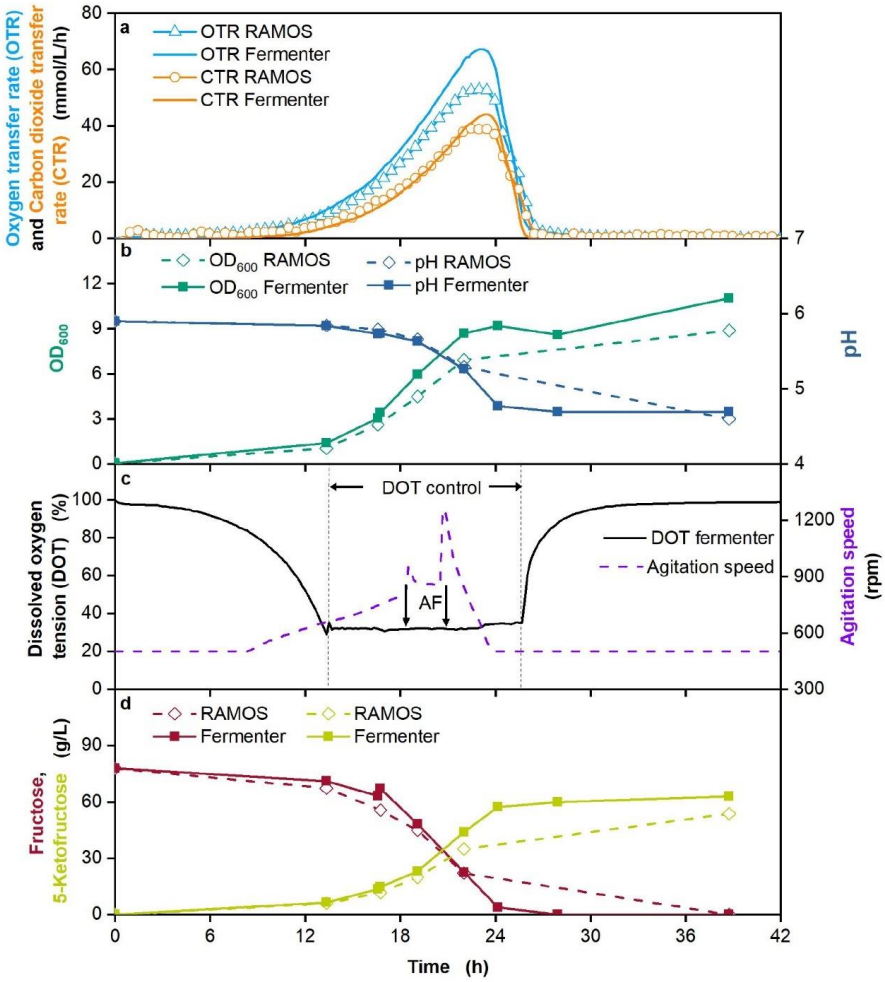

Figure S2. Scale-up of batch fermentation of *G. oxydans* IK003.1-igr3::*fdhSCL* from shake flasks (RAMOS device) to a 2 L fermenter with 80 g/L fructose and 150 mM MES. Depicted are (**a**) oxygen transfer rate (OTR) and carbon dioxide transfer rate (CTR), (**b**) growth as OD_{600} and pH, (**c**) dissolved oxygen tension (DOT), agitation speed during fermentation, addition of antifoam agent (AF), and period of DOT control (indicated by arrows) and (**d**) fructose and 5-ketofructose concentration as determined by HPLC (method B). Cultivations were performed in complex medium with 80 g/L fructose prepared in the fermenter. The shake flask experiment was started with a sterile sample from the fermenter at 30 °C, 350 rpm, V_L = 10 mL in 250 mL flasks, pH_{start} = 6 and a shaking diameter of 50 mm using the RAMOS system. Fermentation was performed with 1 L filling volume in a 2 L fermenter, DOT was kept ≥ 30 % by variation of the agitation speed (500 rpm – 1250 rpm), aeration rate (Q) = 1 L/min, 30 °C.

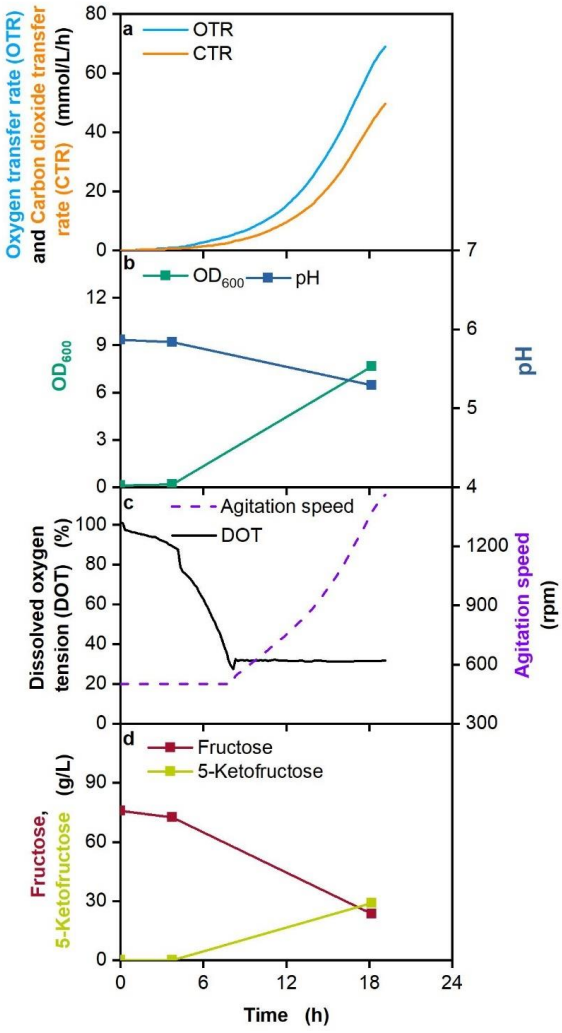

Figure S3. Cultivation of *G. oxydans* IK003.1-igr3::*fdhSCL* in a 2 L fermenter with 100 mM MES and 80 g/L fructose. Depicted is (**a**) the oxygen and carbon dioxide transfer rates (OTR and CTR), (**b**) optical density (OD_{600}) and pH, (**c**) dissolved oxygen tension (DOT) and agitation speed, (**d**) fructose and 5-ketofructose concentrations. The cultivation was performed with 1 L filling volume, DOT ≥ 30 % controlled by agitation speed (500 rpm – 1500 rpm), aeration rate (Q) = 1 L/min, T = 30 °C.

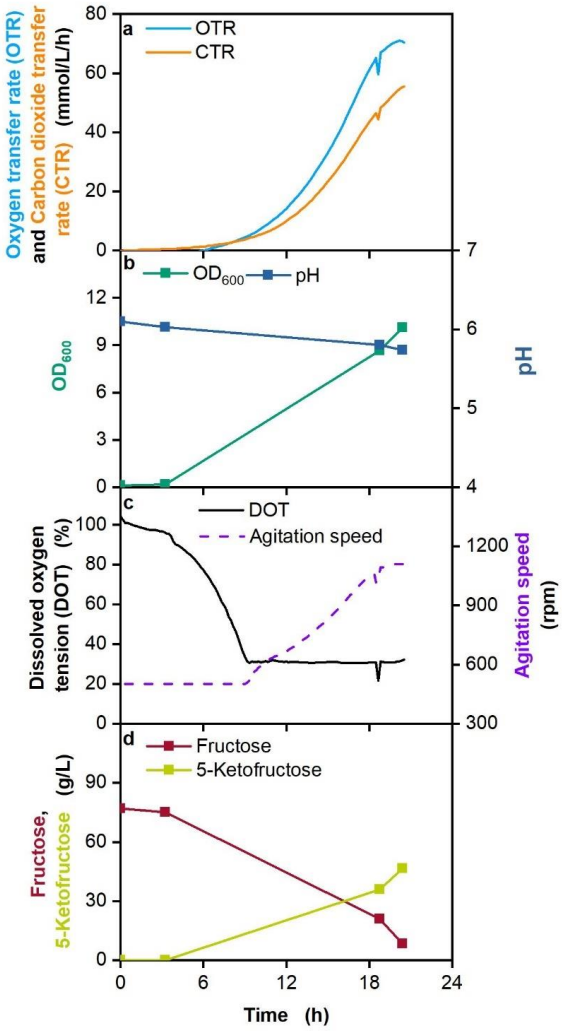

Figure S4. Cultivation of *G. oxydans* IK003.1-igr3::*fdhSCL* in a 2 L fermenter with 80 g/L fructose and pH control. Depicted is (**a**) the oxygen and carbon dioxide transfer rates (OTR and CTR), (**b**) optical density (OD_{600}) and pH, (**c**) dissolved oxygen tension (DOT) and agitation speed, (**d**) fructose and 5-ketofructose concentrations. The cultivation was performed with 1 L filling volume, DOT ≥ 30 % controlled by agitation speed (500 rpm – 1500 rpm), aeration rate (Q) = 1 L/min, T = 30 °C.

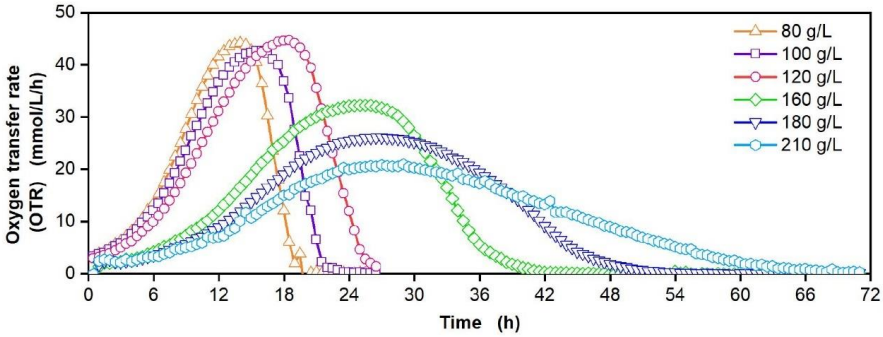

Figure S5. Cultivation of *G. oxydans* IK003.1-igr3::*fdhSCL* in a RAMOS device with different fructose concentrations and 150 mM MES (initial pH of 6). Depicted is the oxygen transfer rate during growth with the indicated concentrations of fructose in complex medium at 30 °C, 350 rpm, V_L = 10 mL in 250 mL flasks, pH_{start} = 6 and a shaking diameter of 50 mm. Shown are mean values of duplicates.

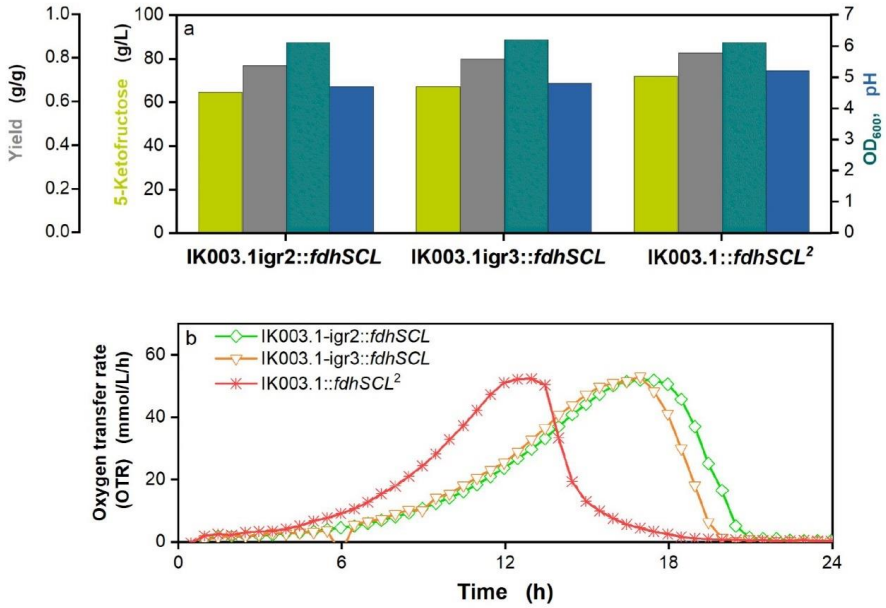

Figure S6. Cultivation of the indicated *G. oxydans* strains in a RAMOS device with 80 g/L fructose and 150 mM MES (initial pH of 6). Depicted is (**a**) the 5-ketofructose concentration (HPLC method B), the yield g/g$_{fr}$, the OD_{600} and the final pH after 29 h and (**b**) the oxygen transfer rate (OTR). Cultivations were performed in complex medium with 80 g/L fructose and 150 mM MES buffer at 30 °C, 350 rpm, V_L = 10 mL in 250 mL flasks, pH_{start} = 6 and a shaking diameter of 50 mm. Shown are mean values of duplicates.

2.2 Metabolic engineering of *Pseudomonas putida* for production of the natural sweetener 5-ketofructose from fructose and sucrose by periplasmic oxidation with a heterologous fructose dehydrogenase

Wohlers, K., Wirtz, A., Reiter, A., Oldiges, M., Baumgart, M., Bott, M. (2021). Microbial Biotechnology, doi: 10.1111/1751-7915.13913

Author contributions:

- KW designed and performed all experiments except the MS analysis, analyzed the data, and drafted the manuscript. All figures and tables resulted from these experiments.
- AW set up the HPLC method.
- AR performed MS analysis, supervised by MO.
- MBa and MBo supervised the study and assisted in data interpretation
- MBo was responsible for the final version of the manuscript.

Overall contribution KW: 90%

microbial biotechnology

Open Access

Metabolic engineering of *Pseudomonas putida* for production of the natural sweetener 5-ketofructose from fructose or sucrose by periplasmic oxidation with a heterologous fructose dehydrogenase

Karen Wohlers,[1] Astrid Wirtz,[1] Alexander Reiter,[1,2] Marco Oldiges,[1,2] Meike Baumgart[1] and Michael Bott[1,3]*

[1]*IBG-1: Biotechnology, Institute of Bio- and Geosciences, Forschungszentrum Jülich, Jülich, 52425, Germany.*

[2]*Institute of Biotechnology, RWTH Aachen University, Aachen, 52062, Germany.*

[3]*The Bioeconomy Science Center (BioSC), Forschungszentrum Jülich, Jülich, D-52425, Germany.*

Summary

5-Ketofructose (5-KF) is a promising low-calorie natural sweetener with the potential to reduce health problems caused by excessive sugar consumption. It is formed by periplasmic oxidation of fructose by fructose dehydrogenase (Fdh) of *Gluconobacter japonicus*, a membrane-bound three-subunit enzyme containing FAD and three haemes *c* as prosthetic groups. This study aimed at establishing *Pseudomonas putida* KT2440 as a new cell factory for 5-KF production, as this host offers a number of advantages compared with the established host *Gluconobacter oxydans*. Genomic expression of the *fdhSCL* genes from *G. japonicus* enabled synthesis of functional Fdh in *P. putida* and successful oxidation of fructose to 5-KF. In a batch fermentation, 129 g l^{-1} 5-KF were formed from 150 g l^{-1} fructose within 23 h, corresponding to a space-time yield of 5.6 g l^{-1} h^{-1}. Besides fructose, also sucrose could be used as substrate for 5-KF production by plasmid-based expression of the invertase gene *inv1417* from *G. japonicus*. In a bioreactor cultivation with pulsed sucrose feeding, 144 g 5-KF were produced from 358 g sucrose within 48 h. These results demonstrate that *P. putida* is an attractive host for 5-KF production.

Received 1 May, 2021; accepted 13 August, 2021.
*For correspondence. E-mail m.bott@fz-juelich.de; Tel. (+49) 2461 613294; Fax (+49) 2461 612710.
Microbial Biotechnology (2021) **0**(0), 1–13
doi:10.1111/1751-7915.13913

Introduction

Consumption of food and beverages with added sugars like sucrose or high-fructose corn syrup is linked to health problems like obesity, diabetes type 2 and cardiovascular diseases (Rippe and Angelopoulos, 2016; Carocho *et al.*, 2017). Reduction of added sugar consumption can be supported with non-nutritive sweeteners (Acero *et al.*, 2020). As such, 5-ketofuctose (5-KF) is an interesting product. It is a naturally occurring compound that has a similar taste and sweetness as fructose (Herweg *et al.*, 2018), but is not metabolized by the human body (Wyrobnik and Wyrobnik, 2006) and, as recently shown, not metabolized by 15 prominent bacterial species of the human gut microbiome (Schiessl *et al.*, 2021). 5-KF therefore meets crucial demands for a new sweetener. 5-KF can be synthesized biologically via fructose oxidation catalyzed by the fructose dehydrogenase (Fdh) of *Gluconobacter japonicus* (Ameyama *et al.*, 1981). This membrane-bound dehydrogenase is a heterotrimeric enzyme consisting of a small subunit FdhS with a Tat signal peptide, a large subunit FdhL with a covalently bound flavin adenine dinucleotide (FAD), and a cytochrome *c* subunit FdhC with three haem-binding motifs CXXCH, a Sec-signal peptide and a C-terminal transmembrane helix that anchors the entire periplasmic Fdh complex in the cytoplasmic membrane. FdhL lacks a signal peptide and is probably secreted into the periplasm pickaback with FdhS via the Tat export system (Kawai *et al.*, 2013). The industrially used cell factory *Gluconobacter oxydans* contains no endogenous Fdh activity (Ameyama *et al.*, 1981) and the genome does not contain homologs of *fdhSCL* (Prust *et al.*, 2005; Kranz *et al.*, 2017). However, plasmid-based heterologous expression of the *fdhSCL* genes from *G. japonicus* in *G.oxydans* led to much higher Fdh activities than observed for wild-type *G. japonicus* (Kawai *et al.*, 2013). Consequently, the subsequent studies on 5-KF production used recombinant strains of *G. oxydans*.

Equipped with various membrane-bound dehydrogenases (Deppenmeier *et al.*, 2002; Peters *et al.*, 2013), *G. oxydans* is an established host in industrial biotechnology for the periplasmic oxidation of substrates in a chemo-, stereo- and regio-specific manner (Reichstein

and Grüssner, 1934; De Muynck *et al.*, 2007). In previous studies, *G. oxydans* with plasmid-encoded Fdh reached high 5-KF production rates and in a fed-batch process, 5-KF titres of almost 500 g l^{-1} with a yield of up to 0.98 $g_{5\text{-KF}}/g_{fructose}$ were obtained (Herweg *et al.*, 2018; Siemen *et al.*, 2018). Hence, *G. oxydans* is a suitable host for 5-KF production from fructose. However, *G. oxydans* also has a number of limitations. It has a very low growth yield compared with other bacteria (Kiefler *et al.*, 2017) and culture media have to be supplemented with yeast extract or other complex nutrient sources in order to obtain fast growth. The number of genetic tools is also limited, although an efficient deletion system (Kostner *et al.*, 2013) and plasmids for constitutive and inducible expression (Kallnik *et al.*, 2010; Fricke *et al.*, 2020) are available. Our knowledge on many aspects of metabolism and in particular regulation in *G. oxydans* is very limited compared with other bacteria used as multipurpose production hosts in biotechnology, although there is continuous progress (Bringer and Bott, 2016; Schweikert *et al.*, 2021). These features impede the development of *G. oxydans* production strains by metabolic engineering and prompted us to search for an alternative host for 5-KF production that lacks the limitations described above.

In this study, we analysed the capabilities of *Pseudomonas putida* KT2440 to serve as production strain for 5-KF. *P. putida* is a metabolically versatile and robust organism for which plenty of knowledge and many tools and techniques for genetic engineering and heterologous expression are available (Loeschcke and Thies, 2015; Zobel *et al.*, 2015; Martínez-García and de Lorenzo, 2017; Nikel and de Lorenzo, 2018). *P. putida* shares a number of features with *G. oxydans* that make it a promising host for 5-KF production. Like *G. oxydans*, *P. putida* KT2440 is a strictly aerobic proteobacterium, which contains two membrane-bound dehydrogenases oxidizing glucose to gluconate and 2-ketogluconate in the periplasm. The glucose dehydrogenase (Gcd) is a PQQ-dependent enzyme (An and Moe, 2016), whereas gluconate dehydrogenase (Gad) consists of a cytochrome *c* subunit with a Sec-signal peptide, an FAD-containing subunit without a signal peptide, and a third small subunit with a Tat-signal peptide (Kumar *et al.*, 2013; Winsor *et al.*, 2016). These properties resemble those of Fdh of *G. japonicus* and suggest that functional expression of the *fdhSCL* genes in *P. putida* might be possible.

In contrast to *G. oxydans*, the oxidized products formed via periplasmic glucose oxidation by *P. putida* do not accumulate in the medium but the majority is taken up and metabolized in the cytoplasm. Similar to *G. oxydans*, *P. putida* lacks a complete Embden-Meyerhof-Parnas pathway and uses the EDEMP cycle for sugar metabolism (del Castillo *et al.*, 2007; Nikel *et al.*, 2015), whereas *G. oxydans* employs a partially cyclic pentose phosphate pathway as major route and the Entner-Doudoroff pathway is dispensable (Hanke *et al.*, 2013; Richhardt *et al.*, 2013). *P. putida*, in contrast to *G. oxydans*, possesses a complete tricarboxylic acid cycle, allowing complete oxidation of acetyl-CoA to CO_2. Differences also exist with respect to the respiratory chain. *P. putida* possesses a proton-pumping complex I-type NADH dehydrogenase, two non-proton-pumping type II NADH dehydrogenases, two ubiquinol oxidases (cytochrome bo_3 and a cyanide-insensitive *bd*-type oxidase CIO), a cytochrome bc_1 complex and three cytochrome *c* oxidases (cytochrome aa_3 and two cytochrome cbb_3 oxidases). *G. oxydans* possesses only a non-proton-pumping NADH dehydrogenase and two quinol oxidases. Consequently, the flexibility of the respiratory chain and the capabilities for proton-motive force generation are much lower for *G. oxydans* than for *P. putida*. As a consequence of these metabolic differences, the biomass yield of *P. putida* (about 0.5 g/g glucose) is about 5-fold higher than the one of *G. oxydans* (about 0.1 g/g glucose) and also the growth rates reported for *P. putida* (about 0.5–0.7 h^{-1}) surpass that of *G. oxydans* (about 0.3–0.5 h^{-1}) (del Castillo *et al.*, 2007; Ebert *et al.*, 2011; Richhardt *et al.*, 2012; Nikel *et al.*, 2015; Kiefler *et al.*, 2017). Another important difference to *G. oxydans* is that *P. putida* grows well in minimal media and does not require complex medium components.

P. putida can utilize fructose as carbon source. Fructose is taken up as fructose 1-phosphate via the PEP-dependent phosphotransferase system PTS^{Fru} composed of the two fusion proteins FruA (EIIB-EIIC) and FruB (EI-HPr-EIIA). Fructose 1-phosphate enters central carbon metabolism after phosphorylation by the kinase FruK to fructose 1,6-bisphosphate (Chavarría *et al.*, 2013). Besides fructose, sucrose is an interesting cheap substrate for 5-KF production, which is present for example in high amounts in sugar beet molasses (Sjölin *et al.*, 2019). Sucrose is naturally not metabolized by *P. putida* KT2440, but strains were constructed which were able to utilize sucrose by expression of the *cscA* and *cscB* genes of *Escherichia coli* W, encoding an invertase and a sucrose permease, respectively (Löwe *et al.*, 2017), or by expression of the *Pseudomonas protegens* Pf-5 *cscRABY* gene cluster for sucrose uptake and metabolism (Löwe *et al.*, 2020).

The aim of this study is the evaluation of *P. putida* as a new host for 5-KF production. As first step, we integrated the *fdhSCL* genes of *G. japonicus* into the chromosome of *P. putida* KT2440 via Tn*7* integration. The recombinant *P. putida::fdhSCL* was able to efficiently oxidize fructose to 5-KF. In order to utilize sucrose as substrate for 5-KF production, the *G. japonicus inv1417*

gene encoding a periplasmic invertase (Hoffmann *et al.*, 2020) was expressed in *P. putida*::*fdhSCL* and the resulting strain was able to grow on sucrose as sole carbon source and produce 5-KF from the disaccharide. In summary, we generated a potent 5-KF production strain of *P. putida* and thus showed that this organism is a suitable host for products requiring periplasmic oxidation.

Results and discussion

Generation of P. putida::fdhSCL *and test for 5-KF production*

To assess whether heterologous expression of the *G. japonicus* fructose dehydrogenase genes enables *P. putida* to oxidize fructose to 5-KF, the *fdhSCL* cluster was integrated into the genome of *P. putida* KT2440. For stable and strong expression, we used a pBG14g-derived vector for site-directed Tn*7* integration of *fdhSCL* under control of the strong constitutive synthetic 14g promoter followed by a BCD2 linker that serves as a translational coupler (Zobel *et al.*, 2015). BCD stands for bicistronic design. The BCD2 DNA sequence includes a ribosome binding site preceding a small ORF of 17 codons, which also includes the ribosome binding for the target gene to be expressed, in our case *fdhS*. The stop codon of this small ORF includes the A of the ATG start codon of the target gene. Translational couplers were shown to reduce effects of the target gene on translation (Mutalik *et al.*, 2013).

The recombinant strain *P. putida*::*fdhSCL* and its parental wild type were cultivated in mineral salts medium (MSM) with 100 mM fructose either as sole carbon source or in combination with 20 mM glucose to test for 5-KF production (Fig. 1). Glucose was added to enable faster growth and potentially increase yield and rate of 5-KF production. The wild type consumed only a small portion of the fructose (35 $\pm$ 4 mM) when grown either on fructose alone or with 20 mM glucose as additional carbon source (22 $\pm$ 4 mM) and did not form 5-KF. *P. putida*::*fdhSCL* consumed the entire fructose within 48 h of cultivation and formed 57 $\pm$ 4 mM 5-KF when cultivated with fructose alone and 67 $\pm$ 4 mM 5-KF when cultivated with fructose and glucose. An example HPLC chromatogram demonstrating 5-KF production in MSM with glucose and fructose as carbon sources is shown in Fig. S1. The molar yields (5-KF formed/fructose consumed) were 0.59 $\pm$ 0.02 in medium with only fructose and 0.68 $\pm$ 0.03 in glucose-supplemented medium. Although the molar yield related to the sum of fructose and glucose consumed (0.56 $\pm$ 0.03) was slightly lower compared with medium with fructose alone, glucose enabled much faster 5-KF production due to a reduced lag phase and an increased growth rate. Hence, glucose addition was also used in the following experiments.

In all cultures an acidification was observed. *P. putida* oxidizes a large fraction of the consumed glucose initially to gluconate, a fraction of which can remain in the medium and contribute to the acidification (Nikel *et al.*, 2015; Kohlstedt and Wittmann, 2019). A preliminary screening for organic acids in culture supernatants via dilute-and-shoot mass spectrometry (Reiter *et al.*, 2021) modified for detection of organic acids qualitatively identified gluconate, pyruvate and several intermediates of the TCA cycle (citrate, isocitrate, succinate, malate), suggesting that the acidification is due to the excretion of a mixture of organic acids. The pH decrease is important for 5-KF production, since Fdh has a pH optimum of about 4 (Kawai *et al.*, 2013).

The results described above show that *P. putida* is a suitable alternative host for 5-KF production and is able to functionally express the *fdhSCL* genes of *G. japonicus*. This is not self-evident as it requires covalent haem attachment to Sec-secreted FdhC, covalent FAD attachment to FdhL and Tat-dependent secretion of the FdhS-FdhL complex. In order to quantify Fdh activity, enzyme assays were performed with cell-free extracts using a spectrophotometric assay (Ameyama and Adachi, 1982) in which ferricyanide serves as electron acceptor and is reduced to ferrocyanide. Ferrocyanide is subsequently quantified as Prussian blue as described in the Experimental procedures section. For *P. putida*::*fdhSCL*, a specific Fdh activity of 1.23 $\pm$ 0.08 μmol min^{-1} (mg protein)$^{-1}$ was determined, which is comparable to the specific Fdh activity measured for *G. oxydans* IK003.1-igr3::*fdhSCL* (1.24 $\pm$ 0.15 μmol min^{-1} (mg protein)$^{-1}$) that served as positive control. No Fdh activity was detected for the parent strains of *P. putida* and *G. oxydans* that do not harbour the *fdhSCL* genes.

Bioreactor cultivation of P. putida::fdhSCL *with 150 g l^{-1} fructose*

The next experiment aimed at determining the potential of *P. putida*::*fdhSCL* for 5-KF production when cultivated under controlled conditions in a bioreactor with a high fructose concentration of 150 g l^{-1} (833 mM). For the cultivation in a DASGIP bioreactor, 1 l MSM medium pH 7 containing 150 g l^{-1} fructose and 3.6 g l^{-1} glucose was used. After the initial acidification phase, the pH was kept at pH 5.0 by automated addition of KOH. To prevent foam formation, headspace gassing was applied at a flow rate of 1 vvm and initial stirring at 500 rpm. The dissolved oxygen concentration (DO) was controlled at 30%. The medium was inoculated using overnight shake flask precultures in MSM with 150 g l^{-1} fructose and 3.6 g l^{-1} glucose. Four biological replicates were performed (Fig. S2) and a representative result of one of these cultivations is shown in Fig. 2. Despite the high

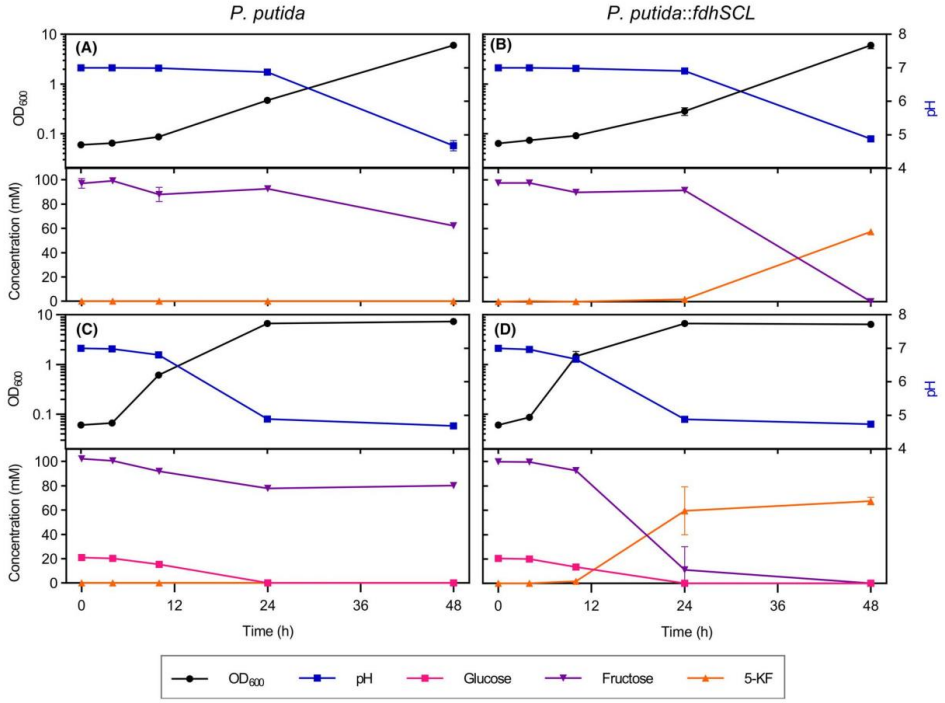

Fig. 1. Growth, pH, sugar consumption and 5-KF formation of *P. putida* and *P. putida::fdhSCL* in shake flasks. *P. putida* wild type (A, C) and *P. putida::fdhSCL* (B, D) were cultivated in 50 ml MSM with 100 mM fructose only (A, B) and MSM with 100 mM fructose and 20 mM glucose (C, D) in 500 ml shake flasks at 30 °C, 85% humidity, and 180 rpm with a shaking diameter of 50 mm. Glucose, fructose and 5-KF concentrations in the culture supernatant were determined by HPLC. Mean values and standard deviations of biological triplicates are shown.

sugar concentration, a growth rate of 0.48 ± 0.02 h^{-1} was observed. Glucose was completely consumed within the first 8 h of cultivation. The pH decreased from 7 to 5 within about 11 h (Fig. 2). 5-KF production correlated with fructose consumption. Within the first 4 h of cultivation, no 5-KF was produced, which might be due to the acidic pH optimum of Fdh (Kawai *et al.*, 2013). After 23 h, fructose had been completely consumed and 129 ± 5 g l^{-1} 5-KF (mean value and standard deviation of four biological replicates) had been formed, resulting in a yield of 0.88 ± 0.01 g 5-KF/g fructose and a space time yield of 5.60 ± 0.22 g l^{-1} h^{-1}. In our previous study with the *G. oxydans* strain IK003.1-igr3::*fdhSCL*, which also contains a genomically encoded Fdh, a 5-KF yield of 0.84 g/g was achieved within 27 h (Battling *et al.*, 2020). Consequently, *P. putida::fdhSCL* shows a comparable performance for 5-KF production as *G. oxydans* IK003.1-igr3::*fdhSCL*, but only requires a minimal medium and not a medium with yeast extract as *G. oxydans*. A comparison of relevant parameters of the two production strains is shown in Table 1.

Biotransformation with resting cells of P. putida *and* G. oxydans

To further compare *P. putida* and *G. oxydans* regarding their ability to produce 5-KF, resting cells of *P. putida*::*fdhSCL* and *G. oxydans* IK003.1-igr3::*fdhSCL* were used for the biotransformation of fructose to 5-KF. For this purpose, cell suspensions with an OD_{600} = 3 prepared in 100 mM potassium phosphate buffer pH 6 containing 150 g l^{-1} fructose were incubated at 30°C and 180 r.p.m. Both strains showed very similar conversion rates of 1.81 ± 0.1 g l^{-1} h^{-1} for *G. oxydans* IK003.1-igr3::*fdhSCL* and 1.80 ± 0.03 g l^{-1} h^{-1} for *P. putida*::*fdhSCL* (Fig. 3). No activity loss was observed during the 48 h

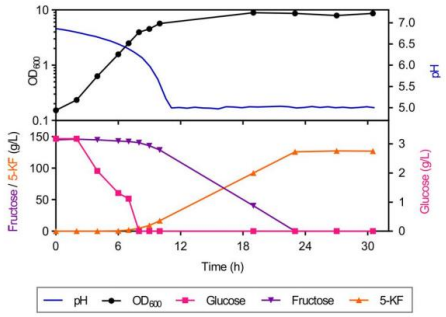

Fig. 2. Growth, pH, sugar consumption and 5-KF formation of *P. putida::fdhSCL* in a batch cultivation. The strain was cultivated in 1 l MSM with 150 g l^{-1} fructose and 3.6 g l^{-1} glucose in a DASGIP bioreactor at 30°C and DO ≥ 30%. After the initial acidification phase, the pH was kept at pH 5 by addition of KOH. For inoculation, overnight shake flask precultures in MSM with 150 g l^{-1} fructose and 3.6 g l^{-1} glucose were used. Fructose, glucose, and 5-KF concentrations in the culture supernatants were determined by HPLC. A representative example of four biological replicates (Fig. S2) is shown here.

Table 1. Comparison of bioreactor cultivations of *G. oxydans* IK003.1-igr3::*fdhSCL* and *P. putida*::*fdhSCL*.

Parameter	*G. oxydans* IK003.1-igr3::*fdhSCL*[a]	*P. putida*::*fdhSCL*[b]
μ (h^{-1})	n.d.	0.48 ± 0.02
Final OD_{600}	9.2	8.55 ± 0.36
Yield (g 5-KF g^{-1} fructose)	0.84	0.88 ± 0.01
Space time yield (g l^{-1} h^{-1})	4.37	5.60 ± 0.22

a. Data for *G. oxydans* IK003.1-igr3::*fdhSCL* cultivated in complex medium with 150 g l^{-1} fructose were taken from Battling *et al.* (2020).
b. Mean values and standard deviations from four biological replicates of *P. putida*::*fdhSCL* in MSM with 150 g l^{-1} fructose and 3.6 g l^{-1} glucose.

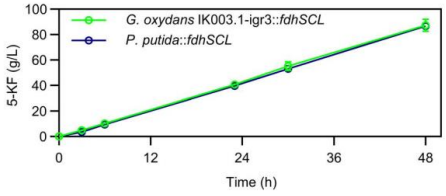

Fig. 3. Biotransformation of fructose to 5-KF with resting cells. Cell suspensions of *G. oxydans* IK003.1-igr3::*fdhSCL* and *P. putida*::*fdhSCL* at an OD_{600} of 3 were incubated in 100 mM potassium phosphate buffer pH 6 with 150 g l^{-1} fructose at 30°C and 180 rpm. 5-KF concentrations were determined by HPLC. Mean values and standard deviations of biological triplicates are shown.

of incubation. However, when these cells were sedimented by centrifugation and used for a second biotransformation, the 5-KF production rate was much lower, indicating that repeated use of the cells is not an option (data not shown).

Expansion of the substrate spectrum for 5-KF production to sucrose

Sucrose represents a cheaper substrate for 5-KF production than fructose and we therefore aimed to construct a *P. putida::fdhSCL* derivative with the ability to utilize sucrose. *P. putida* wild type is unable to metabolize and grow on sucrose, but strains engineered for growth on sucrose were reported (Löwe *et al.*, 2017; Löwe *et al.*, 2020). However, these studies used cytosolic invertases, that is CscA from *E. coli* and CscA from *P. protegens*, whereas we aimed for a periplasmic invertase, which provides fructose for Fdh without the necessity for fructose export from the cytoplasm. Hence, we selected an invertase recently identified in *G. japonicus* LMG1417, which has a high K_M for sucrose (63 ± 11 mM), but the highest specific activity (2300 U mg^{-1}) of all mesophilic invertases. After heterologous *inv1417* expression in *G. oxydans*, 40% of the activity was found in the periplasm and 60% in the cytoplasm (Hoffmann *et al.*, 2020). According to *in silico* prediction, Inv1417 contains a Tat signal peptide (Hoffmann *et al.*, 2020). However, as the protein is not known to contain a cofactor, secretion via the Sec machinery cannot be excluded. The *G. japonicus inv1417* gene was cloned into the expression plasmid pBT'T under the control of the constitutive P_{tac} promoter. *P. putida::fdhSCL* transformed with pBT'T-*inv1417* was cultivated in MSM with 100 mM sucrose as sole carbon source to test whether the invertase is active in *P. putida* and whether efficient 5-KF formation from sucrose can be achieved with this enzyme (Fig. 4).

P. putida::fdhSCL (pBT'T-*inv1417*) grew on sucrose as sole carbon source, but initial growth was slower compared with cultivations with glucose and fructose (see Fig. 1D). Since Inv1417 has an acidic pH optimum at around pH 5 (Hoffmann *et al.*, 2020) and invertase activity is crucial for growth on sucrose as sole carbon source, we compared cultures with an initial pH of 7.0 (Fig. 4A) with cultures having an initial pH of 6.5 (Fig. 4B). The lower initial pH resulted in faster sucrose cleavage, faster 5-KF production and a lower final cell density. After 46.5 h of cultivation, the cultures with a start pH of 6.5 reached an OD_{600} of 4.7 ± 0.1 compared with 6.6 ± 0.3 for the cultures with a start pH of 7.0. Besides faster 5-KF production, the reduced start pH also led to an increased molar yield (5-KF/sucrose) of 0.93 ± 0.02 compared with 0.82 ± 0.01 obtained for the cultures with a start pH of 7.0.

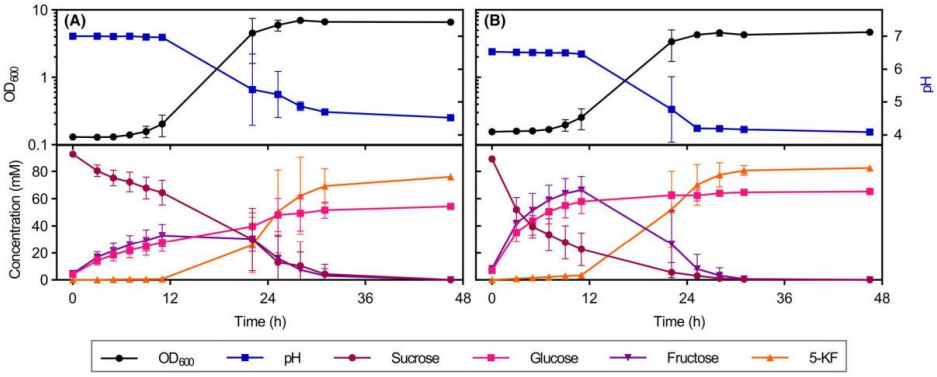

Fig. 4. Growth, pH, sugar consumption and 5-KF formation of *P. putida*::*fdhSCL* (pBT'T-*inv1417*) in shake flasks. The strain was cultivated in 50 mL MSM with 100 mM sucrose in 500 ml shake flasks at 30 °C, 85% humidity, and 180 rpm (shaking diameter of 50 mm) with a start pH of either 7.0 (A) or 6.5 (B). The cultures were inoculated with precultures grown in MSM with 100 mM sucrose and 20 mM glucose. Sucrose, glucose, fructose and 5-KF concentrations in the supernatants were determined by HPLC. Mean values and standard deviations of biological triplicates are shown.

As shown in Fig. 4A and B, both fructose and glucose were formed in the first 11 h of the cultivation with roughly similar kinetics. However, whereas the fructose was completely consumed again by conversion to 5-KF, glucose remained in the medium, reaching final concentrations of 54.3 ± 0.4 mM in the cultures with an initial pH of 7 and 65.1 ± 0.3 mM in the cultures with an initial pH of 6.5. This suggests that glucose consumption is inhibited by acidic pH. We could support this assumption by further growth experiments in which we either doubled the buffer capacity of the medium or adjusted the pH after 24 h to 6.5 with NaOH. In both cases, the higher pH led to a higher glucose consumption and increased OD_{600} values (Fig. S3). The major pathway for glucose catabolism in *P. putida* is the periplasmic oxidation to gluconate, which is then taken up and metabolized in the cytoplasm (Nikel *et al.*, 2015; Kohlstedt and Wittmann, 2019). Hence, the membrane-bound glucose dehydrogenase Gcd plays a crucial role in glucose catabolism. For Gcd of *P. putida*, the pH optimum has not been determined to our knowledge. However, in recent studies on lactobionic acid production with *Pseudomonas taetrolens* it was reported that the PQQ-dependent glucose dehydrogenase is responsible for the oxidation of lactose to lactobionic acid (Oh *et al.*, 2020). In a subsequent study of the same group, it was shown that lactobionic acid production with *P. taetrolens* worked best at pH values above 6, suggesting that the optimum pH of the PQQ-dependent glucose dehydrogenase is in this range (Kim *et al.*, 2020). The PQQ-dependent glucose dehydrogenase of *P. taetrolens* (GenBank: KMM82267.1) shows 49% amino acid sequence identity to the homologous protein of *P. putida* (Gcd, PP_1444), suggesting that the two proteins share comparable properties.

The kinetics of 5-KF production by *P. putida*::*fdhSCL* (pBT'T-*inv1417*) from sucrose is comparable to that directly from fructose (Fig. 1) and even faster compared with *G. oxydans* with genomically integrated *fdhSCL* genes and plasmid-based *inv1417* expression (Hoffmann *et al.*, 2020). This is surprising as Inv1417 is expected to be more active in *G. oxydans* at the beginning of the cultivations due to the lower start pH of 6. A possible limitation might be a higher number of membrane-bound dehydrogenases in *G. oxydans* compared with *P. putida*, which might limit the secretion of Fdh and invertase. A *G. oxydans* multideletion strain lacking eight membrane-bound dehydrogenases showed an increased L-erythrulose production by the native membrane-bound polyol dehydrogenase SldAB compared with the parental wild-type strain, which might be due at least in part to an improved Sec-dependent secretion of SldA (Peters *et al.*, 2013; Burger *et al.*, 2019). In summary, the results shown in Fig. 4 demonstrate that plasmid-based synthesis of the invertase Inv1417 from *G. japonicus* enables good growth of *P. putida*::*fdhSCL* with sucrose and efficient 5-KF production.

We also determined the specific invertase activity in cell-free extracts of *P. putida*::*fdhSCL* (pBT'T-*inv1417*) and the control strain *P. putida*::*fdhSCL* (pBT'T) by measuring sucrose consumption via HPLC. In extracts containing Inv1417, a specific activity of

4.63 ± 0.23 μmol min^{-1} (mg protein)$^{-1}$ was measured, and similar rates were determined for the formation of the products glucose (4.38 ± 0.18 μmol min^{-1} (mg protein)$^{-1}$) and fructose (4.03 ± 0.26 μmol min^{-1} (mg protein)$^{-1}$). In contrast, no sucrose consumption was determined in extracts of the control strain without invertase. This result confirms the functional expression of *inv1417* in *P. putida*.

Bioreactor cultivation of P. putida::fdhSCL *(pBT'T-*inv1417*) with sucrose*

After demonstrating efficient 5-KF production from sucrose in shake flasks by *P. putida::fdhSCL* (pBT'T-*inv1417*), we wanted to test the performance of the strain at elevated substrate concentrations under controlled conditions in a bioreactor. Preliminary tests showed that an initial concentration of 285 g l^{-1} sucrose (corresponding to 150 g l^{-1} fructose) is growth-inhibitory, and we therefore started with an initial sucrose concentration of 150 g l^{-1} and added two pulses of sucrose after 13 and 23 h (Fig. 5). A growth rate of 0.43 h^{-1} was reached with sucrose as sole carbon source and within 46 h 121 g l^{-1} 5-KF were produced. Taking into account the initial sucrose concentration, the two sucrose pulses, and sucrose loss caused by sampling, 358 g sucrose were available in total. Considering 5-KF loss during sampling, 144 g 5-KF were produced in total, corresponding to a mass yield of 0.40 g 5-KF per g sucrose consumed and a molar yield of 0.77 mol 5-KF per mol sucrose. The space-time yield was 2.74 g l^{-1} h^{-1}. After the pH drop and especially after the sucrose pulses, fast sucrose cleavage and fast 5-KF production were observed. As in the shake flask experiment (Fig. 4), high amounts of glucose remained in the medium (150 g l^{-1}), likely because the low pH prevented further metabolization (see discussion above).

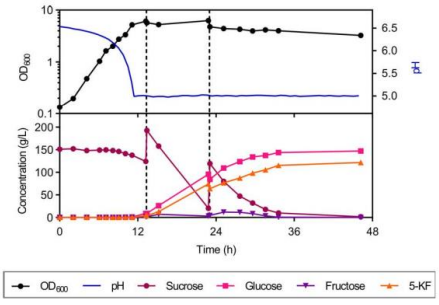

Fig. 5. Growth, pH, sugar consumption and 5-KF formation of *P. putida::fdhSCL* (pBT'T-*inv1417)* in a bioreactor cultivation with pulsed feeding of sucrose. The strain was cultivated in 1 l MSM with 150 g l^{-1} sucrose in a DASGIP bioreactor at 30°C, DO ≥ 30% and pH control at pH 5 by KOH addition after the initial acidification phase. For inoculation overnight shake flask precultures in MSM with 150 g l^{-1} sucrose were used. Additional sucrose was added as pulses of 100 ml and 165 ml of an 839 g l^{-1} sucrose solution after 13 and 23 h of cultivation, respectively (indicated by dashed lines). Sucrose, fructose, glucose, and 5-KF concentrations in the culture supernatants were determined by HPLC. A representative example of two biological replicates (Fig. S4) is shown here.

Conclusions and outlook

In this study, we demonstrated that *P. putida* is able to functionally synthesize the fructose dehydrogenase of *G. japonicus*, which includes a membrane-anchored trihaem cytochrome *c* and an FAD-containing subunit transported pickepack with a small subunit via the Tat secretion system. The recombinant strain with genomically integrated *fdhSCL* genes proved to be an efficient 5-KF producer with comparable performance as *G. oxydans*, the standard host used for periplasmic oxidation reactions. By functional expression of the periplasmic invertase gene *inv1417* from *G. japonicus*, we enabled growth of *P. putida::fdhSCL* on sucrose and 5-KF production from this substrate. Periplasmic conversion of sucrose to glucose and fructose is particularly reasonable for 5-KF production, as the substrate is formed directly in the compartment where it is needed (Fig. 6). Remarkably, the 5-KF production rate from sucrose was comparable to the one obtained directly with fructose, confirming that Inv1417 is a highly active invertase. Furthermore, our results indicate that *P. putida* has a high potential to serve as host for periplasmic oxidations not only with native enzymes, as recently published (Dvořák *et al.*, 2020), but also with complex heterologous enzymes like *G. japonicus* Fdh.

Strategies to further optimize *P. putida* as host for 5-KF production can be envisaged. In *G. oxydans* the chromosomal integration of a second *fdhSCL* copy significantly increased the 5-KF production rate (Battling *et al.*, 2020) and a comparable effect might also occur in *P. putida* with an additional chromosomal copy. Alternatively, plasmid-based expression of *fdhSCL* without the requirement for antibiotics selection could be used to increase the 5-KF production rate. Various antibiotic-free plasmid addiction systems have been described for bacteria (Kroll *et al.*, 2010). For example, *pyrF* (encoding orotidine-5'-phosphate decarboxylase) and *proC* (encoding pyrroline-5-carboxylate reductase) were shown to be suitable plasmid selection markers in Δ*pyrF* and Δ*proC* strains of *Pseudomonas fluorescens* (Schneider *et al.*, 2005). Furthermore, chromosomal expression of *inv1417* or the use of an antibiotic-independent *inv1417* expression plasmid would allow 5 KF production from sucrose without the necessity to use antibiotics. Lastly, process optimization will be important to improve 5 KF production

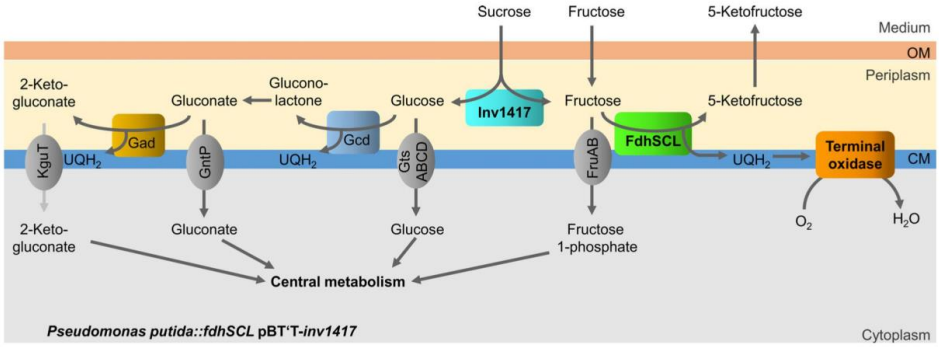

Fig. 6. Schematic overview of sugar metabolism and 5-KF production in *P. putida::fdhSCL* (pBT'T-*inv1417*). Sucrose and fructose enter the periplasm via porins (not shown) in the outer membrane (OM). Sucrose is cleaved by the periplasmic invertase Inv1417 of *G. japonicus* to glucose and fructose. Fructose is oxidized to 5-ketofructose by the membrane-bound fructose dehydrogenase FdhSCL from *G. japonicus*. Glucose can be taken up into the cytosol via the cytoplasmic membrane (CM) by the glucose transport system (GtsABCD) or is oxidized by the PQQ-dependent glucose dehydrogenase (Gcd) to gluconolactone, which is subsequently hydrolyzed to gluconate. Gluconate can be taken up via the gluconate permease (GntP) or is further oxidized by the gluconate dehydrogenase (Gad) to 2-ketogluconate, which can be taken up via the ketogluconate transporter (KguT). Periplasmic oxidation by the membrane-bound dehydrogenases generates ubiquinol, which is oxidized in the respiratory chain either directly by ubiquinol oxidases or via the cytochrome bc_1 complex and cytochrome *c* oxidases.

with the strains generated in this study. For isolation of 5-KF, a method has been described in US patent 3,206,375, which involves removal of the cells, treatment of the supernatant with activated carbon for decolourization, deionization with ion exchange resins, concentration, precipitation and recrystallization (Kinoshita and Terada, 1963).

Experimental procedures

Strains, plasmids and oligonucleotides

All strains and plasmids used in this study are listed in Table 2. Plasmids were cloned in either *E. coli* DH5α or *E. coli* PIR2 (for the integration plasmid with *ori* R6K) via standard Gibson assembly (Gibson, 2011). Oligonucleotides used are listed in Table S1 and were synthesized by Eurofins Genomics (Ebersberg, Germany).

Media composition and cultivation conditions

E. coli strains and *P. putida* precultures were cultivated in LB medium (Bertani, 1951) at 37°C and 130 rpm or at 30°C and 180 rpm respectively. 5-KF production experiments with *P. putida* were conducted at 30°C, 85% humidity and 180 rpm at a shaking diameter of 50 mm in a Kuhner shaker ISF1-X (Kuhner, Birsfelden, Switzerland) using mineral salts medium (MSM) based on Hartmans *et al.* (1989). It contains per l double-distilled H_2O 3.88 g K_2HPO_4, 1.63 g $NaH_2PO_4 \times 2$ H_2O, 2.0 g $(NH_4)_2SO_4$, 0.1 g $MgCl_2 \times 6$ H_2O, 10 mg EDTA, 2 mg ZnSO4 × 7 H_2O, 1 mg $CaCl_2 \times 2$ H_2O, 5 mg $FeSO_4 \times 7$ H_2O, 0.2 mg $Na_2MoO_4 \times 2$ H_2O, 0.2 mg $CuSO_4 \times 5$ H_2O, 0.4 mg $CoCl_2 \times 6$ H_2O and 1 mg $MnCl_2 \times 2$ H_2O with varying carbon sources at the indicated concentrations. When required, 50 μg ml^{-1} kanamycin or 25 μg ml^{-1} gentamycin were added. *G. oxydans* strains were cultivated at 30°C and 180 r.p.m in complex medium containing 40 g l^{-1} mannitol, 5 g l^{-1} yeast extract (BD Biosciences, Heidelberg, Germany), 2.5 g l^{-1} $MgSO_4 \times 7$ H_2O, 1 g l^{-1} $(NH_4)_2SO_4$ and 1 g l^{-1} KH_2PO_4. The initial pH was adjusted to pH 6 with NaOH (Richhardt *et al.*, 2013). The medium was supplemented with 50 μg ml^{-1} cefoxitin and 10 μM thymidine.

Generation of P. putida::fdhSCL *via Tn7 integration*

The Tn*7*-based chromosomal integration of the *fdhSCL* genes from *G. japonicus* was performed according to Zobel *et al.* (2015). $_{ATG}$*fdhSCL* was amplified from pBBR1p264-*fdhSCL*-ST (Siemen *et al.*, 2018) and encodes an FdhS variant with an ATG start codon instead of the original TTG start codon, which was shown to be advantageous (Kawai *et al.*, 2013). Except for the start codon change, the native *G. japonicus* sequence was used. *fdhSCL* was cloned into pBG14g, with the Tn*7*L and Tn*7*R extremes, the left and right ends of Tn*7* and the strong synthetic 14g promotor (Zobel *et al.*, 2015). The resulting strain *E. coli* PIR2 pBG14g-*fdhSCL* was used for mating on LB agar with

Table 2. Bacterial strains and plasmids used in this work.

Strain or plasmid	Relevant characteristic	Source or reference
Bacterial strains		
E. coli		
DH5α	*F⁻ endA1* Φ80d*lacZ*ΔM15 Δ(*lacZYA-argF*)U169 *recA1 relA1 hsdR17*(rK–mK+) *deoR supE44 thi-1 gyrA96 phoA* λ–, strain used for cloning	Hanahan (1983)
PIR2	*F⁻ Δlac169 rpoS(Am) robA1 creC510 hsdR514 endA reacA1 uidA(ΔMlui)::pir*, host for ori R6K replication	Invitrogen
HB101	*F⁻ mcrB mrr hsdS20(rB⁻ mB⁻) recA13 leuB6 ara−14 proA2 lacY1 galK2 xyl-5 mtl-1 rpsL20(SmR) gln V44* λ–	Boyer and Roulland-Dussoix (1969)
DH5α λpir	λpir phage lysogen DH5α derivative; host for ori R6K vectors	Platt *et al.* (2000)
P. putida		
KT2440	Wild-type, mt-2 derivative cured from plasmid pWW0	Bagdasarian *et al.* (1981)
P. putida::*fdhSCL*	KT2440 with *fdhSCL* genes under control of P14g, integrated in *att*Tn*7*, downstream of *glmS*	This study
Plasmids		
pBG14g-*msfgfp*	Kan^R, Gm^R, ori R6K, Tn*7*L and Tn*7*R extremes, BCD2−*msfgfp* fusion, P_{14g}	Zobel *et al.* (2015)
pBG14g-*fdhSCL*	pBG14g derivative for integration of *fdhSCL*	This study
pTnS1	Amp^R, ori R6K, TnSABC+D operon	Choi *et al.* (2005)
pRK2013	Kan^R, oriV(RK2/ColE1), mob^+ tra^+	Figurski and Helinski (1979)
pBT'mcs	Kan^R, ori and rep of pBBR1, P_{tac}	Koopman *et al.* (2010)
pBT'T	pBT'mcs with ribosomal binding site	Wierckx lab, Forschungszentrum Jülich, Germany
pBT'T-*inv1417*	pBT'T derivative for expression of *inv1417*	This study

the *P. putida* KT2440 wild-type recipient, the helper strain *E. coli* HB101 pRK2013 and *E. coli* DH5α λpir pTnS1, carrying the TnS_{ABC+D} operon for site-directed transposition (Choi *et al.*, 2005) according to Wynands *et al.* (2018). *P. putida* integration strains were selected on cetrimide agar with gentamycin and correct integration downstream of the *glmS* gene (PP_5409) was confirmed via colony-PCR.

Cultivation in 2-l bioreactor

Bioreactor cultivations were conducted in a 2 l DASGIP bioreactor. The 1 l main cultures in MSM pH 7 with 150 g l^{-1} fructose and 20 mM glucose or MSM pH 6.5 with 150 g l^{-1} sucrose were inoculated from overnight shake flask precultures in the main culture medium. To prevent foam formation, headspace gassing was used. The DO was controlled at 30% via a cascade of increasing the stirrer speed from 500 to 1200 rpm, the flow rate from 60 to 90 sL h^{-1} and the oxygen concentration from 21 to 80% (vol/vol).

Sugar quantification via HPLC

Culture samples were centrifuged (15 min, 17 000 *g*) and the supernatants stored at −20°C. Thawed samples were diluted with deionized water, heated for 60 min at 60°C to prevent double peaks for 5-KF, which might be caused by the keto and gem-diol forms (Herweg *et al.*, 2018), filtered and analysed via high performance liquid chromatography (HPLC) using a modification of a previously described method (Richhardt *et al.*, 2012). 10 μL samples were analysed with an Agilent LC-1100 system using a Rezex RCM-Monosaccharide 300 × 7.8 mm column (Phenomenex, Aschaffenburg, Germany) equipped with a Carbo-Ca Guard Cartridge (Phenomenex) at 80°C with water as eluent at a flow rate of 0.6 ml min^{-1}. Sucrose, glucose, 5-KF and fructose were detected using a refraction index detector at 35°C at retention times of 9.4, 11.3, 13.1 and 14.5 min respectively.

Preparation of cell free extracts for enzyme activity assays

Overnight cultures of the respective *P. putida* and *G. oxydans* strains were harvested (10 min, 5000 g, 4°C), washed once in ddH_2O (Fdh assay) or 100 mM potassium phosphate buffer pH 6 (invertase assay) and the cells were disrupted in a Precellys 24 homogenizer (Bertin, Frankfurt am Main, Germany). Cell lysates were centrifuged for 10 min at 16 000 *g* and 4°C and the supernatant was collected as cell-free extract for the enzyme activity assays. Protein concentrations were determined via a modified Bradford assay using the Coo Protein Assay (Uptima, Interchim, Montlucon Cedex, France).

Enzyme assays

Fructose dehydrogenase activity was measured in a spectrophotometric assay with potassium ferricyanide as artificial electron acceptor as described (Ameyama and Adachi, 1982). Briefly, 100 μl McIlvaine buffer pH 4.5, 20

µl H_2O, 20 µl 10% Triton X-100, 20 µl 1 M fructose and 20 µl cell-free extract were preincubated for 5 min at 25°C and then the reaction was started by adding 20 µl 0.1 M $K_3[FeIII(CN)_6]$. Samples were incubated for 4-14 min at 25°C, the reaction was stopped by adding 100 µl ferric sulfate-Dupanol reagent (5 g l^{-1} $Fe_2((SO)_4)_3$, 3 g l^{-1} sodium dodecyl sulphate, 95 ml l^{-1} 85% phosphoric acid). 700 µl ddH_2O was added and the samples were incubated for 20 min at 25°C. The formation of Prussian blue colour was measured at 660 nm. The kinetics of the absorbance increase was used to calculate the specific activity. One unit of enzyme activity is defined as the amount of enzyme catalysing the oxidation of 1 µmol D-fructose per minute under the conditions described above; 4.0 absorbance units equal 1 µmol of D-fructose oxidized (Ameyama and Adachi, 1982).

Invertase activity was measured according to a previously published method (Hoffmann *et al.*, 2020) with slight modifications. 100 µl cell-free extract was mixed with 400 µl 100 mM potassium phosphate buffer pH 6 containing 1 M sucrose. The mixtures were incubated at 30°C and samples were taken at different time points after 20–120 min and stored at −20°C. Thawed samples were diluted with ddH_2O and the sucrose, glucose and fructose concentrations were determined via HPLC. The specific activity was determined from the sucrose decrease over time, with one unit of enzyme activity corresponding to 1 µmol sucrose converted per minute.

Acknowledgements

The authors are very grateful for the support by their colleagues Prof. Nick Wierckx, Dr. Maike Otto and Dr. Benedikt Wynands, who provided *Pseudomonas putida* KT2440 and the plasmid vectors and gave advice with respect to cultivation and genetic engineering of *P. putida*. The invertase gene *inv1417* from *Gluconobacter japonicus* was a kind gift from Prof. Uwe Deppenmeier and Dr. Juliane Hoffmann from the Institute of Microbiology and Biotechnology of the University of Bonn. The authors thank Rebecca Schlößer for her contribution to this project during a practical course.

Funding Information

This project was funded by the Bundesministerium für Bildung und Forschung (BMBF) within the project IMPRES (FKZ 031B0370).

Conflict of interest

None declared.

References

Acero, D., Zoellner, J.M., Davy, B.M., and Hedrick, V.E. (2020) Changes in non-nutritive sweetener consumption patterns in response to a sugar-sweetened beverage reduction intervention. *Nutrients* **12:** 3428.

Ameyama, M., and Adachi, O. (1982) D-Fructose dehydrogenase from *Gluconobacter industrius*, membrane-bound. *Meth Enzymol* **89:** 154–159.

Ameyama, M., Shinagawa, E., Matsushita, K., and Adachi, O. (1981) D-Fructose dehydrogenase of *Gluconobacter industrius* - purification, characterization, and application to enzymatic micro-determination of D-fructose. *J Bacteriol* **145:** 814–823.

An, R., and Moe, L.A. (2016) Regulation of pyrroloquinoline quinone-dependent glucose dehydrogenase activity in the model rhizosphere-dwelling bacterium *Pseudomonas putida* KT2440. *Appl Environ Microbiol* **82:** 4955–4964.

Bagdasarian, M., Lurz, R., Ruckert, B., Franklin, F.C., Bagdasarian, M.M., Frey, J., and Timmis, K.N. (1981) Specific-purpose plasmid cloning vectors. II. Broad host range, high copy number, RSF1010-derived vectors, and a host-vector system for gene cloning in *Pseudomonas*. *Gene* **16:** 237–247.

Battling, S., Wohlers, K., Igwe, C., Kranz, A., Pesch, M., Wirtz, A., *et al.* (2020) Novel plasmid-free *Gluconobacter oxydans* strains for production of the natural sweetener 5-ketofructose. *Microb Cell Fact* **19:** 54.

Bertani, G. (1951) Studies on lysogenesis. I. The mode of phage liberation by lysogenic *Escherichia coli*. *J Bacteriol* **62:** 293–300.

Boyer, H.W., and Roulland-Dussoix, D. (1969) A complementation analysis of the restriction and modification of DNA in *Escherichia coli*. *J Mol Biol* **41:** 459–472.

Bringer, S., and Bott, M. (2016) Central carbon metabolism and respiration in *Gluconobacter oxydans*. In *Acetic Acid Bacteria: Ecology and Physiology*. Matsushita, K., Toyama, H., Tonouchi, N., and Okamoto-Kainuma, A. (eds). Springer Japan: Tokyo, pp. 235–253.

Burger, C., Kessler, C., Gruber, S., Ehrenreich, A., Liebl, W., and Weuster-Botz, D. (2019) L-Erythrulose production with a multideletion strain of *Gluconobacter oxydans*. *Appl Microbiol Biotechnol* **103:** 4393–4404.

Carocho, M., Morales, P., and Ferreira, I. (2017) Sweeteners as food additives in the XXI century: a review of what is known, and what is to come. *Food Chem Toxicol* **107:** 302–317.

del Castillo, T., Ramos, J.L., Rodríguez-Herva, J.J., Fuhrer, T., Sauer, U., and Duque, E. (2007) Convergent peripheral pathways catalyze initial glucose catabolism in *Pseudomonas putida*: Genomic and flux analysis. *J Bacteriol* **189:** 5142–5152.

Chavarría, M., Fuhrer, T., Sauer, U., Pflüger-Grau, K., and de Lorenzo, V. (2013) Cra regulates the cross-talk between the two branches of the phosphoenolpyruvate: phosphotransferase system of *Pseudomonas putida*. *Environm Microbiol* **15:** 121–132.

Choi, K.-H., Gaynor, J.B., White, K.G., Lopez, C., Bosio, C.M., Karkhoff-Schweizer, R.R., and Schweizer, H.P. (2005) A Tn*7*-based broad-range bacterial cloning and expression system. *Nat Meth* **2:** 443–448.

Deppenmeier, U., Hoffmeister, M., and Prust, C. (2002) Biochemistry and biotechnological applications of *Gluconobacter* strains. *Appl Microbiol Biotechnol* **60:** 233–242.

Dvořák, P., Kováč, J., and de Lorenzo, V. (2020) Biotransformation of D-xylose to D-xylonate coupled to medium-chain-length polyhydroxyalkanoate production in cellobiose-grown *Pseudomonas putida* EM42. *Microb Biotechnol* **13:** 1273–1283.

Ebert, B.E., Kurth, F., Grund, M., Blank, L.M., and Schmid, A. (2011) Response of *Pseudomonas putida* KT2440 to increased NADH and ATP demand. *Appl Environ Microbiol* **77:** 6597–6605.

Figurski, D.H., and Helinski, D.R. (1979) Replication of an origin-containing derivative of plasmid RK2 dependent on a plasmid function provided in *trans*. *Proc Natl Acad Sci USA* **76:** 1648–1652.

Fricke, P.M., Link, T., Gätgens, J., Sonntag, C., Otto, M., Bott, M., and Polen, T. (2020) A tunable L-arabinose-inducible expression plasmid for the acetic acid bacterium *Gluconobacter oxydans*. *Appl Microbiol Biotechnol* **104:** 9267–9282.

Gibson, D.G. (2011) Enzymatic assembly of overlapping DNA fragments. *Meth Enzymol* **498:** 349–361.

Hanahan, D. (1983) Studies on transformation of *Escherichia coli* with plasmids. *J Mol Biol* **166:** 557–580.

Hanke, T., Nöh, K., Noack, S., Polen, T., Bringer, S., Sahm, H., *et al.* (2013) Combined fluxomics and transcriptomics analysis of glucose catabolism via a partially cyclic pentose phosphate pathway in *Gluconobacter oxydans* 621H. *Appl Environ Microbiol* **79:** 2336–2348.

Hartmans, S., Smits, J.P., van der Werf, M.J., Volkering, F., and de Bont, J.A. (1989) Metabolism of styrene oxide and 2-phenylethanol in the styrene-degrading *Xanthobacter* strain 124X. *Appl Environ Microbiol* **55:** 2850–2855.

Herweg, E., Schöpping, M., Rohr, K., Siemen, A., Frank, O., Hofmann, T., *et al.* (2018) Production of the potential sweetener 5-ketofructose from fructose in fed-batch cultivation with *Gluconobacter oxydans*. *Bioresour Technol* **259:** 164–172.

Hoffmann, J.J., Hövels, M., Kosciow, K., and Deppenmeier, U. (2020) Synthesis of the alternative sweetener 5-ketofructose from sucrose by fructose dehydrogenase and invertase producing *Gluconobacter* strains. *J Biotechnol* **307:** 164–174.

Kallnik, V., Meyer, M., Deppenmeier, U., and Schweiger, P. (2010) Construction of expression vectors for protein production in *Gluconobacter oxydans*. *J Biotechnol* **150:** 460–465.

Kawai, S., Goda-Tsutsumi, M., Yakushi, T., Kano, K., and Matsushita, K. (2013) Heterologous overexpression and characterization of a flavoprotein-cytochrome *c* complex fructose dehydrogenase of *Gluconobacter japonicus* NBRC3260. *Appl Environ Microbiol* **79:** 1654–1660.

Kiefler, I., Bringer, S., and Bott, M. (2017) Metabolic engineering of *Gluconobacter oxydans* 621H for increased biomass yield. *Appl Microbiol Biotechnol* **101:** 5453–5467.

Kim, J.-H., Jang, Y.-A., Seong, S.-B., Jang, S.A., Hong, S.H., Song, J.K., and Eom, G.T. (2020) High-level production and high-yield recovery of lactobionic acid by the control of pH and temperature in fermentation of *Pseudomonas taetrolens*. *Bioproc Biosyst Eng* **43:** 937–944.

Kinoshita, S. & Terada, O. (1963) Method for preparing 5-ketofructose by fermentation. US patent 3,206,375.

Kohlstedt, M., and Wittmann, C. (2019) GC-MS-based ^{13}C metabolic flux analysis resolves the parallel and cyclic glucose metabolism of *Pseudomonas putida* KT2440 and *Pseudomonas aeruginosa* PAO1. *Metab Eng* **54:** 35–53.

Koopman, F., Wierckx, N., de Winde, J.H., and Ruijssenaars, H.J. (2010) Identification and characterization of the furfural and 5-(hydroxymethyl)furfural degradation pathways of *Cupriavidus basilensis* HMF14. *Proc Natl Acad Sci USA* **107:** 4919–4924.

Kostner, D., Peters, B., Mientus, M., Liebel, W., and Ehrenreich, A. (2013) Importance of *codB* for new *codA*-based markerless gene deletion in *Gluconobacter oxydans*. *Appl Microbiol Biotechnol* **97:** 8341–8349.

Kranz, A., Vogel, A., Degner, U., Kiefler, I., Bott, M., Usadel, B., and Polen, T. (2017) High precision genome sequencing of engineered *Gluconobacter oxydans* 621H by combining long nanopore and short accurate Illumina reads. *J Biotechnol* **258:** 197–205.

Kroll, J., Klinter, S., Schneider, C., Voß, I., and Steinbüchel, A. (2010) Plasmid addiction systems: perspectives and applications in biotechnology. *Microb Biotechnol* **3:** 634–657.

Kumar, C., Yadav, K., Archana, G., and Naresh Kumar, G. (2013) 2-Ketogluconic acid secretion by incorporation of *Pseudomonas putida* KT 2440 gluconate dehydrogenase (*gad*) operon in *Enterobacter asburiae* PSI3 improves mineral phosphate solubilization. *Curr Microbiol* **67:** 388–394.

Loeschcke, A., and Thies, S. (2015) *Pseudomonas putida*—a versatile host for the production of natural products. *Appl Microbiol Biotechnol* **99:** 6197–6214.

Löwe, H., Schmauder, L., Hobmeier, K., Kremling, A., and Pflüger-Grau, K. (2017) Metabolic engineering to expand the substrate spectrum of *Pseudomonas putida* toward sucrose. *MicrobiologyOpen* **6:** e00473.

Löwe, H., Sinner, P., Kremling, A. and Pflüger-Grau, K. (2020) Engineering sucrose metabolism in *Pseudomonas putida* highlights the importance of porins. *Microb Biotechnol* **13:** 97–106.

Martínez-García, E., and de Lorenzo, V. (2017) Molecular tools and emerging strategies for deep genetic/genomic refactoring of *Pseudomonas*. *Curr Opin Biotechnol* **47:** 120–132.

Mutalik, V.K., Guimaraes, J.C., Cambray, G., Lam, C., Christoffersen, M.J., Mai, Q.-A., *et al.* (2013) Precise and reliable gene expression via standard transcription and translation initiation elements. *Nat Meth* **10:** 354–360.

De Muynck, C., Pereira, C.S., Naessens, M., Parmentier, S., Soetaert, W., and Vandamme, E.J. (2007) The genus *Gluconobacter oxydans*: comprehensive overview of biochemistry and biotechnological applications. *Crit Rev Biotechnol* **27:** 147–171.

Nikel, P.I., Chavarria, M., Fuhrer, T., Sauer, U., and de Lorenzo, V. (2015) *Pseudomonas putida* KT2440 strain metabolizes glucose through a cycle formed by enzymes of the Entner-Doudoroff, Embden-Meyerhof-Parnas, and

pentose phosphate pathways. *J Biol Chem* **290:** 25920–25932.

Nikel, P.I., and de Lorenzo, V. (2018) *Pseudomonas putida* as a functional chassis for industrial biocatalysis: From native biochemistry to trans-metabolism. *Metab Eng* **50:** 142–155.

Oh, Y.-R., Jang, Y.-A., Lee, S.S., Kim, J.-H., Hong, S.H., Han, J.J., and Eom, G.T. (2020) Enhancement of lactobionic acid productivity by homologous expression of quinoprotein glucose dehydrogenase in *Pseudomonas taetrolens*. *J Agric Food Chem* **68:** 12336–12344.

Peters, B., Mientus, M., Kostner, D., Junker, A., Liebl, W., and Ehrenreich, A. (2013) Characterization of membrane-bound dehydrogenases from *Gluconobacter oxydans* 621H via whole-cell activity assays using multi-deletion strains. *Appl Microbiol Biotechnol* **97:** 6397–6412.

Platt, R., Drescher, C., Park, S.-K., and Phillips, G.J. (2000) Genetic system for reversible integration of DNA constructs and *lacZ* gene fusions into the *Escherichia coli* chromosome. *Plasmid* **43:** 12–23.

Prust, C., Hoffmeister, M., Liesegang, H., Wiezer, A., Fricke, W.F., Ehrenreich, A., *et al.* (2005) Complete genome sequence of the acetic acid bacterium *Gluconobacter oxydans*. *Nat Biotechnol* **23:** 195.

Reichstein, T., and Grüssner, A. (1934) Eine ergiebige synthese der L-Ascorbinsäure (C-Vitamin). *Helv Chim Acta* **17:** 311–328.

Reiter, A., Herbst, L., Wiechert, W., and Oldiges, M. (2021) Need for speed: evaluation of dilute and shoot-mass spectrometry for accelerated metabolic phenotyping in bioprocess development. *Anal Bioanal Chem* **413:** 3253–3268.

Richhardt, J., Bringer, S., and Bott, M. (2012) Mutational analysis of the pentose phosphate and Entner-Doudoroff pathways in *Gluconobacter oxydans* reveals improved growth of a Δ*edd* Δ*eda* mutant on mannitol. *Appl Environ Microbiol* **78:** 6975–6986.

Richhardt, J., Bringer, S., and Bott, M. (2013) Role of the pentose phosphate pathway and the Entner-Doudoroff pathway in glucose metabolism of *Gluconobacter oxydans* 621H. *Appl Microbiol Biotechnol* **97:** 4315–4323.

Rippe, J.M., and Angelopoulos, T.J. (2016) Relationship between added sugars consumption and chronic disease risk factors: current understanding. *Nutrients* **8:** 697.

Schiessl, J., Kosciow, K., Garschagen, L.S., Hoffmann, J.J., Heymuth, J., Franke, T., and Deppenmeier, U. (2021) Degradation of the low-calorie sugar substitute 5-ketofructose by different bacteria. *Appl Microbiol Biotechnol* **105:** 2441–2453.

Schneider, J.C., Jenings, A.F., Mun, D.M., McGovern, P.M., and Chew, L.C. (2005) Auxotrophic markers *pyrF* and *proC* can replace antibiotic markers on protein production plasmids in high-cell-density *Pseudomonas fluorescens* fermentation. *Biotechnol Prog* **21:** 343–348.

Schweikert, S., Kranz, A., Yakushi, T., Filipchyk, A., Polen, T., Etterich, H., *et al.* (2021) The FNR-type regulator GoxR of the obligatory aerobic acetic acid bacterium *Gluconobacter oxydans* affects expression of genes involved in respiration and redox metabolism. *Appl Environ Microbiol* **87:** e00195–e121.

Siemen, A., Kosciow, K., Schweiger, P., and Deppenmeier, U. (2018) Production of 5-ketofructose from fructose or sucrose using genetically modified *Gluconobacter oxydans* strains. *Appl Microbiol Biotechnol* **102:** 1699–1710.

Sjölin, M., Thuvander, J., Wallberg, O., and Lipnizki, F. (2019) Purification of sucrose in sugar beet molasses by utilizing ceramic nanofiltration and ultrafiltration membranes. *Membranes* **10:** 5.

Winsor, G.L., Griffiths, E.J., Lo, R., Dhillon, B.K., Shay, J.A., and Brinkman, F.S. (2016) Enhanced annotations and features for comparing thousands of *Pseudomonas* genomes in the *Pseudomonas* genome database. *Nucleic Acids Res* **44:** D646–653.

Wynands, B., Lenzen, C., Otto, M., Koch, F., Blank, L.M., and Wierckx, N. (2018) Metabolic engineering of *Pseudomonas taiwanensis* VLB120 with minimal genomic modifications for high-yield phenol production. *Metab Eng* **47:** 121–133.

Wyrobnik, D.H., and Wyrobnik, I.H. (2006) Agent for reducing the useable calorie content of food and for therapeutic reduction of weight, in particular for use in the case of adiposity (obesity). EP1951289.

Zobel, S., Benedetti, I., Eisenbach, L., de Lorenzo, V., Wierckx, N., and Blank, L.M. (2015) Tn*7*-based device for calibrated heterologous gene expression in *Pseudomonas putida*. *ACS Synth Biol* **4:** 1341–1351.

Supporting information

Additional supporting information may be found online in the Supporting Information section at the end of the article.

Fig. S1. Analysis of 5-KF formation by HPLC. In panel A, a standard mixture containing 5 g/L glucose, 5-KF and fructose was separated. In panel B, supernatants (10 μl) of a shake flask cultivation of *P. putida*::*fdhSCL* (see Fig. 1) at the start of the cultivation (grey) and after 48 h (black) were analyzed with an Agilent LC-1100 system using a Rezex RCM-Monosaccharide 300 x 7.8 mm column (Phenomenex, Aschaffenburg, Germany) equipped with a Carbo-Ca Guard Cartridge (Phenomenex, Aschaffenburg, Germany) at 80 °C with water as eluent at a flow rate of 0.6 mL/min. A refraction index detector operated at 35 °C was used for detection.

Fig. S2. Growth, pH, sugar consumption and 5-KF formation of *P. putida*::*fdhSCL* in batch cultivation. The strain was cultivated in 1 L MSM with 150 g/L fructose and 3.6 g/L glucose in a DASGIP bioreactor at 30 °C and DO ≥ 30%. After the initial acidification phase, the pH-control kept the pH at 5 by KOH addition. For inoculation, overnight shake flask precultures in MSM with 150 g/L fructose and 3.6 g/L glucose were used. Fructose, glucose, and 5-KF concentrations in the culture supernatants were determined by HPLC. The data for all four biological replicates performed in this study are shown. Panel D is identical to Fig. 2 in the main text.

Fig. S3. Growth, pH, sucrose and glucose consumption of *P. putida*::*fdhSCL* (pBT'T-inv1417) in shake flasks. The strain was cultivated in 50 mL MSM with 100 mM sucrose

in 500 mL shake flasks at 30 °C, 85% humidity, and 180 rpm (shaking diameter of 50 mm). The cultures were grown either under standard conditions with an initial pH of 7.0, or under the same condition, but with a pH shift after 24 h to pH 6.5 by addition of NaOH, or in modified MSM containing 72 mM phosphate buffer instead of 36 mM with an initial pH of 7, or in standard MSM with an initial pH of 6.5 All cultures were inoculated with precultures grown in MSM with 100 mM sucrose and 20 mM glucose, initial pH 7.0. Sucrose and glucose concentrations in the supernatants were determined by HPLC. Mean values and standard deviations of biological triplicates are shown.

Fig. S4. Growth, pH, sugar consumption and 5-KF formation of *P. putida*::*fdhSCL* (pBT'T-inv1417) in a bioreactor cultivation with pulsed feeding of sucrose. The strain was cultivated in 1 L MSM with 150 g/L sucrose in a DASGIP bioreactor at 30 °C and DO ≥ 30%. After the initial acidification phase, the pH was kept at pH 5 by addition of KOH. For inoculation, overnight shake flask precultures in MSM with 150 g/L sucrose were used. Additional sucrose was added as pulses of 100 mL and 165 mL of an 839 g/L sucrose solution after 13 and 23 h of cultivation, respectively (indicated by dashed lines). Sucrose, fructose, glucose, and 5-KF concentrations in the culture supernatants were determined by HPLC. The data for two biological replicates performed in this study are shown. Panel A is identical to Fig. 5 in the main text.

Table S1. Oligonucleotides used in this study.

Supporting information to

Metabolic engineering of *Pseudomonas putida* for production of the natural sweetener 5-ketofructose from fructose or sucrose by periplasmic oxidation with a heterologous fructose dehydrogenase

Karen Wohlers[a], Astrid Wirtz[a], Alexander Reiter[a,b], Marco Oldiges[a,b], Meike Baumgart[a], Michael Bott[a,c]*

[a] IBG-1: Biotechnology, Institute of Bio- and Geosciences, Forschungszentrum Jülich, 52425 Jülich, Germany

[b] Institute of Biotechnology, RWTH Aachen University, 52062, Aachen, Germany

[c] The Bioeconomy Science Center (BioSC), Forschungszentrum Jülich, D-52425 Jülich, Germany

*Corresponding author

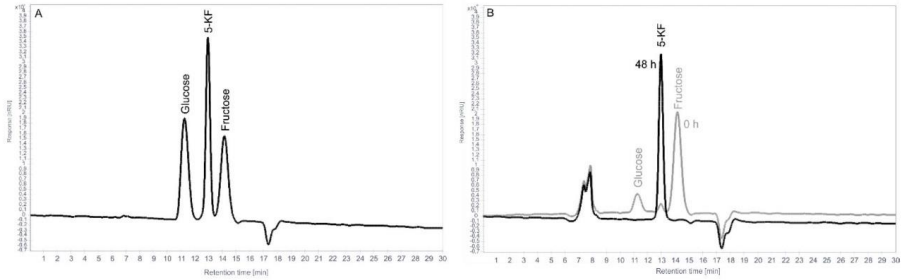

Fig. S1. Analysis of 5-KF formation by HPLC**.** In panel A, a standard mixture containing 5 g/L mM glucose, 5-KF and fructose was separated. In panel B, supernatants (10 µl) of a shake flask cultivation of *P. putida*::*fdhSCL* (see Fig. 1) at the start of the cultivation (grey) and after 48 h (black) were analyzed with an Agilent LC-1100 system using a Rezex RCM-Monosaccharide 300 x 7.8 mm column (Phenomenex, Aschaffenburg, Germany) equipped with a Carbo-Ca Guard Cartridge (Phenomenex, Aschaffenburg, Germany) at 80 °C with water as eluent at a flow rate of 0.6 mL/min. A refraction index detector operated at 35 °C was used for detection.

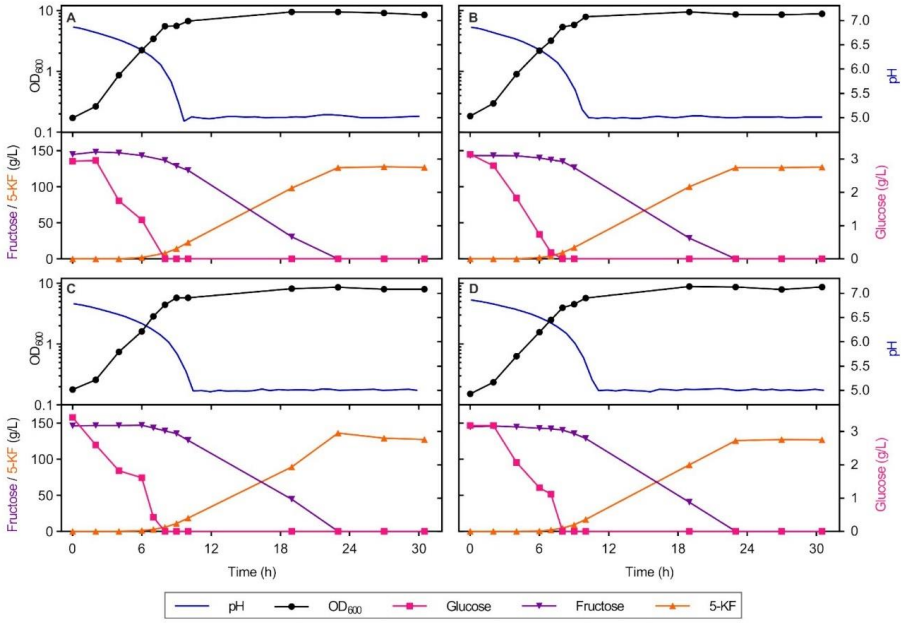

Fig. S2. Growth, pH, sugar consumption and 5-KF formation of *P. putida*::*fdhSCL* in batch cultivation. The strain was cultivated in 1 L MSM with 150 g/L fructose and 3.6 g/L glucose in a DASGIP bioreactor at 30 °C and DO ≥ 30%. After the initial acidification phase, the pH-control kept the pH at 5 by KOH addition. For inoculation, overnight shake flask precultures in MSM with 150 g/L fructose and 3.6 g/L glucose were used. Fructose, glucose, and 5-KF concentrations in the culture supernatants were determined by HPLC. The data for all four biological replicates performed in this study are shown. Panel D is identical to Fig. 2 in the main text.

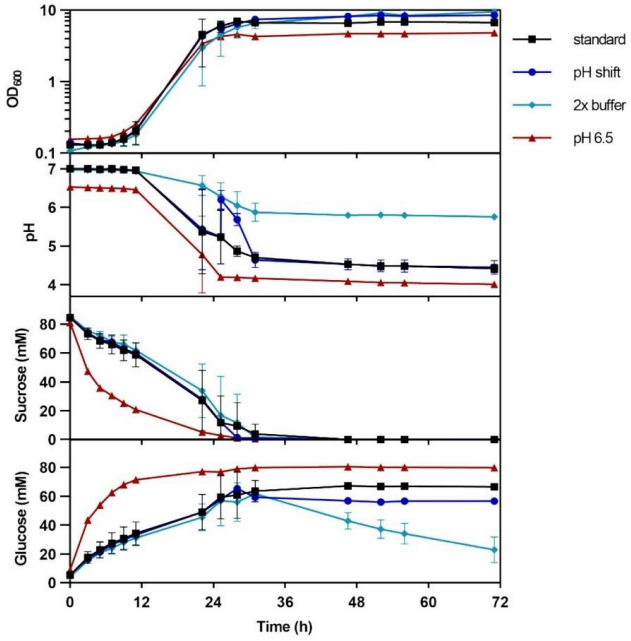

Fig. S3. Growth, pH, sucrose and glucose consumption of *P. putida*::*fdhSCL* (pBT'T-*inv1417*) in shake flasks. The strain was cultivated in 50 mL MSM with 100 mM sucrose in 500 mL shake flasks at 30 °C, 85% humidity, and 180 rpm (shaking diameter of 50 mm). The cultures were grown either under standard conditions with an initial pH of 7.0, or under the same condition, but with a pH shift after 24 h to pH 6.5 by addition of NaOH, or in modified MSM containing 72 mM phosphate buffer instead of 36 mM with an initial pH of 7, or in standard MSM with an initial pH of 6.5 All cultures were inoculated with precultures grown in MSM with 100 mM sucrose and 20 mM glucose, initial pH 7.0. Sucrose and glucose concentrations in the supernatants were determined by HPLC. Mean values and standard deviations of biological triplicates are shown.

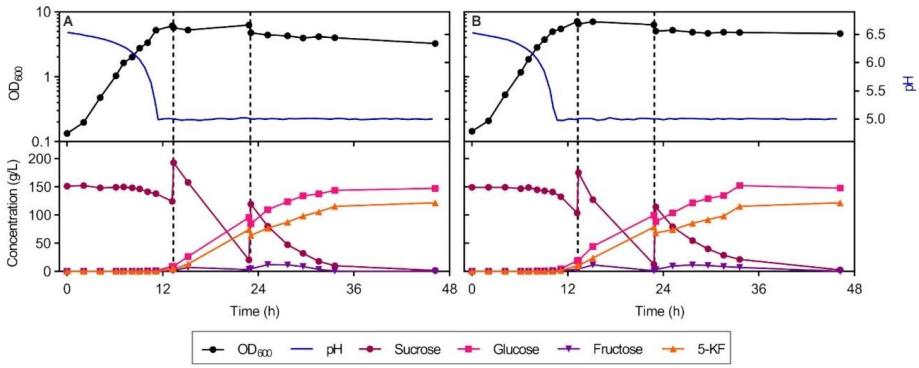

Fig. S4. Growth, pH, sugar consumption and 5-KF formation of *P. putida*::*fdhSCL* (pBT'T-*inv1417*) in a bioreactor cultivation with pulsed feeding of sucrose. The strain was cultivated in 1 L MSM with 150 g/L sucrose in a DASGIP bioreactor at 30 °C and DO ≥ 30%. After the initial acidification phase, the pH was kept at pH 5 by addition of KOH. For inoculation, overnight shake flask precultures in MSM with 150 g/L sucrose were used. Additional sucrose was added as pulses of 100 mL and 165 mL of an 839 g/L sucrose solution after 13 and 23 h of cultivation, respectively (indicated by dashed lines). Sucrose, fructose, glucose, and 5-KF concentrations in the culture supernatants were determined by HPLC. The data for two biological replicates performed in this study are shown. Panel A is identical to Fig. 5 in the main text.

Table S1. Oligonucleotides used in this study

Oligonucleotide	Sequence (5'→ 3') and properties[1]
Oligonucleotides for cloning	
fdhS-fwd-pBG-overlap	**TGCTAAGGAGGTTTTCTAAT**GGAAAAAATAGCTGATTCCG
fdhL-rev-pBG-overlap	**ATCCCCGGGTACCGAGCTCG**TTACCCCTGTTTCAGGTCATTG
inv1417-fwd-pBT'Toverlap	**ACAGGAAACAGGAGGTACCG**ATGCTGCCGGGTATGACGGATC
inv1417-rev-pBT'Toverlap	**GCCCGACGTCGCATGCTCCT**CTACATCGCCGTAGGGCGATTC
Oligonucleotides for sequencing and colony-PCR	
pBG-seq-fwd	AAGCCATGAAAACCGCCACTG
pBG-seq-rev	GAGTTCTGAGGTCATTACTG
fdh-seq-fwd2	GTGGTTATGCCATTTCTTCCCC
fdh-seq-fwd3	AACCGATGGTGCTGCACTC
fdh-seq-fwd4	CCCGCATACCAACTACTTCC
5-Pput-*glmS* UP[2]	AGTCAGAGTTACGGAATTGTAGG
pBT'T-seq-fwd	TGAGCCCCATCCCCCTGTTG
pBT'T-seq-rev	ACTCACTATAGGGCGAATTGGAGC
inv1417-seq-fwd	GTCATCTGCCCCGACGTTGC

[1]Overlaps for Gibson assembly in bold
[2]Zobel *et al.* 2015 ACS Synth Biol 4: 1341-1351

3 Discussion

The increasing demand for new sweeteners makes 5-ketofructose (5-KF) an interesting new product, as it has a similar taste and sweetness as fructose but is not metabolized by humans and major species of the human gut microbiome. In previous studies it was shown that strains of *Gluconobacter oxydans* carrying an expression plasmid for the fructose dehydrogenase of *Gluconobacter japonicus* can serve as highly efficient 5-KF producers. However, for a food additive, plasmid- or at least antibiotic-free microbial production is desirable and needs to be kept in mind when developing an industrial process. Furthermore, as the costs for such a sweetener must be low, besides an efficient producer strain also the substrate and the media composition are highly relevant parameters in process development. In this study efficient 5-KF producer strains with different traits were developed (Battling, et al., 2020, Wohlers, et al., 2021).

3.1 Development of plasmid-free *G. oxydans* strains for 5-KF production

In the first part of this thesis, plasmid-free *G. oxydans* strains for 5-KF production were developed to avoid the necessity to add antibiotics to the media for plasmid-maintenance. For this purpose, the *fdhSCL* genes encoding fructose dehydrogenase were integrated in four selected chromosomal loci. Furthermore, a strain with two genomic copies of the *fdhSCL* genes was created. The resulting integration strains were analyzed were characterized.

3.1.1 Integration site-specific differences in *fdhSCL* expression

Different plasmid-free 5-KF *G. oxydans* producer strains were generated and four suitable chromosomal integration sites for heterologous expression were identified. The comparison of the corresponding *fdhSCL*-integration strains with respect to 5-KF production and the approximately consistent RT-qPCR results, assaying *fdh* expression, revealed slight site-specific differences in *fdhSCL* expression and 5-KF production rate (Battling, et al., 2020). These might be due to the chromosomal organization and secondary structures, since supercoiling and the distribution of nucleoid-associated proteins differ among chromosomal regions and globally influence transcription (Browning, et al., 2010, Lal, et al., 2016, El Houdaigui, et al., 2019). Alternatively, the differences in *fdhSCL* expression could also depend on the cultivation conditions influencing the expression levels of the neighboring genes. For *E. coli* a reduced expression of the reporter gene was observed when the transcription of the neighboring gene was increased and vice versa (Bryant, et al., 2014). Despite the minor differences in *fdhSCL* expression, all four integration sites were shown to be suitable for future projects targeting *G. oxydans* strain development.

3.1.1 Influence of the *fdhSCL* copy number on expression and 5-KF production

As desired, the double integration strain IK003.1::*fdhSCL*^{2} showed approximately twice the 5-KF production rate and relative expression level compared to the corresponding single integration

strains (Battling, et al., 2020). Plasmid-based expression however, only resulted in an about two-fold increase in 5-KF production velocity, compared to the double integration strains. This means that a third or fourth chromosomal *fdhSCL* copy could already lead to 5-KF production rates like in the plasmid-based system. Additionally, a stronger promotor for *fdhSCL* expression could increase Fdh activity. Hoffmann, et al. (2020) reported for a single chromosomal *fdhSCL* integration with the P264 promotor in the *gdhM* locus, together with the native *gdhM* promotor, so actually a double promotor, 38% Fdh activity compared to the plasmid-based Fdh activity. However, the difference between *fdhSCL* transcript levels and 5-KF production in the plasmid-containing strain is striking. For the pBBR1 backbone a copy number of 23 ± 6 copies per cell has been reported for strain *G. oxydans* Δ*hsdR* (Kallnik, et al., 2010). While the expected 20-fold difference between the single integration strains and the plasmid-bearing strain was confirmed by RT-qPCR for the *fdhSCL* expression levels, a much weaker difference was observed with respect to the 5-KF production rate (Battling, et al., 2020).

3.1.2 Limitations in 5-KF production

The discrepancy between *fdhSCL* expression and 5-KF production can have different reasons. One explanation could be a limitation in secretion and correct incorporation of the C-terminal transmembrane helix of FdhC into the inner membrane. This hypothesis seems likely since the cytoplasmic membrane of *G. oxydans* contains a vast number of endogenous dehydrogenases (Peters, et al., 2013b, Mientus, et al., 2017). The native membrane-bound dehydrogenases could limit the incorporation of the heterologous Fdh or the secretion via the Sec- or Tat-pathway since all membrane-bound dehydrogenases with the active site in the periplasm need to be secreted as well. A negative influence of the multitude of membrane-bound dehydrogenases was reported for L-erythrulose production via the native mSldAB (Burger, et al., 2019). Using the *G. oxydans* BP.8 multideletion strain with deletions of the genes for eighth native membrane-bound dehydrogenases, other than mSldAB, was advantageous for L-erythrulose production, regarding rate and final titer, when compared to the corresponding wild type strain. In a biotransformation with resting cells, the multideletion strain reached an about 10% increased cell-specific product formation rate, compared to the wild type strain. The authors explain the effect by a limitation in space for enzyme integration to the cytoplasmic membrane by the different membrane-bound dehydrogenases (Burger, et al., 2019).

Another possible explanation for limited fructose oxidation could be a limitation in oxygen. However this seems unlikely, as the plasmid-carrying strain *G. oxydans* 621H Δ*hsdR* pBBR1p264-*fdhSCL*-ST was not 20-fold faster in 5-KF production than the single integration strain *G. oxydans* IK003.1-igr3::*fdhSCL* in a comparable batch fermentation, where oxygen supply is sufficient (Herweg, et al., 2018, Battling, et al., 2020). It is rather possible that the ubiquinone regeneration via the respiratory chain is limiting. A similar effect was reported for a *G. oxydans*

strain overproducing the membrane-bound glucose dehydrogenase. In the study by Meyer, et al. (2013), plasmid-based *gdhM* expression resulted in nine-fold increased transcript levels, while the membrane fraction showed five-fold increased GdhM activity with an artificial electron accepter, but only three-fold increased oxygen consumption, indicating a limitation in the terminal quinol oxidases of the respiratory chain (Meyer, et al., 2013).

After an improvement of plasmid-free 5-KF production by increasing the *fdhSCL* expression levels with additional copies and/or a different promotor, the transcription-independent limitation in fructose oxidation could be addressed by either deleting genes for endogenous dehydrogenases or, the other way around, integrating the *fdhSCL* genes in an existing multideletion strain, for example *G. oxydans* BP.9 (Peters, et al., 2013b), or alternatively overexpress selected parts of the respiratory chain. Overexpression of the *cyoBACD* genes encoding cytochrome bo_3 oxidase in *G. oxydans* for example led to an improved growth rate and growth yield (Richhardt, et al., 2013b) and improved GdhM- and mSldAB-based production of 5-keto-D-gluconic acid (Yuan, et al., 2016).

Further optimization of the presented 5-KF production strains might be achieved by deletion of the 5-KF reductase genes, GOX1432 and GOX0644, recently discovered in *G. oxydans* 621H (Schiessl, et al., 2021). Although no decrease in 5-KF concentrations was observed in our strains, simultaneous fructose oxidation and 5-KF reduction could decelerate the production rate.

3.1.3 Alternative 5-KF production via native *Gluconobacter* strains

Although plasmid-free and needing no antibiotics, the generated *G. oxydans* 5-KF producer strains are still genetically modified organisms (GMOs) since they carry the *fdhSCL* genes of *G. japonicus*. For consumer perception, a non-GMO production process would be beneficial, since non-GMO labeled foods are unwarrantedly more likely to be related to healthiness, safety, and environmental friendliness by costumers (Sax and Doran, 2016). Consequently, also the possibility of a non-GMO producer strain was investigated. *G. oxydans* 621H has no Fdh but still produces small amounts of 5-KF when grown on fructose as seen in the IK003.1 reference (Battling, et al., 2020). Also, the parental strain *G. oxydans* 621H was previously described to form 5-KF when grown on D-mannitol (Richhardt, et al., 2012). The glycerol dehydrogenase of *G. thailandicus* NBRC 3258, a homolog of the *G. oxydans* 621H polyol dehydrogenase mSldAB, was described to have a broad substrate spectrum and to oxidize fructose to 5-KF (Ano, et al., 2017). We could confirm unspecific 5-KF production in *G. oxydans* 621H by mSldAB with a *sldAB* deletion strain and complementation with plasmid-based *sldAB* expression (Figure S1). However, even plasmid-based *sldAB* expression in the wild type (Figure S2) resulted only in low 5-KF production rates compared to *the fdhSCL* expressing strains, indicating that 5-KF production via the endogenous mSldAB enzyme in *G. oxydans* 621H is not competitive with heterologous production via the highly active FdhSCL.

Another option would be to use a species with an endogenous Fdh, such as *G. japonicus* NBRC3260, the donor of the here used *fdhSCL* genes. However, an initial comparison of a heterologous plasmid-based *fdhSCL* expression in *G. oxydans* was shown to be beneficial when compared to the *G. japonicus* wild type (Kawai, et al., 2013). Even for the strain *G. oxydans* Δ*mgdh*::*fdhSCL* with only one chromosomal *fdhSCL* copy a higher Fdh activity than in different tested *Gluconobacter* strains with native Fdh was reported (Hoffmann, et al., 2020). Also, the recently published example of 5-KF production from mannitol with native *G. frateurii* CHM 43 (Adachi, et al., 2020) seems not competitive, since the reported production rates are lower than in our *fdhSCL* integration strains (Adachi, et al., 2020, Battling, et al., 2020). This indicates that the known hosts with native Fdh would also need optimization prior to efficient 5-KF production and that *G. oxydans* strains are advantageous for 5-KF production.

3.2 *P. putida* as alternative 5-KF production host

In the second part of this thesis, 5-KF production was established in *P. putida* as alternative host. Tn*7*-based chromosomal integration of the *fdhSCL* genes enabled *P. putida* to produce 5-KF from fructose. Furthermore, heterologous expression of *inv1417*, encoding an invertase, allowed 5-KF from sucrose as alternative substrate. The different strains were characterized in shake flask and bioreactor cultivations. Additionally, the new host was compared to *G. oxydans* regarding 5-KF production.

The membrane-bound Fdh, which needs proper secretion via the Sec- and Tat-pathway, the membrane incorporation via the cytochrome *c* subunit and heme *c* and FAD as prosthetic groups for FdhC and FdhL, is a complex enzyme and correct assembly in the new host was not self-evident. However, the presence of the endogenous gluconate dehydrogenase in *P. putida*, which has similar subunits and prosthetic groups (Kumar, et al., 2013), suggested that correct Fdh assembly might be possible. Additionally, the importance of periplasmic glucose oxidation (del Castillo, et al., 2007) and the recently published xylonate production based on periplasmic xylose oxidation with *P. putida* (Dvořák, et al., 2020) led to the assumption that *P. putida* is a suited host for production processes via periplasmic oxidation.

Whether *P. putida* has a sufficient osmotolerance to produce 5-KF at high substrate and product concentrations, whether high fructose oxidation activities can be reached with strong heterologous *fdhSCL* expression and whether the yield can be improved by inhibiting fructose metabolization still needs to be investigated.

3.2.1 *P. putida* at increased osmotic pressure

The adaptation of *P. putida* to osmotic stress conditions via uptake of potassium or betaine and biosynthesis of Nα-acetylglutaminylglutamine amide and mannitol has been described (Kets, et al., 1996a, Kets, et al., 1996b). According to transcriptome studies, *P. putida* responds to osmotic stress also with membrane modifications, biofilm formation and reduced flagella formation

together with a more general stress response (Reva, et al., 2006, Bojanovič, et al., 2017). To assess the ability of *P. putida*::*fdhSCL* to cope with increased osmotic stress at high fructose concentrations a preliminary experiment with different fructose concentrations ranging from 18 g/L – 200 g/L fructose was conducted in the BioLector. The experiment showed an extended lag phase and decreased final biomass with increasing fructose concentrations and no growth with 180 g/L or 200 g/L fructose (Figure S3). In the 1 L batch fermentation in a DASGIP bioreactor with 150 g/L fructose, however, *P. putida*::*fdhSCL* showed good growth and 5-KF production (Wohlers, et al., 2021). This demonstrates that fructose concentrations of at least 150 g/L are tolerated. Also, higher sugar concentrations and osmolarities during a potential 5-KF production process should be no problem, since 150 g/L fructose could be a good initial concentration for a fed-batch process. Since fructose oxidation only started in the late exponential phase after a pH decrease, in a fed-batch process with a balanced fructose feed-rate beginning after the growth phase and optimized conditions, high product concentrations should be possible.

3.2.2 Influence of a second chromosomal *fdhSCL* copy on 5-KF production in *P. putida*

Aiming at increased 5-KF production, like in the *G. oxydans* project, a second chromosomal *fdhSCL* copy was integrated into the genome of *P. putida*. Two serial, adjacent *fdhSCL* copies, together with one 14g promotor, were integrated via Tn*7* transposition into the *P. putida* wild type, yielding *P. putida*::2x*fdhSCL*. Against the expectations, no increase in 5-KF production was observed. Instead, growth was slightly inhibited and 5-KF production delayed, when compared to the single integration strain (Figure S4). This indicates that increased production of the heterologous membrane-bound enzyme complex is growth-inhibiting and consequently fructose oxidation is delayed. Despite having a negative effect under these conditions, the impaired growth suggests that in fact more Fdh is produced and incorporated into the membrane. Despite the growth defect, the second *fdhSCL* copy could be beneficial at higher fructose concentrations, when a later production start but higher fructose oxidation rate outcompetes the earlier start in 5-KF production of the single integration strain. However, it needs to be assessed how much of improvement can be achieved considering the oxidation capacities of the respiratory chain. In *G. oxydans*, even in a plasmid-carrying strain that reaches approximately 20-fold expression levels of a single integration strain, only an about four-fold 5-KF production rate was reached compared to a single integration strain, indicating a limitation in the respiratory chain (Battling, et al., 2020).

3.2.3 Acidification during cultivation of *P. putida*::*fdhSCL* with fructose or sucrose

A strong acidification with a drop from pH 7 to pH values below 5 was observed in the cultivations of *P. putida*::*fdhSCL* when grown in mineral salts medium (MSM) with glucose and fructose or with sucrose as sole carbon source for the *inv1417* expressing strain. A role of Fdh or 5-KF can be excluded since a similar pH decrease was observed in cultures of the wild type (Wohlers, et al., 2021). A similar effect has to our knowledge not yet been described for *P. putida*. However, its

sugar metabolism has mostly been studied for cells grown with glucose. While glucose is predominantly oxidized in the periplasm to gluconate and partially further oxidized to 2-ketogluconate, these acids are described to be later taken up and metabolized via the central carbon metabolism (del Castillo, et al., 2007, Nikel, et al., 2015, Kohlstedt and Wittmann, 2019). This suggests that at least the 20 mM glucose in the medium is not responsible for the strong pH decrease. Admittedly, in the publications describing the complete metabolization of the acids from periplasmic glucose oxidation, only 16-40 mM glucose were applied and this might be different at increased overall sugar concentrations like in the 20 mM glucose with 100 mM fructose used for 5-KF production (del Castillo, et al., 2007, Nikel, et al., 2015, Kohlstedt and Wittmann, 2019, Wohlers, et al., 2021). Additionally, a similarly low pH as in cultures containing glucose and fructose has also been observed in cultures with fructose as sole carbon source (Wohlers, et al., 2021), indicating that acids formed during fructose consumption are causing the pH decrease. To exclude glucose as cause for the acidification, a cultivation with 100 mM or 120 mM glucose would be necessary.

Only recently the periplasmic formation of the acidic compound mannonate has been described for fructose-grown *P. putida*. Fructose is initially isomerized to mannose and then oxidized to mannonate by the periplasmic glucose dehydrogenase (Nguyen, et al., 2021a). However, these reactions were observed under completely different conditions, namely when *P. putida* was grown anaerobically in an artificial bioelectrochemical system and thus this effect might not occur in aerobically grown *P. putida*. The fact that *P. putida*::*fdhSCL* Δ*fruB*, a mutant unable to take up fructose, showed a delayed pH decrease (Figure S5) rather indicates that the reason for acidification of fructose grown *P. putida* lies in cytoplasmic fructose consumption. Furthermore, the strain *P. putida*::*fdhSCL* Δ*gcd*::*inv1417*, lacking the membrane-bound glucose dehydrogenase showed a comparable acidification as the 5-KF strain with *gcd* (Master Thesis Marielle Driller, 2021). Consequently, periplasmic mannonate formation can be excluded as reason for the observed acidification during 5-KF production. The study on anaerobic fructose metabolization additionally describes the formation of acetate and pyruvate as by-products (Nguyen, et al., 2021a). These by-products, however, were also reported for a comparable anaerobic metabolization of glucose (Yu, et al., 2018), while they were not detected during aerobic glucose consumption (Nikel, et al., 2015), indicating that the formation of pyruvate and acetate not necessarily has to be the same for aerobically fructose-grown cells. .

Both uptake and metabolism of fructose and glucose in *P. putida* show differences. Glucose is taken up via the ATP-dependent ABC transporter GtsABCD, while fructose is taken up via PTS^{Fru}. A study by Chavarría, et al. (2012) revealed a different metabolization of both sugars. Glucose is mostly processed via the EDP and only to a small extent (4%) via the PPP, or as later described via the EDEMP cycle, while fructose is metabolized through the EDP (52 %), the EMP (34%), and the PPP (14%). Despite lacking phosphofructokinase, *P. putida* can process fructose via the EMP

since fructose-1-phosphate is directly phosphorylated to fructose-1,6-bisphosphate by FruK (Chavarría, et al., 2012). The distribution among different routes was shown to be influenced by PtsN, a subunit of PTS^{Ntr}, which is interconnected with PTS^{Fru} (Chavarría, et al., 2012). Additionally, fructose-1-phosphate is the effector for Cra, which represses PP_3443, encoding a GAPDH and can consequently influences the upper sugar metabolism at the GA3P node. To ensure efficient PEP supply for PTS^{Fru} in fructose-grown cells the GAPDH flux is increased, in comparison to glucose-grown cells. Hence the distribution between the different pathways, TCA cycle, EDEMP cycle or PPP is different depending on the carbon source (Chavarría, et al., 2012, Chavarría, et al., 2016). The different fluxes of the non-PTS sugar glucose and the PTS sugar fructose, the different metabolization and varying enzyme activities could cause the accumulation of distinct by-products. Consequently, the difference in metabolization of fructose from glucose could possibly cause the strong acidification in cultures of fructose-grown *P. putida* , since a similar acidification has not yet been reported for glucose-grown cells.

A dilute-and-shoot mass spectrometry analysis using a method described by Reiter, et al. (2021) optimized for detection of organic acids, identified the presence of gluconate, pyruvate, and different TCA cycle intermediates (citrate, isocitrate, succinate, malate) in culture supernatants after growth with fructose and glucose (Wohlers, et al., 2021). However, verification via high performance liquid chromatography (HPLC) was challenging and qualitative detection was only possible for some of the compounds following sample preparation via solid phase extraction (SPE), using NH_2-SPE columns as described by Agius, et al. (2018). Pyruvate was found in all tested samples of *P. putida*::*fdhSCL* and *P. putida*::*fdhSCL* pBT'T-*inv1417*, while succinate, malate and 2-ketogluconate could only be detected in some samples. Additionally, unidentified peaks were detected (see example chromatograms in Figure S7). These results suggest that small amounts of different acids are excreted into the medium by fructose- or sucrose-grown *P. putida*, which in combination cause the observed pH shift.

3.2.4 Fructose uptake and metabolism in *P. putida*

An advantage of using the well-studied *P. putida* is the knowledge of the fructose uptake system. In *P. putida* fructose is taken up via the PEP-dependent phosphotransferase system present in this species, PTS^{Fru} encoded by the *fruBKA* operon. PTS^{Fru} has been reported to be the only uptake route for fructose in *P. putida*, since a *fruB* mutant strain cannot grow on fructose as sole carbon source (Velázquez, et al., 2007). Hence, a *P. putida*::*fdhSCL* Δ*fruB* mutant was generated to prevent fructose loss via cytoplasmic fructose metabolization and thereby increase the 5-KF/fructose yield. However, instead of increasing 5-KF production and yield, 5-KF production was decelerated, and an increasing brownish coloring of the medium was observed. Additionally, a slower pH decrease was observed compared to *P. putida*::*fdhSCL*, still carrying the *fruB* gene (Figure S5). The brownish coloring had also been observed previously in the biotransformation experiments with

high fructose and 5-KF concentrations and is likely due to the Maillard reaction. The Maillard reaction actually comprises a set of different reactions following an initial reaction between a carbonyl group of a reducing sugar with an amino group of amino acids or peptides, forming a glycosylamine (Hodge, 1953, Martins, et al., 2000). This initial step is facilitated at neutral to basic pH, since the amino group needs to be unprotonated (Martins, et al., 2000, Lund and Ray, 2017). In the case of 5-KF production with *P. putida*, a lowering of the pH occurred during cultivation. This acidification is not only important to increase Fdh activity, but also decreases the formation of by-products via Maillard reaction, meaning substrate or product loss. Compared to fructose with its single α-hydroxyketo group, 5-KF with two α-hydroxyketo groups is even more prone to the Maillard reaction. Consequently, in the case of *P. putida*::*fdhSCL* Δ*fruB* not only the slower 5-KF production, but possibly also the increased brownish coloring of the culture medium is caused by the slower pH decrease in the mutant lacking the *fruB* gene. This assumption was confirmed when *P. putida*::*fdhSCL* Δ*fruB* was cultivated at different pH conditions. A lower pH was implemented by either doubling the initial glucose concentration for increased gluconate formation and natural acidification, or artificial acidification by addition of HCl after growth was completed. These modifications on the one hand increased 5-KF/fructose yield and on the other hand decreased the brownish coloring of the medium, compared to the standard conditions (Figure S6). In addition to the importance for Fdh activity, the acidification observed during 5-KF production with *P. putida* seems to be important to avoid the formation of brown by-products.

3.2.5 Sucrose as alternative substrate for 5-KF production in *P. putida*

An alternative way to make 5-KF production more cost-efficient is the use of a substrate that is cheaper than fructose, such as sucrose. Plasmid-based expression of the *G. japonicus inv1417* gene in *P. putida*::*fdhSCL* resulted in 5-KF production from sucrose at comparable rates as from fructose (Wohlers, et al., 2021). The invertase Inv1417 has been described to be a periplasmic enzyme and *in silico* predictions suggest the presence of a Tat signal peptide (Hoffmann, et al., 2020). However, in our lab the suitability of Inv1417 to be anchored to the outer membrane via Sec-dependent surface display was shown (data not shown, Master Thesis Marielle Driller, 2021), indicating that Inv1417 is secreted via the Sec pathway and not via the Tat pathway. Regardless of the secretion mechanism, periplasmic sucrose cleavage is advantageous for 5-KF production in comparison to the previously reported heterologous sucrose cleavage in the cytosol (Löwe, et al., 2020), as fructose is formed in the compartment where also its oxidation by Fdh takes place.

When studying 5-KF formation from sucrose, large amounts of the glucose fraction were not metabolized. From 100 mM sucrose up to 65 mM glucose remained in the culture medium (Wohlers, et al., 2021). This effect was not reported for the sucrose-consuming *P. putida* strains described in literature, but in these studies, only low sucrose concentrations of 3 g/L sucrose (=8.7 mM) were used (Löwe, et al., 2017, Löwe, et al., 2020). Since in our studies more glucose was

accumulated in cultures with a start pH of 6.5 compared to cultures with a start pH of 7, a connection of glucose accumulation and the low pH was assumed. This assumption was confirmed when comparing different pH adjustments with the standard cultivation conditions. In cultures with increased pH, either by NaOH addition or with increased buffer capacity, less glucose was accumulated compared to the standard conditions (Wohlers, et al., 2021). The major route for glucose consumption in *P. putida* is the oxidation to gluconate via the periplasmic PQQ-dependent glucose dehydrogenase Gcd (Daddaoua, et al., 2010, Nikel, et al., 2015, Kohlstedt and Wittmann, 2019). Hence, a limitation in Gcd activity at low pH seems to be a possible reason for glucose accumulation. The pH optimum of Gcd for glucose oxidation has not been determined. However, the production of lactobionic acid in *Pseudomonas taetrolens* via its native PQQ-dependent glucose dehydrogenase was described to be most efficient at pH values above 6, indicating a neutral pH optimum for the glucose dehydrogenase (Kim, et al., 2020, Oh, et al., 2020). Since the *P. taetrolens* glucose dehydrogenase (Genbank KMM82267.1) shows 49% amino acid sequence identity to the homologous protein of *P. putida* (Gcd, PP_1444), comparable properties and a similar pH optimum are likely. Considering the role of glucose oxidation by *P. putida* in the soil or rhizosphere, where gluconic acid formation leads to acidification causing phosphate solubilization, reduced Gcd activity at acidic pH seems reasonable. Phosphate limiting conditions were shown to increase expression of *gcd* and genes encoding enzymes for PQQ biosynthesis, together leading to acidification by gluconate formation (An and Moe, 2016). Consequently, a Gcd inhibition or downregulation at acidic pH could also be possible.

If inactive Gcd would lead to the glucose accumulation, a strain without *gcd* should accumulate even more glucose. However, *P. putida*::*fdhSCL* Δ*gcd*::*inv1417* showed a similar glucose accumulation when compared to a strain that has the *gcd* (data not shown, Master Thesis Marielle Driller, 2021). This suggests, that reduced or inhibited Gcd activity is not the only reason for glucose accumulation.

Considering not directly the acidic pH but the organic acids causing it, catabolite repression could be of importance here. *Pseudomonads* are described to prefer organic acids like succinate and citrate over glucose (Collier, et al., 1996). For *P. aeruginosa* citrate and succinate were shown to repress enzymes of glucose metabolism. For example, gluconate dehydrogenase, glucose 6-phosphate dehydrogenase, and KDPG aldolase were downregulated when the organic acids were present. Concentrations as little as 5 mM succinate or 8 mM citrate were sufficient for downregulation (Ng and Dawes, 1973, Siegel, et al., 1977, Collier, et al., 1996, Rojo, 2010). For *P. putida*, succinate also results in catabolite repression of glucose, however, both carbon sources are consumed simultaneously, while succinate is consumed faster (La Rosa, et al., 2015). While in the publication by La Rosa, et al. (2015) glucose is still metabolized when succinate is present, this could be different under the conditions in our study.

Also, a general pH inhibition of growth and the overall enzyme activities and a stop in glucose consumption as consequence are possible. The observed pH values below 5 are rather untypical for *P. putida*, which is described to grow at a pH range of 5.5-10 (Bagdasarian and Timmis, 1982, Reva, et al., 2006). Thus, inactivity of the organism's metabolism seems to be a possible explanation for the glucose accumulation.

Regardless of the reason for glucose accumulation during growth on sucrose, this effect can be beneficial in future studies. For maximal 5-KF production from sucrose, also the glucose units need to be converted to 5-KF. Hence, glucose accumulation is favorable since it allows 5-KF production also of the glucose units after isomerization to fructose.

3.3 Comparison of *G. oxydans* and *P. putida* regarding their qualification for 5-KF production

When comparing *G. oxydans* and *P. putida* with respect to 5-KF production, important traits of the host organism are a high osmotolerance, sufficient oxidation capacity of the respiratory chain and the ability to grow and survive at acidic pH.

3.3.1 Comparison of osmotolerance

G. oxydans as natural habitant of sugary niches is an organism renowned for its osmotolerance (Deppenmeier, et al., 2002, Sievers and Swings, 2015, Zahid, et al., 2015). However, the molecular basis of the osmotolerance of the acetic acid bacterium has not been completely elucidated. 2-Keto-L-gulonic acid, which can be synthesized from sorbitol in *G. oxydans*, was proposed to have a function in osmotic stress control (Saito, et al., 1998), but so far only mannitol accumulation was demonstrated as strategy in osmoprotection (Zahid, et al., 2015). A fed-batch process for 5-KF production already proved sufficient osmotolerance of *G. oxydans*. Only at osmolalities ≥ 1.08 osmol/kg, corresponding to the initial fructose concentration of 150 g/L fructose, growth of *G. oxydans* 621H Δ*hsdR* pBBR1p264-*fdhSCL*-ST was delayed and product concentrations up to 489 g/L 5-KF could be reached (Herweg, et al., 2018). The ability of *P. putida* to tolerate concentration above 150 g/L fructose or 5-KF still needs to be investigated. For *P. putida* facing osmotic stress, mannitol accumulation was also shown as strategy and transcriptome data suggest further adaptation mechanisms like the accumulation or synthesis of further osmoprotectans like glycine or N-acetylglutaminylglutamine amide (NAGGN), a modification of the cell envelope, activation of transmembrane transporters, motility reduction by downregulation of flagella genes and upregulation of biofilm formation (Kets, et al., 1996a, Reva, et al., 2006, Bojanovič, et al., 2017). However, if the endogenous adaptation capabilities should not be sufficient, exogenous osmoprotectants like proline or betaine could be added to the medium. The uptake of these compounds should be possible, as the gene PP_2914 was annotated as a proline/betaine

symporter (ProP) and was upregulated under osmotic stress (Belda, et al., 2016, Bojanovič, et al., 2017).

3.3.2 Comparison of the respiratory chain and oxidation capacity

Regardless of the organism, the respiratory chain or more specifically the terminal oxidases and their oxidation capacity is of high importance for fast 5-KF oxidation. At least in *G. oxydans* with plasmid-based *fdhSCL* expression, rather the regeneration of ubiquinol via the terminal oxidases than the *fdhSCL* expression seems to be limiting (see 3.1.2).

P. putida and *G. oxydans* both have a cytochrome *bd*- and a cytochrome bo_3- type quinol oxidase and a cytochrome bc_1 complex. However, *G. oxydans* lacks cytochrome *c* oxidase and therefore the role of the cytochrome bc_1 complex is unclear. *P. putida*, on the other hand, contains three cytochrome *c* oxidases, one aa_3- and two cbb_3-type cytochrome *c* terminal oxidases. The higher number and broader variety of terminal oxidases in *P. putida* in theory imply a higher oxidation capacity. Especially cbb_3-type cytochrome oxidases are known to have a high oxygen affinity and hence could be important at high oxidation rates (Morales, et al., 2006, Hanke, et al., 2012, Richhardt, et al., 2013b, Belda, et al., 2016). Probably more important than the number of terminal oxidases are the expression of the genes and the actual activity. In both organisms the cytochrome bo_3 oxidase encoded by respective *cyo* operons has been reported to be the main oxidase under aerobic conditions (Sweet and Peterson, 1978, Dinamarca, et al., 2002, Richhardt, et al., 2013b).

For *G. oxydans* the overexpression of the *cyoBACD* genes coding the bo_3 oxidase has been described to increase the growth rate, the growth yield, and the ubiquinol oxidase activity and led to accelerated and increased production of 5-ketogluconate via GdhM and mSldAB (Richhardt, et al., 2013b, Yuan, et al., 2016). A similar overexpression of the *cyoBACD* genes could also improve 5-KF production with *G. oxydans*. Correspondingly, overexpression of the terminal oxidase genes might improve 5-KF production in *P. putida*, despite no such study has been published yet. In *P. aeruginosa*, however, the overexpression of the *cioAB* genes for cytochrome *bd* oxidase led to a cell division defect and increased antibiotic sensitivity (Tavankar, et al., 2003). This could be different in *P. putida* and the alternative overproduction of the cytochrome bo_3 oxidase might be possible without negative effects. Instead of direct overexpression of quinol oxidase-coding genes, the titration of regulatory effects might increase the terminal oxidase activity and consequently accelerate ubiquinol and fructose oxidation. For example the hybrid sensor kinase HskA was shown to play a role in the composition of the electron transport chain in *P. putida* depending on oxygen availability by sensing the redox status of the respiratory ubiquinones (Sevilla, et al., 2013a, Sevilla, et al., 2013b). HskA upregulates the expression of the genes coding for the cytochrome bc_1 complex and the cytochrome cbb_3-1 oxidase at aerobic conditions. At semiaerobic conditions, HskA upregulates the genes coding for the cytochrome *bd*, aa_3 and cbb_3-1 oxidases and

the cytochrome bc_1 complex, while the cytochrome bo_3 and the cbb_3-2 oxidases are not regulated by HskA (Sevilla, et al., 2013a). Consequently, *hskA* overexpression could possibly increase the oxidation capacity and accelerate 5-KF production in *P. putida*.

The respiratory chain of the acid-tolerant *G. oxydans* has been described to adapt to acidic pH by increasing the amount of the cyanide-insensitive cytochrome *bd* oxidase. At pH 4 compared to pH 6 expression of the *cydAB* genes is 2.2- and 1.6 fold upregulated (Matsushita, et al., 1989, Hanke, et al., 2012). The cytochrome *bd* oxidase has high quinol oxidase activity, also at low pH, whereas the cytochrome bo_3 oxidase shows decreasing activity at lower pH (Miura, et al., 2013). Despite no cytochrome *c* oxidase was identified in *G. oxydans*, the cytochrome bc_1 complex was described to play a role at acidic pH, as a deletion mutant showed a growth defect at acidic pH (Hanke, et al., 2012). In *P. putida*, no transcriptional changes were detected for the terminal oxidase genes at acidic conditions of pH 4.5 (Reva, et al., 2006). However, the cytochrome bo_3 oxidase has been described to be crucial for adaptation to acidic pH (Reva, et al., 2006).

3.3.3 Comparison of acid tolerance

For 5-KF production with Fdh and its acidic pH optimum, both organisms need to adapt to acidic conditions. For *G. oxydans* the ability is self-evident as the natural metabolism involving incomplete periplasmic oxidation of various substrates is causing acidification. The pH adaptation mechanisms of *G. oxydans*, however, have not yet been elucidated. A transcriptome study comparing global gene expression at pH 4 and pH 6 showed no typical acid stress responses, suggesting functionality of all crucial *G. oxydans* enzymes at neutral to acidic pH (Hanke, et al., 2012).

In the soil as natural habitat, *P. putida* can also be exposed to pH stress and in general *P. putida* is renown as robust host. In a study on the influence of acidic pH (pH 4.5, HCl) on the *P. putida* transcriptome, only a few changes were noted. PP_1656, encoding RelA, the major ppGpp synthetase, was upregulated. Also, PP_2914, coding for a proline/betaine transporter, was upregulated, potentially to stimulate the uptake of proline or betaine from the medium. Additionally, PP_2196, encoding an agmatinase, was upregulated. Agmatinase hydrolyzes agmatine to putrescine and urea. The authors assume that this causes the observed alkalization from pH 4.5 to 8 during the cultivation (Reva, et al., 2006). This unbuffered increase of the pH during the experiment might have falsified the strength of transcriptome change upon acid stress. The genome sequence of *P. putida* revealed that most acid resistance mechanisms of Enterobacteria are missing in *P. putida* (Bearson, et al., 1997, Belda, et al., 2016). However, also *P. putida* possesses a gene PP_4140 coding for a lysine decarboxylase, which in *E. coli* plays a role in acid resistance (Belda, et al., 2016). Despite the limited knowledge on the mechanisms and ability for acid adaptation in *P. putida*, 5-KF production upon acidification below pH 5 showed clearly that the cells are able to withstand the acidic condition (Wohlers, et al., 2021).

3.4 Conclusion and outlook

Both *G. oxydans* and *P. putida* were shown to be suitable hosts for 5-KF production and of both organisms potent producer strains were generated in this work (Battling, et al., 2020, Wohlers, et al., 2021). While *G. oxydans* is a well renowned host for periplasmic oxidations, *P. putida* was first shown in this work to be a suited host for heterologous periplasmic oxidation. For further project development and potential industrial implementation, however, one of the two hosts needs to be chosen eventually. The choice is between the classical periplasmic oxidizer *G. oxydans* with a high osmotolerance and strong oxidation capacities but limitations in engineering tools and expression systems and, on the other side, the well-studied *P. putida*, with many genetic tools available, good growth in minimal media and a better biomass yield than *G. oxydans*, but possible limitations in periplasmic oxidation capacities, at acidic pH and when facing highly osmotic conditions.

For a potential industrial process, space time yield and product titer are especially important. Consequently, the production ability of *P. putida* to produce high 5-KF concentrations in a fed-batch process with fructose as substrate need to be evaluated and compared to that of *G. oxydans* to decide which organism should be used for further strain and process optimization.

For both organisms, an increase in fructose oxidation abilities seems possible and should be addressed first, e.g., by introducing further chromosomal *fdhSCL* copies or promotor exchanges for increased expression. Also it is necessary to check whether the capacity of the terminal oxidases is sufficient by comparing oxygen consumption during fructose oxidation with Fdh activity in an oxygen-independent reaction with artificial electron acceptors, similar as described by Meyer, et al. (2013).

Sucrose utilization for 5-KF production in the generated strain *G. oxydans* IK003.1::*fdhSCL*^{2} via heterologous *inv1417* expression, as first described by Hoffmann, et al. (2020), was already tested and is possible (Figure S8). This means that 5-KF production from sucrose is an option with both organisms at choice via plasmid-based *inv1417* expression. For antibiotic-free production, however, a chromosomal integration or change for an antibiotic-independent plasmid system would be needed. For efficient use of sucrose, eventually also the glucose fraction needs to be converted to 5-KF. Therefore, the conversion of glucose to fructose by glucose isomerase is necessary. Upon identifying or developing a suited isomerase, glucose isomerization seems possible since both organisms accumulate the majority of the glucose units after sucrose cleavage (Figure S8; Wohlers, et al. (2021)).

Regarding sucrose as substrate, also the potential of a surface display of invertase and further heterologous enzymes should be assessed. The development of a surface display system for enzymes needed for the utilization of alternative substrates was tested to obtain a reusable cell catalyst for conversion of substrates without the need of an uptake via the membranes. The difficulties to establish a surface display system in *G. oxydans* were the most important reason for testing *P. putida* as alternative 5-KF production host. Hence, an assessment of the advantages and

applicability of a surface display of the invertase and potentially an isomerase in comparison with soluble, periplasmic enzymes is of importance for the selection of the organism. The surface display of Inv1417 was achieved in *P. putida*::*fdhSCL* with *E. coli* Lpp-OmpA or *P. aeruginosa* OprF as membrane anchors (data not shown, Master Thesis Marielle Driller, 2021). However, additional proof of surface display and optimization would be needed before application.

Eventually, process development will lead to optimization of media composition, pH, starting substrate concentration, and feed-rate. Additionally, a process for product purification needs to be established. An approach for 5-KF purification from the culture broth has been described by Kinoshita and Terada (1963).

Independent of the choice of the producer strain and further strain and process optimization, the applicability and stability of 5-KF in different foods and preparation methods needs to be tested prior to market introduction as not all sweeteners are equally suited for all applications (Carocho, et al., 2017). Since 5-KF is prone to Maillard reactions, which are enhanced at high temperature, it is perhaps not suited for baking. More importantly, approval of 5-KF as food ingredient by the authorities (FDA, EFSA) is needed before it can be commercialized. This approval process requires a broad set of toxicity tests, which need to be completed before submitting a petition (Rulis and Levitt, 2009).

4 References

Ackermann, Y.S., Li, W.-J., Op de Hipt, L., Niehoff, P.-J., Casey, W., Polen, T., Köbbing, S., Ballerstedt, H., Wynands, B., O'Connor, K., Blank, L.M., and Wierckx, N. (2021) Engineering adipic acid metabolism in *Pseudomonas putida*. *Metab. Eng.* 67: 29-40.

Adachi, O., Moonmangmee, D., Toyama, H., Yamada, M., Shinagawa, E., and Matsushita, K. (2003) New developments in oxidative fermentation. *Appl. Microbiol. Biotechnol.* 60: 643-653.

Adachi, O., Nguyen, T.M., Hours, R.A., Kataoka, N., Matsushita, K., Akakabe, Y., and Yakushi, T. (2020) 5-Keto-D-fructose production from sugar alcohol by isolated wild strain *Gluconobacter frateurii* CHM 43. *Biosci. Biotechnol. Biochem.* 84: 1745-1747.

Agius, C., von Tucher, S., Poppenberger, B., and Rozhon, W. (2018) Quantification of sugars and organic acids in tomato fruits. *MethodsX* 5: 537-550.

Aida, K., and Yamada, Y. (1964) A new enzyme, 5-ketofructose reductase. *Agric. Biol. Chem.* 28: 74-75.

Ameyama, M., Matsushita, K., Shinagawa, E., and Adachi, O. (1981a) 5-Keto-D-fructose reductase of *Gluconobacter industrius*: Purification, crystallization and properties. *Agric. Biol. Chem.* 45: 863-869.

Ameyama, M., Shinagawa, E., Matsushita, K., and Adachi, O. (1981b) D-Fructose dehydrogenase of *Gluconobacter industrius* - purification, characterization, and application to enzymatic micro-determination of D-fructose. *J. Bacteriol.* 145: 814-823.

An, R., and Moe, L.A. (2016) Regulation of pyrroloquinoline quinone-dependent glucose dehydrogenase activity in the model rhizosphere-dwelling bacterium *Pseudomonas putida* KT2440. *Appl. Environ. Microbiol.* 82: 4955-4964.

Ankenbauer, A., Schäfer, R.A., Viegas, S.C., Pobre, V., Voß, B., Arraiano, C.M., and Takors, R. (2020) *Pseudomonas putida* KT2440 is naturally endowed to withstand industrial-scale stress conditions. *Microb. Biotechnol.* 13: 1145-1161.

Ano, Y., Hours, R.A., Akakabe, Y., Kataoka, N., Yakushi, T., Matsushita, K., and Adachi, O. (2017) Membrane-bound glycerol dehydrogenase catalyzes oxidation of D-pentonates to 4-keto-D-pentonates, D-fructose to 5-keto-D-fructose, and D-psicose to 5-keto-D-psicose. *Biosci. Biotechnol. Biochem.* 81: 411-418.

Asai, T. (1935) Taxonomic studies on acetic acid bacteria and allied oxidative bacteria isolated from fruits. A new classification of the oxidative bacteria. *J. Agric. Chem. Soc. Japan* 11: 674-708.

Avantium (2021) Avantium reaches key commercial milestone for its FDCA flagship plant with commitments for >50% of its output, web page, https://www.avantium.com/press-releases/avantium-reaches-key-commercial-milestone-for-its-fdca-flagship-plant-with-commitments-for-50-of-its-output/, accessed October 8, 2021.

Avigad, G., and Englard, S. (1974) 5-Keto-D-fructose. VIII. Synthesis of 5-keto-D-fructose 1,6-bisphosphate and some of its properties. *Biochim. Biophys. Acta, Gen. Subj.* 343: 330.

Avigad, G., and Englard, S. (1965) 5-Keto-D-fructose: I. Chemical characterization and analytical determination of the dicarbonylhexose produced by *Gluconobacter cerinus*. *J. Biol. Chem.* 240: 2290-2296.

Avigad, G., and Englard, S. (1968) 5-Keto-D-fructose: V. Phosphorylation by yeast hexokinase. *J. Biol. Chem.* 243: 1511-1513.

Avigad, G., Englard, S., and Pifko, S. (1966) 5-Keto-D-fructose: IV. A specific reduced nicotinamide adenine dinucleotide phosphate-linked reductase from *Gluconobacter cerinus*. *J. Biol. Chem.* 241: 373-378.

Azeez, O.H., Alkass, S.Y., and Persike, D.S. (2019) Long-term saccharin consumption and increased risk of obesity, diabetes, hepatic dysfunction, and renal impairment in rats. *Medicina* 55: 681.

Bagdasarian, M., Lurz, R., Ruckert, B., Franklin, F.C., Bagdasarian, M.M., Frey, J., and Timmis, K.N. (1981) Specific-purpose plasmid cloning vectors. II. Broad host range, high copy number, RSF1010-derived vectors, and a host-vector system for gene cloning in *Pseudomonas*. *Gene* 16: 237-247.

Bagdasarian, M., and Timmis, K.N. (1982) Host: vector systems for gene cloning in *Pseudomonas*. *Curr. Top. Microbiol. Immunol.* 96: 47-67.

Barbe, J.-C., De Revel, G., Joyeux, A., Bertrand, A., and Lonvaud-Funel, A. (2001) Role of botrytized grape micro-organisms in SO_2 binding phenomena. *J. Appl. Microbiol.* 90: 34-42.

Battling, S., Wohlers, K., Igwe, C., Kranz, A., Pesch, M., Wirtz, A., Baumgart, M., Büchs, J., and Bott, M. (2020) Novel plasmid-free *Gluconobacter oxydans* strains for production of the natural sweetener 5-ketofructose. *Microb. Cell Fact.* 19: 54.

Bearson, S., Bearson, B., and Foster, J.W. (1997) Acid stress responses in enterobacteria. *FEMS Microbiol. Lett.* 147: 173-180.

Belda, E., van Heck, R.G., Jose Lopez-Sanchez, M., Cruveiller, S., Barbe, V., Fraser, C., Klenk, H.P., Petersen, J., Morgat, A., Nikel, P.I., Vallenet, D., Rouy, Z., Sekowska, A., Martins Dos Santos, V.A., de Lorenzo, V., Danchin, A., and Medigue, C. (2016) The revisited genome of *Pseudomonas putida* KT2440 enlightens its value as a robust metabolic *chassis*. *Environ. Microbiol.* 18: 3403-3424.

Blanchard, J.S., Brewer, C.F., Englard, S., and Avigad, G. (1982) Solution structure of 5-keto-D-fructose: relevance to the specificity of hexose kinases. *Biochemistry* 21: 75-81.

Blank, L.M., Ionidis, G., Ebert, B.E., Bühler, B., and Schmid, A. (2008) Metabolic response of *Pseudomonas putida* during redox biocatalysis in the presence of a second octanol phase. *FEBS J.* 275: 5173-5190.

Blasi, M., Barbe, J.C., Dubourdieu, D., and Deleuze, H. (2008) New method for reducing the binding power of sweet white wines. *J. Agric. Food Chem.* 56: 8470-8474.

Bojanovič, K., D'Arrigo, I., and Long, K.S. (2017) Global transcriptional responses to osmotic, oxidative, and imipenem stress conditions in *Pseudomonas putida*. *Appl. Environ. Microbiol.* 83: e03236-03216.

Breiteneder, H. (2004) Thaumatin-like proteins – a new family of pollen and fruit allergens. *Allergy* 59: 479-481.

Bremus, C., Herrmann, U., Bringer-Meyer, S., and Sahm, H. (2006) The use of microorganisms in L-ascorbic acid production. *J. Biotechnol.* 124: 196-205.

Brewer, C.F., Blanchard, J.S., Englard, S., Jacob, G., and Avigad, G. (1982) Solid-state ^{13}C-N.M.R. spectroscopy of D-threo-2,5-hexodiulose (5-keto-D-fructose). *Carbohydr. Res.* 102: 294-297.

Browning, D.F., Grainger, D.C., and Busby, S.J.W. (2010) Effects of nucleoid-associated proteins on bacterial chromosome structure and gene expression. *Curr. Opin. Microbiol.* 13: 773-780.

Bryant, J.A., Sellars, L.E., Busby, S.J.W., and Lee, D.J. (2014) Chromosome position effects on gene expression in *Escherichia coli* K-12. *Nucleic Acids Res.* 42: 11383-11392.

Burger, C., Kessler, C., Gruber, S., Ehrenreich, A., Liebl, W., and Weuster-Botz, D. (2019) L-Erythrulose production with a multideletion strain of *Gluconobacter oxydans*. *Appl. Microbiol. Biotechnol.* 103: 4393-4404.

Calero, P., Jensen, S.I., and Nielsen, A.T. (2016) Broad-host-range ProUSER vectors enable fast characterization of inducible promoters and optimization of *p*-coumaric acid production in *Pseudomonas putida* KT2440. *ACS Synth. Biol.* 5: 741-753.

Carocho, M., Morales, P., and Ferreira, I. (2017) Sweeteners as food additives in the XXI century: a review of what is known, and what is to come. *Food Chem. Toxicol.* 107: 302-317.

Cases, I., Lopez, J.-A., Albar, J.-P., and de Lorenzo, V. (2001) Evidence of multiple regulatory functions for the PtsN (IIA^{Ntr}) protein of *Pseudomonas putida*. *J. Bacteriol.* 183: 1032-1037.

Castagno, L.N., Estrella, M.J., Sannazzaro, A.I., Grassano, A.E., and Ruiz, O.A. (2011) Phosphate-solubilization mechanism and *in vitro* plant growth promotion activity mediated by *Pantoea eucalypti* isolated from *Lotus tenuis* rhizosphere in the Salado River Basin (Argentina). *J. Appl. Microbiol.* 110: 1151-1165.

Chattopadhyay, S., Raychaudhuri, U., and Chakraborty, R. (2014) Artificial sweeteners – a review. *J. Food Sci. Technol.* 51: 611-621.

Chavarría, M., Durante-Rodríguez, G., Krell, T., Santiago, C., Brezovsky, J., Damborsky, J., and de Lorenzo, V. (2014) Fructose 1-phosphate is the one and only physiological effector of the Cra (FruR) regulator of *Pseudomonas putida*. *FEBS Open Bio* 4: 377-386.

Chavarría, M., Fuhrer, T., Sauer, U., Pflüger-Grau, K., and de Lorenzo, V. (2013) Cra regulates the cross-talk between the two branches of the phosphoenolpyruvate : phosphotransferase system of *Pseudomonas putida*. *Environ. Microbiol.* 15: 121-132.

Chavarría, M., Goñi-Moreno, Á., de Lorenzo, V., and Nikel, P.I. (2016) A metabolic widget adjusts the phosphoenolpyruvate-dependent fructose influx in *Pseudomonas putida*. *mSystems* 1: e00154-00116.

Chavarría, M., Kleijn, R.J., Sauer, U., Pflüger-Grau, K., and de Lorenzo, V. (2012) Regulatory tasks of the phosphoenolpyruvate-phosphotransferase system of *Pseudomonas putida* in central carbon metabolism. *mBio* 3.

Chia, C.W., Shardell, M., Tanaka, T., Liu, D.D., Gravenstein, K.S., Simonsick, E.M., Egan, J.M., and Ferrucci, L. (2016) Chronic low-calorie sweetener use and risk of abdominal obesity among older adults: a cohort study. *PLOS ONE* 11: e0167241.

Coines, J., Acosta-Gutierrez, S., Bodrenko, I., Rovira, C., and Ceccarelli, M. (2019) Glucose transport via the pseudomonad porin OprB: implications for the design of Trojan Horse anti-infectives. *Physical Chemistry Chemical Physics* 21: 8457-8463.

Collier, D.N., Hager, P.W., and Phibbs, P.V., Jr. (1996) Catabolite repression control in the *Pseudomonads*. *Res. Microbiol.* 147: 551-561.

Daddaoua, A., Krell, T., Alfonso, C., Morel, B., and Ramos, J.-L. (2010) Compartmentalized glucose metabolism in *Pseudomonas putida* is controlled by the PtxS repressor. *J. Bacteriol.* 192: 4357-4366.

Daniell, S., Mellits, K.H., Faus, I., and Connerton, I. (2000) Refolding the sweet-tasting protein thaumatin II from insoluble inclusion bodies synthesised in *Escherichia coli*. *Food Chem.* 71: 105-110.

Danneel, H.-J., Rössner, E., Zeeck, A., and Giffhorn, F. (1993) Purification and characterization of a pyranose oxidase from the basidiomycete *Peniophora gigantea* and chemical analyses of its reaction products. *Eur. J. Biochem.* 214: 795-802.

de Koning, L., Malik, V.S., Rimm, E.B., Willett, W.C., and Hu, F.B. (2011) Sugar-sweetened and artificially sweetened beverage consumption and risk of type 2 diabetes in men. *Am. J. Clin. Nutr.* 93: 1321-1327.

del Castillo, T., Ramos, J.L., Rodríguez-Herva, J.J., Fuhrer, T., Sauer, U., and Duque, E. (2007) Convergent peripheral pathways catalyze initial glucose catabolism in *Pseudomonas putida*: genomic and flux analysis. *J. Bacteriol.* 189: 5142-5152.

Deppenmeier, U., and Ehrenreich, A. (2009) Physiology of acetic acid bacteria in light of the genome sequence of *Gluconobacter oxydans*. *J. Mol. Microbiol. Biotechnol.* 16: 69-80.

Deppenmeier, U., Hoffmeister, M., and Prust, C. (2002) Biochemistry and biotechnological applications of *Gluconobacter* strains. *Appl. Microbiol. Biotechnol.* 60: 233-242.

Deshpande, A., and Jadad, A.R. (2008) The impact of polyol-containing chewing gums on dental caries: a systematic review of original randomized controlled trials and observational studies. *J. Am. Dent. Assoc.* 139: 1602-1614.

Dinamarca, M.A., Ruiz-Manzano, A., and Rojo, F. (2002) Inactivation of cytochrome *o* ubiquinol oxidase relieves catabolic repression of the *Pseudomonas putida* GPo1 alkane degradation pathway. *J. Bacteriol.* 184: 3785-3793.

DiNicolantonio, J.J., O'Keefe, J.H., and Lucan, S.C. (2015) Added fructose: a principal driver of type 2 diabetes mellitus and its consequences. *Mayo Clin. Proc.* 90: 372-381.

Dvořák, P., Kováč, J., and de Lorenzo, V. (2020) Biotransformation of D-xylose to D-xylonate coupled to medium-chain-length polyhydroxyalkanoate production in cellobiose-grown *Pseudomonas putida* EM42. *Microb. Biotechnol.* 13: 1273-1283.

Ebert, B.E., Kurth, F., Grund, M., Blank, L.M., and Schmid, A. (2011) Response of *Pseudomonas putida* KT2440 to increased NADH and ATP demand. *Appl. Environ. Microbiol.* 77: 6597-6605.

El Houdaigui, B., Forquet, R., Hindré, T., Schneider, D., Nasser, W., Reverchon, S., and Meyer, S. (2019) Bacterial genome architecture shapes global transcriptional regulation by DNA supercoiling. *Nucleic Acids Res.* 47: 5648-5657.

Elmore, J.R., Dexter, G.N., Salvachúa, D., Martinez-Baird, J., Hatmaker, E.A., Huenemann, J.D., Klingeman, D.M., Peabody, G.L.t., Peterson, D.J., Singer, C., Beckham, G.T., and Guss, A.M.

(2021) Production of itaconic acid from alkali pretreated lignin by dynamic two stage bioconversion. *Nat. Commun.* 12: 2261.

Englard, S., and Avigad, G. (1975a) 5-Keto-D-fructose reductase from *Gluconobacter cerinus*. In: *Methods Enzymol.* Wood, W.A. (ed): Academic Press. 127-131.

Englard, S., and Avigad, G. (1975b) 5-Keto-D-fructose reductase from yeast. In: *Methods Enzymol.* Wood, W.A. (ed): Academic Press. 132-138.

Englard, S., Avigad, G., and Prosky, L. (1965) 5-keto-D-fructose: III. Proof of structure based on stereospecific patterns of enzymatic reduction. *J. Biol. Chem.* 240: 2302-2307.

Englard, S., Kaysen, G., and Avigad, G. (1970) 5-keto-D-fructose. VI. A specific reduced nicotinamide adenine dinucleotide phosphate-linked reductase from yeast. *J. Biol. Chem.* 245: 1311-1318.

Fagherazzi, G., Vilier, A., Saes Sartorelli, D., Lajous, M., Balkau, B., and Clavel-Chapelon, F. (2013) Consumption of artificially and sugar-sweetened beverages and incident type 2 diabetes in the Etude Epidémiologique auprès des femmes de la Mutuelle Générale de l'Education Nationale–European Prospective Investigation into Cancer and Nutrition cohort. *Am. J. Clin. Nutr.* 97: 517-523.

Firsov, A.P., Pushin, A.S., and Dolgov, S.V. (2018) Transgenic plants as producers of supersweet protein thaumatin II. In: *Sweeteners: Pharmacology, Biotechnology, and Applications*. Mérillon, J.-M., and Ramawat, K.G. (eds). Cham: Springer International Publishing. 185-209.

Frey, J.C. (2012) Natural low-calorie sweeteners. In: *Natural Food Additives, Ingredients and Flavourings*. Baines, D., and Seal, R. (eds): Woodhead Publishing. 41-75.

Fricke, P.M., Klemm, A., Bott, M., and Polen, T. (2021a) On the way toward regulatable expression systems in acetic acid bacteria: target gene expression and use cases. *Appl. Microbiol. Biotechnol.* 105: 3423-3456.

Fricke, P.M., Link, T., Gätgens, J., Sonntag, C., Otto, M., Bott, M., and Polen, T. (2020) A tunable L-arabinose-inducible expression plasmid for the acetic acid bacterium *Gluconobacter oxydans*. *Appl. Microbiol. Biotechnol.* 104: 9267-9282.

Fricke, P.M., Lürkens, M., Hünnefeld, M., Sonntag, C.K., Bott, M., Davari, M.D., and Polen, T. (2021b) Highly tunable TetR-dependent target gene expression in the acetic acid bacterium *Gluconobacter oxydans*. *Appl. Microbiol. Biotechnol.* 105: 6835-6852.

Gätgens, C., Degner, U., Bringer-Meyer, S., and Herrmann, U. (2007) Biotransformation of glycerol to dihydroxyacetone by recombinant *Gluconobacter oxydans* DSM 2343. *Appl. Microbiol. Biotechnol.* 76: 553-559.

Ghosh, S., and Sudha, M.L. (2012) A review on polyols: new frontiers for health-based bakery products. *Int. J. Food Sci. Nutr.* 63: 372-379.

Grazi, E., Mangiarotti, M., and Pontremoli, S. (1962) The enzymic production of 2,5-D-threo-diketohexose. *Biochemistry* 1: 628-631.

Greenfield, S., and Claus, G.W. (1972) Nonfunctional tricarboxylic acid cycle and the mechanism of glutamate biosynthesis in *Acetobacter suboxydans*. *J. Bacteriol.* 112: 1295-1301.

Grembecka, M. (2015) Sugar alcohols—their role in the modern world of sweeteners: a review. *Eur. Food Res. Technol.* 241: 1-14.

Gupta, A., Singh, V.K., Qazi, G.N., and Kumar, A. (2001) *Gluconobacter oxydans*: Its biotechnological applications. *J. Mol. Microbiol. Biotechnol.* 3: 445-456.

Hanke, T., Nöh, K., Noack, S., Polen, T., Bringer, S., Sahm, H., Wiechert, W., and Bott, M. (2013) Combined fluxomics and transcriptomics analysis of glucose catabolism via a partially cyclic pentose phosphate pathway in *Gluconobacter oxydans* 621H. *Appl. Environ. Microbiol.* 79: 2336-2348.

Hanke, T., Richhardt, J., Polen, T., Sahm, H., Bringer, S., and Bott, M. (2012) Influence of oxygen limitation, absence of the cytochrome bc_1 complex and low pH on global gene expression in *Gluconobacter oxydans* 621H using DNA microarray technology. *J. Biotechnol.* 157: 359-372.

Hansen, L.K., Hordvik, A., and Hove, R. (1976) Crystal and molecular structure of D-threo-hexo-2,5-diulose; dimeric form in the solid state. *J. Chem. Soc., Chem. Commun.*: 572-573.

Hekmat, D., Bauer, R., and Fricke, J. (2003) Optimization of the microbial synthesis of dihydroxyacetone from glycerol with *Gluconobacter oxydans*. *Bioprocess Biosystems Eng.* 26: 109-116.

Herweg, E., Schöpping, M., Rohr, K., Siemen, A., Frank, O., Hofmann, T., Deppenmeier, U., and Büchs, J. (2018) Production of the potential sweetener 5-ketofructose from fructose in fed-batch cultivation with *Gluconobacter oxydans*. *Bioresour. Technol.* 259: 164-172.

Hickey, D.P., Giroud, F., Schmidtke, D.W., Glatzhofer, D.T., and Minteer, S.D. (2013) Enzyme cascade for catalyzing sucrose oxidation in a biofuel cell. *ACS Catalysis* 3: 2729-2737.

Hodge, J.E. (1953) Dehydrated foods, chemistry of browning reactions in model systems. *J. Agric. Food Chem.* 1: 928-943.

Hoffmann, J.J., Hövels, M., Kosciow, K., and Deppenmeier, U. (2020) Synthesis of the alternative sweetener 5-ketofructose from sucrose by fructose dehydrogenase and invertase producing *Gluconobacter* strains. *J. Biotechnol.* 307: 164-174.

Hui, H., Huang, D., McArthur, D., Nissen, N., Boros, L.G., and Heaney, A.P. (2009) Direct spectrophotometric determination of serum fructose in pancreatic cancer patients. *Pancreas* 38: 706-712.

Ibrahim, S.A., Crack, J.C., Rolfe, M.D., Acuña, J.M.B.-d., Thomson, A.J., Le Brun, N.E., Schobert, M., Stapleton, M.R., and Green, J. (2015) Three *Pseudomonas putida* FNR family proteins with different sensitivities to O_2. *J. Biol. Chem.* 290: 16812-16823.

Isbell, H.S., and Karabinos, J.V. (1952) Preparation of D-mannitol-C^{14} and its conversion to D-fructose-l-(and 6)-C^{14} by *Acetobacter suboxydans J. Res. Natl. Bur. Stand.* 48: 438-440.

Joseph, J.A., Akkermans, S., Nimmegeers, P., and Van Impe, J.F.M. (2019) Bioproduction of the recombinant sweet protein thaumatin: current state of the art and perspectives. *Front. Microbiol.* 10.

Kallnik, V., Meyer, M., Deppenmeier, U., and Schweiger, P. (2010) Construction of expression vectors for protein production in *Gluconobacter oxydans*. *J. Biotechnol.* 150: 460-465.

Kamitaka, Y., Tsujimura, S., and Kano, K. (2006) High current density bioelectrolysis of D-fructose at fructose dehydrogenase-adsorbed and Ketjen black-modified electrodes without a mediator. *Chem. Lett.* 36: 218-219.

Kampers, L.F.C., Volkers, R.J.M., and Martins Dos Santos, V.A.P. (2019) *Pseudomonas putida* KT2440 is HV1 certified, not GRAS. *Microb. Biotechnol.* 12: 845-848.

Kawai, S., Goda-Tsutsumi, M., Yakushi, T., Kano, K., and Matsushita, K. (2013) Heterologous overexpression and characterization of a flavoprotein-cytochrome *c* complex fructose dehydrogenase of *Gluconobacter japonicus* NBRC3260. *Appl. Environ. Microbiol.* 79: 1654-1660.

Kawai, S., Yakushi, T., Matsushita, K., Kitazumi, Y., Shirai, O., and Kano, K. (2014) The electron transfer pathway in direct electrochemical communication of fructose dehydrogenase with electrodes. *Electrochem. Commun.* 38: 28-31.

Ke, X., Pan-Hong, Y., Hu, Z.C., Chen, L., Sun, X.Q., and Zheng, Y.G. (2019) Synergistic improvement of PQQ-dependent D-sorbitol dehydrogenase activity from *Gluconobacter oxydans* for the biosynthesis of miglitol precursor 6-(N-hydroxyethyl)-amino-6-deoxy-alpha-L-sorbofuranose. *J. Biotechnol.* 300: 55-62.

Kelada, K.D., Tusé, D., Gleba, Y., McDonald, K.A., and Nandi, S. (2021) Process simulation and techno-economic analysis of large-scale bioproduction of sweet protein thaumatin II. *Foods* 10.

Kets, E.P., Galinski, E.A., de Wit, M., de Bont, J.A., and Heipieper, H.J. (1996a) Mannitol, a novel bacterial compatible solute in *Pseudomonas putida* S12. *J. Bacteriol.* 178: 6665-6670.

Kets, E.P.W., de Bont, J.A.M., and Heipieper, H.J. (1996b) Physiological response of *Pseudomonas putida* S12 subjected to reduced water activity. *FEMS Microbiol. Lett.* 139: 133-137.

Kiefler, I., Bringer, S., and Bott, M. (2017) Metabolic engineering of *Gluconobacter oxydans* 621H for increased biomass yield. *Appl. Microbiol. Biotechnol.* 101: 5453-5467.

Kim, J.-H., Jang, Y.-A., Seong, S.-B., Jang, S.A., Hong, S.H., Song, J.K., and Eom, G.T. (2020) High-level production and high-yield recovery of lactobionic acid by the control of pH and temperature in fermentation of *Pseudomonas taetrolens*. *Bioprocess Biosyst. Eng.* 43: 937-944.

Kinoshita, S., and Terada, O. (1963) Method for preparing 5-ketofructose by fermentation. US3206375A

Kohlstedt, M., Starck, S., Barton, N., Stolzenberger, J., Selzer, M., Mehlmann, K., Schneider, R., Pleissner, D., Rinkel, J., Dickschat, J.S., Venus, J., B.J.H. van Duuren, J., and Wittmann, C. (2018) From lignin to nylon: cascaded chemical and biochemical conversion using metabolically engineered *Pseudomonas putida*. *Metab. Eng.* 47: 279-293.

Kohlstedt, M., and Wittmann, C. (2019) GC-MS-based ^{13}C metabolic flux analysis resolves the parallel and cyclic glucose metabolism of *Pseudomonas putida* KT2440 and *Pseudomonas aeruginosa* PAO1. *Metab. Eng.* 54: 35-53.

Kostner, D., Peters, B., Mientus, M., Liebl, W., and Ehrenreich, A. (2013) Importance of *codB* for new *codA*-based markerless gene deletion in *Gluconobacter* strains. *Appl. Microbiol. Biotechnol.* 97: 8341-8349.

Kovach, M.E., Elzer, P.H., Steven Hill, D., Robertson, G.T., Farris, M.A., Roop, R.M., and Peterson, K.M. (1995) Four new derivatives of the broad-host-range cloning vector pBBR1MCS, carrying different antibiotic-resistance cassettes. *Gene* 166: 175-176.

Krajewski, V., Simic, P., Mouncey, N.J., Bringer, S., Sahm, H., and Bott, M. (2010) Metabolic engineering of *Gluconobacter oxydans* for improved growth rate and growth yield on glucose by elimination of gluconate formation. *Appl. Environ. Microbiol.* 76: 4369-4376.

Kranz, A., Busche, T., Vogel, A., Usadel, B., Kalinowski, J., Bott, M., and Polen, T. (2018) RNAseq analysis of α-proteobacterium *Gluconobacter oxydans* 621H. *BMC Genomics* 19: 24.

Kranz, A., Vogel, A., Degner, U., Kiefler, I., Bott, M., Usadel, B., and Polen, T. (2017) High precision genome sequencing of engineered *Gluconobacter oxydans* 621H by combining long nanopore and short accurate Illumina reads. *J. Biotechnol.* 258: 197-205.

Kumar, C., Yadav, K., Archana, G., and Naresh Kumar, G. (2013) 2-Ketogluconic acid secretion by incorporation of *Pseudomonas putida* KT 2440 gluconate dehydrogenase (*gad*) operon in *Enterobacter asburiae* PSI3 improves mineral phosphate solubilization. *Curr. Microbiol.* 67: 388-394.

La Rosa, R., Nogales, J., and Rojo, F. (2015) The Crc/CrcZ-CrcY global regulatory system helps the integration of gluconeogenic and glycolytic metabolism in *Pseudomonas putida*. *Environ. Microbiol.* 17: 3362-3378.

Lal, A., Dhar, A., Trostel, A., Kouzine, F., Seshasayee, A.S., and Adhya, S. (2016) Genome scale patterns of supercoiling in a bacterial chromosome. *Nat. Commun.* 7: 11055.

Lee, S.H., Choi, J.i., Han, M.J., Choi, J.H., and Lee, S.Y. (2005) Display of lipase on the cell surface of *Escherichia coli* using OprF as an anchor and its application to enantioselective resolution in organic solvent. *Biotechnol. Bioeng.* 90: 223-230.

Lenhart, A., and Chey, W.D. (2017) A systematic review of the effects of polyols on gastrointestinal health and irritable bowel syndrome. *Adv. Nutr.* 8: 587-596.

Lessie, T.G., and Phibbs, P.V., Jr. (1984) Alternative pathways of carbohydrate utilization in *Pseudomonads*. *Annu. Rev. Microbiol.* 38: 359-388.

Li, S., Ma, Y., and Wei, D. (2016) Identification of an interaction between EI and a histidine kinase-response regulator hybrid protein in *Gluconobacter oxydans*. *Biochem. Biophys. Res. Commun.* 470: 331-335.

Li, W.J., Narancic, T., Kenny, S.T., Niehoff, P.J., O'Connor, K., Blank, L.M., and Wierckx, N. (2020) Unraveling 1,4-butanediol metabolism in *Pseudomonas putida* KT2440. *Front. Microbiol.* 11: 382.

Livesey, G. (2003) Health potential of polyols as sugar replacers, with emphasis on low glycaemic properties. *Nutr. Res. Rev.* 16: 163-191.

Loeschcke, A., Markert, A., Wilhelm, S., Wirtz, A., Rosenau, F., Jaeger, K.-E., and Drepper, T. (2013) TREX: A universal tool for the transfer and expression of biosynthetic pathways in bacteria. *ACS Synth. Biol.* 2: 22-33.

Loeschcke, A., and Thies, S. (2015) *Pseudomonas putida*—a versatile host for the production of natural products. *Appl. Microbiol. Biotechnol.* 99: 6197-6214.

Longley, R.P., and Perlman, D. (1972) Conversion of L-sorbose to 5-keto-D-fructose by *Pseudomonads*. *Biotechnol. Bioeng.* 14: 843-846.

Löwe, H., Schmauder, L., Hobmeier, K., Kremling, A., and Pflüger-Grau, K. (2017) Metabolic engineering to expand the substrate spectrum of *Pseudomonas putida* toward sucrose. *MicrobiologyOpen* 6: e00473.

Löwe, H., Sinner, P., Kremling, A., and Pflüger-Grau, K. (2020) Engineering sucrose metabolism in *Pseudomonas putida* highlights the importance of porins. *Microb. Biotechnol.* 13: 97-106.

Lund, M.N., and Ray, C.A. (2017) Control of Maillard reactions in foods: strategies and chemical mechanisms. *J. Agric. Food Chem.* 65: 4537-4552.

Malik, V.S., Popkin, B.M., Bray, G.A., Després, J.P., Willett, W.C., and Hu, F.B. (2010) Sugar-sweetened beverages and risk of metabolic syndrome and type 2 diabetes. *Diabetes Care* 33: 2477-2483.

Martínez-García, E., and de Lorenzo, V. (2011) Engineering multiple genomic deletions in Gram-negative bacteria: analysis of the multi-resistant antibiotic profile of *Pseudomonas putida* KT2440. *Environ. Microbiol.* 13: 2702-2716.

Martínez-García, E., and de Lorenzo, V. (2017) Molecular tools and emerging strategies for deep genetic/genomic refactoring of *Pseudomonas*. *Curr. Opin. Biotechnol.* 47: 120-132.

Martínez-García, E., Fraile, S., Rodriguez Espeso, D., Vecchietti, D., Bertoni, G., and de Lorenzo, V. (2020) Naked bacterium: emerging properties of a surfome-streamlined *Pseudomonas putida* strain. *ACS Synth. Biol.* 9: 2477-2492.

Martins, S.I.F.S., Jongen, W.M.F., and van Boekel, M.A.J.S. (2000) A review of Maillard reaction in food and implications to kinetic modelling. *Trends Food Sci. Technol.* 11: 364-373.

Masuda, T. (2017) Sweet-tasting protein thaumatin: physical and chemical properties. In: *Sweeteners: Pharmacology, Biotechnology, and Applications*. Merillon, J.-M., and Ramawat, K.G. (eds): Springer International Publishing. 493-523.

Matsushita, K., Fujii, Y., Ano, Y., Toyama, H., Shinjoh, M., Tomiyama, N., Miyazaki, T., Sugisawa, T., Hoshino, T., and Adachi, O. (2003) 5-Keto-D-gluconate production is catalyzed by a quinoprotein glycerol dehydrogenase, major polyol dehydrogenase, in *Gluconobacter* species. *Appl. Environ. Microbiol.* 69: 1959-1966.

Matsushita, K., Nagatani, Y.-i., Shinagawa, E., Adachi, O., and Ameyama, M. (1989) Effect of extracellular pH on the respiratory chain and energetics of *Gluconobacter suboxydans*. *Agric. Biol. Chem.* 53: 2895-2902.

Matsushita, K., Toyama, H., and Adachi, O. (1994) Respiratory chains and bioenergetics of acetic acid bacteria. In: *Adv. Microb. Physiol.* Rose, A.H., and Tempest, D.W. (eds): Academic Press. 247-301.

Mattes, R.D., and Popkin, B.M. (2009) Nonnutritive sweetener consumption in humans: effects on appetite and food intake and their putative mechanisms. *Am. J. Clin. Nutr.* 89: 1-14.

Mazur, R.H., Schlatter, J.M., and Goldkamp, A.H. (1969) Structure-taste relationships of some dipeptides. *J. Am. Chem. Soc.* 91: 2684-2691.

Meyer, M., Schweiger, P., and Deppenmeier, U. (2013) Effects of membrane-bound glucose dehydrogenase overproduction on the respiratory chain of *Gluconobacter oxydans*. *Appl. Microbiol. Biotechnol.* 97: 3457-3466.

Micheel, F., and Horn, K. (1934) A fermentable diketose, 5-ketofructose (5-fructonose). *Justus Liebigs Ann. Chem.* 515: 1-10.

Mientus, M., Kostner, D., Peters, B., Liebl, W., and Ehrenreich, A. (2017) Characterization of membrane-bound dehydrogenases of *Gluconobacter oxydans* 621H using a new system for their functional expression. *Appl. Microbiol. Biotechnol.* 101: 3189-3200.

Miller, P.E., and Perez, V. (2014) Low-calorie sweeteners and body weight and composition: a meta-analysis of randomized controlled trials and prospective cohort studies. *Am. J. Clin. Nutr.* 100: 765-777.

Mitchell, N.S., Catenacci, V.A., Wyatt, H.R., and Hill, J.O. (2011) Obesity: overview of an epidemic. *Psychiatr. Clin. N. Am.* 34: 717-732.

Miura, H., Mogi, T., Ano, Y., Migita, C.T., Matsutani, M., Yakushi, T., Kita, K., and Matsushita, K. (2013) Cyanide-insensitive quinol oxidase (CIO) from *Gluconobacter oxydans* is a unique terminal oxidase subfamily of cytochrome *bd*. *J. Biochem.* 153: 535-545.

Momtazi-Borojeni, A.A., Esmaeili, S.A., Abdollahi, E., and Sahebkar, A. (2017) A review on the pharmacology and toxicology of steviol glycosides extracted from *Stevia rebaudiana*. *Curr. Pharm. Des.* 23: 1616-1622.

Morales, G., Ugidos, A., and Rojo, F. (2006) Inactivation of the *Pseudomonas putida* cytochrome *o* ubiquinol oxidase leads to a significant change in the transcriptome and to increased expression of the CIO and *cbb3*-1 terminal oxidases. *Environ. Microbiol.* 8: 1764-1774.

Moriconi, E., Feraco, A., Marzolla, V., Infante, M., Lombardo, M., Fabbri, A., and Caprio, M. (2020) Neuroendocrine and metabolic effects of low-calorie and non-calorie sweeteners. *Front. Endocrinol.* 11: 444.

Mowshowitz, S., Avigad, G., and Englard, S. (1974a) 5-Keto-D-fructose: formation and utilization in the course of D-fructose as similation by *Gluconabacter cerinus*. *J. Bacteriol.* 118: 1051-1058.

Mowshowitz, S., Englard, S., and Avigad, G. (1974b) Metabolic consequences of a block in the synthesis of 5-keto-D-fructose in a mutant of *Gluconobacter cerinus*. *J. Bacteriol.* 119: 363-370.

Moynihan, P. (2016) Sugars and dental caries: evidence for setting a recommended threshold for intake. *Adv. Nutr.* 7: 149-156.

Moynihan, P.J., and Kelly, S.A.M. (2014) Effect on caries of restricting sugars intake: systematic review to inform WHO guidelines. *J. Dent. Res.* 93: 8-18.

Murray, K., Duggleby, C.J., Sala-Trepat, J.M., and Williams, P.A. (1972) The metabolism of benzoate and methylbenzoates via the meta-cleavage pathway by *Pseudomonas arvilla* mt-2. *Eur. J. Biochem.* 28: 301-310.

Nelson, K.E., Weinel, C., Paulsen, I.T., Dodson, R.J., Hilbert, H., Martins dos Santos, V.A., Fouts, D.E., Gill, S.R., Pop, M., Holmes, M., Brinkac, L., Beanan, M., DeBoy, R.T., Daugherty, S., Kolonay, J., Madupu, R., Nelson, W., White, O., Peterson, J., Khouri, H., Hance, I., Chris Lee, P., Holtzapple, E., Scanlan, D., Tran, K., Moazzez, A., Utterback, T., Rizzo, M., Lee, K., Kosack, D., Moestl, D., Wedler, H., Lauber, J., Stjepandic, D., Hoheisel, J., Straetz, M., Heim, S., Kiewitz, C., Eisen, J.A., Timmis, K.N., Düsterhöft, A., Tümmler, B., and Fraser, C.M. (2002) Complete genome sequence and comparative analysis of the metabolically versatile *Pseudomonas putida* KT2440. *Environ. Microbiol.* 4: 799-808.

Ng, F.M.-W., and Dawes, E.A. (1973) Chemostat studies on the regulation of glucose metabolism in *Pseudomonas aeruginosa* by citrate. *Biochem. J.* 132: 129-140.

Ng, H. (1969) Effect of decreasing growth temperature on cell yield of *Escherichia coli*. *J. Bacteriol.* 98: 232-237.

Nguyen, A.V., Lai, B., Adrian, L., and Kromer, J.O. (2021a) The anoxic electrode-driven fructose catabolism of *Pseudomonas putida* KT2440. *Microb. Biotechnol.* 14: 1784-1796.

Nguyen, T.M., Goto, M., Noda, S., Matsutani, M., Hodoya, Y., Kataoka, N., Adachi, O., Matsushita, K., and Yakushi, T. (2021b) The 5-ketofructose reductase of *Gluconobacter* sp. strain CHM43 is a novel class in the shikimate dehydrogenase family. *J. Bacteriol.*: Jb0055820.

Nikel, P.I., Chavarria, M., Fuhrer, T., Sauer, U., and de Lorenzo, V. (2015) *Pseudomonas putida* KT2440 strain metabolizes glucose through a cycle formed by enzymes of the Entner-Doudoroff, Embden-Meyerhof-Parnas, and pentose phosphate pathways. *J. Biol. Chem.* 290: 25920-25932.

Nikel, P.I., and de Lorenzo, V. (2018) *Pseudomonas putida* as a functional *chassis* for industrial biocatalysis: from native biochemistry to trans-metabolism. *Metab. Eng.* 50: 142-155.

Nikel, P.I., Martínez-García, E., and de Lorenzo, V. (2014) Biotechnological domestication of pseudomonads using synthetic biology. *Nat. Rev. Microbiol.* 12: 368-379.

Nikel, P.I., Pérez-Pantoja, D., and de Lorenzo, V. (2016) Pyridine nucleotide transhydrogenases enable redox balance of *Pseudomonas putida* during biodegradation of aromatic compounds. *Environ. Microbiol.* 18: 3565-3582.

Oh, Y.-R., Jang, Y.-A., Lee, S.S., Kim, J.-H., Hong, S.H., Han, J.J., and Eom, G.T. (2020) Enhancement of lactobionic acid productivity by homologous expression of quinoprotein glucose dehydrogenase in *Pseudomonas taetrolens*. *J. Agric. Food Chem.* 68: 12336-12344.

Olsson, K., Carlsen, S., Semmler, A., Simón, E., Mikkelsen, M.D., and Møller, B.L. (2016) Microbial production of next-generation stevia sweeteners. *Microb. Cell Fact.* 15: 207.

Palleroni, N.J. (2015) *Pseudomonas*. In: *Bergey's Manual of Systematics of Archaea and Bacteria*. Whitman, W.B. (ed). 1-1.

Pepino, M.Y. (2015) Metabolic effects of non-nutritive sweeteners. *Physiol. Behav.* 152: 450-455.

Peters, B., Junker, A., Brauer, K., Mühlthaler, B., Kostner, D., Mientus, M., Liebl, W., and Ehrenreich, A. (2013a) Deletion of pyruvate decarboxylase by a new method for efficient markerless gene deletions in *Gluconobacter oxydans*. *Appl. Microbiol. Biotechnol.* 97: 2521-2530.

Peters, B., Mientus, M., Kostner, D., Junker, A., Liebl, W., and Ehrenreich, A. (2013b) Characterization of membrane-bound dehydrogenases from *Gluconobacter oxydans* 621H via whole-cell activity assays using multideletion strains. *Appl. Microbiol. Biotechnol.* 97: 6397-6412.

Pflüger, K., and de Lorenzo, V. (2008) Evidence of *in vivo* cross talk between the nitrogen-related and fructose-related branches of the carbohydrate phosphotransferase system of *Pseudomonas putida*. *J. Bacteriol.* 190: 3374-3380.

Poltronieri, P., and Kumar, P. (2017) Polyhydroxyalkanoates (PHAs) in industrial applications. In: *Handbook of Ecomaterials*. Martínez, L.M.T., Kharissova, O.V., and Kharisov, B.I. (eds). Cham: Springer International Publishing. 1-30.

Prust, C., Hoffmeister, M., Liesegang, H., Wiezer, A., Fricke, W.F., Ehrenreich, A., Gottschalk, G., and Deppenmeier, U. (2005) Complete genome sequence of the acetic acid bacterium *Gluconobacter oxydans*. *Nat. Biotechnol.* 23: 195.

Reichstein, T., and Grüssner, A. (1934) Eine ergiebige Synthese der L-Ascorbinsäure (C-Vitamin). *Helv. Chim. Acta* 17: 311-328.

Reiter, A., Herbst, L., Wiechert, W., and Oldiges, M. (2021) Need for speed: evaluation of dilute and shoot-mass spectrometry for accelerated metabolic phenotyping in bioprocess development. *Anal. Bioanal. Chem.* 413: 3253-3268.

Reva, O.N., Weinel, C., Weinel, M., Böhm, K., Stjepandic, D., Hoheisel, J.D., and Tümmler, B. (2006) Functional genomics of stress response in *Pseudomonas putida* KT2440. *J. Bacteriol.* 188: 4079-4092.

Richhardt, J., Bringer, S., and Bott, M. (2012) Mutational analysis of the pentose phosphate and Entner-Doudoroff pathways in *Gluconobacter oxydans* reveals improved growth of a Δ*edd* Δ*eda* mutant on mannitol. *Appl. Environ. Microbiol.* 78: 6975-6986.

Richhardt, J., Bringer, S., and Bott, M. (2013a) Role of the pentose phosphate pathway and the Entner-Doudoroff pathway in glucose metabolism of *Gluconobacter oxydans* 621H. *Appl. Microbiol. Biotechnol.* 97: 4315-4323.

Richhardt, J., Luchterhand, B., Bringer, S., Büchs, J., and Bott, M. (2013b) Evidence for a key role of cytochrome bo_3 oxidase in respiratory energy metabolism of *Gluconobacter oxydans*. *J. Bacteriol.* 195: 4210-4220.

Rippe, J.M., and Angelopoulos, T.J. (2016) Relationship between added sugars consumption and chronic disease risk factors: current understanding. *Nutrients* 8: 697.

Rojo, F. (2010) Carbon catabolite repression in *Pseudomonas*: optimizing metabolic versatility and interactions with the environment. *FEMS Microbiol. Rev.* 34: 658-684.

Ruiz-Ojeda, F.J., Plaza-Díaz, J., Sáez-Lara, M.J., and Gil, A. (2019) Effects of sweeteners on the gut microbiota: a review of experimental studies and clinical trials. *Adv. Nutr.* 10: S31-S48.

Rulis, A.M., and Levitt, J.A. (2009) FDA'S food ingredient approval process: safety assurance based on scientific assessment. *Regul. Toxicol. Pharmacol.* 53: 20-31.

Saito, Y., Ishii, Y., Hayashi, H., Yoshikawa, K., Noguchi, Y., Yoshida, S., Soeda, S., and Yoshida, M. (1998) Direct fermentation of 2-keto-L-gulonic acid in recombinant *Gluconobacter oxydans*. *Biotechnol. Bioeng.* 58: 309-315.

Saravolac, E.G., Taylor, N.F., Benz, R., and Hancock, R.E. (1991) Purification of glucose-inducible outer membrane protein OprB of *Pseudomonas putida* and reconstitution of glucose-specific pores. *J. Bacteriol.* 173: 4970-4976.

Sasajima, K.-i., and Isono, M. (1968) Polyol dehydrogenases in the soluble fraction of *Acetobacter melanogenum*. *Agric. Biol. Chem.* 32: 161-169.

Sato, K., Yamada, Y., Aida, K., and Uemura, T. (1967) On the formation of 5-keto-D-fructose and three γ-pyrone compounds from D-sorbitol by *Acetobacter suboxydans*. *Agric. Biol. Chem.* 31: 877-879.

Sawyer, M.H., Baumann, P., Baumann, L., Berman, S.M., Cánovas, J.L., and Berman, R.H. (1977) Pathways of D-fructose catabolism in species of *Pseudomonas*. *Arch. Microbiol.* 112: 49-55.

Sax, J.K., and Doran, N. (2016) Food labeling and consumer associations with health, safety, and environment. *J. Law Med. Ethics* 44: 630-638.

Schedel, M. (2000) Regioselective oxidation of aminosorbitol with *Gluconobacter oxydans*, key reaction in the industrial 1-deoxynojirimycin synthesis. In: *Biotechnology*. Rehm, H.-J., and Reed, G. (eds). 295-311.

Schienkiewitz, A., Mensink, G., Kuhnert, R., and Lange, C. (2017) Übergewicht und Adipositas bei Erwachsenen in Deutschland. *Journal of Health Monitoring* 2: 21-28.

Schiessl, J., Kosciow, K., Garschagen, L.S., Hoffmann, J.J., Heymuth, J., Franke, T., and Deppenmeier, U. (2021) Degradation of the low-calorie sugar substitute 5-ketofructose by different bacteria. *Appl. Microbiol. Biotechnol.* 105: 2441-2453.

Schneider, K., Dorscheid, S., Witte, K., Giffhorn, F., and Heinzle, E. (2012) Controlled feeding of hydrogen peroxide as oxygen source improves production of 5-ketofructose from L-sorbose using engineered pyranose 2-oxidase from *Peniophora gigantea*. *Biotechnol. Bioeng.* 109: 2941-2945.

Schrimsher, J.L., Wingfield, P.T., Bernard, A., Mattaliano, R., and Payton, M.A. (1988) Purification and characterization of 5-ketofructose reductase from *Erwinia citreus*. *Biochem. J.* 253: 511-516.

Schweikert, S., Kranz, A., Yakushi, T., Filipchyk, A., Polen, T., Etterich, H., Bringer, S., and Bott, M. (2021) The FNR-type regulator GoxR of the obligatory aerobic acetic acid bacterium *Gluconobacter oxydans* affects expression of genes involved in respiration and redox metabolism. *Appl. Environ. Microbiol.* 87: e00195-00121.

Sevilla, E., Alvarez-Ortega, C., Krell, T., and Rojo, F. (2013a) The *Pseudomonas putida* HskA hybrid sensor kinase responds to redox signals and contributes to the adaptation of the electron transport chain composition in response to oxygen availability. *Environ. Microbiol. Rep.* 5: 825-834.

Sevilla, E., Silva-Jiménez, H., Duque, E., Krell, T., and Rojo, F. (2013b) The *Pseudomonas putida* HskA hybrid sensor kinase controls the composition of the electron transport chain. *Environ. Microbiol. Rep.* 5: 291-300.

Sharma, A., Amarnath, S., Thulasimani, M., and Ramaswamy, S. (2016) Artificial sweeteners as a sugar substitute: are they really safe? *Indian J. Pharmacol.* 48: 237-240.

Siegel, L.S., Hylemon, P.B., and Phibbs, P.V., Jr. (1977) Cyclic adenosine 3',5'-monophosphate levels and activities of adenylate cyclase and cyclic adenosine 3',5'-monophosphate phosphodiesterase in *Pseudomonas* and *Bacteroides*. *J. Bacteriol.* 129: 87-96.

Siemen, A., Kosciow, K., Schweiger, P., and Deppenmeier, U. (2018) Production of 5-ketofructose from fructose or sucrose using genetically modified *Gluconobacter oxydans* strains. *Appl. Microbiol. Biotechnol.* 102: 1699-1710.

Sievers, M., and Swings, J. (2015) *Gluconobacter*. In: *Bergey's Manual of Systematics of Archaea and Bacteria*. Whitman, W.B. (ed). 1-9.

Soffritti, M., Belpoggi, F., Esposti, D.D., Lambertini, L., Tibaldi, E., and Rigano, A. (2006) First experimental demonstration of the multipotential carcinogenic effects of aspartame administered in the feed to Sprague-Dawley rats. *Environ. Health Perspect.* 114: 379-385.

Stricker, S., Rudloff, S., Geier, A., Steveling, A., Roeb, E., and Zimmer, K.P. (2021) Fructose consumption-free sugars and their health effects. *Dtsch. Arztebl. Int.* 118: 71-78.

Sun, W., Vallooran, J.J., Fong, W.-K., and Mezzenga, R. (2016) Lyotropic liquid crystalline cubic phases as versatile host matrices for membrane-bound enzymes. *J. Phys. Chem. Lett.* 7: 1507-1512.

Sweet, W.J., and Peterson, J.A. (1978) Changes in cytochrome content and electron transport patterns in *Pseudomonas putida* as a function of growth phase. *J. Bacteriol.* 133: 217-224.

Tan, S.Z., Reisch, C.R., and Prather, K.L.J. (2018) A robust CRISPR interference gene repression system in *Pseudomonas*. *J. Bacteriol.* 200: e00575-00517.

Tandel, K.R. (2011) Sugar substitutes: health controversy over perceived benefits. *J. Pharmacol. Pharmacother.* 2: 236-243.

Tavankar, G.R., Mossialos, D., and Williams, H.D. (2003) Mutation or overexpression of a terminal oxidase leads to a cell division defect and multiple antibiotic sensitivity in *Pseudomonas aeruginosa*. *J. Biol. Chem.* 278: 4524-4530.

Terada, O., Suzuki, S., and Kinoshita, S. (1961) Occurrence of 5-ketofructose during kojic acid formation from sorbose by *Acetobacter* species. *Agric. Biol. Chem.* 25: 871-872.

Terada, O., Tomizawa, K., Suzuki, S., and Kinoshita, S. (1960) Formation of 5-dehydrofructose by members of *Acetobacter*. *Bull. Agr. Chem. Soc. Japan* 24: 535-536.

Tiso, T., Ihling, N., Kubicki, S., Biselli, A., Schonhoff, A., Bator, I., Thies, S., Karmainski, T., Kruth, S., Willenbrink, A.-L., Loeschcke, A., Zapp, P., Jupke, A., Jaeger, K.-E., Büchs, J., and Blank, L.M. (2020) Integration of genetic and process engineering for optimized rhamnolipid production using *Pseudomonas putida*. *Front. Bioeng. Biotechnol.* 8: 976.

Tiso, T., Narancic, T., Wei, R., Pollet, E., Beagan, N., Schröder, K., Honak, A., Jiang, M., Kenny, S.T., Wierckx, N., Perrin, R., Avérous, L., Zimmermann, W., O'Connor, K., and Blank, L.M. (2021) Towards bio-upcycling of polyethylene terephthalate. *Metab. Eng.* 66: 167-178.

Tozakidis, I.E.P., Lüken, L.M., Üffing, A., Meyers, A., and Jose, J. (2020) Improving the autotransporter-based surface display of enzymes in *Pseudomonas putida* KT2440. *Microb. Biotechnol.* 13: 176-184.

Tschannen, M.P., Glück, U., Bircher, A.J., Heijnen, I., and Pletscher, C. (2017) Thaumatin and gum arabic allergy in chewing gum factory workers. *Am. J. Ind. Med.* 60: 664-669.

Tsujimura, S., Nishina, A., Kamitaka, Y., and Kano, K. (2009) Coulometric D-fructose biosensor based on direct electron transfer using D-fructose dehydrogenase. *Anal. Chem.* 81: 9383-9387.

Uebanso, T., Ohnishi, A., Kitayama, R., Yoshimoto, A., Nakahashi, M., Shimohata, T., Mawatari, K., and Takahashi, A. (2017) Effects of low-dose non-caloric sweetener consumption on gut microbiota in mice. *Nutrients* 9: 560.

Ugidos, A., Morales, G., Rial, E., Williams, H.D., and Rojo, F. (2008) The coordinate regulation of multiple terminal oxidases by the *Pseudomonas putida* ANR global regulator. *Environ. Microbiol.* 10: 1690-1702.

van Buul, V.J., Tappy, L., and Brouns, F.J.P.H. (2014) Misconceptions about fructose-containing sugars and their role in the obesity epidemic. *Nutr. Res. Rev.* 27: 119-130.

Velázquez, F., Pflüger, K., Cases, I., De Eugenio, L.I., and de Lorenzo, V. (2007) The phosphotransferase system formed by PtsP, PtsO, and PtsN proteins controls production of polyhydroxyalkanoates in *Pseudomonas putida*. *J. Bacteriol.* 189: 4529.

Weidenhagen, R., and Bernsee, G. (1960) Über ein bakterielles Dehydrierungsprodukt der Fructose (6-aldo-D-Fructose) 93: 2924-2928.

Weimer, A., Kohlstedt, M., Volke, D.C., Nikel, P.I., and Wittmann, C. (2020) Industrial biotechnology of *Pseudomonas putida*: advances and prospects. *Appl. Microbiol. Biotechnol.* 104: 7745-7766.

WHO (2020) Obesity and overweight, web page, https://www.who.int/news-room/fact-sheets/detail/obesity-and-overweight, accessed May 19, 2021.

WHO Consultation on Obesity, and World Health Organization (2000) Obesity: preventing and managing the global epidemic: report of a WHO consultation. Geneva: World Health Organization.

Wierckx, N.J., Ballerstedt, H., de Bont, J.A., and Wery, J. (2005) Engineering of solvent-tolerant *Pseudomonas putida* S12 for bioproduction of phenol from glucose. *Appl. Environ. Microbiol.* 71: 8221-8227.

Winsor, G.L., Griffiths, E.J., Lo, R., Dhillon, B.K., Shay, J.A., and Brinkman, F.S. (2016) Enhanced annotations and features for comparing thousands of *Pseudomonas* genomes in the Pseudomonas genome database. *Nucleic Acids Res.* 44: D646-653.

Wohlers, K., Wirtz, A., Reiter, A., Oldiges, M., Baumgart, M., and Bott, M. (2021) Metabolic engineering of *Pseudomonas putida* for production of the natural sweetener 5-ketofructose from fructose or sucrose by periplasmic oxidation with a heterologous fructose dehydrogenase. *Microb. Biotechnol.* n/a.

Wolf, S., Pflüger-Grau, K., and Kremling, A. (2015) Modeling the interplay of *Pseudomonas putida* EIIA with the potassium transporter KdpFABC. *J. Mol. Microbiol. Biotechnol.* 25: 178-194.

Wyrobnik, D.H., Wyrobnik, I.H., and Silcoff, E.R. (2009) Agent for reducing the useable calorie content of food and for therapeutic reduction of weight, in particular for use in the case of adiposity (obesity). US 2009/0060956A1

Yagi, S., Kobayashi, K., and Sonoyama, T. (1989) Purification and properties of 5-keto-D-fructose reductase from a mutant strain derived from *Corynebacterium* sp. *J. Ferment. Bioeng.* 67: 212-214.

Yamada, Y., Aida, K., ocirc, and Uemura, T. (1966a) A new enzyme, D-fructose dehydrogenase. *Agric. Biol. Chem.* 30: 95-96.

Yamada, Y., Iizuka, K., Aida, K., and Uemura, T. (1966b) L-Sorbose oxidase from *Trametes sanguinea*. *Agric. Biol. Chem.* 30: 97-98.

Yang, Q., Zhang, Z., Gregg, E.W., Flanders, W.D., Merritt, R., and Hu, F.B. (2014) Added sugar intake and cardiovascular diseases mortality among US adults. *JAMA Intern. Med.* 174: 516-524.

Yu, S., Lai, B., Plan, M.R., Hodson, M.P., Lestari, E.A., Song, H., and Krömer, J.O. (2018) Improved performance of *Pseudomonas putida* in a bioelectrochemical system through overexpression of periplasmic glucose dehydrogenase. *Biotechnol. Bioeng.* 115: 145-155.

Yuan, J., Wu, M., Lin, J., and Yang, L. (2016) Combinatorial metabolic engineering of industrial *Gluconobacter oxydans* DSM2343 for boosting 5-keto-D-gluconic acid accumulation. *BMC Biotechnol.* 16: 42.

Zahid, N., Schweiger, P., Galinski, E., and Deppenmeier, U. (2015) Identification of mannitol as compatible solute in *Gluconobacter oxydans*. *Appl. Microbiol. Biotechnol.* 99: 5511-5521.

Zhao, L., Li, W., Wichmann, G., Khankhoje, A., Gonzalo, C.G.d., MahatdejkuL-Meadows, T., Jackson, S., Leavell, M., and Platt, D. (2018) UDP-dependent glycosyltransferase for high efficiency production of rebaudiosides. WO2018031955A2

Zobel, S., Benedetti, I., Eisenbach, L., de Lorenzo, V., Wierckx, N., and Blank, L.M. (2015) Tn*7*-based device for calibrated heterologous gene expression in *Pseudomonas putida*. *ACS Synth. Biol.* 4: 1341-1351.

5 Appendix

References given in the Appendix are part of the reference list given for the general discussion.

5.1 Supplementary figures

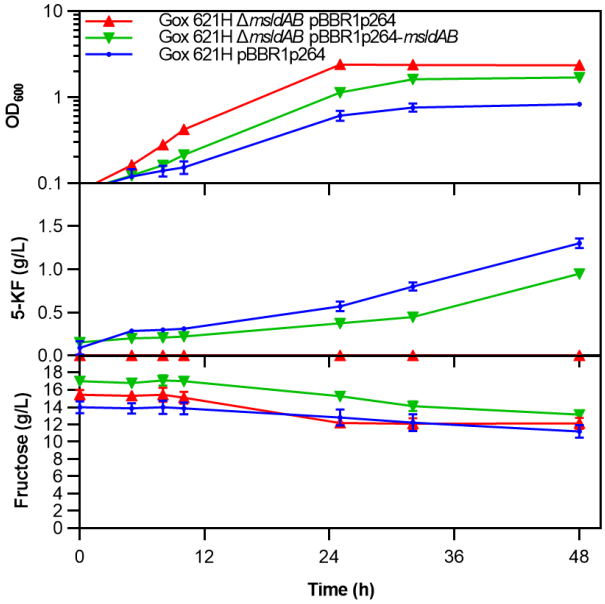

Figure S1 Shake flask cultivation of *G. oxydans* 621H Δ*msldAB* with pBBR1p264 and pBBR1p264-*msldAB*. Depicted is the growth as OD_{600}, the 5-KF production, and fructose consumption of *G. oxydans* 621H pBBR1p264 and *G. oxydans* 621H Δ*msldAB* with either the empty vector control pBBR1p264 or the expression plasmid pBBR1p264-*msldAB*, cultivated in 100 mL complex medium with 18 g/L fructose in 500 mL baffled shake flasks that were incubated at 30°C and 130 rpm. The *msldAB* genes encode the major polyol dehydrogenase, which has a broad substrate specificity (Peters, et al., 2013b, Ano, et al., 2017) Shown are mean values of biological triplicates. This experiment was conducted by Philipp Wirtz during his Bachelor Thesis.

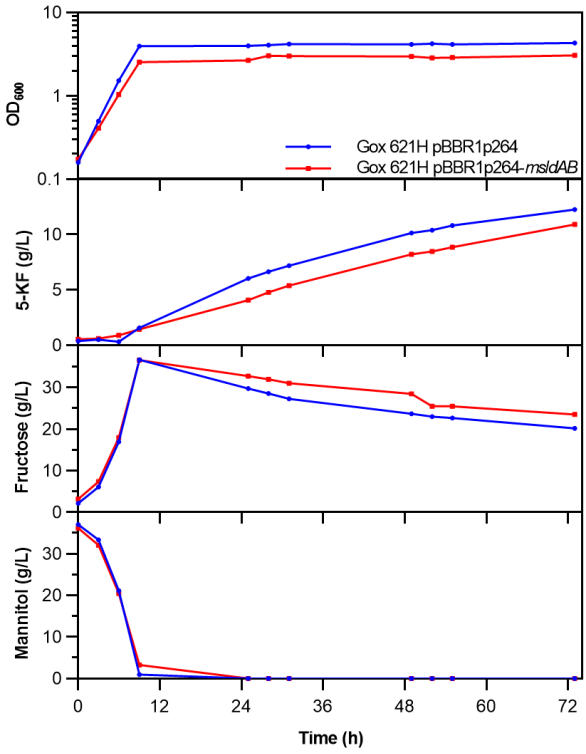

Figure S2 Shake flask cultivation of *G. oxydans* 621H with pBBR1p264 and pBBR1p264-*msldAB*. Depicted is the growth as OD_{600}, 5-KF production, fructose formation and consumption, and mannitol consumption of *G. oxydans* 621H with either the empty vector control pBBR1p264 or the expression plasmid pBBR1p264-*msldAB*, cultivated in 100 mL complex medium with 40 g/L mannitol in 500 mL baffled shake flasks that were incubated at 30°C and 130 rpm. Shown are mean values of biological duplicates. This experiment was conducted by Philipp Wirtz during his Bachelor Thesis.

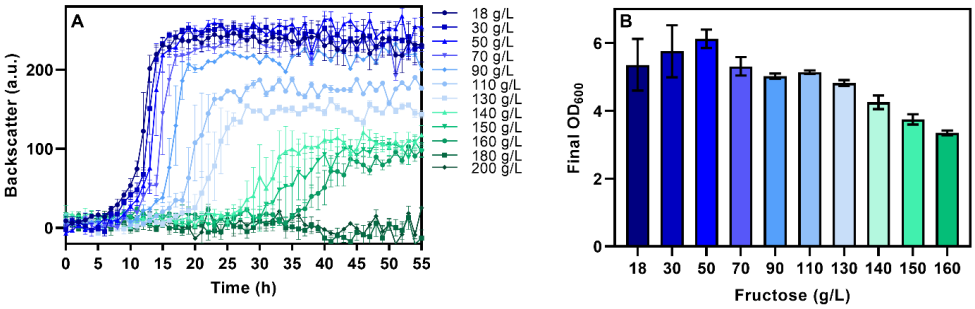

Figure S3 Growth of *P. putida*::*fdhSCL* with different fructose concentrations. Depicted is the growth as backscatter (arbitrary units, a.u.)(A) and the final cell density as OD_{600} (B) of *P. putida*::*fdhSCL* grown in MSM with 20 mM glucose (3.6 g/L glucose) and 18-200 g/L fructose. The main cultures were inoculated from precultures grown in MSM with 20 mM glucose and 18 g/L fructose. 800 µL cultures were incubated in a Flowerplate in a BioLector at 30 °C, 1200 rpm and 85 % humidity. Depicted are mean values and standard deviations of biological triplicates.

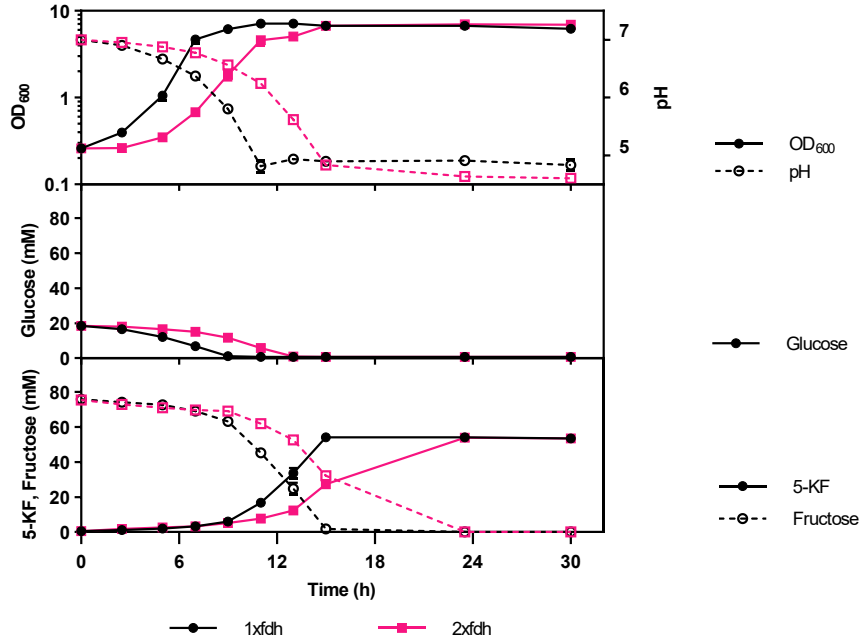

Figure S4 Shake flask cultivation of *P. putida*::*fdhSCL* and *P. putida*::2x*fdhSCL*. Depicted are the OD_{600}, pH, and the concentrations of glucose, fructose and 5-KF for *P. putida*::*fdhSCL* and *P. putida*::2x*fdhSCL* grown in 500 mL shake flasks with 50 mL MSM containing 100 mM fructose and 20 mM glucose. The cultures were incubated at 30 °C and 180 rpm. Shown are mean values and standard deviations of four biological replicates.

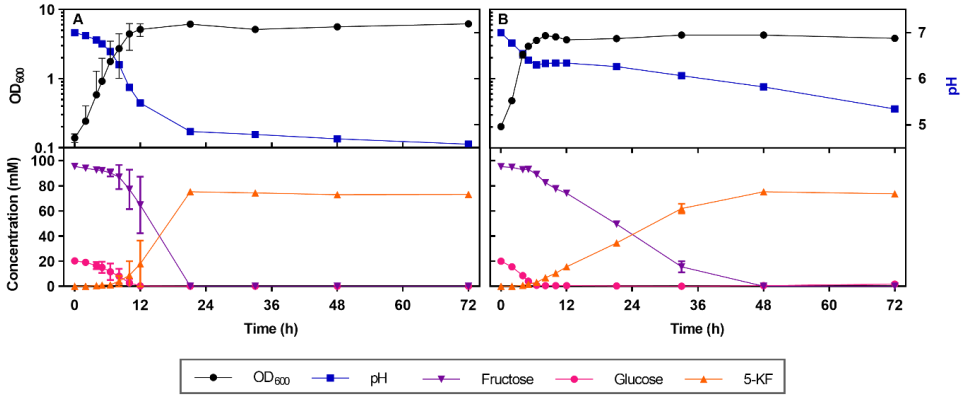

Figure S5 Shake flask cultivation of *P. putida*::*fdhSCL* and *P. putida*::*fdhSCL* Δ*fruB*. Depicted are OD_{600}, pH, and the concentrations of glucose, fructose and 5-KF concentrations for *P. putida*::*fdhSCL* (A) and *P. putida*::*fdhSCL* Δ*fruB* (B) grown in 500 mL shakeflasks with 50 mL MSM containing 100 mM fructose and 20 mM glucose. The cultures were incubated at 30 °C and 180 rpm. Shown are mean values and standard deviations of biological triplicates.

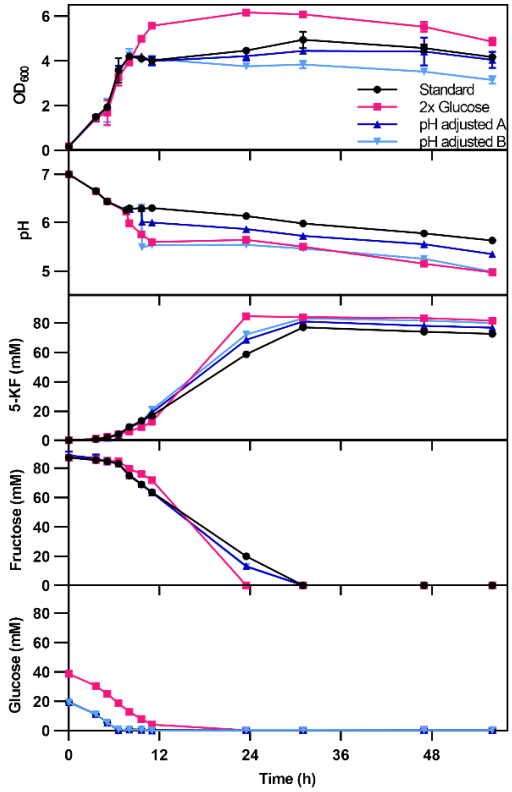

Figure S6 Shake flask cultivation of *P. putida*::*fdhSCL* Δ*fruB* under different conditions. Depicted are OD_{600}, pH, and the concentrations of glucose, fructose and 5-KF for *P. putida*::*fdhSCL* Δ*fruB* grown in 500 mL shake flasks with 50 mL MSM containing 100 mM fructose and 20 mM glucose, with either no adjustments (standard), 2x glucose (40 mM), addition of 3.6 mM HCl (pH adjusted A), or addition of 6 mM HCl (pH adjusted B). The cultures were incubated at 30 °C and 180 rpm. Shown are mean values and standard deviations of biological triplicates.

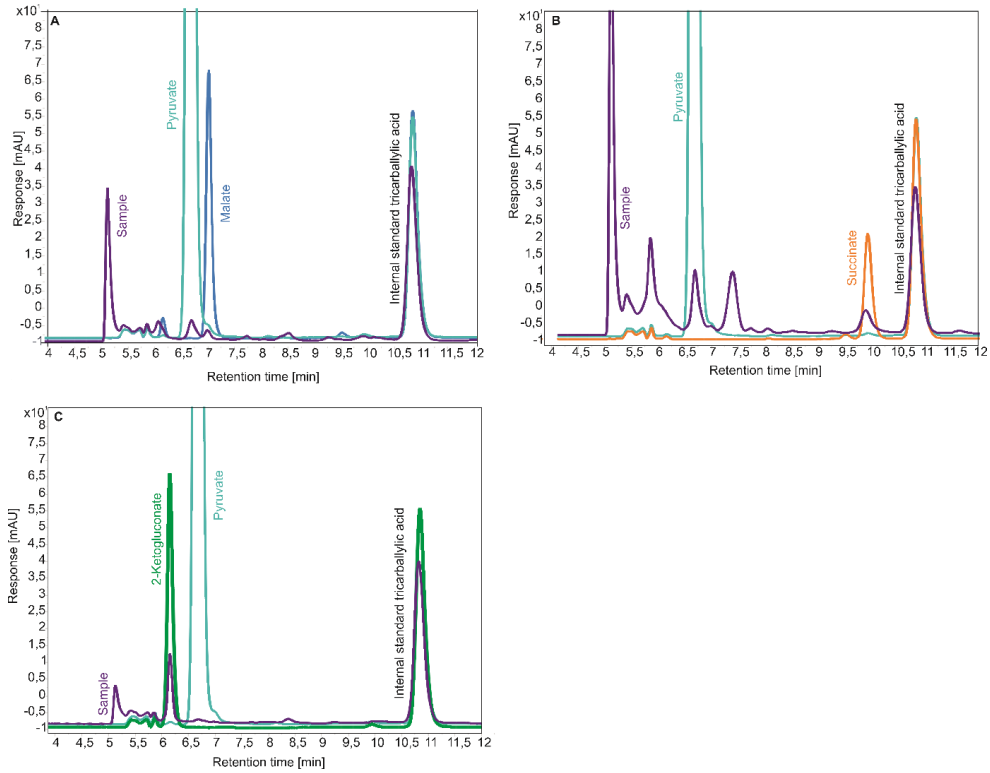

Figure S7 Example chromatograms of organic acid analysis in culture supernatants after SPE. A: Overlay of 32 h sample of *P. putida*::*fdhSCL* cultivated in a shake flask with 100 mM fructose (1:2 dilution of culture supernatant with water) and standard solutions of 10 mM pyruvate and 10 mM malate. B: Overlay of 23 h sample of *P. putida*::*fdhSCL* pBT'T-*inv1417* cultivated in a bioreactor with 150 g/L sucrose (3:4 dilution of culture supernatant with water) together with standard solutions of 10 mM pyruvate and 10 mM succinate. C: Overlay of 22 h sample of *P. putida*::*fdhSCL* pBT'T-*inv1417* cultivated in shake flasks with 100 mM sucrose (1:5 dilution of culture supernatant with water) and standard solutions of 10 mM pyruvate and 10 mM 2-ketogluconate. All samples and standard solutions contained tricarballylic acid as internal standard. Samples were prepared vie NH_2 SPE, acids were eluted with phosphoric acid according to a method described by Agius, et al. (2018). Eluted acids were separated in an Agilent LC-1200 system (Agilent, Santa Clara, CA, USA), equipped with a 250*4.6 mm Synergi 4u polar RP 80Å column (Phenomenex, Germany) with 20 mM ammonium phosphate buffer, pH 2.6 with an acetonitrile gradient according to the published method.

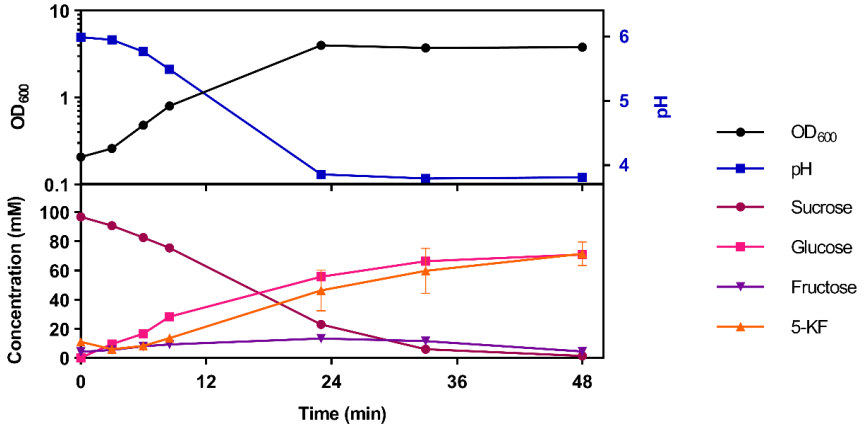

Figure S8 Shake flask cultivation of *G. oxydans* IK003.1::*fdhSCL*^{2} pBBR1p264-*inv1417*. Depicted is the growth as OD_{600} together with the pH and the concentrations of sucrose, glucose, fructose, and 5-ketofructose determined by HPLC for a shake flask cultivation of *G. oxydans* IK003.1 *fdhSCL*^{2} pBBR1p264-*inv1417*. Cells were cultivated in 50 mL *Gluconobacter* complex medium, pH 6.0, with 100 mM sucrose using 500 mL shake flasks that were incubated at 30°C and 180 rpm. Shown are mean values and standard deviations of biological triplicates.

5.2 Studies on cell surface display in *G. oxydans*

5.2.1 Background

To obtain a reusable cell catalyst for 5-KF production from alternative substrates like sucrose and starch, a surface display of the heterologous enzymes required for conversion of these substrates was planned. The reusability of the cells aimed to compensate for the low biomass yield of *G. oxydans*. Additionally, this would have the advantage that bulky substrates like starch, that cannot enter the cell, could also be used.

Cell surface display in Gram-negative bacteria by using heterologous membrane anchors has been described in literature for various examples and hence seemed possible in *G. oxydans* (Becker, et al., 2005, Schüürmann, et al., 2014, Tozakidis, et al., 2015, Schulte, et al., 2017). For sucrose conversion to 5-KF, two enzymes are required, namely an invertase and a glucose isomerase. For starch as alternative substrate, four additional enzymes would be needed, namely an α-amylase, a pullulanase, an α-glucosidase, and a glucose isomerase (see Figure S9).

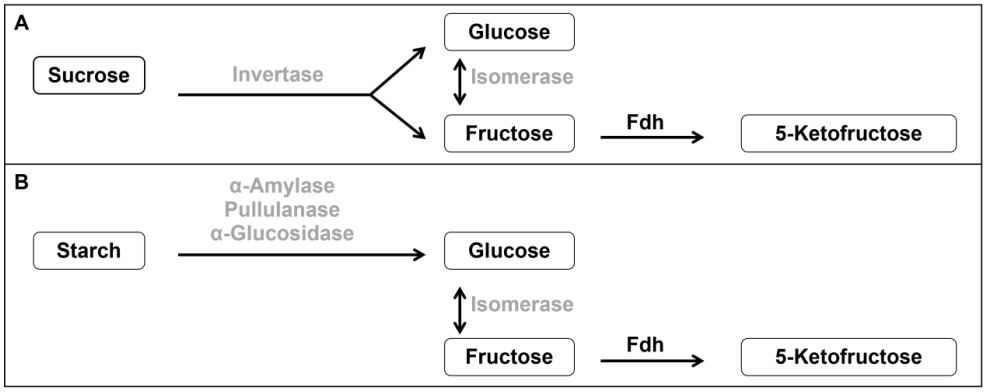

Figure S9 Planned heterologous utilization of alternative substrates. Shown is an overview of the needed enzymes for 5-KF production from sucrose (A) and starch (B). The enzymes for surface display are written in grey.

5.2.2 Amylases

α-Amylase was selected as test enzyme because starch as a substrate cannot cross the outer membrane of Gram-negative bacterial cells. Hence, amylase activity observed in cell suspensions would indicate extracellular amylase activity. For the selection of the amylases, the molecular mass and the pH range of the enzymes were considered. The pH range of the amylase needed to overlap with the slightly acidic pH range of *G. oxydans* and Fdh activity and the molecular mass was relevant, as smaller passenger enzymes are thought to be more suited for secretion and surface display.

At first, two different amylases, that of *Bacillus licheniformis* DSM 13 and that of *Streptomyces griseus* IMRU 3570, were selected due to their characteristics. Later a third enzyme, the α-amylase of *Streptococcus bovis* 148, was included. This enzyme was shown to be actively

expressed in *G. oxydans* in the group of Prof. U. Deppenmeier (University of Bonn, Germany). Additionally, for the *S. bovis* amylase functional surface display has been described in literature (Narita, et al., 2006). An overview of the selected enzymes with the corresponding characteristics is shown in Table S1.

Table S1 Selected α-amylases for surface display in *G. oxydans*

Organism	Molecular mass	pH range	References
Bacillus licheniformis DSM 13	55 kDa	5-8	(Saito, 1973, Yuuki, et al., 1985)
Streptomyces griseus IMRU 3570	57 kDa	6-8	(Vigal, et al., 1991, Seibold, et al., 2006)
Streptococcus bovis 148	77 kDa	4.5-7.5	(Satoh, et al., 1993, Satoh, et al., 1997, Narita, et al., 2006)

5.2.3 Membrane anchors

As membrane anchors first the autotransporters EstA and EhaA were selected. The autotransporter domain of *P. aeruginosa* EstA is a well-studied membrane anchor in heterologous surface display (Yang, et al., 2004, Becker, et al., 2005, Nicolay, et al., 2012, Chung, et al., 2020). The *E. coli* EhaA autotransporter domain has already been used in several examples in heterologous surface display, among other hosts also in *Zymomonas mobilis* (Wells, et al., 2008, Tozakidis, et al., 2014, Sichwart, et al., 2015, Schulte, et al., 2017). *Z. mobilis*, like *G. oxydans*, is an alphaproteobacterium, suggesting that the membrane anchor could also be functional in *G. oxydans*.

To broaden the spectrum of membrane anchors and increasing the variety, later also the outer membrane protein (OMP)-derived N-terminal membrane anchors OprF and Lpp-OmpA were included. $OprF_{188}$, a truncated version of *P. aeruginosa* OprF (Lee, et al., 2005), was selected, since it has been described for functional surface display in *G. oxydans* (Blank and Schweiger, 2018). The fusion construct Lpp-OmpA of the *E. coli* lipoprotein signal peptide and a truncated *E. coli* OmpA fragment adds variety to the set of membrane anchors (Francisco, et al., 1992, Earhart, 2000). An overview of the selected membrane anchors together with their size and original reference is listed in Table S2.

Table S2 Selected membrane anchors tested for surface display in *G. oxydans*

Membrane anchor	Organism	Size	Reference
Autotransporter			
EstA	*P. aeruginosa*	326 aa / 36 kDa	(Becker, et al., 2005)
EhaA	*E. coli*	339 aa/ 38 kDa	(Wells, et al., 2008)
OMP			
$OprF_{188}$	*P. aeruginosa*	188 aa / 20 kDa	(Lee, et al., 2005)
Lpp-OmpA	*E. coli*	122 aa /13 kDa	(Francisco, et al., 1992)

5.2.4 Cloning and testing

For strong constitutive expression, the respective amylase membrane anchor constructs were cloned into the plasmid pBBR1p264. All autotransporter constructs were cloned with the N-terminal signal sequence of EstA to avoid differences between the EhaA and EstA constructs caused by secretion differences due to different signal peptides. The plasmids were used to transform *G. oxydans* IK003.1 via conjugation, since electroporation was not successful, likely due to the large plasmid size.

As a first assay, the strains were tested for amylase activity on starch agar plates. For that purpose, *Gluconobacter* mannitol medium agar plates, additionally containing 1 g/L starch, were used to streak out the relevant strains and incubate them for 1-2 days at 30 °C. After growth, the plates were layered with Lugols' solution (3.3 g/L iodine and 6.6 g/L potassium iodine). During incubation for some minutes at room temperature, the iodine stains the starch in the agar plates. Areas not or only weakly stained indicate starch degradation by amylase activity. Additionally, cells from liquid cultures, either whole cells or cell fractions, were assayed in the Phadebas assay (Phadebas AB, Kristianstad, Sweden), the dinitro salicylic assay (Miller, 1959), or the Red Starch assay (Megazyme Ltd., Wicklow, Ireland). The Phadebas and the Red Starch assay are both based on modified starch molecules enabling colorimetric detection of starch hydrolysis. Dinitro salicylic acid allows colorimetric detection of reducing sugars formed by starch hydrolysis.

All tests showed that, at least in combination with the selected membrane anchors, AmyA of *S. bovis* is the most suited amylase for expression in *G. oxydans*. The starch plate assay showed strong starch cleavage activity for the Lpp-OmpA-AmyA construct and selected experiments with the most promising strain *G. oxydans* IK003.1pBBR1p264-*lpp-ompA-amyA* are shown in Figure S10. Cell fractionation and proteinase K treatment prior to enzyme assays showed only very low amylase activity for the membrane fraction compared to the soluble fraction and no activity decrease upon proteinase K treatment (Figure S10). These results suggest that the extracellular amylase activity was due to cell lysis or secretion into the medium and that the surface display was not successful.

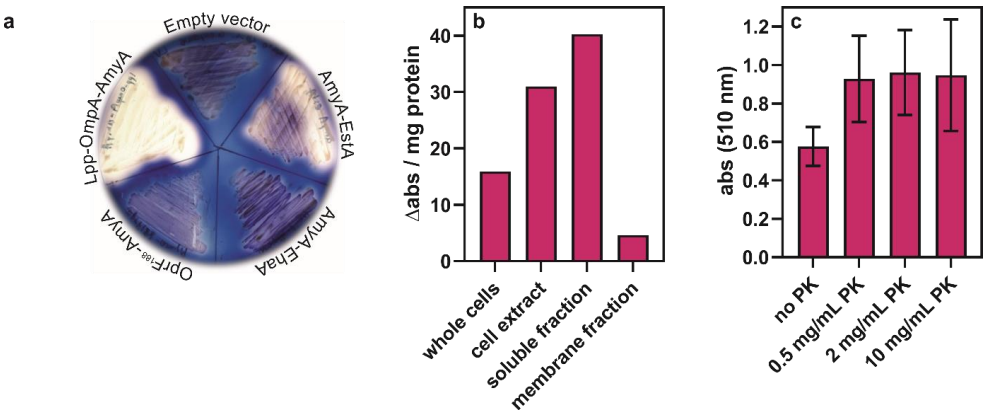

Figure S10 Surface display experiments with AmyA of *S. bovis* in *G. oxydans* IK003.1. (a) *G. oxydans* IK003.1 strains with pBBR1-p264-plasmids for the synthesis of AmyA fusion proteins with EstA, EhaA, OprF188 or Lpp-OmpA as membrane anchors were cultivated on starch agar and stained with Lugols' solution. (b, c) Amylase activity of *G. oxydans* IK003.1 pBBR1-p264-*lpp-ompA-amyA* with the artificial substrate Red Starch either in cell fractions, incubated for 20.5 h at 30 °C (b) or with whole cells of an OD_{600} of 20, after proteinase K (PK) incubation for 15 min at room temperature (c). The lower activity in the cells incubated without PK suggests that PK leads to cell lysis and release of intracellular amylase.

5.2.5 Conclusion

Despite testing different amylases and different membrane anchors, the surface display of an α-amylase in *G. oxydans* was not successful. This could have different reasons. It is possible that the selected enzymes are not suitable for functional expression in *G. oxydans*. At least the amylase AmyA of *S. bovis* is suited for *G. oxydans* as reported by our project partners at the University of Bonn (Prof. Deppenmeier) and shown here in the amylase assays with the membrane-anchor constructs. Also, the membrane anchor might not be functional in *G. oxydans*. However, the selected anchoring sequences had a broad variety including N-terminal OMPs and C-terminal autotransporter domains. Additionally, the OprF188 membrane anchor has been described to be functional in *G. oxydans* (Blank and Schweiger, 2018). When using a functional amylase and a functional membrane anchor, it is still possible that the combination of both is not optimal. The membrane anchor is described to influence the activity of the displayed passenger enzyme (Tozakidis, et al., 2020). For the autotransporters also the choice of the signal peptide can strongly influence the surface display (Tozakidis, et al., 2020). Since different signal peptides described to be functional in *G. oxydans* were tested, the choice of the signal peptide was at least not the only reason for the problems with surface display in *G. oxydans*. The most likely explanation at present is that the expression was too strong and that also constitutive expression might not be ideal for surface display. In literature, inducible expression has been used for surface display. The strong constitutive expression with pBBR1p264 in our study was likely too strong for a heterologous,

secreted, and membrane-integrated fusion protein. This hypothesis was supported by the fact that the DNA sequencing of some of the expression plasmids after isolation from *G. oxydans* revealed disrupted plasmids.

To enable surface display in *G. oxydans* it would likely be best to first test an endogenous enzyme as passenger or an enzyme of a more related organism and to use an inducible expression system. Also, the fusion with one of *G. oxydans* native OMPs as membrane anchor could be an option.

5.3 Influence of 5-KF on the *P. putida* KT2440 transcriptome

5.3.1 Background and experimental settings

To test whether 5-KF influences the alternative host *P. putida*, the effect of 5-KF on the transcriptome was analyzed in a DNA microarray experiment. LB precultures (four biological replicates) were used to inoculate a second preculture in mineral salts medium (MSM) (Hartmans, et al., 1989, Wohlers, et al., 2021) with 20 mM glucose. The second preculture was used to inoculate two 10 mL main cultures in MSM with 100 mM glucose. After incubation for 4.5 h at 30 °C and 180 rpm to an approximate OD_{600} of 4, 2 mL samples were taken for RNA isolation and 100 mM 5-KF or the same volume of water were added to the cultures together with concentrated medium to avoid a dilution effect. After continued incubation for 30 minutes, again 2 mL samples were taken for RNA isolation. The experiment was performed in four biological replicates.

5.3.2 Results

In the microarray experiment the genome-wide changes in transcript levels upon addition of 5-KF or water were analyzed. First, the mRNA ratio of the samples +5-KF 30 min vs. +5-KF 0 min and +water 30 min vs. +water 0 min were formed. Subsequently, the ratio of these two ratios was formed to exclude changes in gene expression not caused by 5-KF, but just by incubating the cultures for 30 min. The differentially expressed genes are listed in Table S3.

Table S3 List for transcriptome changes in *P. putida* KT2440 caused by addition of 100 mM 5-KF. Listed are genes that were differentially expressed with a signal to noise ratio >3, signals in at least 2 out of 4 replicates, ≥2-fold change and p-values ≤0.1. Stated are the fold changes after incubation for 30 min with 100 mM 5-KF or water as control and the ratio of the fold-changes in 5-KF compared to H_2O. Mean values of 4 biological replicates are shown. The genes were ordered into functional groups and listed with the corresponding p-values.

Locus tag	Gene name, annotation	Fold changes			p-values	
		5-KF / H_2O	5-KF	H_2O	5-KF	H_2O
Respiration and energy metabolism						
PP_0103	cytochrome *c* oxidase, *aa*$_3$-type, subunit II	0.49	0.18	0.37	2×10^{-3}	4×10^{-4}
PP_0104	cytochrome *c* oxidase, *aa*$_3$-type, subunit I	0.17	0.11	0.65	7×10^{-5}	5×10^{-2}
PP_0105	cytochrome *c* oxidase assembly protein	0.39	0.18	0.46	2×10^{-3}	8×10^{-3}
PP_0106	cytochrome *c* oxidase, *aa*$_3$-type, subunit III	0.26	0.18	0.67	3×10^{-4}	4×10^{-2}
PP_0109	cytochrome oxidase assembly protein	0.44	0.26	0.61	4×10^{-3}	6×10^{-2}
PP_0810	cyoups1 protein, gene upstream of *cyoABCD* operon	2.48	5.10	2.06	3×10^{-4}	9×10^{-2}
PP_0811	cyoups2 protein, gene upstream of *cyoABCD* operon	2.29	6.99	3.05	3×10^{-4}	2×10^{-3}
PP_0812	*cyoA*, cytochrome *o* ubiquinol oxidase, subunit II	3.22	8.55	2.66	3×10^{-3}	7×10^{-2}
PP_0814	*cyoC*, cytochrome *o* ubiquinol oxidase, subunit III	2.58	8.57	3.32	1×10^{-3}	5×10^{-2}
PP_4251	*ccoO-1*, cytochrome *c* oxidase, *cbb*$_3$-type, subunit II	10.20	4.38	0.43	3×10^{-2}	4×10^{-2}

Locus tag	Gene name, annotation	Fold changes			p-values	
		5-KF / H_2O	5-KF	H_2O	5-KF	H_2O
PP_4253	*ccoP-1*, cytochrome *c* oxidase, *cbb*$_3$-type, subunit III	7.53	4.09	0.54	2×10^{-2}	8×10^{-2}
PP_4258	*ccoP-2*, cytochrome *c* oxidase, *cbb*$_3$-type, subunit III	3.81	2.21	0.58	3×10^{-2}	7×10^{-2}
PP_4870	azurin	2.09	0.67	0.32	9×10^{-2}	2×10^{-2}
Metabolism						
PP_0056	oxidoreductase, GMC family	0.38	0.07	0.17	1×10^{-3}	1×10^{-3}
PP_0154	acetyl-CoA hydrolase/transferase family protein	2.60	1.51	0.58	1×10^{-2}	3×10^{-2}
PP_0205	oxidoreductase	2.43	1.94	0.80	4×10^{-2}	8×10^{-2}
PP_0323	*soxB*, sarcosine oxidase, beta subunit	0.44	0.31	0.71	2×10^{-5}	4×10^{-2}
PP_0397	serine proteine kinase PrkA	0.41	0.26	0.62	4×10^{-3}	2×10^{-2}
PP_0490	formate dehydrogenase, iron-sulfur subunit	17.66	10.57	0.60	2×10^{-3}	3×10^{-2}
PP_0491	formate dehydrogenase, cytochrome *b*556 subunit	6.45	3.75	0.58	9×10^{-4}	9×10^{-3}
PP_0552	*adh*, 2,3-butanediol dehydrogenase	2.28	11.44	5.02	3×10^{-4}	1×10^{-2}
PP_0596	beta-alanine-pyruvate transaminase	0.43	0.09	0.20	4×10^{-3}	2×10^{-3}
PP_0763	long chain fatty acid-CoA synthetase	0.47	0.12	0.26	1×10^{-5}	1×10^{-2}
PP_0794	*fruK*, 1-phosphofructokinase	7.18	4.41	0.61	3×10^{-3}	9×10^{-3}
PP_0903	type 11 methyltransferase	0.40	0.61	1.52	3×10^{-3}	7×10^{-2}
PP_1033	sulfatase domain protein	0.33	0.20	0.61	1×10^{-3}	3×10^{-2}
PP_1303	*cysD*, sulfate adenylyl transferase subunit II	2.18	3.13	1.43	6×10^{-5}	3×10^{-2}
PP_1343	*lpxC*, UDP-3-O-[3-hydroxymyristoyl] N-acetylglucosamine deacetylase	0.49	0.78	1.61	8×10^{-2}	6×10^{-2}
PP_1811	*wecB*, UDP-N-acetylglucosamine 2-epimerase	0.47	0.26	0.55	1×10^{-3}	3×10^{-2}
PP_2036	dihydrodipicolinate synthase, putative	0.50	2.49	5.00	6×10^{-4}	1×10^{-3}
PP_2052	hydrolase, haloacid dehalogenase-like family	10.93	8.57	0.78	3×10^{-4}	4×10^{-2}
PP_2183	formate dehydrogenase, subunit gamma	0.39	0.28	0.73	9×10^{-3}	5×10^{-2}
PP_2206	peptidase, U32 family	3.83	6.70	1.75	2×10^{-3}	2×10^{-2}
PP_2351	acetyl-CoA synthetase, putative	0.26	0.18	0.66	6×10^{-3}	6×10^{-3}
PP_2439	*ahpC*, alkyl hydroperoxide reductase, C subunit	6.11	4.43	0.72	1×10^{-3}	3×10^{-3}
PP_2453	*ansA*, L-asparaginase II	0.44	0.50	1.15	7×10^{-2}	3×10^{-2}
PP_2795	acyl-CoA synthetase	0.46	0.79	1.71	7×10^{-2}	4×10^{-4}
PP_2926	UDP-glucose dehydrogenase, putative	2.00	1.51	0.75	1×10^{-1}	8×10^{-2}
PP_2928	saccharopin dehydrogenase	2.12	5.00	2.36	7×10^{-3}	2×10^{-3}
PP_3136	serine O-acetyltransferase, putative	0.49	0.38	0.77	2×10^{-4}	9×10^{-2}
PP_3443	glyceraldehyde-3-phosphate dehydrogenase	4.15	2.26	0.55	3×10^{-3}	4×10^{-3}
PP_3623	gluconate 2-dehydrogenase, cytochrome *c* family protein	0.48	0.41	0.84	1×10^{-2}	4×10^{-2}
PP_3745	*glcD*, glycolate oxidase subunit	22.10	7.42	0.34	7×10^{-6}	6×10^{-3}
PP_3746	*glcE*, glycolate oxidase, FAD binding subunit	26.59	10.36	0.39	4×10^{-3}	5×10^{-2}

Locus tag	Gene name, annotation	Fold changes			p-values	
		5-KF / H_2O	5-KF	H_2O	5-KF	H_2O
PP_3747	*glcF*, glycolate oxidase, iron-sulfur subunit	33.47	18.42	0.55	3×10^{-4}	2×10^{-2}
PP_3748	*glcG*, hypothetical protein	32.35	20.08	0.62	7×10^{-4}	6×10^{-2}
PP_3786	aminotransferase	0.41	1.41	3.42	6×10^{-2}	3×10^{-2}
PP_4278	*xdhA*, xanthine dehydrogenase, subunit A	0.48	0.11	0.23	1×10^{-3}	7×10^{-3}
PP_4286	polysaccharide deacetylase family protein	0.45	0.14	0.30	4×10^{-3}	2×10^{-4}
PP_4403	*bkdB*, branched-chain alpha-keto acid dehydrogenase, subunit E2	0.37	0.21	0.57	1×10^{-3}	2×10^{-2}
PP_4493	oxidoreductase, FAD-linked, putative	2.99	1.34	0.45	7×10^{-2}	7×10^{-2}
PP_4752	aminopeptidase, putative	0.41	0.27	0.68	6×10^{-3}	5×10^{-2}
PP_5346	*oadA*, pyruvate carboxylase subunit B	2.18	2.66	1.22	3×10^{-3}	4×10^{-2}
PP_5008	polyhydroxyalkanoate granule-associated protein GA1	0.42	0.20	0.47	3×10^{-3}	1×10^{-2}
Transport						
PP_0233	*tauA*, taurine ABC transporter, periplasmic substrate-binding protein	4.43	2.63	0.59	5×10^{-3}	2×10^{-2}
PP_0284	gamma-aminobutyrate transporter, putative	0.33	0.41	1.24	2×10^{-3}	5×10^{-2}
PP_0295	glycine betaine/L-proline ABC transporter, permease protein	0.22	0.45	2.05	3×10^{-3}	7×10^{-2}
PP_0304	hypothetical protein (BlastP: choline ABC transporter)	0.36	0.25	0.70	1×10^{-4}	7×10^{-3}
PP_0411	polyamine ABC transporter, ATPase	0.22	0.13	0.56	1×10^{-2}	4×10^{-2}
PP_0412	polyamine ABC transporter, periplasmic substrate-binding protein	0.40	0.17	0.42	2×10^{-3}	2×10^{-2}
PP_0496	sodium/alanine symporter	0.49	1.34	2.71	2×10^{-2}	6×10^{-3}
PP_0618	branched-chain amino acid ABC transporter, permease protein	0.49	0.17	0.35	9×10^{-4}	6×10^{-3}
PP_0619	branched-chain amino acid ABC transporter, periplasmic substrate-binding protein	0.45	0.10	0.21	5×10^{-5}	6×10^{-3}
PP_0709	NCS1 nucleoside transporter family	0.38	0.49	1.31	3×10^{-2}	6×10^{-3}
PP_0884	dipeptide ABC transporter, periplasmic peptide-binding protein	0.38	0.22	0.58	6×10^{-4}	5×10^{-2}
PP_0885	dipeptide ABC transporter, periplasmic peptide-binding protein	0.37	0.16	0.44	5×10^{-3}	3×10^{-2}
PP_0970	cyanate MFS transporter	2.18	1.52	0.70	7×10^{-2}	1×10^{-1}
PP_1015	sugar/glucose ABC transporter, periplasmic sugar-binding protein	0.24	0.47	1.92	5×10^{-3}	5×10^{-3}
PP_1016	Sugar/glucose ABC transporter, permease protein	0.30	0.64	2.12	9×10^{-2}	5×10^{-2}
PP_1017	Sugar/glucose ABC transporter, permease protein	0.31	0.68	2.21	5×10^{-2}	5×10^{-2}

Locus tag	Gene name, annotation	Fold changes			p-values	
		5-KF / H_2O	5-KF	H_2O	5-KF	H_2O
PP_1071	amino acid ABC transporter, periplasmic substrate-binding protein	0.37	0.56	1.54	2×10^{-2}	8×10^{-2}
PP_1137	*braG*, branched-chain amino acid ABC transporter, ATP-binding protein	0.36	0.27	0.75	5×10^{-4}	6×10^{-2}
PP_1297	*aapJ*, general amino acid ABC transporter, periplasmic substrate-binding protein	0.06	0.04	0.68	3×10^{-4}	7×10^{-2}
PP_1486	polyamine ABC transporter, periplasmic polyamine-binding protein	0.36	0.21	0.58	7×10^{-4}	6×10^{-2}
PP_2264	sugar ABC transporter, periplasmic sugar-binding protein, putative	0.47	0.76	1.60	2×10^{-2}	2×10^{-2}
PP_2454	*rbsB*, ribose ABC transporter, periplasmic ribose-binding protein	0.30	0.17	0.57	5×10^{-4}	9×10^{-3}
PP_2558	outer membrane efflux protein, TolC family type	0.46	0.35	0.76	1×10^{-2}	2×10^{-2}
PP_2569	metabolite MFS transporter, MHS family	0.46	0.24	0.51	8×10^{-3}	2×10^{-3}
PP_2604	major facilitator family transporter	0.45	0.66	1.48	8×10^{-2}	6×10^{-2}
PP_2830	major facilitator family transporter	0.41	0.73	1.77	1×10^{-2}	5×10^{-3}
PP_3165	*benK*, benzoate MFS transporter	0.42	1.73	4.09	5×10^{-2}	7×10^{-3}
PP_3658	aromatic compound MFS transporter, putative	0.45	0.54	1.20	1×10^{-1}	5×10^{-2}
PP_4309	transporter, NCS1 nucleoside transporter family	0.49	0.23	0.47	3×10^{-2}	6×10^{-3}
PP_4735	*lctP*, L-lactate transporter	0.19	0.05	0.28	1×10^{-5}	5×10^{-3}
PP_4863	branched-chain amino acid ABC transporter, ATP-binding protein	0.15	0.12	0.79	7×10^{-3}	6×10^{-2}
PP_4865	branched-chain amino acid ABC transporter, permease protein	0.19	0.14	0.70	5×10^{-4}	8×10^{-2}
PP_5171	*cysP*, sulfate ABC transporter, periplasmic sulfate-binding protein	2.25	1.70	0.76	4×10^{-2}	9×10^{-2}
PP_5174	efflux membrane fusion protein, RND family	0.48	0.35	0.74	4×10^{-4}	2×10^{-2}
PP_5279	amino acid ABC transporter permease	4.76	3.72	0.78	7×10^{-3}	5×10^{-2}
Membrane						
PP_0092	lipoprotein, putative	2.26	4.14	1.83	5×10^{-4}	9×10^{-2}
PP_0504	*oprG*, outer membrane protein, OmpW family protein	2.57	1.77	0.69	7×10^{-2}	2×10^{-2}
PP_1122	OmpA family protein	0.39	0.27	0.69	6×10^{-3}	5×10^{-2}
PP_1153	lipoprotein, putative	2.36	0.49	0.21	3×10^{-2}	2×10^{-2}
PP_3090	OmpA domain protein	3.56	2.06	0.58	8×10^{-2}	6×10^{-2}
PP_3236	lipoprotein OprI	2.20	0.38	0.17	4×10^{-3}	9×10^{-4}
PP_4282	aquaporin Z	0.47	0.33	0.70	4×10^{-3}	2×10^{-3}
Regulation and signal transduction						

Locus tag	Gene name, annotation	Fold changes			p-values	
		5-KF / H_2O	5-KF	H_2O	5-KF	H_2O
PP_0386	sensory box protein	0.37	0.30	0.81	5×10^{-3}	7×10^{-2}
PP_1063	*metR-1*, transcriptional activator	2.22	1.86	0.84	1×10^{-3}	8×10^{-2}
PP_1144	diguanylate cyclase, GGDEF domain protein	0.48	0.31	0.64	1×10^{-3}	3×10^{-2}
PP_1313	transcriptional regulator, AraC family	0.41	0.67	1.63	4×10^{-4}	2×10^{-2}
PP_1644	*wrbA*, trp repressor binding protein	2.19	1.66	0.76	4×10^{-2}	2×10^{-2}
PP_2259	sigma-54 dependent transcriptional regulator	0.43	0.33	0.78	8×10^{-3}	5×10^{-2}
PP_2944	sensor histidine kinase	0.46	0.32	0.69	2×10^{-3}	2×10^{-2}
PP_2945	sensor histidine kinase/response regulator	0.46	0.30	0.65	3×10^{-4}	2×10^{-2}
PP_3159	*benR*, transcriptional activator of *benABC* operon	0.38	0.59	1.58	1×10^{-2}	9×10^{-2}
PP_3420	sensor histidine kinase	0.41	0.20	0.49	8×10^{-4}	8×10^{-3}
PP_3592	transcriptional regulator, RpiR family	0.34	0.23	0.68	4×10^{-4}	3×10^{-2}
Motility						
PP_2310	methyl-accepting chemotaxis transducer	2.49	1.48	0.59	1×10^{-3}	2×10^{-2}
PP_4376	*fliD*, flagellar cap protein	0.30	0.47	1.56	5×10^{-3}	1×10^{-1}
PP_4388	*flgE*, flagellar hook protein	0.46	0.87	1.91	2×10^{-2}	5×10^{-2}
PP_4888	methyl-accepting chemotaxis transducer, putative	0.36	0.27	0.74	3×10^{-2}	5×10^{-2}
Stress						
PP_0985	cold-shock domain family protein	0.42	0.78	1.84	4×10^{-2}	5×10^{-2}
PP_1522	*cspA*, cold shock protein	0.35	0.60	1.70	2×10^{-3}	5×10^{-2}
PP_3234	heat shock protein, HSP20 family	2.48	0.33	0.13	7×10^{-4}	8×10^{-4}
PP_3290	universal stress protein family	2.07	0.46	0.22	7×10^{-3}	3×10^{-3}
PP_4855	osmotically-inducible lipoprotein OsmE	22.96	15.79	0.69	4×10^{-4}	9×10^{-3}
Transcriptional and translational machinery						
PP_0493	*selA*, selenocysteine synthase	2.25	1.68	0.75	8×10^{-2}	2×10^{-2}
PP_0719	*ychF*, GTP-dependent nucleic acid-binding protein	2.10	4.03	1.92	7×10^{-3}	4×10^{-2}
PP_2006	hypothetical protein (BlastP: TULIP family P47 like protein)	0.24	0.41	1.75	2×10^{-2}	1×10^{-2}
PP_2007	P-47-related protein	0.32	0.23	0.70	3×10^{-3}	4×10^{-2}
PP_t12	tRNA-Pro	0.39	0.83	2.13	2×10^{-3}	8×10^{-2}
Others						
PP_0052	metallo-beta-lactamase family protein	0.47	0.31	0.66	3×10^{-3}	4×10^{-2}
PP_1083	bacterioferritin-associated ferredoxin, putative	0.31	0.75	2.41	8×10^{-2}	6×10^{-2}
PP_1116	site-specific recombinase, resolvase family	2.05	2.67	1.30	4×10^{-3}	3×10^{-2}
PP_3448	*nfrB*, bacteriophage N4 adsorption protein B	0.45	0.30	0.67	2×10^{-2}	4×10^{-2}
PP_4259	iron-sulfur cluster-binding protein	2.74	1.75	0.64	5×10^{-3}	2×10^{-2}
PP_4856	bacterioferritin, putative	14.63	14.13	0.97	3×10^{-4}	3×10^{-2}
Hypothetical proteins						

Locus tag	Gene name, annotation	Fold changes			p-values	
		5-KF / H_2O	5-KF	H_2O	5-KF	H_2O
PP_0273	hypothetical protein	3.19	1.53	0.48	2×10^{-2}	2×10^{-2}
PP_2874	hypothetical protein	2.71	1.40	0.52	5×10^{-2}	3×10^{-3}
PP_3094	hypothetical protein	4.49	6.78	1.51	5×10^{-4}	7×10^{-2}
PP_3097	hypothetical protein	3.51	4.90	1.40	3×10^{-4}	6×10^{-2}
PP_3100	hypothetical protein	3.52	4.91	1.39	5×10^{-5}	8×10^{-2}
PP_3235	hypothetical protein	2.17	0.45	0.21	4×10^{-3}	4×10^{-3}
PP_3307	hypothetical protein	3.07	2.29	0.75	2×10^{-2}	8×10^{-2}
PP_3401	hypothetical protein	2.14	2.45	1.14	5×10^{-2}	5×10^{-2}
PP_3610	hypothetical protein (BlastP: DNA alkylation repair protein)	2.15	1.34	0.62	8×10^{-2}	2×10^{-2}
PP_4615	hypothetical protein, phosphate-starvation-inducible E	4.70	2.29	0.49	6×10^{-2}	7×10^{-2}
PP_5167	hypothetical protein (BlastP: alpha/beta hydrolase)	2.03	1.44	0.71	8×10^{-2}	6×10^{-2}
PP_0712	hypothetical protein (BlastP: polyphosphate kinase)	0.43	0.29	0.69	4×10^{-3}	5×10^{-3}
PP_0764	hypothetical protein PP_0764	0.29	0.19	0.65	6×10^{-3}	3×10^{-2}
PP_0765	hypothetical protein PP_0765	0.37	0.16	0.44	5×10^{-3}	1×10^{-2}
PP_0766	hypothetical protein PP_0766	0.16	0.11	0.70	2×10^{-3}	4×10^{-2}
PP_0819	hypothetical protein PP_0819	0.47	0.69	1.46	7×10^{-2}	2×10^{-2}
PP_0905	hypothetical protein PP_0905	0.36	0.51	1.43	1×10^{-2}	5×10^{-2}
PP_1640	hypothetical protein (BlastP:YIP1 family protein)	0.25	0.16	0.67	1×10^{-3}	3×10^{-2}
PP_1662	hypothetical protein PP_1662	0.47	0.28	0.60	3×10^{-3}	7×10^{-3}
PP_1742	hypothetical protein PP_1742	0.29	0.07	0.25	6×10^{-3}	2×10^{-2}
PP_1762	hypothetical protein (BlastP: Pyrroloquinoline quinone (Coenzyme PQQ)	0.45	0.36	0.81	1×10^{-2}	3×10^{-2}
PP_1958	hypothetical protein PP_1958	0.41	0.73	1.79	3×10^{-2}	2×10^{-3}
PP_2292	hypothetical protein PP_2292	0.44	0.59	1.34	9×10^{-2}	5×10^{-2}
PP_2396	hypothetical protein PP_2396	0.49	0.39	0.79	4×10^{-3}	7×10^{-2}
PP_2401	hypothetical protein (BlastP: ferric reductase-like transmembrane domain-containing protein)	0.44	0.33	0.76	1×10^{-3}	6×10^{-2}
PP_2510	hypothetical protein PP_2510	0.46	0.94	2.06	8×10^{-4}	5×10^{-2}
PP_2796	hypothetical protein PP_2796	0.47	0.89	1.90	8×10^{-2}	8×10^{-3}
PP_3782	hypothetical protein (BlastP: acyl carrier protein)	0.46	1.39	2.99	6×10^{-4}	8×10^{-2}
PP_3784	hypothetical protein (BlastP:dioxygenase)	0.44	1.25	2.82	6×10^{-2}	6×10^{-2}
PP_4062	hypothetical protein PP_4062	0.33	0.63	1.92	3×10^{-2}	1×10^{-3}
PP_4207	hypothetical protein (BlastP: histidin kinase/ response regulator)	0.48	0.37	0.76	5×10^{-3}	4×10^{-2}
PP_4593	hypothetical protein PP_4593	0.47	0.32	0.68	2×10^{-3}	4×10^{-2}

Locus tag	Gene name, annotation	Fold changes			p-values	
		5-KF / H_2O	5-KF	H_2O	5-KF	H_2O
PP_4640	hypothetical protein (BlastP: YbdD/YjiX family protein)	0.36	0.54	1.50	4×10^{-3}	3×10^{-2}
PP_4685	hypothetical protein (BlastP: TfoX/Sxy family DNA transformation protein)	0.48	0.43	0.89	2×10^{-3}	9×10^{-2}
PP_5319	hypothetical protein (BlastP: conserved exported protein of unknown function)	0.46	0.27	0.59	1×10^{-3}	2×10^{-2}

Of the selected genes, 58 were upregulated and 104 were downregulated with respect to the ratio of 5-KF-fold change/water-fold change. Genes that are of particular interest are those related to fructose metabolism and those with a particularly strong expression change (up or down). A selection of these genes is discussed in the following sections.

5.3.3 Genes involved in respiration and energy metabolism

The genes for the cytochrome *o* quinol oxidase and the *cbb*$_3$-type cytochrome *c* oxidase, especially *cbb*$_3$-1, were upregulated upon 5-KF addition, while the genes for the *aa*$_3$-type cytochrome *c* oxidase were downregulated compared to the control. Opposing results were observed for an experiment involving 60 min incubation of cells after addition of 30 g/L (=513 mM) NaCl. The osmotic stress was shown to downregulate the genes for the cytochrome *o* oxidase and the *cbb*$_3$-2 oxidase (Bojanovič, et al., 2017). The genes for the cytochrome *o* quinol oxidase are usually downregulated under oxygen limitation due to the low oxygen affinity of the *bo*$_3$ oxidase. *cbb*$_3$-type oxidases on the other hand have a very high oxygen affinity and are important for growth under microaerobic conditions (Williams, et al., 2007, Ugidos, et al., 2008). For *P. aeruginosa*, which like *P. putida* possesses two *cbb*$_3$ oxidases, the *cbb*$_3$-1 oxidase, corresponding to the *P. putida cbb*$_3$-2 oxidase, also plays an important role at high oxygen tension, while the other is more important at low oxygen tension (Williams, et al., 2007, Ugidos, et al., 2008). The composition of the respiratory chain in dependence of oxygen availability in *P. putida* is regulated by the oxygen-sensitive global regulator ANR, which activates the expression of *cbb*$_3$-1 oxidase but represses the *bo*$_3$ oxidase (Ugidos, et al., 2008). The hybrid sensor kinase HskA is also known to regulate the expression of the electron transport chain components depending on the oxygen availability, the oxidation state of ubiquinone, and the growth phase. HskA activates the cytochrome *cbb*$_3$-1 oxidase genes but does not regulate the cytochrome *bo*$_3$ oxidase genes (Sevilla, et al., 2013a, Sevilla, et al., 2013b). The observation that 5-KF addition causes upregulation of both, *bo*$_3$ oxidase and *cbb*$_3$-1 oxidase, suggests ANR or HskA might be responsible for activation of the *cbb*$_3$-1 oxidase genes and that another regulatory system is responsible for activation of the *bo*$_3$ oxidase genes. Also, the water control does not show these effects, and both cultures under the

same incubation conditions, should have comparable oxygen concentrations. The 5-KF addition should not change the oxygen availability.

5.3.4 Genes involved in metabolism

An interesting result of the transcriptome study is the upregulation of *fruK*, encoding the phosphofructokinase, which phosphorylates fructose-1-phosphate to fructose-1,6-bisphosphate. Expression of the *fruK* gene was previously shown to be upregulated after fructose addition when compared to glucose-grown cells (Chavarría, et al., 2013, Sudarsan, et al., 2014). Also, the GAPDH gene PP_3443 was upregulated by 5-KF addition, which was also previously observed when comparing fructose-grown cells and glucose-grown cells (Chavarría, et al., 2016). PP_3443 is upregulated by Cra, for which fructose-1-phosphate is the effector (Chavarría, et al., 2016). The upregulation of PP_3443 and *fruK* by the addition of 5-KF suggests that 5-KF is taken up and phosphorylated like fructose by PTS^{Fru}. 5-KF phosphorylation to 5-ketofructose-1-phosphate has already been described for a yeast hexokinase (Avigad and Englard, 1968). It would be interesting to confirm the formation of 5-KF-1-phosphate in future and elucidate the fate of this new metabolite.

Strongly upregulated by 5-KF addition are also the genes for glycolate oxidase. However, these genes seem to be part of a general stress response in *P. putida*. RNAseq data for oxidative, imipenem, and osmotic stress all showed an upregulation of the genes for the glycolate oxidase (Bojanovič, et al., 2017). Also, the formate dehydrogenase genes and PP_2052, encoding a hydrolase of the haloacid dehalogenase family, are strongly upregulated by 5-KF and these genes are also upregulated by oxidative and osmotic stress (Bojanovič, et al., 2017) and hence are probably not specifically related to 5-KF .

5.3.5 Genes involved in transport

The genes for a taurine transporter were strongly upregulated (in the list only *tauA*, in the whole data set also further subunits are upregulated, but do not fulfill the set criteria (fewer replicates or p-values > 0.1). The upregulation of these genes is reported for oxidative stress, not for osmotic stress. Taurine is an antioxidant and membrane stabilizer (Bojanovič, et al., 2017). The upregulation of the taurine transporter could thus be a response to the osmotic stress caused by 5-KF addition.

Striking is the downregulation of the glycine betaine/proline ABC transporter subunit (PP_0295) since these compounds serve as compatible solutes and enable protection against hyperosmotic stress.

Interesting is also the downregulation of sugar ABC transporters, especially the PP_1015-1018 operon, which is known to take up glucose (del Castillo, et al., 2007). This could indicate a conversion from glucose to fructose metabolism. However, the sugar ABC transporters are also

downregulated under osmotic stress conditions in Bojanovič, et al. (2017), this is rather a strategy for osmoprotection, to limit intracellular sugar concentrations.

5.3.6 Genes involved in motility

As expected for osmotic stress and as reported by Bojanovič, et al. (2017), genes involved in flagella synthesis are downregulated. Here only two are listed, but further were downregulated in the entire data set, but either were changed in a small number of replicates or had p-values >0.1.

5.3.7 Genes involved in stress response

The added 5-KF concentration of 100 mM 5-KF in comparison to the start concentration of 100 mM glucose seems to have caused osmotic stress. Some targets correspond with those reported for osmotic stress response upon NaCl addition (Bojanovič, et al., 2017). Remarkably is the upregulation of *osmE*, which is upregulated upon osmotic stress in *E. coli* and *P. putida*, but besides being a lipoprotein, the function is not known (Gutierrez, et al., 1995, Bojanovič, et al., 2017).

5.3.8 5-KF reductases

Different organisms were described to reduce 5-KF to fructose and thus enable its metabolism (see 1.2.3). Only recently different 5-KF reductases were identified in different organisms (Nguyen, et al., 2021b, Schiessl, et al., 2021). When analyzing the transcriptome changes of *P. putida* upon 5-KF addition, the question whether this bacterium can reduce 5-KF is important when using it as a 5-KF production host. The known 5-KF reductase sequences reported by Schiessl, et al. (2021) and Nguyen, et al. (2021b) were used for a TBlastN search (Altschul, et al., 1990) against the *P. putida* KT2440 genome. The results are listed in Table S4. Nine genes were identified as homologs for 5-KF reductases, but no significant upregulation was found for any of the genes upon 5-KF addition. Since a 5-KF reducing enzyme would likely be upregulated upon 5-KF addition, this indicates that *P. putida* KT2440 has no 5-KF reductase or at least none with is subject to 5-KF dependent regulation.

Table S4 5-KF reductase homologs in *P. putida* KT2440. Listed are TBlastN results for the 5-KF reductases reported by Schiessl, et al. (2021) and Nguyen, et al. (2021b)

5-KF reductase	Protein	Homologous BLAST hit for *P. putida* KT2440 locus tag and annotation
Tatumella morbirosei	KGD75378.1	PP_2406, putative quinate/shikimate dehydrogenase PP_3768, putative shikimate 5-dehydrogenase
Clostridium pasteurianum	AJA48273.1	PP_2368, 2,5-diketo-d-gluconate reductase PP_3671, oxidoreductase, aldo/keto reductase family
Gluconobacter oxydans	GOX0644, AAW60421.1	PP_2368, 2,5-diketo- d-gluconate reductase PP_3671, oxidoreductase, aldo/keto reductase family PP_3120, aldo/keto reductase PP_3174, putative oxidoreductase PP_2902, UDP-2,3-diacylglucosamine hydrolase PP_4872, hypothetical protein
	GOX1432, AAW61182.1	No hits
Gluconobacter thailandicus	GAP25168.1	PP_2406, putative quinate/shikimate dehydrogenase
		PP_2608, shikimate dehydrogenase

5.3.9 Conclusions

The microarray results indicate that the addition of 100 mM 5-KF apparently caused osmotic stress, as some genes showed changed expression that were previously reported to be part of the osmotic or general stress response. To avoid the stress response and get a more 5-KF-specific result, a similar experiment could either be performed with a lower 5-KF concentration to avoid the stress effect or in comparison to glucose addition to have the same osmotic effect in the control samples.

Striking is the differential expression of genes involved in respiration. Whether these changes are related to stress or other effects remains unclear.

The most remarkable observations are the upregulation of *fruK*, encoding the phosphofructokinase, and PP_3443, encoding a GAPDH, which are both also upregulated in fructose-grown cells, suggesting that the cells seem to recognize 5-KF as fructose or potentially can even metabolize it similarly, at least the initial steps.

The observation that none of the 5-KF reductase homologs was upregulated upon 5-KF addition suggests that *P. putida* can likely not reduce 5-KF, which is beneficial for its use as 5-KF production host.

5.4 References Appendix

Agius, C., von Tucher, S., Poppenberger, B., and Rozhon, W. (2018) Quantification of sugars and organic acids in tomato fruits. *MethodsX* 5: 537-550.

Altschul, S.F., Gish, W., Miller, W., Myers, E.W., and Lipman, D.J. (1990) Basic local alignment search tool. *J. Mol. Biol.* 215: 403-410.

Ano, Y., Hours, R.A., Akakabe, Y., Kataoka, N., Yakushi, T., Matsushita, K., and Adachi, O. (2017) Membrane-bound glycerol dehydrogenase catalyzes oxidation of D-pentonates to 4-keto-D-pentonates, D-fructose to 5-keto-D-fructose, and D-psicose to 5-keto-D-psicose. *Biosci. Biotechnol. Biochem.* 81: 411-418.

Avigad, G., and Englard, S. (1968) 5-Keto-D-fructose: V. Phosphorylation by yeast hexokinase. *J. Biol. Chem.* 243: 1511-1513.

Becker, S., Theile, S., Heppeler, N., Michalczyk, A., Wentzel, A., Wilhelm, S., Jaeger, K.E., and Kolmar, H. (2005) A generic system for the *Escherichia coli* cell-surface display of lipolytic enzymes. *FEBS Lett.* 579: 1177-1182.

Blank, M., and Schweiger, P. (2018) Surface display for metabolic engineering of industrially important acetic acid bacteria. *PeerJ* 6: e4626.

Bojanovič, K., D'Arrigo, I., and Long, K.S. (2017) Global transcriptional responses to osmotic, oxidative, and imipenem stress conditions in *Pseudomonas putida*. *Appl. Environ. Microbiol.* 83: e03236-03216.

Chavarría, M., Fuhrer, T., Sauer, U., Pflüger-Grau, K., and de Lorenzo, V. (2013) Cra regulates the cross-talk between the two branches of the phosphoenolpyruvate : phosphotransferase system of *Pseudomonas putida*. *Environ. Microbiol.* 15: 121-132.

Chavarría, M., Goñi-Moreno, Á., de Lorenzo, V., and Nikel, P.I. (2016) A metabolic widget adjusts the phosphoenolpyruvate-dependent fructose influx in *Pseudomonas putida*. *mSystems* 1: e00154-00116.

Chung, M.E., Goroncy, K., Kolesnikova, A., Schönauer, D., and Schwaneberg, U. (2020) Display of functional nucleic acid polymerase on *Escherichia coli* surface and its application in directed polymerase evolution. *Biotechnol. Bioeng.* 117: 3699-3711.

del Castillo, T., Ramos, J.L., Rodríguez-Herva, J.J., Fuhrer, T., Sauer, U., and Duque, E. (2007) Convergent peripheral pathways catalyze initial glucose catabolism in *Pseudomonas putida*: genomic and flux analysis. *J. Bacteriol.* 189: 5142-5152.

Earhart, C.F. (2000) Use of an Lpp-OmpA fusion vehicle for bacterial surface display. In: *Methods Enzymol.*: Academic Press. 506-516.

Francisco, J.A., Earhart, C.F., and Georgiou, G. (1992) Transport and anchoring of beta-lactamase to the external surface of *Escherichia coli*. *Proc. Natl. Acad. Sci. USA* 89: 2713-2717.

Gutierrez, C., Gordia, S., and Bonnassie, S. (1995) Characterization of the osmotically inducible gene *osmE* of *Escherichia coli* K-12. *Mol. Microbiol.* 16: 553-563.

Hartmans, S., Smits, J.P., van der Werf, M.J., Volkering, F., and de Bont, J.A. (1989) Metabolism of styrene oxide and 2-phenylethanol in the styrene-degrading *Xanthobacter* strain 124X. *Appl. Environ. Microbiol.* 55: 2850-2855.

Lee, S.H., Choi, J.i., Han, M.J., Choi, J.H., and Lee, S.Y. (2005) Display of lipase on the cell surface of *Escherichia coli* using OprF as an anchor and its application to enantioselective resolution in organic solvent. *Biotechnol. Bioeng.* 90: 223-230.

Miller, G.L. (1959) Use of dinitrosalicylic acid reagent for determination of reducing sugar. *Anal. Chem.* 31: 426-428.

Narita, J., Okano, K., Kitao, T., Ishida, S., Sewaki, T., Sung, M.H., Fukuda, H., and Kondo, A. (2006) Display of alpha-amylase on the surface of *Lactobacillus casei* cells by use of the PgsA anchor protein, and production of lactic acid from starch. *Appl. Environ. Microbiol.* 72: 269-275.

Nguyen, T.M., Goto, M., Noda, S., Matsutani, M., Hodoya, Y., Kataoka, N., Adachi, O., Matsushita, K., and Yakushi, T. (2021) The 5-ketofructose reductase of *Gluconobacter* sp. strain CHM43 is a novel class in the shikimate dehydrogenase family. *J. Bacteriol.*: Jb0055820.

Nicolay, T., Lemoine, L., Lievens, E., Balzarini, S., Vanderleyden, J., and Spaepen, S. (2012) Probing the applicability of autotransporter based surface display with the EstA autotransporter of *Pseudomonas stutzeri* A15. *Microb. Cell Fact.* 11: 158.

Peters, B., Mientus, M., Kostner, D., Junker, A., Liebl, W., and Ehrenreich, A. (2013) Characterization of membrane-bound dehydrogenases from *Gluconobacter oxydans* 621H via whole-cell activity assays using multideletion strains. *Appl. Microbiol. Biotechnol.* 97: 6397-6412.

Saito, N. (1973) A thermophilic extracellular α-amylase from *Bacillus licheniformis*. *Arch. Biochem. Biophys.* 155: 290-298.

Satoh, E., Niimura, Y., Uchimura, T., Kozaki, M., and Komagata, K. (1993) Molecular cloning and expression of two alpha-amylase genes from *Streptococcus bovis* 148 in *Escherichia coli*. *Appl. Environ. Microbiol.* 59: 3669-3673.

Satoh, E., Uchimura, T., Kudo, T., and Komagata, K. (1997) Purification, characterization, and nucleotide sequence of an intracellular maltotriose-producing alpha-amylase from *Streptococcus bovis* 148. *Appl. Environ. Microbiol.* 63: 4941-4944.

Schiessl, J., Kosciow, K., Garschagen, L.S., Hoffmann, J.J., Heymuth, J., Franke, T., and Deppenmeier, U. (2021) Degradation of the low-calorie sugar substitute 5-ketofructose by different bacteria. *Appl. Microbiol. Biotechnol.* 105: 2441-2453.

Schulte, M.F., Tozakidis, I.E.P., and Jose, J. (2017) Autotransporter-based surface display of hemicellulases on *Pseudomonas putida*: whole-cell biocatalysts for the degradation of biomass. *ChemCatChem* 9: 3955-3964.

Schüürmann, J., Quehl, P., Festel, G., and Jose, J. (2014) Bacterial whole-cell biocatalysts by surface display of enzymes: toward industrial application. *Appl. Microbiol. Biotechnol.* 98: 8031-8046.

Seibold, G., Auchter, M., Berens, S., Kalinowski, J., and Eikmanns, B.J. (2006) Utilization of soluble starch by a recombinant *Corynebacterium glutamicum* strain: growth and lysine production. *J. Biotechnol.* 124: 381-391.

Sevilla, E., Alvarez-Ortega, C., Krell, T., and Rojo, F. (2013a) The *Pseudomonas putida* HskA hybrid sensor kinase responds to redox signals and contributes to the adaptation of the electron transport chain composition in response to oxygen availability. *Environ. Microbiol. Rep.* 5: 825-834.

Sevilla, E., Silva-Jiménez, H., Duque, E., Krell, T., and Rojo, F. (2013b) The *Pseudomonas putida* HskA hybrid sensor kinase controls the composition of the electron transport chain. *Environ. Microbiol. Rep.* 5: 291-300.

Sichwart, S., Tozakidis, I.E., Teese, M., and Jose, J. (2015) Maximized autotransporter-mediated expression (MATE) for surface display and secretion of recombinant proteins in *Escherichia coli*. *Food Technol. Biotechnol.* 53: 251-260.

Sudarsan, S., Dethlefsen, S., Blank, L.M., Siemann-Herzberg, M., and Schmid, A. (2014) The functional structure of central carbon metabolism in *Pseudomonas putida* KT2440. *Appl. Environ. Microbiol.* 80: 5292-5303.

Tozakidis, I.E., Sichwart, S., and Jose, J. (2015) Going beyond *E. coli*: autotransporter based surface display on alternative host organisms. *N. Biotechnol.* 32: 644-650.

Tozakidis, I.E., Sichwart, S., Teese, M.G., and Jose, J. (2014) Autotransporter mediated esterase display on *Zymomonas mobilis* and *Zymobacter palmae*. *J. Biotechnol.* 191: 228-235.

Tozakidis, I.E.P., Lüken, L.M., Üffing, A., Meyers, A., and Jose, J. (2020) Improving the autotransporter-based surface display of enzymes in *Pseudomonas putida* KT2440. *Microb. Biotechnol.* 13: 176-184.

Ugidos, A., Morales, G., Rial, E., Williams, H.D., and Rojo, F. (2008) The coordinate regulation of multiple terminal oxidases by the *Pseudomonas putida* ANR global regulator. *Environ. Microbiol.* 10: 1690-1702.

Vigal, T., Gil, J.A., Daza, A., Garcia-Gonzalez, M.D., and Martin, J.F. (1991) Cloning, characterization and expression of an alpha-amylase gene from *Streptomyces griseus* IMRU3570. *Mol. Gen. Genet.* 225: 278-288.

Wells, T.J., Sherlock, O., Rivas, L., Mahajan, A., Beatson, S.A., Torpdahl, M., Webb, R.I., Allsopp, L.P., Gobius, K.S., Gally, D.L., and Schembri, M.A. (2008) EhaA is a novel autotransporter protein

of enterohemorrhagic *Escherichia coli* O157 : H7 that contributes to adhesion and biofilm formation. *Environ. Microbiol.* 10: 589-604.

Williams, H.D., Zlosnik, J.E., and Ryall, B. (2007) Oxygen, cyanide and energy generation in the cystic fibrosis pathogen *Pseudomonas aeruginosa*. *Adv. Microb. Physiol.* 52: 1-71.

Wohlers, K., Wirtz, A., Reiter, A., Oldiges, M., Baumgart, M., and Bott, M. (2021) Metabolic engineering of *Pseudomonas putida* for production of the natural sweetener 5-ketofructose from fructose or sucrose by periplasmic oxidation with a heterologous fructose dehydrogenase. *Microb. Biotechnol.* n/a.

Yang, T.H., Pan, J.G., Seo, Y.S., and Rhee, J.S. (2004) Use of *Pseudomonas putida* EstA as an anchoring motif for display of a periplasmic enzyme on the surface of *Escherichia coli*. *Appl. Environ. Microbiol.* 70: 6968-6976.

Yuuki, T., Nomura, T., Tezuka, H., Tsuboi, A., Yamagata, H., Tsukagoshi, N., and Udaka, S. (1985) Complete nucleotide sequence of a gene coding for heat- and pH-stable alpha-amylase of *Bacillus licheniformis*: comparison of the amino acid sequences of three bacterial liquefying alpha-amylases deduced from the DNA sequences. *J. Biochem.* 98: 1147-1156.

Danksagung

Besonders danken möchte ich Professor Dr. Michael Bott für die Überlassung des spannenden Themas, das Interesse am Fortgang meines Projektes, die Diskussionen und die Durchsicht dieser Arbeit.

Bei Dr. Meike Baumgart bedanke ich mich herzlich für das spannende Thema, das Interesse am Fortgang meines Projektes, viele Diskussionen und das Durchsprechen von Versuchen und Texten.

Bei Professorin Dr. Martina Pohl bedanke ich mich für die freundliche Übernahme des Zweitgutachtens meiner Arbeit.

Vielen Dank an alle, die mich fachlich und technisch bei meinen Arbeiten zur 5-Ketofructose unterstützt haben. Vielen Dank an Astrid Wirtz für die tolle, geduldige Unterstützung an der HPLC. Vielen Dank an Dr. Tino Polen und Christina Mack für die Unterstützung für das Microarray Experiment und die Auswertung. Vielen Dank an Svenja Battling für die gelungene Zusammenarbeit und den Austausch zur 5-Ketofructose in *Gluconobacter*. Vielen Dank an Philipp Fricke für die Zusammenarbeit im IMPRES Projekt und die Unterstützung in Bezug auf *Gluconobacter*. Vielen Dank an alle Mitglieder des IMPRES Projektes für die Zusammenarbeit. Vielen Dank an Professor Dr. Nick Wierckx, Dr. Maike Otto und Dr. Benedikt Wynands für die Bereitstellung von Stämmen, Plasmiden und hilfreichen Tipps zum Thema *Pseudomonas*. Vielen Dank an Alexander Reiter, für die MS-Messungen, um die Ansäuerung in meinen Proben aufzuklären. Vielen Dank an Ronja Weskott und Apilaasha Tharmasothirajan für die Hilfe mit der DASGIP.

Ich bedanke mich bei allen Studenten, die mich in Praktika und Abschlussarbeiten unterstützt haben. Danke an Alexander, Karolina, Marielle, Philipp, und Rebecca.

Bei allen Kollegen in der AG Regulation möchte ich mich für viel Unterstützung und eine wunderschöne Zeit bedanken. Danke an Alexander, Alina, Angela, Brita, Cedric, Friederike, Helga, Jan-Gerrit, Johanna, Johanna, Kai, Kiki, Lea, Lingfeng, Lukas, Marielle, Natalie, Paul, Philipp, Rico, Srushti, Susana und Tina. Mit Euch hat die Zeit im Labor, im Büro, in den Kaffeepausen und bei gemeinsamen Unternehmungen immer viel Spaß gemacht. Ihr seid die Besten!

Ein großes Dankeschön geht auch an alle Mitarbeiter des IBG-1 für die freundliche Arbeitsatmosphäre und die Unterstützung bei verschiedensten Problemen. Danke an die Infrastruktur, die IT, die Werkstatt sowie die anderen Arbeitsgruppen.

Bei meiner Familie bedanke ich mich für die Unterstützung auf meinem bisherigen Lebensweg und während des Studiums.

Ein großes Dankeschön an Carsten, weil Du immer für mich da bist, auch während dieser Arbeit.

Erklärung

Ich versichere an Eides Statt, dass die vorgelegte Dissertation von mir selbständig und ohne unzulässige fremde Hilfe unter Beachtung der „Grundsätze zur Sicherung guter wissenschaftlicher Praxis an der Heinrich-Heine-Universität Düsseldorf“ erstellt worden ist. Die Dissertation wurde in der vorgelegten oder in ähnlicher Form noch bei keiner anderen Institution eingereicht. Ich habe bisher keine erfolglosen Promotionsversuche unternommen.

_____

Jülich, den 25.10.2021

Band / Volume 239
Single crystal growth and neutron scattering studies of novel quantum materials
X. Wang (2021), VI, 145 pp
ISBN: 978-3-95806-546-8

Band / Volume 240
Structure and Dynamics of Magnetocaloric Materials
N. A. Maraytta (2021), vii, 146 pp
ISBN: 978-3-95806-557-4

Band / Volume 241
Novel insights into the transcriptional regulation of cell division in *Corynebacterium glutamicum*
K. J. Kraxner (2021), V, 83 pp
ISBN: 978-3-95806-560-4

Band / Volume 242
Interplay of proximity effects in superconductor/ferromagnet heterostructures
A. Stellhorn (2021), ix, 219 pp
ISBN: 978-3-95806-562-8

Band / Volume 243
Silencing and counter-silencing of the Lsr2-like protein CgpS in *Corynebacterium glutamicum*
J. Wiechert (2021), IV, 265 pp
ISBN: 978-3-95806-569-7

Band / Volume 244
Molecular Layer Functionalized Neuroelectronic Interfaces:
From Sub-Nanometer Molecular Surface Functionalization to Improved Mechanical and Electronic Cell-Chip Coupling
N. R. Wolf (2021), IV, 101, xx pp
ISBN: 978-3-95806-570-3

Band / Volume 245
Surface Acoustic Waves in Strain-Engineered Thin (K,Na)NbO_3 Films:
From Basic Research to Application in Molecular Sensing
S. Liang (2021), VI, 125 pp
ISBN: 978-3-95806-571-0

Band / Volume 246
Tailoring neuroelectronic interfaces via combinations of oxides and molecular layers
X. Yuan (2021), 113 pp
ISBN: 978-3-95806-572-7

Band / Volume 247
Stoichiometric control and magnetoelectric coupling in artificial multiferroic heterostructures
P. Schöffmann (2021), vii, 176 pp
ISBN: 978-3-95806-575-8

Band / Volume 248
A Unified Framework for Functional Renormalisation Group Calculations and its Application to Three Dimensional Hubbard Models
J. Ehrlich (2021), xvi, 213 pp
ISBN: 978-3-95806-582-6

Band / Volume 249
Photoemission electron microscopy of magneto-ionic effects in $La_{0.7}Sr_{0.3}MnO_3$
M. Wilhelm (2021), 134 pp
ISBN: 978-3-95806-592-5

Band / Volume 250
Development of a Multiplexer System and Measurement of the Neutron Yield for a Low-Energy Accelerator-Driven Neutron Source
M. Rimmler (2021), v, 200 pp
ISBN: 978-3-95806-600-7

Band / Volume 251
Resolving interface effects in voltage controlled magnetic heterostructures using advanced neutron scattering and electron microscopy methods
T. Bhatnagar-Schöffmann (2021), ix, 171 pp
ISBN: 978-3-95806-604-5

Band / Volume 252
Strain development of *Gluconobacter oxydans* and *Pseudomonas putida* for production of the sweetener 5-ketofructose
K. Wohlers (2022), VI, 118 pp
ISBN: 978-3-95806-612-0

Weitere ***Schriften des Verlags im Forschungszentrum Jülich*** unter
http://wwwzb1.fz-juelich.de/verlagextern1/index.asp

Schlüsseltechnologien / Key Technologies
Band / Volume 252
ISBN 978-3-95806-612-0

Mitglied der Helmholtz-Gemeinschaft

JÜLICH
Forschungszentrum